Functional characterisation of asparaginase and glutaminase in *Klebsiella pneumoniae* KR3167

Thesis submitted for the degree of

Doctor of Philosophy

at the University of Leicester

by

Rashed Mohammed Alghamdi

Department of Infection, Immunity and Inflammation

University of Leicester

April 2019

UNIVERSITY OF LEICESTER

Statement of originality

This accompanying thesis submitted for the degree of PhD entitled "Functional characterisation of asparaginase and glutaminase in *Klebsiella pneumoniae* KR3167" is based on work conducted by the author in the Department of Infection, Immunity and Inflammation of the University of Leicester during the period between September 2014 and September 2018.

All the work recorded in this thesis is original unless otherwise acknowledged in the text or by references.

None of this work has been submitted for another degree in this or any other University.

Signed …… Date ……

Abstract

Functional characterisation of asparaginase and glutaminase in *Klebsiella pneumoniae* KR3167

Rashed Alghamdi

Asparaginase and glutaminase are sets of enzymes that assist *Klebsiella pneumoniae* in acquiring necessary nitrogen sources when ammonia (NH_3), the preferred nitrogen source, is low or absent. *K. pneumoniae* contains four putative asparaginase and glutaminase genes (*yneH*, *ansA*, *ybiK*, and *KPN_01165*) but their functions are unknown. Therefore, the aim of my Ph.D. project was to investigate the contribution of these enzymes to *K. pneumoniae* KR3167 biology and virulence by creating unmarked mutant strains using Lambda Red system and Flp-recombinase-mediated excision mutagenesis.

A phenotypic assessment of the mutants was undertaken to determine the impact of asparaginase and glutaminase enzymes in survival and virulence of *K. pneumoniae* by using *in vitro* and *in vivo* assays. In growth medium not limited in nitrogen content, there was no significant difference in growth between the wild type and the mutants. In all assays, the *yneH* mutant showed no difference in phenotype compared to the wild type. However, all the other stains showed variation in asparaginase/glutaminase activity levels. In particular, the *KPN_01165* mutation produced the greatest effects. The mutant strain suffered reduced growth and had low asparaginase and glutaminase activities.

Moreover, this strain had less capsule synthesis and was attenuated in growth in serum-containing medium. My results showed that Lectin Pathway of complement (LP) is activated on the surface of *K. pneumoniae* KR3167 following the binding of the carbohydrate recognition molecule Collectin-11 (CL-11) which enhances C3 deposition. The role of LP was confirmed by using different mouse sera that were deficient of mannan-binding lectin serine protease (MASP-2), Ficolin A, and CL-11. Survival and killing assays using *G.mellonella* also revealed significant attenuation in virulence of *ΔansA*, *ΔybiK* , *ΔKPN_01165*, and *ΔybiK/ΔKPN_01165* strains compared to wild-type KR3167. Collectively, these results show that asparaginase and glutaminase enzymes are important in survival and virulence of *K. pneumoniae*.

Acknowledgements and dedications

In the name of God the most gracious the most merciful, that followed by thanking God for giving me strength and determination to complete to finish this work then, my deep appreciation to my family my mother (Maedah), my father (Mohammed), my wife (Sadia), and my children (Tala and Talal) for their continuous love and prayers.

I would like also to take this opportunity to thank everyone who has contributed to the success of this project. Deep thanks to my supervisor, Dr, Hasan Yesilkaya for his endless support throughout this PhD project: his patience, and suggestions allow me, easily adapt working environment in the lab and gaining the required skills needed for the lab research. His encouragement motivated me to accomplish my objectives. My special thanks to Dr. Primrose Freestone, for peoviding me support and kind words during this study.

I am grateful for Dr. Nicholas J Lynch, and Professor Jose Bengoechea School of Medicine, Dentistry and Biomedical Sciences, Queen's University Belfast, for accepting to train me in the serum bactericidal experments and *Galleria mellonella* infection model, respectively. Their assesstance had a great influence on the success of this project.

Special thanks to Albaha University (my scholarship provider), for giving me the opportunity to proceed postgraduate study.

Many thanks to all my friends in lab 125 for your encouragement and support.

This thesis is dedicated to my beloved parents, wife, and my kids for their endless love, and encouragement throughout this project.

Abbreviations

AP	Alternative pathway	ng	Nanogram
APS	Ammonium persulphate	nM	Nanomolar
bp	Base pair	OD	Optical density
BSA	Bovine serum albumin	PCR	Polymerase chain reaction
cDNA	Complementary DNA	RNA	Ribonucleic acid
CFU	Colony forming unit	SDS	Sodium dodecyl sulphate
CP	Classical pathway	TAE	Tris acetic acid EDTA
DNA	Deoxyribonucleic acid	TCA	Tricarboxylic acid cycle
dNTP	Deoxynucleotide triphosphate	µM	Micromolar
EDTA	Ethylene diamine tetra acetic acid		
kb	Kilobase	v/v	Volume per volume
LA	Luria-Bertani agar	w/v	Weight per volume
LB	Luria-Bertani broth	x g	Gravity force

Table of contents:

1 Chapter-1: Introduction

1.1 Klebsiella pneumoniae: Overview

Klebsiella pneumoniae is a Gram-negative bacterium and belongs to the Family Enterobacteriaceae. The bacterium is non-motile, has a capsule, and appears rod-shaped. When *K. pneumoniae* is grown in agar, it appears as opaque and mucoid (Straus, 1998). It is found in the mouth, skin, and intestine (in 5% of healthy humans) and also in the environment (Wu and Li, 2015). It is also found in the soil and can fix nitrogen in aerobic conditions. As a free-living diazotroph, it has been reported to increase agricultural crop yield (De Bruijn and Ausubel, 1983). It is an opportunistic pathogen and causes a broad spectrum of diseases which include pneumonia, urinary tract infection, enteritis, meningitis, septic lesions, otitis, and sinusitis. Up to 20% of hospital patients are found to be affected by it (Brabb *et al.*, 2012). Bronchopneumonia is the general condition in people after infection with *K. pneumoniae,* and the formation of ulcer is also common. It is also linked with ventilator-associated pneumoniae in 10-13% patients and also causes acute respiratory distress syndrome when co-infection occurs with *Streptococcus pneumoniae* and *Mycoplasma pneumoniae* (Wu and Li, 2015). In hospitalized people, incidences of septicemia, pneumonia, urinary tract infection are common due to *K. pneumoniae* infections. Faeces and direct contact with contaminated instruments are the main sources of infection (Rammaert *et al*., 2011). *K. pneumoniae* is notorious for its drug resistance because of extended-spectrum β-lactamase (ESBL) resistance, which can be due to the accumulation of resistance-conferring mutations or can be inherited from the transfer of mobile genetic elements from another organism. Treatment of infections due to resistant *K. pneumoniae* with ESBL is very difficult (Broberg *et al.*, 2014). Therefore, it is imperative to understand the microbe's biology in detail in order to develop effective anti-infectives.

1.2 *Klebsiella pneumoniae* virulence factors

The driver of pathogenicity for *K. pneumoniae* is multifactorial and includes capsule, lipopolysaccharides (LPS), urease, adhesins, biofilms as well as proteins located in the outer membrane (Wu and Li, 2015). *Klebsiella* genus members express two different

types of antigens on their surface. O antigen is a component of the lipopolysaccharide layer while K antigen is a capsular polysaccharide. The K virulent antigen attaches to the host cell membrane and alters the bacterial cell surface thereby hindering phagocytosis. The capsule also plays a vital role in infection of the host cell and inhibition of phagocytosis. Apart from these, *Klebsiella* also produces an endotoxin (Highsmith and Jarvis, 1985). The virulence factors help the bacteria to evade phagocytosis (Liverman and Orth, 2008). Although certain determinants of *K. pneumoniae* virulence have been identified, what controls the disease-causing ability of this microbe is not fully understood. Some other determinants of *K. pneumoniae* virulence include fimbriae F1 and F3, the high-affinity siderophore enterobactin that acquires iron (Fe^{3+}), and hyper-mucoviscosity, which is a feature of certain strains (El Fertas-Aissani *et al*., 2013). Although these factors are essential for survival within the host, it has been suggested that *K. pneumoniae* may have other undiscovered factors that may contribute to its ability to colonise and cause disease within its host. Elusive virulence mechanisms, numerous infection sites, the appearance of antibiotic-resistant strains and difficult to control outbreaks are all reasons to investigate the biology of *K. pneumoniae* further. Therefore, the objective of this study is to identify if there are nutrient related influences on *K. pneumoniae* virulence, such as nitrogen availability.

1.2.1 Capsular polysaccharide

cellrole in virulence as the acapsular bacteria show less virulence than the bacteria with the capsule (Podschun and Ullmann, 1998; Yoshida *et al.*, 2000) (Figure 1.1). Hypervirulent strains are characterized by the presence of the extra thick capsule, which is also known as hypermucoviscous. Hypermucoviscosity differs from the presence of the ordinary capsule in that it consists of a mucoviscous exopolysaccharide which forms the bacterial coating and it is also robust in comparison (Fang *et al.*, 2004). Capsules, both classical and hypervirulent are termed as K antigens, and the variation in capsular polysaccharide is strain specific. There are about 78 different capsule types (Pan *et al.*, 2008). The genes needed for synthesizing capsule are chromosomally located and organized in an operon (*cps*). *Cps* is highly conserved among *K. pneumoniae* strains (Arakawa *et al.*, 1991; Shu *et al.*, 2009). The K antigen is synthesized by *wzi* gene locus of the *cps* gene cluster (Pan *et al.*, 2013). In acapsular bacteria, the *wzi* gene is absent and less susceptible to phagocytosis no matter if opsonin is present or absent (Lawlor *et al.*, 2006). For example, *K. pneumoniae* strains producing K1 or K2 serotypes are more

virulent than the other *K. pneumoniae*, and they can a cause community-acquired pyogenic liver abscess (Podschun and Ullmann, 1998, Siu *et al.*, 2012). Other *K. pneumoniae*withK8, K9, K10, and K24 serotypes were less virulent and were isolated from human urinary tract infections(Brooks *et al.*, 2001).

1.2.2 Lipopolysaccharide (LPS)

Lipopolysaccharide (LPS) is a component of the cell capsule of Gram-negative bacteria, and it is also known as endotoxin (Figure 1.1). The components of LPS include O antigen, core oligosaccharide, and lipid A (Merino *et al.*, 2000; De Majumdar *et al.*, 2015). There are 9 different O-antigens present in the capsule, and among them, O1 is the most common. LPS can serve as a virulence factor and also as a factor that triggers an immune response (Hansen *et al.*, 1999). The endotoxin property of lipopolysaccharide is considered to play a direct role in septicaemia (Tomas *et al.*, 1988). Lipid A component of the LPS, is a potent target for Toll-like receptor 4 (TLR4) (pattern recognition receptor) that stimulates the release of cytokines and chemokines from cellular components such as neutrophils and macrophages. Stimulation of the immune system causes clearance of *K. pneumoniae*. Lack of TLR4 causes pneumonia and systemic spread in the host, although TLR4 signaling can be dampened by the activity of hyper capsule (Branger *et al.*, 2004; Cai *et al.*, 2009; Standiford *et al.*, 2012). Dynamic flexibility has been demonstrated in the lipid A component in tissues like lungs where lipid A could change itself in to a 2-hydroxy acyl modification, and that may protect the bacterial against antimicrobial peptides (Llobet *et al.*, 2015).

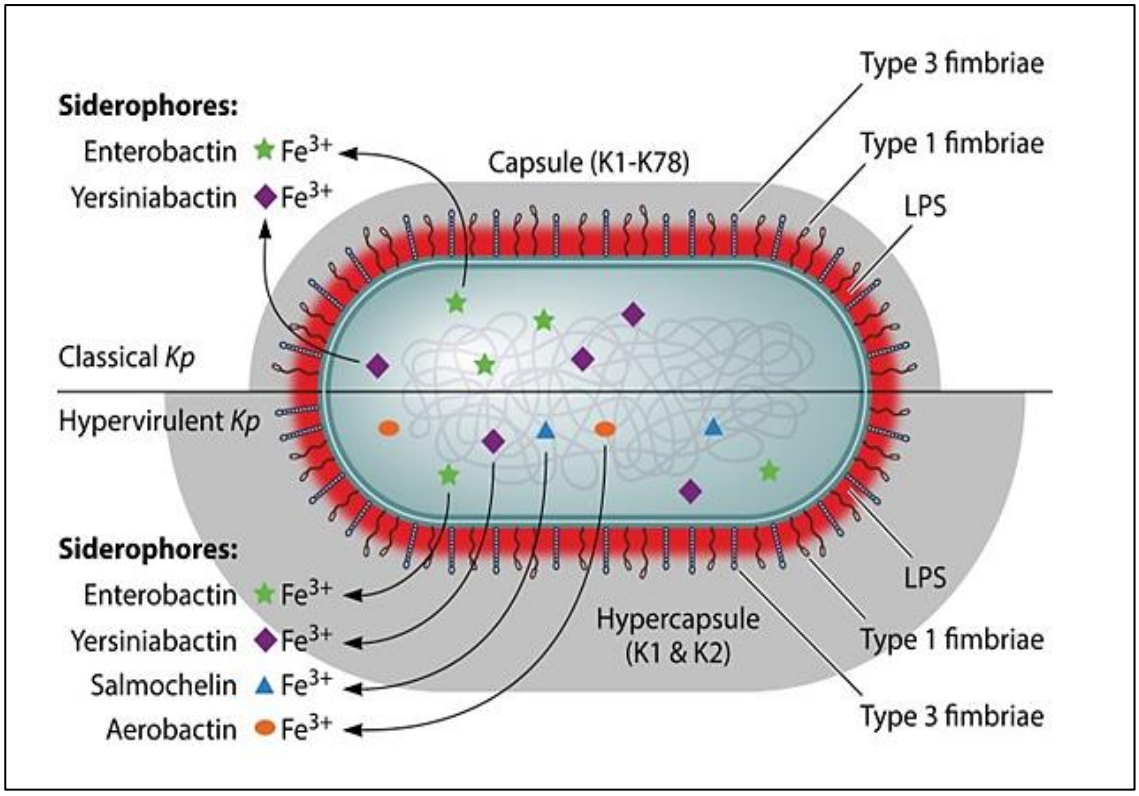

Figure 1.1. *Schematic representation of Klebsiella virulence factors. Diagram adopted from (Paczosa and Mecsas, 2016).*

1.3 Role of nutrition in pathogenicity

The pathogenicity of bacteria is accomplished by the production of virulence factors that can harm host organisms. Hence, it is not surprising that the regulation of virulence factor production is under the control of nutrient availability (Somerville and Proctor, 2009). The connection between virulence factor production and nutrient availability has been noted in earlier studies, but the mechanism by which the nutrient availability affected the virulence remained elusive for different types of nutrients and bacterial species (Batt and Brown, 1974). Bacterial cells are challenged continuously by various environmental conditions inside their host. Like other pathogenic bacteria, *Klebsiella* needs to evade the host immune response and adapt to the limited supply of oxygen and nutrients. Therefore, it needs to regulate the expression of virulence genes in response to the external and internal signals (Bassler, 1999). For example, *K. pneumoniae* needs to aqquire iron which is limited within the host. The reason behind its limited resource during an infection is because it is part of the non-specific immune response, and the host preserves it to prevent the growth of pathogens (Bullen, Rogers and Griffiths, 1972; Carniel, 2001). Usually, in mammals, iron remains bound to transferrin protein but during infection the binding of the iron shifts from transferrin to lactoferrin; this mechanism is associated with the innate

immune response (Bullen *et al*., 1972; Miethke and Marahiel, 2007). In this condition, the bacteria *K. pneumoniae* must acquire some strategies that will help it to acquire iron to support its survival in the host cell. The most used tactics are related to proteins called siderophores which are virulence factor. The siderophores have a property of affinity for iron which is higher than the proteins in host cells do. Siderophores can bind to the iron and acquire it from chelating protein (with which the protein usually remains bound) and scavenge it from the environment (Miethke and Marahiel, 2007). The variation could be observed in siderophores according to strain, and this variation also contributes to virulence of the strain. Production of more than one siderophore supports its colonization in different tissues and also prevents its neutralization by the host (Miethke and Marahiel, 2007; Bachman *et al.*, 2012). The expressed siderophores in *K. pneumoniae* are enterobactin, salmochelin, yersiniabactin and aerobactin (Perry *et al.*, 1999).

1.4 *Klebsiella pneumoniae* is a metabolically adaptive microbe

Klebsiella pneumoniae needs different sources of nutrients for growth. These nutrients are acquired by the catabolism of macromolecules. Non-pathogenic *Klebsiella* can obtain nutrients from the environment as a free-living organism or a symbiotic whereas pathogenic strains acquire them from other living organisms (Batt and Brown, 1974).

Carbon and nitrogen are two elements that are required by *Klebsiella pneumoniae* for its growth (Gottschalk, 2012). Most pathogenic bacteria are able to grow by using simple carbon sources such as glucose (Gottschalk, 2012). In the presence of oxygen, glucose via the glycolytic pathways produces pyruvate, which is then further dissimilated by pyruvate dehydrogenase in oxidative and decarboxylation steps to produce acetyl-coenzyme A. Consequently, the acetyl part will be consumed by the tricarboxylic acid (TCA) cycle (Gottschalk, 2012). TCA is a central metabolic pathway that occurs during aerobic metabolism. The TCA cycle generates intermediates such as the acetyl group and dicarboxylic acids, which are precursor molecules needed to produce many materials such as amino acids, and nucleotide bases (Kornberg, 2000). In terms of obtaining nitrogen, which accounts for about 10% of the bacterium's dry weight (Ronneau *et al*., 2014), *K. pneumoniae,* like all other organisms requires nitrogen or nitrogen-containing compounds during growth which can be used in formation of different amino acids, proteins, amino sugars and a number of co-enzymes. Sonawane et al. (2003) indicated that bacteria could use different amino acids such as glutamine or asparagine as carbon and nitrogen sources.

There are six classes of amino acids which are classified according to the precursor from which they originate. These include glutamate or α-ketoglutarate family, aspartate family, pyruvate family, serine-glycine or triose family, aromatic amino acid family and histidine. Among them, glutamine and asparagine (belongs to the aspartate family) are important as they are linked to the assimilation of ammonia (Hirokawa *et al*., 1998). In general, the ultimate products of amino acid metabolism are alpha-keto acids that can enter several metabolic pathways and serve as a carbon source. Gluconeogenic amino acids such as glutamine, asparagine, alanine, and cysteine, produce pyruvate and serve as a precursor for gluconeogenesis. Ketogenic amino acids such as leucine and lysine produce acetyl coA as their end product which serves as a precursor for the synthesis of fats. Transamination reactions provide amino groups required for the synthesis of several amino acids (Batt and Brown, 1974). Transamination reactions not only produce different amino acids, but they are also used to remove excess nitrogen in the form of small compounds which are then deaminated to produce ammonia or enter the urea cycle. Most transaminases require pyridoxal phosphate (the co-enzyme that is required for glutaminase to work) as a co-factor. Some enzymes also use pyruvate as substrate (Paul and Cooksey 1981).

However, if a high concentration of glucose is also provided with these amino acids, the microbe prefers to use glucose first. The reason for inhibition of asparagine and glutamine utilisation in the presence of glucose is because asparagine and glutamine, and glucose are degraded by the TCA cycle to 2-oxoglutarate and fumarate intermediates. A feedback inhibition can arise if this occurs because if these cycle intermediates are already at maximal, the need to utilize the amino acids as carbon sources will be reduced (Sanchez *et al*., 2007; Sonawane *et al*., 2003). All of these diverse metabolic pathways raise the possibility of the presence of a powerful adaptation system that enables *K. pneumoniae* to grow in different environments in which the access to nutrients is limited.

1.5 Nitrogen limitation and catabolite repression

Carbon catabolite repression is a regulatory mechanism that allows microorganisms to quickly adapt to the most rapidly metabolised carbon source first. Catabolite repression is achieved by the inhibition of enzymes required for the metabolism of other carbon sources other than the rapidly metabolizable source. It is an essential global regulatory system found in several microorganisms to efficiently use nutrients with low energy cost

(Stülke and Hillen, 1999). *Klebsiella* prefers glucose over lignocellulose hydroxylates due to catabolite repression (Gottschalk, 2012). Several genes involved in catabolite repression are identified in *Klebsiella.* For example, *crp* which codes for Cyclic adenosine monophosphate cAMP receptor, that mediate the utilization of glucose as well as xylose simultaneously (Ji *et al*., 2010). In the presence of glucose, cAMP mediates signalling process that blocks the induction of genes that is responsible for the utilization of other available sugars. However, in the absence of glucose, cAMP bind *crp* causes the induction of carbon catabolite repressed genes (Gosset 2005).

The nitrogen limitation does not result in the elimination of catabolite repression. In fact, nitrogen limitation leads to increased expression of traditional indicators like β-galactosidase and tryptophanase. It also activates the formation of glutamine synthase and glutamate dehydrogenase. However, nitrogen limitation represses the formation of glutamate synthetase and glutaminase (Prusiner *et al*., 1972) (Figure 1.2). Also, it was shown that there is a connection between *crp* and virulence regulation in some pathogens. For example, *Vibrio cholerae* Crp was reported to affect intestinal colonisation after controlling the expression of the genes responsible for that (Deutscher, 2008).

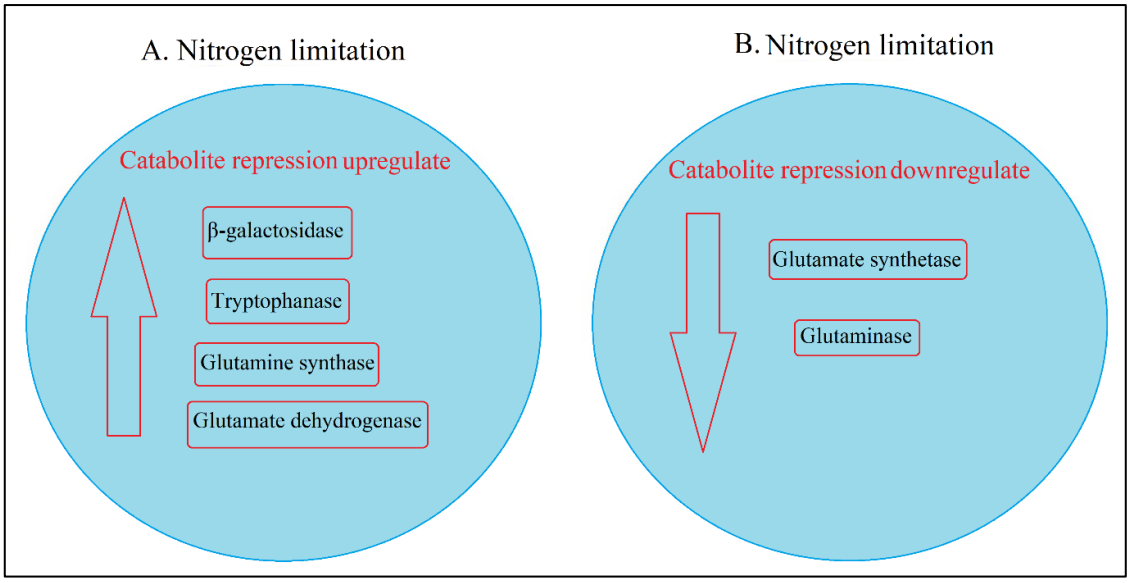

Figure 1.2. *Schematic representation of the effect of nitrogen limitation on catabolite repression signalling. A. Catabolite repression responds to nitrogen limitation by increased expression of β-galactosidase, tryptophanase, glutamine synthase and glutamate dehydrogenase. B. Under same condition (nitrogen limitation) catabolite repression also downregulate the formation of glutamate synthetase and glutaminase.*

1.6 Nitrogen metabolism in *K. pneumoniae*

Ronneau et al. (2014) suggested, bacteria obviously are in need of nitrogen or nitrogen containing compounds during their growth whether that growth is on a symbiotic or pathogenic basis. Moreover, nitrogen cannot usually be used in its elemental form; it should be combined with other bio elements such as oxygen, carbon, and hydrogen. It is present in diverse forms, however, the preferable form of nitrogen for bacteria is ammonium ion (NH_4^+) because it can be used efficiently by many nitrogen metabolism systems without consumption of high energy, but this requires an active transporter (Reitzer, 2003; Ronneau *et al*., 2014). *K. pneumoniae* has the capability to fix atmospheric nitrogen i.e., they can convert atmospheric nitrogen into ammonium. *K. pneumoniae* that is found in the soil as free-living can fix nitrogen by synthesizing an enzyme called nitrogenase which binds to the molecular nitrogen and reduces it to ammonia. Nitrogenase is synthesized by involving 20 genes which are also termed *nif* genes, located in a 24kb region of the chromosome. Nitrogen-fixing bacteria are also known as diazotrophic. Nitrogen fixation is an energy-intensive process which requires 16 ATP molecules and Mg^{2+} as a cofactor to catalyze the reaction of reduction of nitrogen into

ammonia. *K. pneumoniae* fixes nitrogen only under aerobic conditions and when the bacteria is under starvation (Streicher *et al.*, 1974; Schmitz *et al.*, 2002).

At high concentrations of ammonia, nitrogen fixation would not be needed. . The intracellular ratio of alpha-ketoglutarate to glutamine could be the critical parameter that determines the activity of glutamine synthetase. Glutamate and glutamine are two very important amino acids in bacterial nitrogen metabolism.

Despite the fact that the preferred nitrogen source is ammonium ion, bacteria have evolved many strategies to acquire the essential nitrogen through other compounds when ammonium ion is unavailable (Reitzer, 2003). In the absence of ammonium or ammonia, *K. pneumoniae* use organic nitrogen-containing compounds such as amino acids, polyamine, and short peptides (Ronneau *et al*., 2014). The nitrogen that comes from organic sources usually has an amino group which can be used in the biosynthesis of other amino acids (Reitzer, 2003; Bender, 2012; Ronneau *et al*., 2014).

Asparaginase and glutaminase are enzymes that hydrolyse asparagine and glutamine to aspartate and glutamate respectively, to produces NH_4^+ (Sonawane *et al*., 2003).

Taken together, these data may suggest that NH_4^+ availability is what control any nitrogen metabolism process and under such condition, asparaginase and glutaminase genes may become a conditionally important source for providing the essential nitrogen. Moreover,

in *K. pneumoniae* any system that involves glutamine or glutamate metabolism may regarded as important because it could help bacteria in keeping the nitrogen metabolism process balanced.

1.7 Metabolic utility of glutamine and asparagine

Glutamine is the primary nitrogen source for enteric bacteria (Soupene *et al*., 1998). Other examples are asparagine and serine, which are considered valuable donors for carbon as both can be linked to chemotaxis (Reitzer, 2003). Sonawane et al. (2003) have used different amino acids in growth studies. It has been found that glutamine and asparagine produced the highest growth yield compared with other amino acids, and they can be used solely to provide nitrogen and carbon. .

1.7.1 Glutamate and glutamine as nitrogen donors

Glutamate is the primary substrate of transaminase (aminotransferase), whereas glutamine is the precursor of many compounds, such as pyrimidines, purines, and other essential amino acids. Furthermore, these two amino acids can be utilized by *Mycobacterium smegmatis* as the sole source of nitrogen and carbon (Harper *et al*., 2010). It has been found that *E. coli* and *Klebsiella aerogenes* use glutamate and glutamine as major donors for nitrogen in the absence of NH_4^+ (Goss *et al*., 2001). According to Yan (2007), glutamate and glutamine have a similar effect when they were used as nitrogen sources for enteric bacteria because there was no difference in growth rate and yield. In addition, it was suggested that intracellular glutamine concentration acts as a sensor of extracellular nitrogen availability. According to Goss et al. (2001), in enteric bacteria, *E. coli* and *K. aerogenes*, 88% and 12% of nitrogen are produced from glutamate and glutamine, respectively. These findings indicate the importance of glutamine and glutamate metabolism in bacteria. However, there is a massive gap of knowledge in *K. pneumoniae* glutamine and asparagine metabolism and this project aims to fill this gap.

1.7.2 Asparagine as a nitrogen donor

Asparagine is a nonessential naturally occurring amino acid that is known to have a high proportion of both carbon and nitrogen. This high ratio leads to asparagine being involved in nitrogen homeosyasis and protein synthesis functions (Loureiro *et al*., 2013). Furthermore, it is considered as a part of the amino acid family that can be used to supply nitrogen. Asparagine synthesis depends on glutamine and/or NH_4^+because glutamine provides nitrogen to this amino acid when the NH_4^+ concentration in the cell is low (Loureiro *et al*., 2013; Reitzer, 2003). As Loureiro et al. (2013) pointed out, there are two enzymes [asparagine synthase A (AS-A) and asparagine synthase B (AS-B)] encoded by *asnA* and *asnB* genes, respectively, that are responsible for biosynthesis of asparagine. In addition, it was described that AS-A relies only on NH_4^+ to produce asparagine, while AS-B can use both NH_4^+ and glutamine. AS-A is found in both eukaryotes and prokaryotes, while AS-B is restricted to prokaryotes (Loureiro *et al*., 2013). Asparagine metabolism produces three intermediates containing carboxylic acids (fumarate and 2-oxoglutarate) (Sonawane *et al*., 2003). 2-Oxoglutarate can be used to produce glutamate and NH_3 through glutamate-oxoglutarate amidotransferase (GOGAT) (Harper *et al*., 2010).. Interestingly, it has been found that the absence of 2-oxoglutarate leads to activation of the nitrogen fixation process in *K. pneumoniae* (Glöer *et al*., 2008). It can

be concluded that among all of the amino acids, glutamine is the primary nitrogen provider, then comes asparagine. Hence, their presence is essential in balanced bacterial nitrogen metabolism. All the available published data emphasise the role of glutamine and asparagine as nitrogen providers, and this may suggest the physiological importance of the systems that allow utilisation of these sources

The presented data suggest the importance of amino acids and the metabolic mechanisms involved with it in *K. pneumoniae* biology.

1.7.3 The physiological importance of glutamine and asparagine

Glutamine is the most abundant amino acid in the human body and is involved in more cellular processes than any other amino acid (Newsholme, 2001). In humans, glutamine is an essential precursor for glucose synthesis and plays a significant role in maintaining the glucose carbon pool. Glutamine is the predominant renal gluconeogenic substance as it accounts for 20-25% of total glucose production. Glutamine boosts net muscle glycogen storage as well as gluconeogenesis (Stark *et al*., 1997). In patients with type II diabetes, conversion of glutamine to glucose is increased (Stumvoll *et al*., 1999). Even though glutamine is a nonessential amino acid, its increased consumption during surgery, trauma, and chemotherapy make it a conditionally essential amino acid (Bender, 2012). Glutamine is a crucial substrate for ammoniagenesis in the kidney and gut due to its predominant role in acid-base homeostasis (Tapiero *et al*., 2002). Glutamine is the key link between protein and carbohydrate metabolism and plays a notable role in the development of enterocytes, fibroblasts, and lymphocytes. Deamidation of glutamine produces alpha-ketoglutarate, which serves as a neurotransmitter inhibitor (Harper *et al*., 2010). Most of the glutamine in the brain is synthesized from TCA cycle intermediates. Glutamine also plays a dominant role in synaptic maintenance and plasticity. It serves as a precursor for the biosynthesis of glutathione and polyglutamated folic acid (Tapiero *et al*., 2002). Since cancer cells are addicted to nutrients due to metabolism alteration, pathways involved in glutamine metabolism can be used for therapeutic purposes (Altman *et al*., 2016).

Glutamine has many essential functions in the human body (Newsholme, 2001). In many tissues, serum and blood, it is the major amino acid and is considered an essential source and transporter for nitrogen. Human serum has a glutamine level that varies between 0.2 to 0.5 mM, and this level drops during infections, burns, and after surgery (Haber *et al.*,

2017). Also, it is a vital source of energy that is especially needed by dividing lymphocytes and macrophages. In the intestinal tract, this amino acid is essential for the epithelial cells and for maintaining normal physiological status (Bender, 2012; Stark *et al*., 1997). Bender (2012) stated that mammalian liver uses transported NH_3, which is the outcome of deamination of different amino acids in peripheral tissues, to produce glutamine and glutamate by GS and glutamate dehydrogenase (GDH). Furthermore, these two enzymes utilize most NH_3 to ensure that there is no or little passed out into the bloodstream (Bender, 2012). All this shows that mammalian tissues contain plentiful glutamine for colonising and invading bacteria.

Asparagine is a nonessential amino acid and is categorized as a part of the oxo-acids amino acid family. In addition, despite their presence in low concentration (blood level approximately 50 µM), this family depends on glutamine to offer nitrogen for their transamination(Bender, 2012; Schalk *et al*., 2014). After the hydrolysis of glutamine to glutamate, the glutamine dependant asparagine synthesis (*asnB*) synthesize asparagine from aspartate after receiving NH_3 that arise as a result of glutamine to glutamate hydrolyzation (Bender, 2012).

Giving that *K. pneumoniae* survive in different tissues that have several sources of nutrients including amino acids in different concentrations, the presence of energy efficient asparagine/ glutamine-acquiring systems may allow this microbe to prioritise, uptake and catabolise preferred nutrient sources with efficient metabolic energy use.

1.8 Asparaginase/glutaminase activities

The primary objective of this project is to evaluate the role of asparaginase and glutaminase enzymes in *K. pneumoniae* survival and virulence. This set of enzymes happens to be common among prokaryotes, eukaryotes, and plants and their main function is to hydrolyse asparagine and glutamine to aspartate and glutamate, respectively, which produces NH_3 (Pokrovskii *et al*., 2013; Sanches *et al*., 2007; Sonawane *et al*., 2003). Attention was drawn to these enzymes in the 1950s, as it was discovered that they have anticancer properties. Since then, asparaginase enzymes have been screened, cloned and expressed in numerous microorganisms and plants for their use in medicine, or in the food industry (Shrivastava *et al*., 2015). Both *E. coli* (EcA) and *Erwinia chrysanthemi* asparaginase are commonly used to treat acute lymphoblastic leukaemia (ALL), but they also possess a glutaminase activity which causes unwanted

side effects (Pokrovskii *et al*., 2013; Sanches *et al*., 2007). The glutaminase reaction is reversible, and the resulting glutamate is converted to α-ketoglutarate by the tricarboxylic acid cycle and is incorporated into the carbon skeletons; α-ketoglutarate is also used as a substrate for amino acid synthesis (Shibayama *et al*., 2011).

Although many other amino acids can provide carbon and nitrogen, which can be integrated into other amino acids or nucleotides, in different ratios (Reitzer, 2003). In*Pseudomonads* glutamine and asparagine produce the highest culture growth yield compared with other amino acids (Sonawane *et al*., 2003).

1.8.1 Asparaginase types

There are three types of asparaginase: bacterial type, plant type, and *Rhizobium etli* asparaginase (Cedar and Schwartz, 1967). In bacteria, the asparaginase/glutaminase enzyme family is generally called asparaginase because these enzymes have a higher affinity to asparagine than to glutamine (Sonawane *et al*., 2003). Bacterial asparaginase enzymes can be categorized into type I and type II, depending on substrate specificity, and location. The former is an anaerobically activated enzyme that has an intracellular location, and has a low affinity towards L-asparagine, while type II can be isolated from periplasmic space, and its activity can be directed to both L-glutamine, and L-asparagine (Sanches *et al*., 2007; Sonawane *et al*., 2003). In addition, it has been found that some bacteria, such as the *Pseudomonads*, have additional asparaginase–glutaminase enzyme in their periplasm, with a function and structure that can be considered similar to the type II asparaginases (Sonawane *et al*., 2003). Srikhanta et al. (2013), indicated that *E. coli* have two asparaginase genes, one with high affinity towards asparagine found in cytoplasm encoded by *ansA* (type I asparaginase), and a second one (type II asparaginase) in periplasm that has low K_m (3.5 μM), encoded by *ansB*.

Regarding the physiological functions of asparaginase, experimental studies have demonstrated that it promotes cell growth when ammonia is not present in the medium, and it uses asparagine and glutamine as a source of nitrogen and uses it to fulfil the nutritional requirement of the cell. Several studies have demonstrated high activity of these enzymes in cell growth (Cedar and Schwartz, 1967; Müller and Boos, 1998; Asselin, 1999; Avramis and Panosyan, 2005). Also, in recent years it was reported by many studies, the importance of the bacterial asparaginase in infection by enhancing

colonisation by *Helicobacter pylori, Salmonella typhimurium,* and *Campylobacter jejuni* (Srikhanta *et al*., 2013).

1.8.2 Bacterial glutaminases

Glutaminase enzymes are common among prokaryotes and eukaryotes (Brown *et al*., 2008). In *E. coli,* there are two types of glutaminases: type A, the major glutaminase, and type B, minor glutaminase, which are encoded by two putative genes, *yneH* and *ybaS*, respectively (Brown *et al*., 2008). Brown et al. (2008) suggested that bacterial glutaminase belongs to the asparaginase/glutaminase family and they are strictly specific for their substrates (glutamine) with low-affinity K_m that range from 1.5 to 9.5 mM. Also, glutaminase mainly regulates the pool of glutamine in the cell which is used as the central metabolite for nitrogen. It was concluded that asparaginase and glutaminase play a role in supporting bacterial growth when nitrogen is limited (Sanches *et al*., 2007). Moreover, Sanches et al. (2007) noted that in *K. aerogenes* when NH_4^+ is low, glutamine synthesis (GS) will be activated which is requires to overexpress asparaginase and glutaminase genes.

1.8.3 Mechanism of action asparaginase and glutaminase

Bacterial asparaginase is amidohydrolase enzymes that catalysed asparagine, glutamine, aspartate and glutamate to produce ammonia. The structural information of all known bacterial asparaginase showed high similarity. This structure can be described as a tetramer of identical subunits (Figure 1.3). Each subunit contains an active site between the adjacent monomers. (Clarissa *et al*., 1997; David ,2005). Kozak et al. (2002) indicated that the active site is under the control of a flexible loop that is hypothesised to be in a closed conformation when the active site engages with its substrate. Besides, the same study suggests that the conformation of the flexible loop is affected by the pH status as the interaction of aspartate and this enzyme is high in acidic pH, and in high pH, the loop will be open. The open conformation structure of bacterial asparaginase is determined and reported by Lubkowski et al., (1994) as threonine (Thr), aspartate (Asp), and lysine (Lys) which are highly conserved among bacterial asparaginase. The threonine residues in the active side are involved in the catalytic activity of those enzymes. (Miller *et al*.,1993).

The flexible loop of the active site controls accesses to the binding pocket. Threonine residues freeze the mobility of the loop when bound covalently to the primary catalytic

nucleophile. The result of this binding is a closed conformation of enzyme (Ortlund *et al*.,2000). A sulphate and ammonium ions provide suitable electrostatic interactions to stabilize the active site loop in the closed conformation (Lebioda et al., 1993).

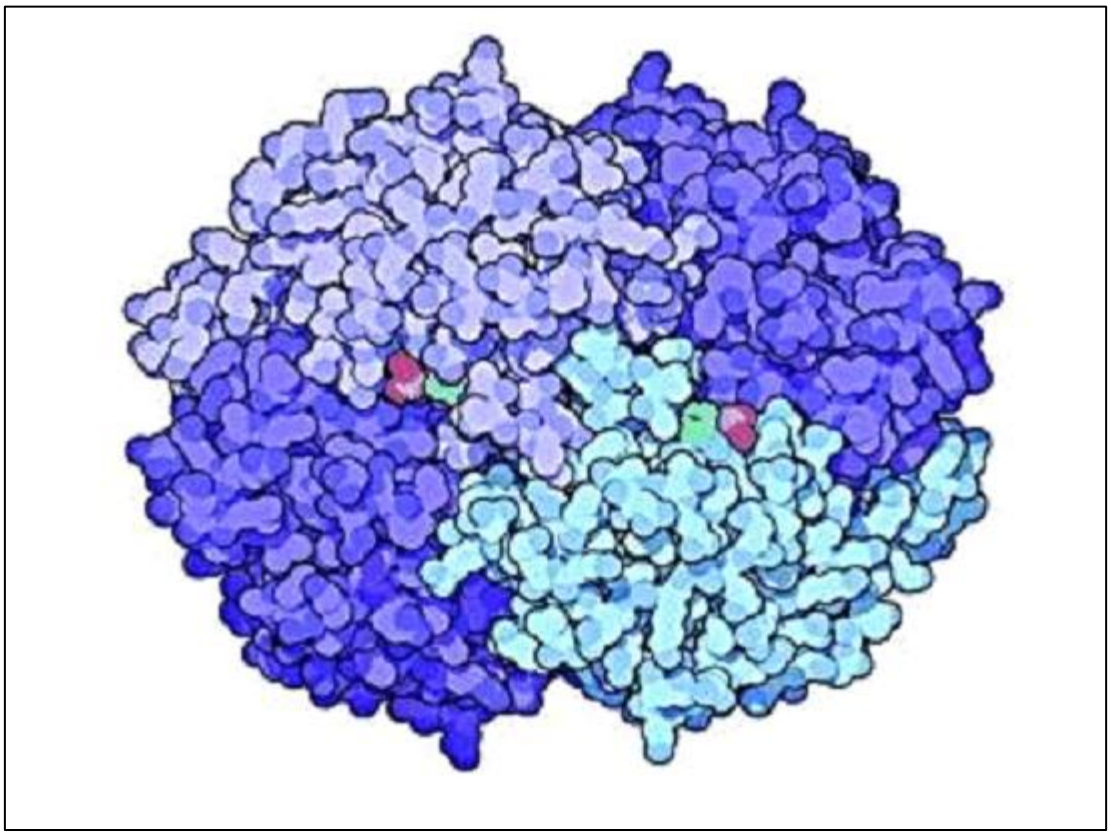

Figure 1.3. *Purified bacterial asparaginase II, which is composed of four identical subunits. Red spots represent the four active sites which also havethreonine amino acid that cleave this enzyme (Goodsell, 2005).*

1.8.4 Asparaginase/glutaminase enzyme nomenclature

Enzyme nomenclature is an enzyme classification system that simplifies enzymes' organization (Ako and Nip, 2012). According to Sanches et al. (2007), the bacterial asparaginase II is called EC 3.5.1.1. According to this nomenclature system, EC 3 means that these enzymes are hydrolysing enzymes that cleave carbon bonds, and as the name indicates, H_2O is an essential substrate for this process. After reviewing the Kyoto Encyclopaedia of Genes and Genomes (KEGG) database, National Center for Biotechnology Information (NCBI) and Ako and Nip (2012), it has been found that *K. pneumoniae* MGH 78578 contains three asparaginase/glutaminase enzymes encoded by

four genes, EC 3.5.1.1 (encoded by *ansA*, *ybiK*, and *KPN_01165*), while EC 3.5.1.2 is encoded by *yneH*. EC 3.5.1 means that the enzyme is working on carbon-nitrogen and peptidase bonds, as the last digit in EC 3.5.1.1 means this is an asparaginase enzyme, whereas EC 3.5.1.2 is a glutaminase enzyme. It has been proposed by Sinsuwan et al. (2012), that the EC 3.5.1.1 enzyme can hydrolyse both asparagine and glutamine, while EC 3.5.1.2 is highly specific for its substrate (glutamine) (Ako& Nip, 2012).

1.8.5 Expression of asparaginase/glutaminase

The expression of glutaminase and asparaginase is strongly regulated by the substrate of these enzymes, and/or reaction products and also by carbon sources such as glucose or carboxylic acids. Glutamine and asparagine also produce the intermediates of Krebs cycle. Deficiency of ammonia induces synthesis of glutamine synthetase and production of asparaginases (Sanches *et al*., 2007). The key function of asparaginase and glutaminase enzymes is to provide NH_3 (Pokrovskii *et al*., 2013). In *K. pneumoniae*, the synthesis, and acquisition of the available nitrogen are highly regulated processes. Under conditions of nitrogen limitation, nitrogen uptake is regulated by the Nitrogen Assimilation Control protein (NAC) and Nitrogen Regulatory System (NTR) (Jennings and Beacham, 1990; Macaluso *et al*., 1990; Merrick and Edwards, 1995). The NAC is a regulatory protein that provides a link between sigma factor σ54 and σ70 (Macaluso *et al*., 1990). The NTR system has four enzymes, uridylyl transferase/uridylyl-removing enzyme encoded by the *glnD*, a small-sized protein PII that is encoded by *glnB*, a two-component regulatory system composed of the NtrB and the response regulator NtrC (Merrick and Edwards, 1995). Mutations affecting NTR in *Klebsiella* impacts the regulation of several nitrogen metabolism genes like *nif*, *nas*, and asparaginase.

Mutations at NAC locus change the expression of asparaginase, tryptophan permease, nitrate reductase and nitrite reductase (Macaluso *et al*., 1990). Expression of asparaginase in *E. coli* is shown to be regulated by cAMP signalling and anaerobiosis (Jennings and Beacham, 1990). All mentioned data suggests that asparaginase is vital in bacterial nitrogen/carbon metabolism and the transcriptional control of asparaginase is critical for asparaginase function.

1.9 Asparaginase/glutaminase and virulence

Bacteria have various strategies to enhance their virulence and evade their host's immune system. One great example of this phenomenon is the production of certain enzymes like,

secretion of endotoxin and type III secretion system that can affect host cells. In one hand, those enzymes is clear, and it may result in hydrolysing of the cell membrane . On the other hand, there are other enzymes involved in metabolism that may produce very moderate changes, but those modifications can be essential for the pathogenesis and controlling the host cell mechanism. One such enzymatic reaction is asparaginase deamination. This reaction is irreversible, and it produces a substrate that cannot be used by the host (Washington *et al*., 2013). The irreversible deamidation of host glutamine and asparagine to glutamic acid and aspartic acid can result in a replacement of an amide group with a carboxylate group. As a result, an increase in the targeted protein mass and the total negative charge may occur. These modifications could change specific protein residues that are important in acquiring glutamic acid or aspartic acid which may impact host cell function (Washington *et al*., 2013).

Amino acid uptake by bacteria is mainly for fulfilling the requirement of protein synthesis and as a nitrogen source for other metabolic activities. The contribution of these enzymes to virulence may be linked to the ability to utilise their primary substrates (asparagine and glutamine) as the depletion in enzyme activity level may affect the normal amino acid balance of the bacterial cell.

1.9.1 Asparaginase as a virulence factor

Many studies have linked asparaginase with the infection processes of various bacteria. For example, *H. pylori* is a major pathogen responsible for gastric cancer and peptic ulcer in humans. Biochemical analysis revealed that cell cycle inhibition in the host's fibroblasts and gastric cells is mediated by asparaginase. Its effect on the cell cycle is confirmed by knockout lines, inhibitors and recombinant proteins. This data suggests that asparaginase is a major component of the *H. pylori* virulence and pathogenesis (Scotti *et al*., 2010).

In another study done by Leduc et al. (2010) that is related to H. *pylori*, it has been found that deamidases-transport system in *H. pylori* plays an important role in its colonization. The asparaginase II is a periplasmic deamidase enzyme in *H. pylori* that hydrolyse asparagine and glutamine to produce ammonia. During colonisation, *H. pylori* consums many amino acids, but asparagine and glutamine were the highest. In the same study, this enzyme was shown to be important in survival, colonisation and acid resistance (ammonia makes the environment basic) of *H. pylori*. Another example is the enhanced ability of

asparaginase of *Helicobacter pylori* to consume extracellular asparagine in the gastrointestinal tract, which helps this microbe in colonisation by interfering with the normal function of lymphocytes at the infection site using asparaginase activity (Shibayama *et al*., 2011). The authors also showed that *H. pylori's* asparaginase has no effect on gastric epithelial cells, but the mutation on the asparaginase gene makes this microbe unable to colonise as efficiently as the wild type.

Pathogens such as *Salmonella* use asparaginase enzymes to convert asparagine and glutamine into aspartate and glutamate respectively which they then use as nutrients. Because of asparaginase deamination, the host immune cellular signalling mechanisms are disrupted, and this has been shown to promote the *Salmonella's* ability to maintain an infection (Washington *et al*., 2013). Kullas et al. (2012) found that asparaginase II activity of *Salmonella typhimurium* suppresses T cells, which allows the microbe to avoid the needed cell-mediated immune response and that was helpful during this organism's colonisation. The mechanism of T-cell suppression includes interfering with normal development from the blast cells, inhibiting T-cell receptor (TCR-β) expression that is required for T-cell functions, and interrupting production of cytokines such as interleukin (IL-2) and interferon (INF-γ). According to the same study, T cells need asparagine to accomplish these functions, but the activity of asparaginase II reduced their level. As *S. typhimurium* strain 14028 lacks *ansB* (cytoplasmic asparaginase gene), it was unable to achieve the same degree of suppression as the wild type.

Several protozoan parasites also utilize asparaginase for pathogenesis. For example, small molecule inhibitors against asparaginase of Leishmania could inhibit the growth of the protozoan (Singh *et al*., 2015).

Porphyromonas gingivalis is a well-adapted pathogen of the oral cavity. On addition to the buccal cells, hemagglutination of the pathogen was reduced when treated with asparaginase, thus indicating the critical role of asparaginase in its virulence (Budu *et al*., 2003).

These results confirm the importance of nitrogen metabolism and the role of asparaginase in the virulence of pathogenic bacteria. So, if bacteria are defective in the production of asparaginase, they show poor pathogenicity.

1.9.2 Glutaminase as a virulence factor

The effect of glutaminase on virulence may come from decreasing glutamine level, which, as discussed before, is a semi-essential amino acid in many parts of the human body (Newsholme, 2001). Also, most of the glutamine that comes from the diet is consumed by cells in the intestine, which is used as respiratory fuel. It has been found that *H. pylori* depend largely on amino acid metabolism found in gastric juice during the infection process (Shibayama *et al*., 2011). Additionally, it was mentioned that *H. pylori* do not have NH_3 cytosol efflux pump to remove the resulting NH_3 from the urease activity. As a result, it depends on asparaginase and γ-glutamyl transpeptidase (GGT) to remove the cytosol accumulated ammonia. This ammonia assimilated by synthesis of asparagine and glutamine then will be released to the periplasm. *H. pylori's* GGT consumption of glutamine damages the epithelial cells and affects lymphocyte functions, which leads to inhibition of the immune response (Shibayama *et al*., 2011). Sonawane et al. (2003) indicated that bacterial asparaginase II also hydrolyses glutamine because of its similarity to asparagine and this could be the reason for the many side effects that arise when these enzymes are used to treat leukaemia.

1.10 Aims and Objectives.

The putative asparaginase/glutaminase activity in *K. pneumoniae* are coded by *yneH*, *ybiK*, *ansA*, and *KPN_01165*. As there is no experimental data to verify their functional role of these four genes, the main aim of my project is to evaluate the role of asparaginase and glutaminase in *K. pneumoniae* survival and virulence. In recent years, several studies have linked asparaginase and glutaminase enzymes with virulence in several microorganisms such as *Helicobacter pylori*, *Salmonella typhimurium*, and *Campylobacter jejuni* (Srikhanta *et al.*, 2013). These findings are reminders of the importance of nitrogen metabolism and in particular, the key role of asparaginase enzymes in the virulence of pathogenic bacteria. I, therefore, hypothesise that the asparaginase and glutaminase enzymes are important for *K. pneumoniae* nitrogen metabolism, and for *in vivo* colonisation and survival of this pathogen.

The objectives of this study are therefore to:

Determine the contribution of asparaginases and glutaminases in *K. pneumoniae* biology by:

i.) Constructing markerless mutants

ii.) Test the mutants' ability to use asparagine/glutamine as sole carbon/nitrogen source

iii.) Determine the phenotypic features of these mutants by growth studies and biochemical assays

iv.) Evaluate the role of asparaginase and glutaminase in *K. pneumoniae* pathogenicity *in vitro* by testing the susceptibly of *K. pneumoniae* KR3167 strains for complement-mediated recognition, then *in vivo* using *Galleria mellonella* larvae.

2 Chapter- 2: Genetic manipulation of *K. pneumoniae* KR3167 genome

Section A: Introduction

2.1 Overview

As described in the introduction, the aim of this study was to characterise role of asparaginase and glutaminase enzymes in *K. pneumoniae* KR3167 biology and virulence. It was therefore essential to this project to construct mutant alleles targeting putative genes coding for these enzymes, including *yneH*, *ansA*, *ybiK* and *KPN_01165*. Generally, to understand a function of a gene, genetic modification tools are applied to target that gene, and the resulting phenotypic change is studied by microbiological, genetic, and biochemical assays (Egan *et al.*, 2016). The lambda (λ) Red-based system is an allelic exchange technique that employs a liner transformation principle by using a suitable plasmid that carry phage related genes to disrupt a pre-targeted gene on its native genetic location. The resulting mutant allele will have an antibiotic resistance cassette that is flanked by regions with homology to upstream and downstream of the targeted area (Murphy, 1998). This technique has been adapted to study gene expression in *K. pneumoniae*, *E. coli* and other Gram-negative bacteria (Murphy, 1998; Datsenko and Wanner, 2000; Ishikawa and Hori, 2013). However, there are many considerations for application of this system, including the drug resistance status of host strain, capsule thickness, capsule mucoviscosity, and plasmid transformation efficiency as some strains does not support the commonly used lambda Red recombination plasmid (Sheng *et al*, 1995; Datsenko and Wanner, 2000).

This chapter will first consider the tools and protocols that are needed for successful mutagenesis processes. Then the results section will illustrate in detail how the lambda Red-based mutagenesis was used to make mutants in the *K. pneumoniae* KR3167 strain, and the application of Flp recombinase-mediated deletion of antibiotic resistance cassettes to create marker less mutants. This happens due to Flp recombinase activity on flippase recognition targets (FRT) which flank the antibiotic cassette. Also, genetic complementation experiments were carried out to rule out the possibility of polarity of mutations.

2.2 Mutant construction by lambda red-based allelic exchange

The lambda-derived Red recombination system allows for the efficient and specific deletion of genes on a native genetic locus. Over the years, numerus allelic-exchange mutagenesis techniques have been developed, and unlike the lambda Red system, a large number of these techniques apply suicide vectors that rely on restriction enzymes, DNA ligases, and cloning. Then during cell division, the vector needs to be cured after a few generations or the mutation process may fail (Hoang *et al.*, 1998a; Hoang *et al.*, 1998b; Datsenko and Wanner, 2000; Chuang *et al.*, 2006). On the other hand, the lambda Red exchange method possesses many useful characteristics including site specificity and higher efficiency, and it is less labour intensive. The system relies on generation of *in vitro* mutagenized allele by creating a construct containing an antibiotic cassette that is flanked by the upstream and downstream nucleotides of a target genetic location. The *in vitro* mutageneis can be achieved by two rounds of PCR, known as splicing overlap extension (Heckman and Pease, 2007; Egan *et al.*, 2016). Also, this system uses an easily curable low copy number plasmid that have an inducible phage related recombinase Gam, Bet, and Exo (Υ, β, and *exo*), to remove the antibiotic resistance cassette subsequently to create unmarked mutations.

The lambda Red proteins facilitate linear DNA exchange in Gram-negative bacteria. Gram-negative bacteria possess exonuclease activities that is done by RecBCD and SbcCD to protect bacteria from foreign DNA. The Gam protein in the system helps in recombination by inhibiting bacterial RecBCD and SbcCD exonuclease activity that may degrade the mutagenised alleles, while the Bet protein is an annealing protein that aids homologous recombination to the host genome, while Exo protein degrades double stranded DNA in 5' prime end to 3' end to create 3' 30-50 bp single-stranded DNA tails (Murphy, 1998; Mosberg, Lajoie and Church, 2010; Wei *et al.*, 2013; Egan *et al.*, 2016).

In this project, the mutant construction by lambda red-based allelic exchange was done on *K. pneumoniae* KR3167 using the pKOBEG-Apra plasmid, after following a previously described protocol (Murphy, 1998). The *K. pneumoniae* KR3167 strain is a clinical strain and was chosen for this study because its mucoviscosity is low, which is ideal for genetic manipulation. As illustrated in Figure 2.1, the first step in the mutagenesis programme was the insertion of pKOBEG-Apra plasmid by electroporation to a wild type *K. pneumoniae* KR3167. The KR3167/ pKOBEG strain was then used to

transform *in vitro* mutagenised allele, which contains approximately 1.5 kb *aph (3')-II*$_{FRT}$ (kanamycin resistance cassette) flanked by FRT, and approximately 500 bp of both left and right flanks of putative asparaginase/ glutaminase genes (Figure 2.1, B). Subsequently, arabinose was added to the growing cells that contained both pKOBEG plasmid, and the mutagenised PCR products, as this addition would induce the lambda red protein to initiate the homologous recombination, which will lead to replacement of target genes with the *aph (3')-II*$_{FRT}$ (Figure 2.1, C and D).

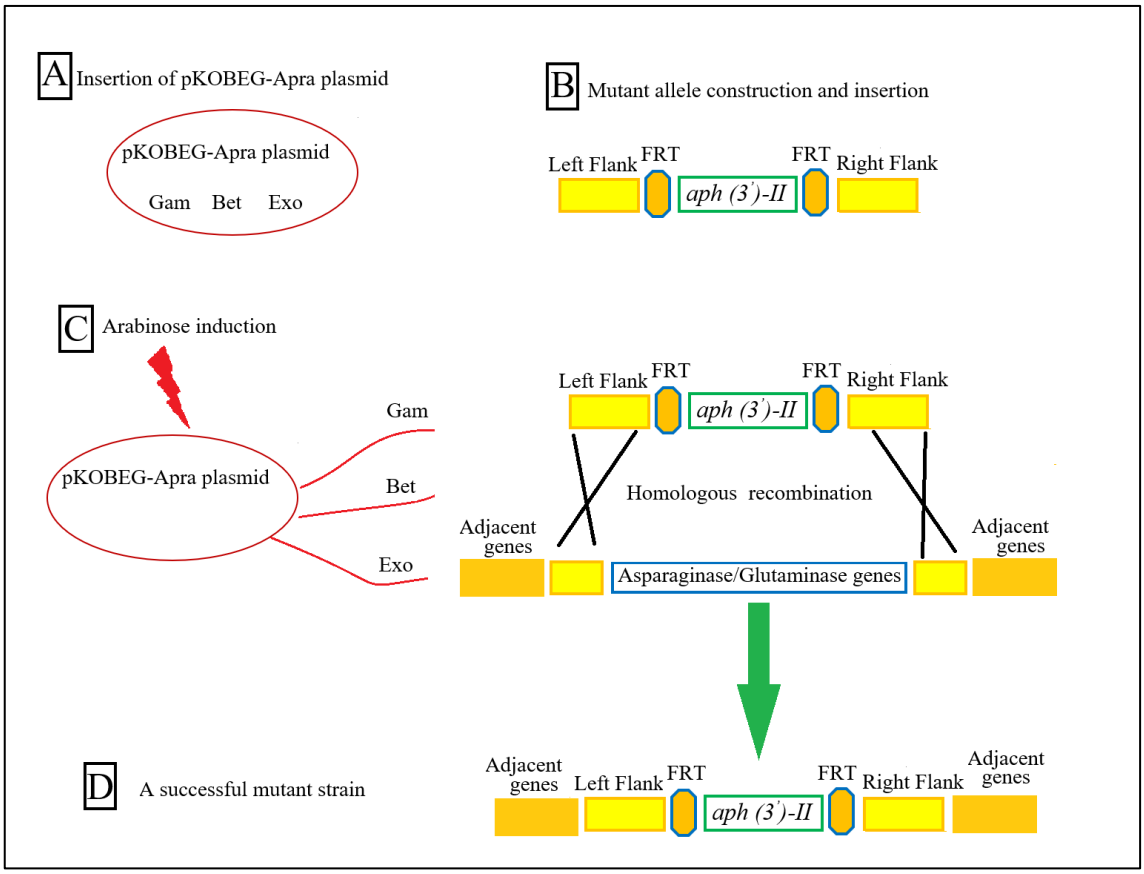

Figure 2.1: Schematic representation of lambda red-based allelic exchange. *It consists of three main steps. In step A: pKOBEG was electrotransformed to wild type* K. pneumoniae *KR316. In B: in vitro mutagenised construct transferred to KR3167/ pKOBEG strain. The third step represents arabinose induction of lambda red proteins that mediate homologous recombination represented by a 'x'. D: depicts a marked mutant strain resulting from the homologous recombination.*

Section B: Tools and protocols

2.3 Cultural media preparation

In the genetic manipulation experiments both *K. pneumoniae*, and *E. coli* strains were propagated in nutrient rich media. The nutrient-rich Lysogeny broth (LB), and Lysogeny agar (LA), provided by Oxoid, and Sigma-Aldrich, were regularly used for cultivation, and long-term storage of *K. pneumoniae*, and *E. coli* strains. These media are widely used for Gram negative bacteria growth, and contain high concentration of peptides, amino acids and carbohydrates. The LB media recipe comprised deionized water, 1 L 10 g tryptone, 5 g yeast extract, and 5 g NaCl, and for LA preparation, 15 g of Bacteriological agar was added (Thermo Scientific, UK). Super Optimal broth with Catabolite repression (SOC), was another enriched broth that was used post-transformation to recover transformed bacteria. A 200 ml SOC was prepared by dissolving 5 g tryptone, 2.5 g yeast extract and 5 g of NaCl into dH_2O. After autoclaving, sterile 100 mM $MgCl_2$, and 200 mM glucose were added before use (Sheng *et al*, 1995).

2.4 Bacterial strains

Strains of *K. pneumoniae* and *E. coli*, and different plasmid bearing hosts were used in this study. All bacterial strains are listed in Table 2.1. The strains were stored at -80ºC in LB broth with 30 % (v/v) sterile glycerol, and routinely grown at 37ºC using LB or agar LA. When required, 50 µg/ml kanamycin, 1200 µg/ml ampicillin, and 50 µg/ml apramycin, were added to the culture media unless otherwise specified.

2.5 Plasmids used in this study

This project relied on construction of unmarked mutants. This aim was achieved by using two plasmids: pKOBEG-Apra that have apramycin antibiotic marker, which was kindly provided by Anne Derbise and Sylvie Letoffe from Unité de Génétique des Biofilms, Département de Microbiologie, France (Chaveroche *et al*., 2000) and pFLP2 with ampicillin resistance that was kindly provided by Harbert Scheizer from College of Veterinary Medicine and Biomedical Sciences, Colorado State University, USA (Hoang *et al*, 1998). For protein expression experiments, I used pLEICS-01 plasmid with embedded ampicillin resistance gene, that was acquired from protein expression laboratory (PROTEX), University of Leicester.

Table 2.1*: Bacterial strains that used in this study.*

Strain	**Relevant description**	**Source**
E. coli DH5α	Plasmid propogation	Dr. Yesilkaya, University of Leicester, UK
E. coli BL21 DE3	Express and purify recombinant proteins	Agilent Technology Ltd., UK
K. pneumoniae MGH 78578	Reference strain	Dr. Kumar Rajakumar, University of Leicester, UK
K. pneumoniae KR 3167	Clinical strain isolated from bloodstream infection at Leicester Royal Infirmary. This strain was used for mutations.	Dr. Kumar Rajakumar, University of Leicester, UK
K. pneumoniae KR2021	To amplify *aph (3')-II*$_{FRT}$ (kanamycin resistance cassette)	Dr. Kumar Rajakumar, University of Leicester, UK
ΔKPN_01636 (*ΔyneH*)	Glutaminase A activity, putative	This study
ΔKPN_01203 (*ΔansA*)	Cytoplasmic asparaginase type II activity, putative	This study
ΔKPN_00861 (*ΔybiK*)	Periplasmic asparaginase type II activity, putative	This study

ΔKPN_01165	Periplasmic putative asparaginase/glutaminase activity	This study
ΔybiK /ΔKPN_01165	Double mutant strain	This study

2.6 DNA-extraction methods

2.6.1 Bacterial DNA extraction

The bacterial DNA extraction method used for *K. pneumoniae* was as described previously (Saito and Miura, 1963). Briefly, this phenol/chloroform extraction protocol was applied on overnight grown bacterial pellet. Usually, 400 µl of TE buffer containing 25% (w/v) sucrose, 60 µl of 500 mM Na_2EDTA, 40 µl of 10% (w/v) sodium dodecyl sulphate (SDS) and 2 µl of proteinase K (from 12.5 mg/ml stock), was used to re-suspend the harvested pellet. After incubation at 37˚C for 2 hours, this mixture was centrifuged for 5 min at 13,000 rpm (Hettich MIKRO 22R, Germany). The clear lysate was added with equal volume of liqufied phenol in Tris buffer pH 7.6 and was gently mixed until an emulsion formed. Then 10 min centrifugation at 13,000 rpm was performed, which produce a three-layer solution, in which the upper aqueous phase contains DNA. This layer was transferred without disturbing the white protein layer, to a fresh tube with an equal volume of chloroform: isoamyl alcohol (24:1) (Sigma Aldrich Ltd, UK). A second centrifugation at 13,000 rpm for 10 min was done. Then 1 volume of upper phase was mixed with 4 volumes of 100% ethanol that had 30 mM sodium acetate, pH 5.2. This mixture was centrifuged at 13,000 rpm for 5 min and the supernatant was discarded. The pellet was washed with 500 µl of 70% (v/v) ethanol and centrifuged again at 13,000 rpm for 5 min. The ethanol was discarded, and the pellet was left to dry before re-suspension in 250 µl TE buffer pH 7.0, and the concentration was measured using a NANODROP 1000 spectrophotometer before use (Thermo Scientific).

2.6.2 Small-scale Plasmid extraction (Mini Prep kit)

Plasmids were propagated in *E. coli* DH5α, and *E. coli* BL21 DE3 using LB broth medium supplemented with appropriate antibiotic. From *E. coli*, desired plasmid was extracted according to manufacturer's instructions (QIAprep®, Qiagen). Briefly, a single colony from fresh *E. coli* culture was incubated overnight at 37°C in 5 ml LB broth. Next day,

the culture was pelleted by centrifugation at 6000x g for 5 min at room temperature. A 250 µl aliquot of P1 buffer addition was used to re-suspend and transfer the pellet to a 1.5 ml micro-centrifuge tube, then 250 µl of P2 Buffer was added and the mixture was inverted gently 4 to 6 times. Before the lysate was centrifuged for 10 min at 13,000 rpm in a bench top micro-centrifuge (Micro centaur), 350 µl of N3 buffer was added, and mixed by inverting the tube 4 to 6 times. The resulting supernatant was transferred to the QIAprep column without touching the pelleted layer. This column was centrifuged for 1 min at 13,000 rpm and the residual liquid was discarded. The filter was washed by 500 µl PB Buffer through centrifugation for 1 min at 13,000 rpm, and flow-through was discarded. Any trace of nucleases was removed by adding 750 µl of PE buffer to the column, then centrifugation at 13000 rpm for 1 min was done. Subsequently, the column filter was treated with 40 µl EB buffer, incubated at room temperature for 1min, centrifugated for 2 min at 13000 rpm, and the eluate was kept. Then the concentration of DNA was determined using the NANODROP 1000 spectrophotomer. After measurement, plasmid DNA samples were stored at -20°C for further use.

2.7 Agarose gel procedures

2.7.1 TAE buffer Preparation

TAE buffer was prepared containing Tris base, acetic acid and EDTA, and was used in agarose gel preparation and electrophoresis. Regularly, 50X TAE buffer was prepared, comprising 242 g Tris base (Fisher, UK), and 37.2 g $Na_2EDTA.H_2O$ (Sigma Aldrich Ltd, UK), 57.1 ml of glacial acetic acid (Sigma Aldrich Ltd, UK), and distilled water to a volume of 800 ml. After mixing the components, pH was adjusted to 8.5 before topping up the volume to one litre. 1X working TAE buffer was prepared by diluting the 50X TAE buffer with distilled water.

2.7.2 Agarose gel preparation and gel electrophoresis

In this project, DNA, and RNA samples were analysed using 1 % w/v agarose gel (Oxoid, UK) which was prepared in 1X TAE buffer. The mixture was dissolved by boiling using a microwave and left at room temperature to cool down (40°C) before addition of 0.1 µg / ml of ethidium bromide (Sigma Aldrich Ltd, Germany). Then this gel was poured into a gel tray and left to solidify at room temperature (Heckman and Pease, 2007).

Usually, 2 % (v/v) 10X loading dye (NEB) was mixed with the tested DNA and RNA samples before loading into a solidified agarose gel along with 1 kb or 100 bp DNA ladder (New England Biolabs). The gel was placed in a gel electrophoresis tank containing 1X TAE buffer and an electric charge of 90–100 V was applied. DNA and RNA samples would migrate from negative to positive at a speed that was size dependent. Ethidium bromide stained gels were visualised using an UV transilluminator ChemiDoc Touch (Bio-Rad), which allows identification of the approximate molecular weight of tested sample in comparison with the known DNA bands sizes of the DNA ladder.

2.7.3 DNA purification

Gel electrophoresis was routinely performed to visualize DNA fragments embedded in agarose gels. When required, DNA fragments on agarose gel were excised by a clean scalpel under minimal ultraviolet light. A commercial kit (Promega), was used to clean DNA fragments out from the gel using the manufacturer's instructions. Briefly, an excised band of interest was placed into a 1.5 ml Eppendorf tube, and its weight recorded. For each 1 mg of gel slice, 1 µl of membrane binding solution (guanidine isothiocyanate 4.5 M) was added, and the mixture was vortexed, and incubated at 65°C until all the gel was dissolved. The Promega kit provided an SV mini-column assembly which was used to host the dissolved mixture. After incubation for 1 min at room temperature, and centrifugation using bench top micro-centrifuge at 14000 rpm for 1 min, the DNA binding liquid was removed. Recovered DNA was placed on the column, and then underwent two washing steps that aimed to remove any excess debris. Using top micro-centrifuge at 14000 rpm for 1 min , a membrane wash solution (10 mM potassium acetate pH 5.0, 80% ethanol and 16.7 µM EDTA pH 8.0) was added twice in two volumes 700 µl, and 500 µl, respectively. After each step, the flow through was discarded. At the end, the mini-column, was transferred to a new 1.5 ml tube, and the DNA was eluted after addition of 35 µl nuclease-free water to the filter, followed by centrifugation at 14000 rpm for 1 min. The collected DNA solution was stored at 4°C or for longer term storage –20°C.

2.8 PCR techniques

2.8.1 Polymerase chain reaction (PCR)

All PCR products in this work were generated using a thermo cycler (Biometra, Germany), and were amplified using HotStarTaq Plus DNA polymerase (Qiagen, UK), and the PrimeSTAR HS DNA polymerase (Takara, Japan), which was used when high

fidelity amplification was required. The usage of all enzymes was according to manufacturer's instructions. Cycling conditions for each enzyme are shown in Table 2.2. The conditions were altered according to amplicon size, and primer melting temperature (Tm).

2.8.2 Colony PCR

A single well-isolated bacterial colony was resuspended in 100 µl of nuclease free water and heated at 95ºC for 10 min. This suspension was then pelleted at 12 000 x g for 2 min and 2 µl of the supernatant was used as template in PCR. When a broth of a bacterial culture was used for colony PCR reaction, a 500 µl culture was centrifuged at 10000 *g*, re-suspended in 300 µl of nuclease free water, and 2 µl of the lysate was used as template. different sets of primers were used for routine PCR procedure as listed in Table 2.2.

Table 2.2: PCR Conditions used in this study.

HotStarTaq polymerase cycling conditions in a routine PCR reaction	
3 PCR stages	**Settings**
1st (1-cycle)	Initial denaturation at 95°C for 5 minutes (m)
2nd (30 cycles)	Denaturation at 94°C for 45 seconds (s)
	Annealing at (Lowest Tm) usually 55 °C for 45 s
	Extension at 72°C (1 min per kb)
3rd (1-cycle)	Final extension at 72°C for 10 min
	Final hold at 4°C
PrimeStar polymerase Cycling Conditions in a Splicing overlap extension-PCR	
1 PCR stage	**Settings**
(30 cycles)	Denaturation at 95°C for 10 s
	Annealing at 55°C for 5 s
	Extension at 72°C for 3 min

2.9 Oligonucleotides (primers) design and synthesis

Asparaginase/glutaminase gene sequences for *K. pneumoniae* MGH 78578 were acquired from National Centre for Biotechnology Information (NCBI) website, and were used for primer design. All primers were designed using the APE plasmid editor software and NCBI primer designer, then synthesized by the Eurofins Genomic company (Germany).

Primers design is an essential step for any successful PCR, and the first primer design strategy was used to investigate sequence homology between *K. pneumoniae* MGH 78578 and *K. pneumoniae* KR 3167. These primers would yield approximately 3 kb products, that resulted from the sum of ~ 1kb upstream flank, ~ 1kb of the asparaginase / glutaminase genes, and ~ 1kb of the downstream flank. Also, these sequences were used as screening primers (S1, and S2), in which S1 was forward primer (FP), and S2 was reverse primer (RP), for instance, the primer set that was used in the *yneH* mutation confirmation by sequencing, were called screening-yneH / FP (S1), and screening-yneH / RP (S2) (Figure 2.2 A, Table 2.4).

Other primers were used in the mutagenesis process, as the targeted genomic region of asparaginase/glutaminase genes were divided in three regions: left flank region (LF) ~ 0.5 kb, targeted genes (*yneH*, *ansA*, *ybiK*, and *KPN_01165*); which in the mutant constructs were replaced by *aph(3')-II*$_{FRT}$ (kanamycin resistance cassette) ~ 1.5 kb, and ~ 0.5 kb of right flank region (RF). For each mutation target, designated primers ranged from P1 (primer 1) to P6 (primer 6), in which P1 (FP), and P2 (RP) would target LF; P3 (FP), and P4 (RP) would amplify *aph (3')-II*$_{FRT}$; and P5 (FP) and P6 (RP) were designed to generate the right flank. Furthermore, the P2 and P5 primers would have homologous region with *aph (3')-II*$_{FRT}$, that served as an important role during mutant allele construction (Figure 2.2 B, Table 2.3).

The last primer design strategy aimed to amplify asparaginase/glutaminase genes plus ~ 50 bp of left flank. For each gene, two primers were created, forward and reverse, and after a PCR reaction, these primers would generate ~ 1 kb amplicons that corresponded to the target genes (*yneH*, *ansA*, *ybiK*, and *KPN_01165*). These primers were also used to confirm the mutation by sequencing and creation of *cis*-complementations. These primers were designated as Complementation and Screening primers, CS1 for forward primer, and CS2 for reverse primer. The primer set that used to amplify *yneH*, were called CS-yneH / FP (CS1), and CS-yneH / RP (CS2) (Figure 2.2 C, Table 2.3).

2.10 Mutant allele construction: Splicing overlap extension-PCR

Mutant alleles for each target gene consisted of a left homologous flank (LF), antibiotic resistance cassette (*aph(3')-II*$_{FRT}$), and a right homologous flank (RF). The homologous sequences were in a size of approximately 0.5 kb. Splicing overlap extension-PCR (SOE-PCR) was used to construct the mutant alleles (Horton *et al.*, 1989). To create the

mutagenesis products, two PCR reactions were carried out. Figure 2.3 illustrates the strategy of mutant allele creation. In the first PCR steps (Table 2.2), primer pairs P1/P2, P3/P4, and P5/P6 were used to separately amplify PCR fragments for LF, antibiotic cassette (*aph(3')-II*$_{FRT}$) and RF, respectively (Table 2.3). The *aph (3')-II*$_{FRT}$ cassette was amplified using P3/P4 primers from the *K. pneumoniae* KR2021strain. After gel electrophoresis, DNA fragments were gel purified as described in section 2.7.3, and the DNA concentration of isolated products adjusted to 20 ng/µl. The P2 and P5 primers were designed to contain at their ends a complementary sequence of ~ 20 bp to the kanamycin resistance gene primers P3 and P4, respectively. This homology is needed for the second PCR reaction (SOE-PCR) (Table 2.2), in which it creates a fusion between the DNA fragments by providing homology as demonstrated in step B (Figure 2.3). A 50 µl SOE-PCR reaction mixture included 4 µl 20 ng/µl of both LF, and RF amplicons mixed with 4 µl of the 20 ng/µl antibiotic cassette fragment, 2XPrimStar polymerase (PrimSTAR Hs premix TaKara, Japan), and 10 pmol P1/P6 primers. PCR cycling conditions were given in Table 2.2. The SOE-PCR amplicons were purified as described in section 2.7.3.

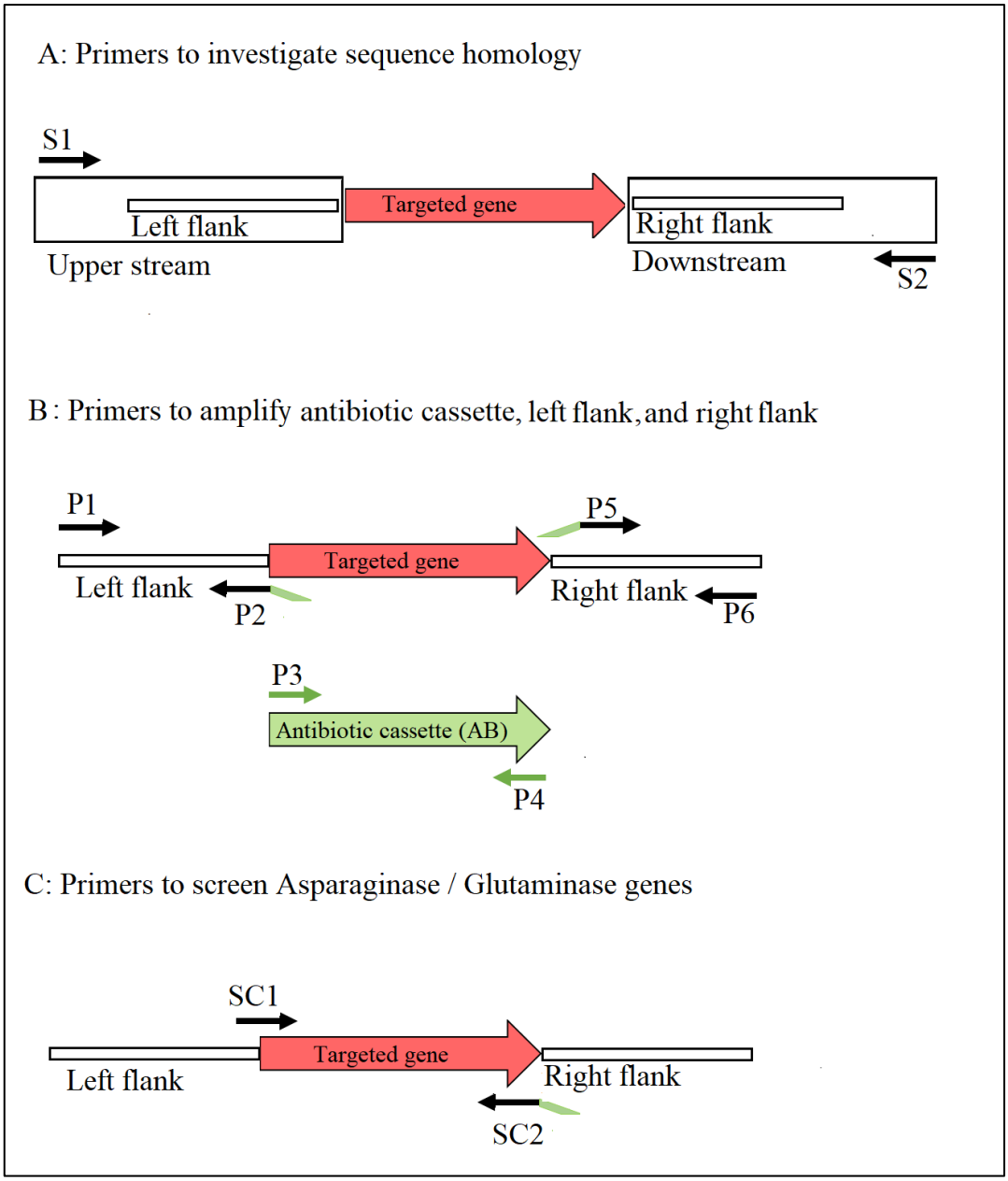

Figure 2.2: Schematic representation of amplification and confirmation strategies using different sets of primers. *A. The aim was to generate a ~ 3 kb genomic location to test if the gene of interest was present in* K. pneumoniae *KR 3167. B. The primers were used to separately amplify LF, antibiotic resistance cassette, and RF, and for construction of mutagenised construct. C. The primers were used in cis-complementation, and for mutation confirmation presence or absence of asparaginase/ glutaminase genes.*

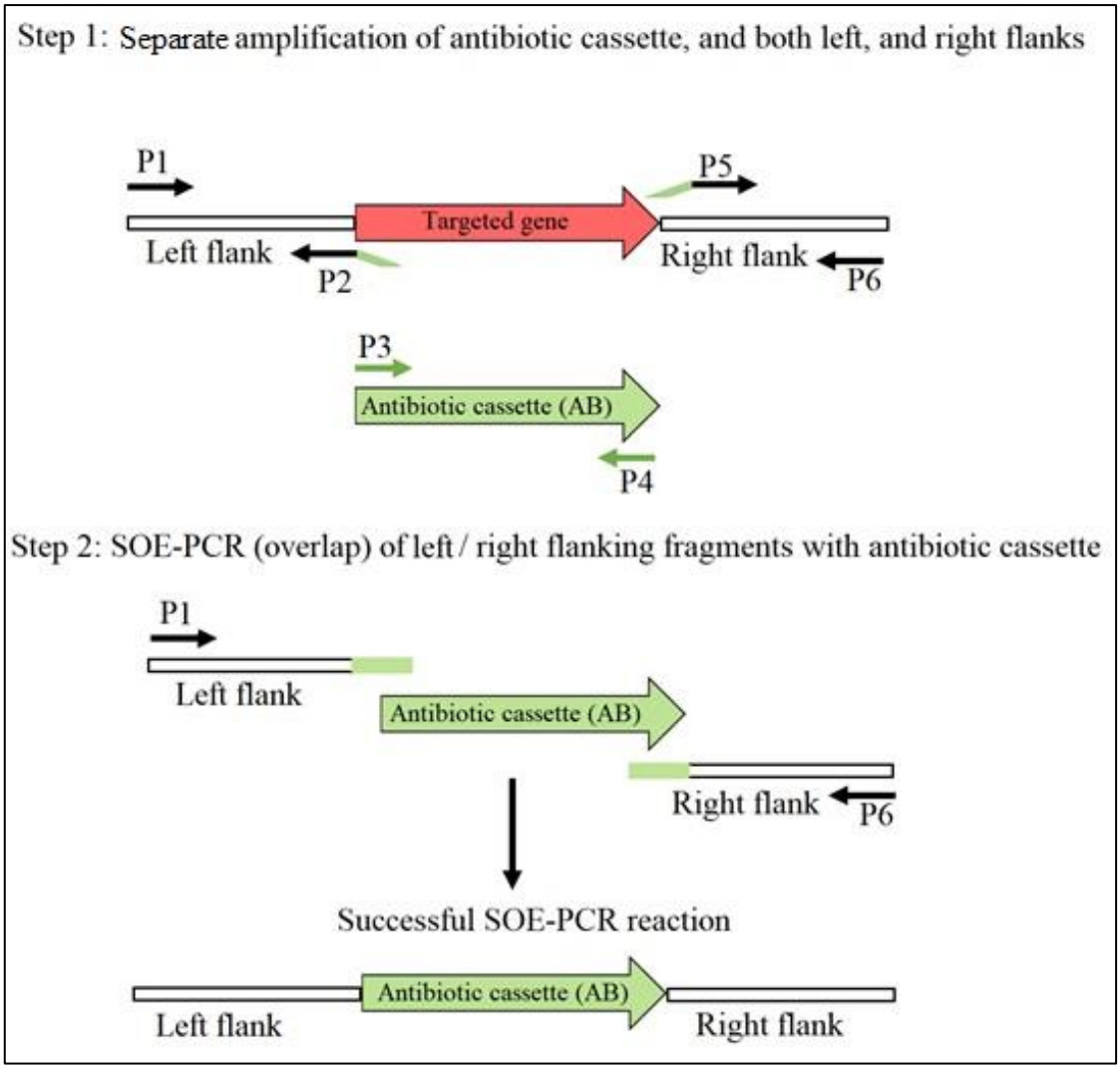

Figure 2.3: Schematic representation of SOE-PCR. *SOE-PCR consists of two main steps. In step 1 the left flank (LF) and right flank (RF) fragments, corresponding to the region targeted for allelic exchange, and the antibiotic resistance cassette (AB) were amplified and separately gel purified. The green tails of the P2 and P5 primers represent the sequence of homology to P3 and P4 primers, respectively. In step 2 the desired mutant allele was produced after SOE-PCR reaction in which LF and RF fragments are joined with the AB cassette using P1 and P6 primers.*

Table 2.3: *Primers used to construct mutants, and genetically complemented strains.*

Primers for *yneH* mutant allele, and deletion screening		
Primer name	Sequence (5′----3′)	Product size
(P1) *yneH* LF / FP	GCCGGGATGACCGGCTTT	

(P2) *yneH* LF / RP+Kan1	**GAAGCAGCTCCAGCCTACA** **C**ACGCGGCTCCTTGCCCAC	459 bp	
(P3) Kan1 / FP	GTGTAGGCTGGAGCTGCTTC	1496 bp	
(P4) Kan2 / RP	ATGGGAATTAGCCATGGTCC		
(P5) *yneH* RF / FP+Kan2	**GGACCATGGCTAATTCCCA** **T**TGGTCGATCAGGATCGCT	524 bp	
(P6) *yneH* RF / RP	GCCGGAGTATGCCTGATAAA		
(CS1) CS-*yneH* / FP	ATGGTGGGCAAGGAGCCGCG	948 bp By CS1/CS2	1407 bp By P1/CS2
(CS2) CS-*yneH* / RP	**GAAGCAGCTCCAGCCTACA** **C**GGGGAGGTCGGTGTTCTGA		
Primer for *ansA* mutant allele, and deletion screening.			
(P1) *ansA* LF / FP	CGGTGACCGTTGTCAAAGAA	493 bp	
(P2) *ansA* LF / RP+ Kan1	**GAAGCAGCTCCAGCCTACAC** GCATCGCTTAGGTTGG		
(P3) Kan1 / FP	GTGTAGGCTGGAGCTGCTTC	1496 bp	
(P4) Kan2 / RP	ATGGGAATTAGCCATGGTCC		
(P5) *ansA* RF / FP+ Kan2	**GGACCATGGCTAATTCCCAT** AGCATCGCTTAGGTTGGT	520 bp	
(P6) *ansA* RF / RP	CGCCGGAGAAAATCGATCAG		
(CS1) CS-*ansA* / FP	TTAAGCCTCGTCGGGGG	1020 bp By CS1/CS 2	1513 bp By P1/CS2
(CS2) CS-*ansA* / RP	**GAAGCAGCTCCAGCCTACAC** TGTAGGCAACGTAAATCGA		
Primer for *ybiK* mutant allele, and deletion screening.			

(P1) *ybiK* LF / FP	TTATCAAAGCCGGGCACATC	512 bp	
(P2) *ybiK* LF/ RP+ Kan1	**GAAGCAGCTCCAGCCTACAC**TCGTTAAGGACTGGCGAA		
(P3) Kan1 / FP	GTGTAGGCTGGAGCTGCTTC	1496 bp	
(P4) Kan2 / RP	ATGGGAATTAGCCATGGTCC		
(P5) *ybiK* RF / FP+ Kan2	**GGACCATGGCTAATTCCCAT**AACAAGGGAGAGGGCGAG	527 bp	
(P6) *ybiK* RF / RP	GATAGCCGATGAGCCAACCAC		
(CS1) CS-*ybiK* / FP	ATGGGCAAGGCGGTTATA	942 bp By CS1/CS2	1454 bp By P1/CS2
(CS2) CS- *ybiK* / RP	**GAAGCAGCTCCAGCCTACA**TTGGCATTTATCGCGAATAG		
Primers for *KPN_01165* mutant allele, and deletion screening.			
(P1) *KPN_01165* LF / FP	TGACGGTGAAAAGCAACAA	504 bp	
(P2) *KPN_01165* LF / RP+ Kan1	**GAAGCAGCTCCAGCCTACAC** GGTCGTTAAGCACCACCATT		
(P3) Kan1 / FP	GTGTAGGCTGGAGCTGCTTC		

(P4) Kan2 / RP	ATGGGAATTAGCCATGGTCC	1496 bp	
(P5) *KPN_01165* RF / FP+ Kan2	**GGACCATGGCTAATTCCCAT**CGGAGAACAGCATCACTTCA	532 bp	
(P6) *KPN_01165* RF / RP	CCACCACGACACCAAGATA		
(CS1) CS-*KPN_01165* / FP	ATGAGCAGCCTGGCGTTTAG	1005 bp By CS1/CS2	1509 bp By P1/CS2
(CS2) CS-*KPN_01165* / RP	**GAAGCAGCTCCAGCCTACA**ATATTTCCATACCTACTGA		

Bold letters *are complementary sequences to the P3 and P4 primers incorporated into P2, P5, and CS2 primers, to aid in the SOE-PCR fusion reaction between the fragments that contain them. APE software and NCBI primer designer software were used to design primers, which were then synthesized by the Eurofins genomic company (Germany).*

2.11 Justification for *K. pneumoniae* KR 3167 usage in this study

The *K. pneumoniae* KR 3167 strain was chosen for mutant construction for three reasons. Sensitivity of this strain to antibiotic resistance conferred by the plasmid used for mutagenesis was the first reason for selection (section 2.2). In addition, this strain had the same asparaginase/glutaminase genetic loci as the *K. pneumoniae* MGH 78578 reference strain, which allowed for an informed mutagenesis strategy. This was confirmed by PCR analyses using primers listed in (Table 2.4). In addition, this strain was less muco-viscous than the reference strain, which eased molecular manipulations.

Table 2.4: *List of primers used to interrogate asparaginase/glutaminase loci in* K. pneumoniae *KR 3167.*

Primers name	Sequence (5′----3′)	Product size
(S1) screening-*yneH* / FP	GCGATGAGCAAAACTACGTC	2889 bp
(S2) screening-*yneH* / RP	CAGAAGAAAGAGAGCTCCTG	
(S1) screening-*ansA* /FP	CTCCATAAACGCCTGGCT	2979 bp
(S2) screening-*ansA* /RP	GGCTCCATTGGCATCTTT	
(S1) screening- *ybiK* /FP	GTCTCTTCCTGCATCACCAC	3021 bp
(S2) screening- *ybiK* / RP	GATAGCCGATGAGCCAACCA	
(S1) screening-*KPN_01165* /FP	TTCCACTACTGTTCGCTGGA	2961 bp
(S2) screening- *KPN_01165* / RP	TGGTCATCATCAGGGCATTA	

2.12 Mutagenesis steps

2.12.1 Competent cell preparation

From both *K. pneumoniae* and *E. coli* strains, competent cells were prepared for plasmids propagation as described previously (Philippe *et al.*, 2004). First, 5 ml of LB was inoculated with a single colony from either *K. pneumoniae* or *E. coli*, which then were grown overnight with shaking at 180 rpm at 37ºC. Next day, this culture was used to inoculate fresh LB media at a ratio of 1:100 (50 µl to 5 ml), then the culture was grown to an OD_{600} of around 1.0. The cells were harvested using a refrigerated centrifuge for 10 min at 3000 x g, at 4ºC, then on the same centrifuge setting, the pellets were gently washed three times with 2 ml ice cold 10 % (v/v) glycerol. After the final wash, the cells were resuspended in 1 ml ice cold 10 % (v/v) glycerol, and 50 µl aliquots were stored at -80°C until needed.

2.12.2 Transformation of electro-competent bacteria

This technique was used to introduce exogenous SOE-PCR products and plasmids, to competent bacterial cells that had been prepared in section 2.12.1, to either accomplish a gene mutagenesis process, or for plasmid propagation. The transformation was achieved by electroporation, in which competent cells were exposed to a high voltage that may allow foreign DNA to be taken up by the recipient cells (Philippe *et al.*, 2004). To accomplish electroporation, special 0.2 cm cuvettes (Bio-Rad) were used. After cooling cuvettes on ice, 5-10 µl (20-60 ng/µl) of extracted plasmid or SOEing product was mixed with 50 µl of electrocompetent *E. coli* or *K. pneumoniae*. Then, the cuvette was placed in a Bio-Rad Gene Pulser system (Bio-Rad), which delivers an electric shock via the following settings: 2.5 kV (voltage), 25 µF (capacitance), and 200 Ω (ohm resistance), for 4.2 ms. After the electroshock was applied, the mixture was transferred into 1.5 ml centrifuge tubes along with 1000 µl SOC media that helps recover the bacteria from the electroporation stress, which was prepared as described in section 2.3, and was incubated with constant shaking 200 rpm, at 30°C or 37°C for 1 h. Transformed cells were then plated onto LA plates containing appropriate antibiotics and incubated at 37ºC or 30°C overnight (Sheng *et al.*, 1995).

2.12.3 Genetic confirmation of recombinant plasmid transformation

For genetic detection of thermosensitive pKOBEG-Apra, and pFLP2, well-isolated colonies were used for colony PCR as described in section 2.8.2, using the primers LRS 1, LRS 2, and FLP1, FLP2 as listed in Table 2.5, respectively. Beside these primers, P3/P4 primers (Table 2.3) were also used to confirm the presence of kanamycin cassette. A LRS 1, LRS 2 screen was used to identify the presence of *araC*, codes for apramycin resistance, and FLP1, FLP2 for *sacB*. Both genes were found in pKOBEG-Apra, and pFLP2 backbone, respectively.

Table 2.5: *Primers for genetic confirmation of plasmid transformation.*

Primers name	Sequence (5′----3′)	Product size
(LRS 1) Lambda Red Sequence *araC* /FP	CTAATCAGCCCGGCATTTCG	1542 bp
(LRS 2) Lambda Red Sequence *araC* /RP	AACGGGCATTTCAGTTCAAG	
(FLP1) pFLP2 SacB/FP	AAAGTGACGGTGAAAGGTCC	2144 bp
(FLP2) pFLP2 SacB/RP	TGGCTTGGCGAAACCATC	

2.12.4 Induction of Lambda red, and curing both pKOBEG-Apra, and *aph (3')-II*$_{FRT}$

After successful transfer of pKOBEG-Apra to *K. pneumoniae* KR3167 by electroporation as described in section 2.12.2, the presence of the plasmid was confirmed by colony PCR using LRS1, and LRS2 primers listed in Table 2.5 (section 2.12.3). After confirmation, an induction procedure was needed to activate Lambda Red recombinase in order to accomplish the intended mutagenesis. The induction procedure was started by using a single colony, which was cultured overnight at 30ºC in LB supplemented with apramycin. The same culture was then re-inoculated at a dilution ratio of 1:100 into fresh LB containing 50 µg / ml apramycin and when the OD_{600} reached 0.2., a 0.2 % (w/v) L-arabinose solution (Sigma, UK) was added. Then this culture was allowed to grow at 30ºC until it reached an OD_{600} of 1.0. The harvested cells were used for electrocompetent cells preparation (section 2.12.1), to introduce SOE-PCR products (mutant alleles) (section 2.10). The electrocompetent cells were grown in SOC broth for 1 h at 37°C to recover transformants and to cure the thermosensitive pKOBEG-Apra immediately. This mixture was distributed on LA supplemented with 50 µg / ml kanamycin and incubated at 37°C. Next day, the kanamycin resistant colonies were screened by PCR to confirm both pKOBEG-Apra plasmid absence, and mutant allele presence, using primers listed in Table 2.5, and Table 2.3, respectively.

After successfully mutating the putative asparaginase/glutaminase genes by homologous recombination, the *aph* cassette, was removed by the activity of flippase (FLP) recombinase found in the backbone of the pFLP2 plasmid which targets the FRT sites of the antibiotic cassette (Hoang *et al.*, 1998). From each mutant strain, *ΔyneH*, *ΔansA*, *ΔybiK* and *ΔKPN_01165*, a batch of electrocompetent cells was prepared (section 2.12.1). Then the pFLP2 plasmid was electroporated (section 2.12.2). After the electroporation process, the cells were selected on LA supplemented with 1200 µg ml/l ampicillin and incubated over night at 37°C. Next day, selected single colonies (ampicillin resistant) were re-grown by patching overnight at 37°C on two separate LA plates: one supplemented with ampicillin, and the other with 50 µg/ ml kanamycin. Only colonies that were resistant to ampicillin and sensitive to kanamycin were selected. Subsequently, they were screened by PCR for positive *sacB* and negative *aph (3')-IIFRT* using FLP1/FLP2 and P3/P4 primers, respectively (Table 2.5 and Table 2.3).

Later, the positive pFLP2 bacteria were grown overnight at 37°C on LA supplemented with 5 % (w/v) sucrose to cure this plasmid (Hoang *et al*, 1998). The resulted single colonies were assessed again through re-growing them in broth that had ampicillin and kanamycin. No growth on both ampicillin and kanamycin, and negative PCR results for both *sacB* and *aph* indicated that the unmarked mutant was successfully produced. The same procedures were applied on unmarked *ΔansA*, *ΔybiK* and *ΔKPN_01165* mutant production.

2.13 Complementation of mutant strains

The putative asparaginase and glutaminase genes were reintroduced back to the unmarked *ΔyneH*, *ΔansA*, *ΔybiK* and *ΔKPN_01165*, to verify that phenotypes of mutants were due to lack of these genes and not due to the polar effects of mutation. Lambda red system was reused to generate genetically complemented strains, and splicing overlap extension reaction was used to construct *cis*-complementation strains of *yneH*, *ansA*, *ybiK* and *KPN_01165*. A *cis*-complementation SOEing product contained an approximately 1 kb asparaginase / glutaminase gene with its approximately 50 bp left flank, 1.5 kb *aph (3')-II*$_{FRT}$, and 500 bp right flank (Figure 2.4). Initially, CS1/CS2, P3/P4, P5/P6, primers were used to separately amplify the putative asparaginase / glutaminase genes plus ~ 50 bp left flank, *aph (3')-II*$_{FRT}$, and right flanks, respectively (Table 2.3). Then, these fragments were gel purified as described in section 2.7.3. Afterwards, SOE-PCR reactions using

CS1/P6 primers were carried out, as described in section 2.10. Successfully constructed SOE-PCR amplicons were separated by agarose gel electrophoresis and were excised and purified from agarose gel using gel purification kit as described in section 2.7.3. The purified products were then electroporated into *ΔyneH, ΔansA, ΔybiK* and *ΔKPN_01165*, as described in section 2.12.

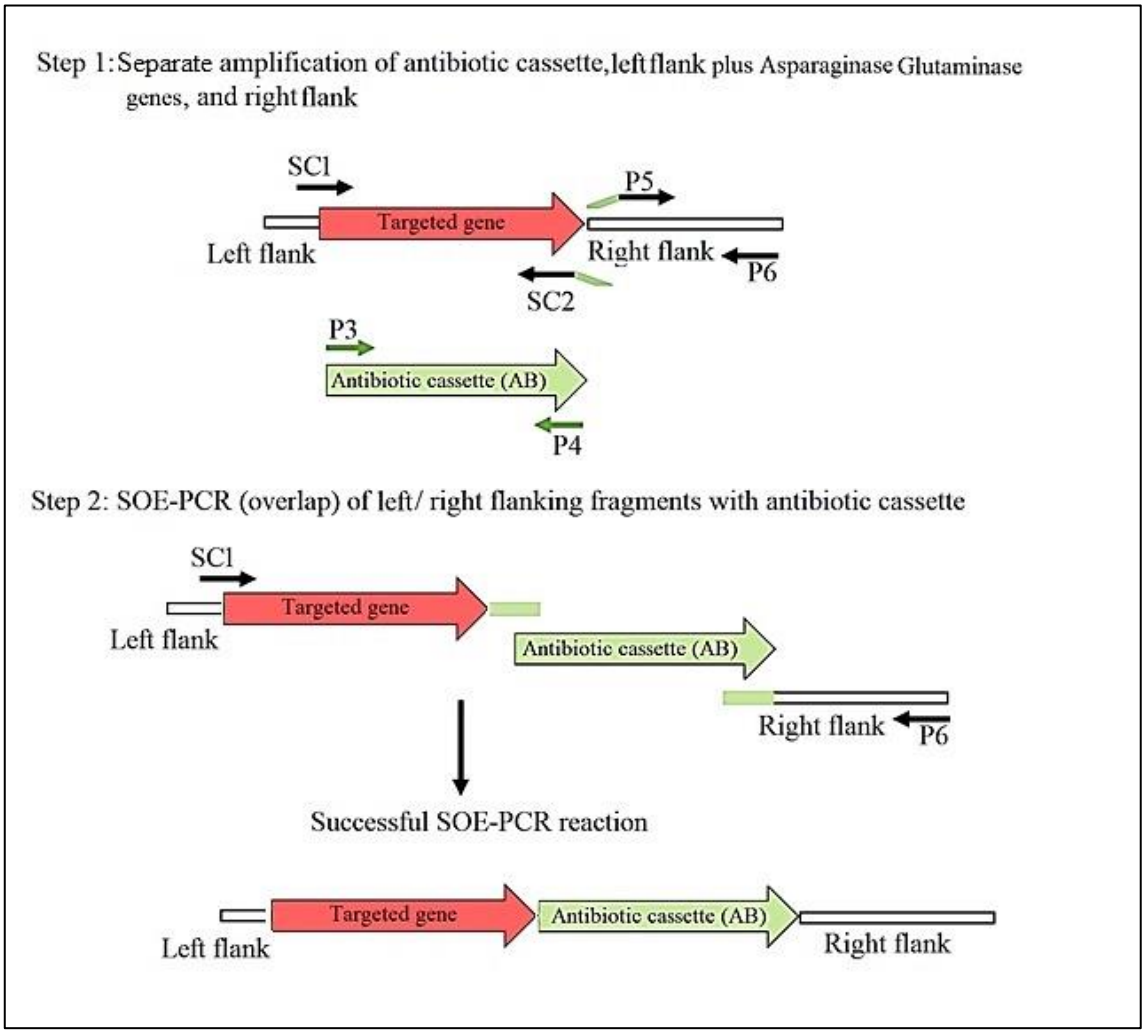

Figure 2.4: Schematic representation of cis-complementation. *SOE-PCR consists of two main steps. In step 1: Left flank plus asparaginase / glutaminase genes, right flank, and antibiotic cassette were PCR amplified and gel purified separately. The green line in CS2 and P5 primers represent the sequence of homology to the P3 and P4 primers, respectively. In step 2 the amplicons from the first step fused together using SC1 and P6.*

2.14 DNA sequencing

Each *cis*-complementation, marked and unmarked mutation was verified by DNA sequencing. Initially, DNA sample was extracted from the strain that was intended for

sequencing as described section in 2.6.1. Then S1 and S2 primers were used to amplify asparaginase/ glutaminase gene regions (Table 2.4). Gel electrophoresis, and the subsequent excision and purification of the DNA fragments was carried out for the amplicons as described in section 2.7.3. Afterward, the NANODROP1000 spectrophotometer was used to adjust DNA concentrations to 20 ng /µl. The DNA products were sent for sequencing along with the CS1 and CS2 primers pair (Table 2.3). To analyse the sequence data, BLAST software was used, available at www.ncbi.nlm.nih.gov (Appendix 1). The gene sequencing was done at Protein & Nucleic Acid Chemistry Laboratory (PNACL)/ University of Leicester).

Section C: Results: Strain selection and molecular work

2.15 *Klebsiella pneumoniae* strain selection for the study

In this project the selection of *K. pneumoniae* KR3167 was determined by its antibiotic resistance status and viscosity. These two criteria were important for successful mutagenesis process. Antibiotic sensitivity test showed that KR3167 strain is sensitive to kanamycin and apramycin which enabled the use of plasmid vectors utilised in this study. In addition, this strain was less muco-viscous compared to *K. pneumoniae* MGH78578 reference strain, which allowed for more efficient DNA transformation.

All primers were designed based on *K. pneumoniae* MGH78578 reference strain genome sequence. To ensure that there was no difference in the targeted genomic regions between the selected strain and reference strain *K. pneumniae* MGH78578, the loci of targeted regions containing asparaginase and glutaminase genes were analysed by PCR as described in section 2.11. The primers used for this genetic analysis, and product sizes are listed in Table 2.4. For each target an approximately 3 kb DNA fragment representing upsteam flanking region, downsteam flanking region, and the coding regions were amplified. The 3 kb implicons represente the predicited sizes from the MGH78578 sequences on the NCBI website. The analysis of PCR products revealed no differences between the two strains (MGH78578 and KR3167) (Figure 2.5 L2 -L9).The *yneH* amplicon size was 2889 bp in both KR3167, and MGH78578 (Figure 2.5 L2, and L3, respectively), and *ansA* PCR products in L4, and L5 were approximately 2979 bp, in both strains (Figure 2.5). The analysis of *ybiK* locus in *K. pneumoniae* KR3167 indicated that it was 3020 bp, which was like that of *K. pneumoniae* MGH78578 (Figure 2.5 L6, and L7, respectively). Similarly, there was no difference in *KPN_01165* product sizes (2961bp), that resulted from KR3167, and MGH78578 strains (Figure 2.5, L8, and L9, respectively).

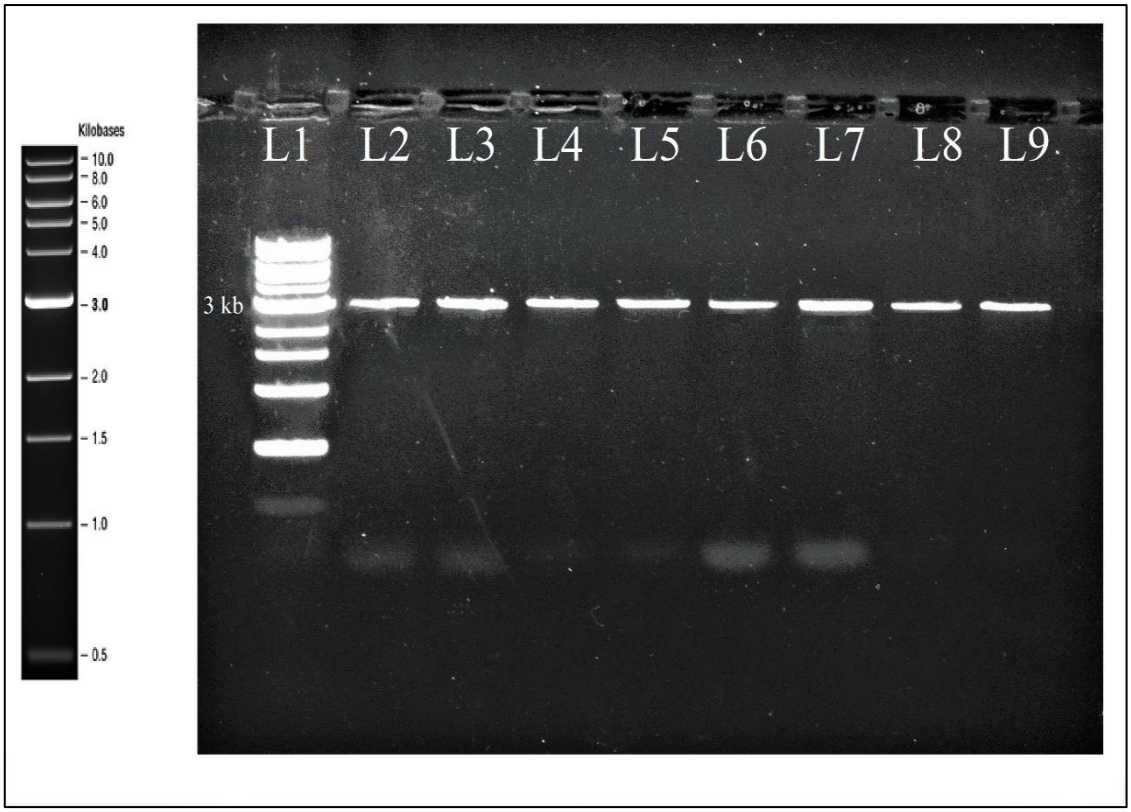

Figure 2.5: *Ethidium bromide-stained 1% (w/v) agarose gel showing the amplicons for loci containing putative asparaginase and glutaminases in KR3167, and MGH78578 K.* pneumoniae *strains. L1: 500 ng 1 kb DNA ladder (NEB); Lane 2, 4, 6, and 8 represent amplicons for* yneH, ansA, ybiK, *and* KPN_01165, *respectively, from* K. pneumoniae *KR3167. L3, 5, 7, and 9 contain reference strain* K. pneumoniae *MGH78578 amplicons that represent* yneH, ansA, ybiK, *and* KPN_01165, *respectively. Primers used for the amplifications are listed in Table 2.4.*

2.16 Mutagenesis results

2.16.1 Construction of lambda Red-compatible strain

In this study, the pKOBEG-Apra plasmid was transformed by electroporation (see section 2.12) to comptent cells of wild type *K. pneumoniae* KR3167, which was prepared as described in section 2.12.1. After electroporation, the transformants were selected on LB agar supplemented with 50 µg/ml apramycin. Then the well isolated colonies were screened for the presence of *araC*, apramycin resistance gene, by colony PCR (section 2.8.2 and section 2.12.3), using LRS1/LRS2 primers listed in Table 2.5. The results showed a successful transformation of apramycin resistant *araC* in tested colonies positive for the pKOBEG-Apra plasmid, which is approximately 1.5 kb (Figure 2.6).

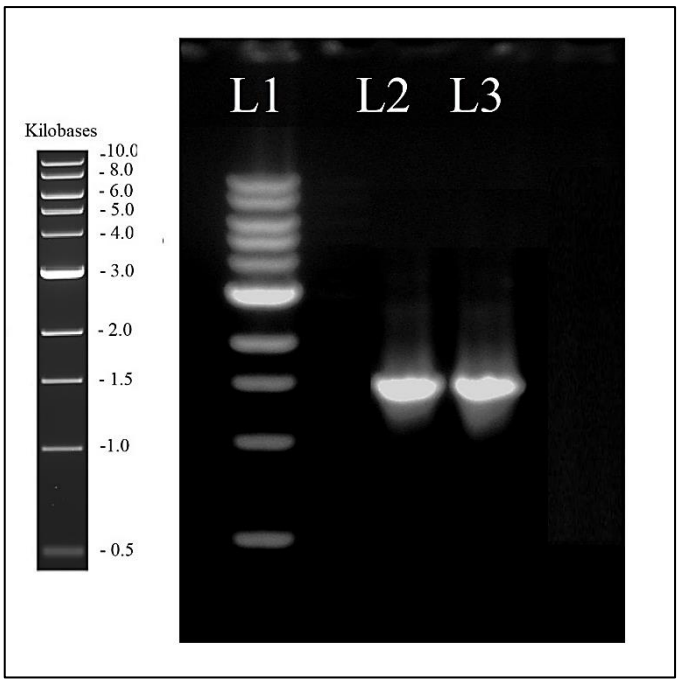

Figure 2.6: *A gel electrophoresis represent a successful transformation of pKOBEG-Apra to a wild type* K. pneumoniae *KR3167. L1 500 ng 1 kb DNA ladder (NEB); L2, and L3 confirm Lambda Red plasmid transformation after using primers (LRS 1/2) that amplify 1500 bp. Full primer sequences are listed in Table 2.5.*

2.16.2 Construction of mutant alleles with *aph (3')-II*$_{FRT}$ cassette

Splicing overlap extension PCR (SOE PCR) was used to create the construct for mutation as described in section 2.10. The antibiotic cassette in the construct holds two identical FLP flippase recognition targets (FRT). Flippase found in pFLP2 plasmid aid in removing this cassette leaving marker less mutant strains (Hoang *et al*, 1998). The first reaction was used to individually amplify LF, antibiotic cassette AB, and RF fragments. Initially, primer pairs P1/P2, P3/P4, and P5/P6 were used to separately amplify the LF, antibiotic cassette, and RF fragments, respectively (Section 2.10 and Figure 2.3). For the LF, primers were designed to yield PCR fragments with an approximate size of 459 bp, 495 bp, 512 bp, and 504 bp for *yneH*, *ansA*, *ybiK*, and *KPN_01165*, respectively (Figure, 2.7. L2, in A, B, C and D respectively). The right flank portions of *yneH*, *ansA*, *ybiK*, and *KPN_01165* fragments were 524 bp, 520 bp, 527 bp, and 532 bp respectively (Figure, 2.7. L3, in A, B, C and D respectively). The kanamycin resistance cassette size was ~ 1.5 kb, and it was PCR amplified from *K. pneumoniae* KR2021 using primers P3, and P4 (Figure, 2.7 and L4 in A, B, C and D respectively). All fragments were gel purified, as described in section 2.7.3. The size of flanks used in overlap extension reactions were

approximately 0.5 kb. A homology of 0.5 kb was shown, in previous studies, to be an appropriate length for efficient homologous recombination (Wei *et al.*, 2012). As previously described in section 2.10, in each mutant allele construction, primers P1 (LF, FP), and P6 (RF, RP) were used in the SOE-PCR reaction to join the gel purified fragments. The ultimate product will have all fragments (LF+AB+RF) joined together to a final product size of approximately 2.5 kb (Figure, 2.7. L5 in A, B, C and D). Lane 5 in Figure 2.7 A, B, C and D represent the expected size of the SOEing products from prospective mutant constructs. In Figure 2.7 A and B, 2479 bp, and 2509 bp products in L5 represent *yneH*, and *ansA* mutant alleles, respectively, and in Figure 2.7 C and D L5 shows the successful amplification of the overlap extension products for *ybiK* (2535 bp), and *KPN_01165* (2532 bp), respectively.

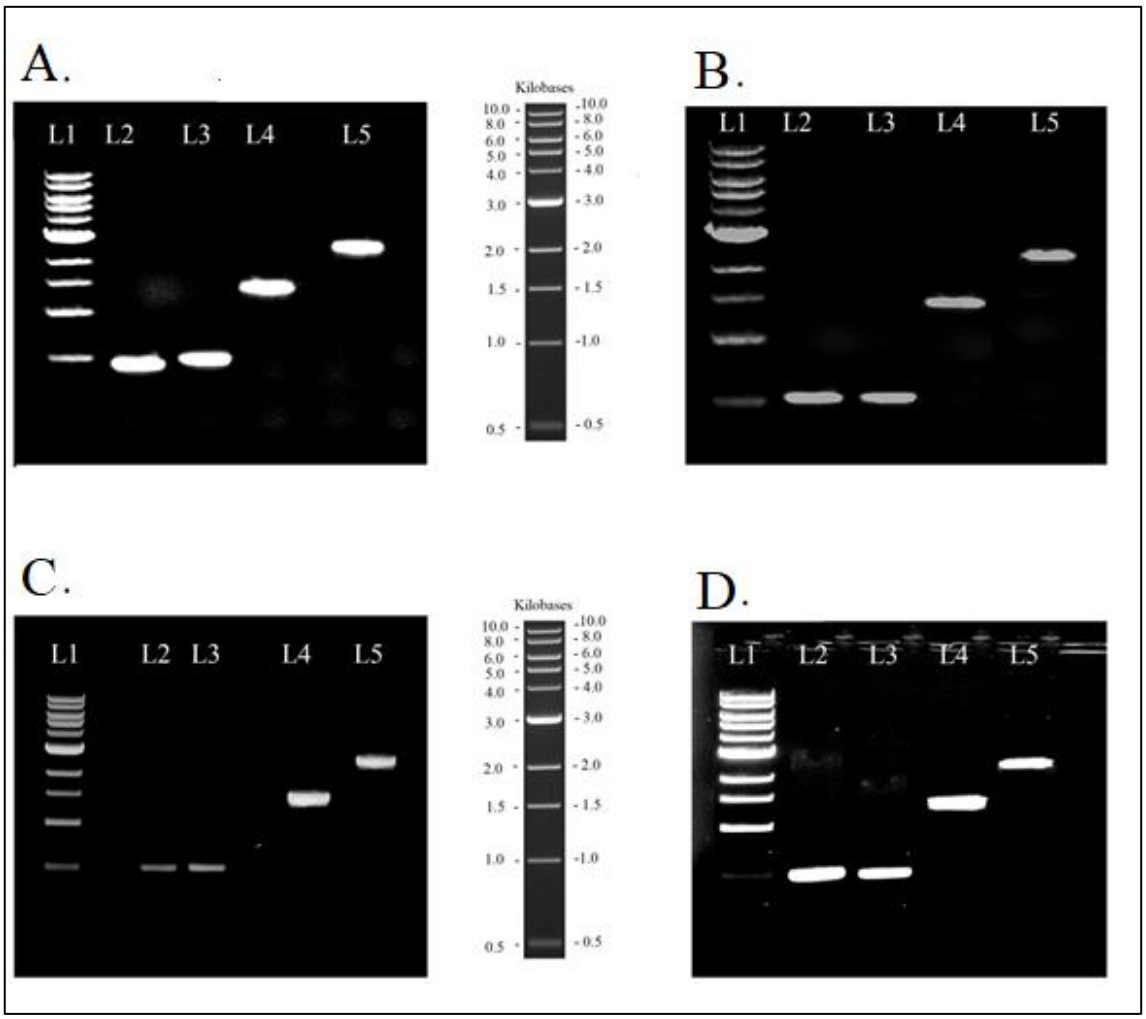

Figure 2.7: *Agarose gels electrophoresis of amplicons representing mutant allele construction for* yneH ***(A)****,* ansA ***(B)****,* ybiK ***(C)****, and* KPN_01165 ***(D)****. In* ***A****,* ***B****,* ***C*** *and* ***D****, L2 and L3 represent the amplicons for left and right flanks for* yneH, ansA, ybiK, *and*

KPN_01165, *L4 is for aph, and L5 is the SOEing product after the fragments fused for* yneH, ansA, ybiK, *and* KPN_01165, *respectively. L1 -500 ng of 1 kb DNA ladder. The primers used for PCR reactions are listed in Table 2.3.*

2.16.3 Transformation of SOE-PCR products into lambda Red-compatible strains

Electrocompetent wild type *K. pneumoniae* KR3167/pKOBEG-Apra cells were prepared from fresh culture in LB supplemented with 50 µg / ml of apramycin and 0.2 % arabinose to induce the pBAD promoter (embedded in the plasmid) that controls the Red recombination system (Lesic and Rahme, 2008) (section 2.12.1). The culture was grown to an OD_{600} of 1.0, and the mutant alleles (SOEing PCR product Figure 2.7, L5) were electroporated at a setting of 2.5 kV. After non-selective growth at 37ºC for 1 h, the transformation mixture was plated onto LA containing 50 µg / ml kanamycin and incubated overnight at 37ºC. The pKOBEG-Apra plasmid has a thermosensitive origin of replication that can replicate at 30ºC but not 37ºC (37ºC was used to cure this plasmid). The pKOBEG-Apra plasmid would mediate the gene deletion process, through inhibition of the restriction modification system of the microbe, after induction by arabinose. This method was efficient, as 1 to 30 transformants were regularly obtained. Mutant alleles were determined to be correct phenotypically if they were able to grow in 50 µg / ml kanamycinas and contained the antibiotic cassettes. This confirmation process was carried out after every successful transformation. An example is shown in Figure 2.8 (lane 2-9), which represents the amplification products of primer set P1/P6 (of each designated gene), and P3/P4; both primer sets were used to confirm the successful insertion of the mutant allele (SOEing product), and *aph (3')-II*$_{FRT}$ presence. In the putative mutants, P1/P6 primer set of *yneH*, *ansA*, *ybiK*, and *KPN_01165*, would generate an amplicon with expected size of ~ 2.5 kb (Figure 2.8, lanes 2, 4,6, and 8). Each amplicon resulted from the fusion of upstream (LF) (~ 0.5 kb), the integrated kanamycin cassette (~ 1.5 kb), and downstream (RF) (~ 0.5 kb) regions. The amplicons in Figure 2.8, lane 2 (2479 bp) represent the successful fusion between right (459 bp) and left (524 bp) flanking regions of *yneH* combined with *aph (3')-II*$_{FRT}$ (1496 bp), respectively. Lane 4 represented the PCR product (2509 bp) for the deletion of *ansA*, in which *aph (3')-II*$_{FRT}$ successfully replaced *ansA*. The mutant strain of *ybiK* was confirmed by a PCR reaction which produced a 2495 bp product as shown in lane 6 that represented the kanamycin resistance gene plus 512 bp upstream, and 527 bp downstream product. The construction of *ΔKPN_01165* was also confirmed by obtaining an amplicon size of 2484 bp in lane 8,

which is a summation of 504 bp left flank, 1496 bp antibiotic cassette, and 532 bp right flank. The amplicons representing kanamycin resistance gene (approximately 1.5 kb) were also obtained in each tested strain using P3/P4 primers as shown in Figure 2.8, lanes 3, 5, 7, and 9, which representing the expected size of antibiotic resistance gene. Furthermore, the P1/P6 primer set for each target was tested using wild type DNA as a control (Figure 2.8, Lane 10-13). The expected product size for all target loci was approximately 2 kb, which represents the combination of right flank (0.5 kb), asparaginase/ glutaminase genes approximately 1 kb, and left flank (0.5 kb). The PCR products shown in Figure 2.8, Lane 10-13 confirms this. In the figure L10 this includes 1931 bp amplicon (948 bp *yneH* sequence, plus 459 bp of upstream, and 524 bp of downstream). L11 in Figure 2.8 contains the *ansA* locus (2033 bp), which consists of 493 bp left flank, 520 bp right flank, and 1020 bp *ansA* coding region. L12 represents the amplicons for *ybiK* locus (942 bp), plus 512 bp (upstream region), and 527 bp (downstream region), totalling 1981 bp. Finally, L13 amplicons (2041 bp) belong to *KPN_01165* (1005 bp), and 504 bp of upstream and 532 bp of downstream region.

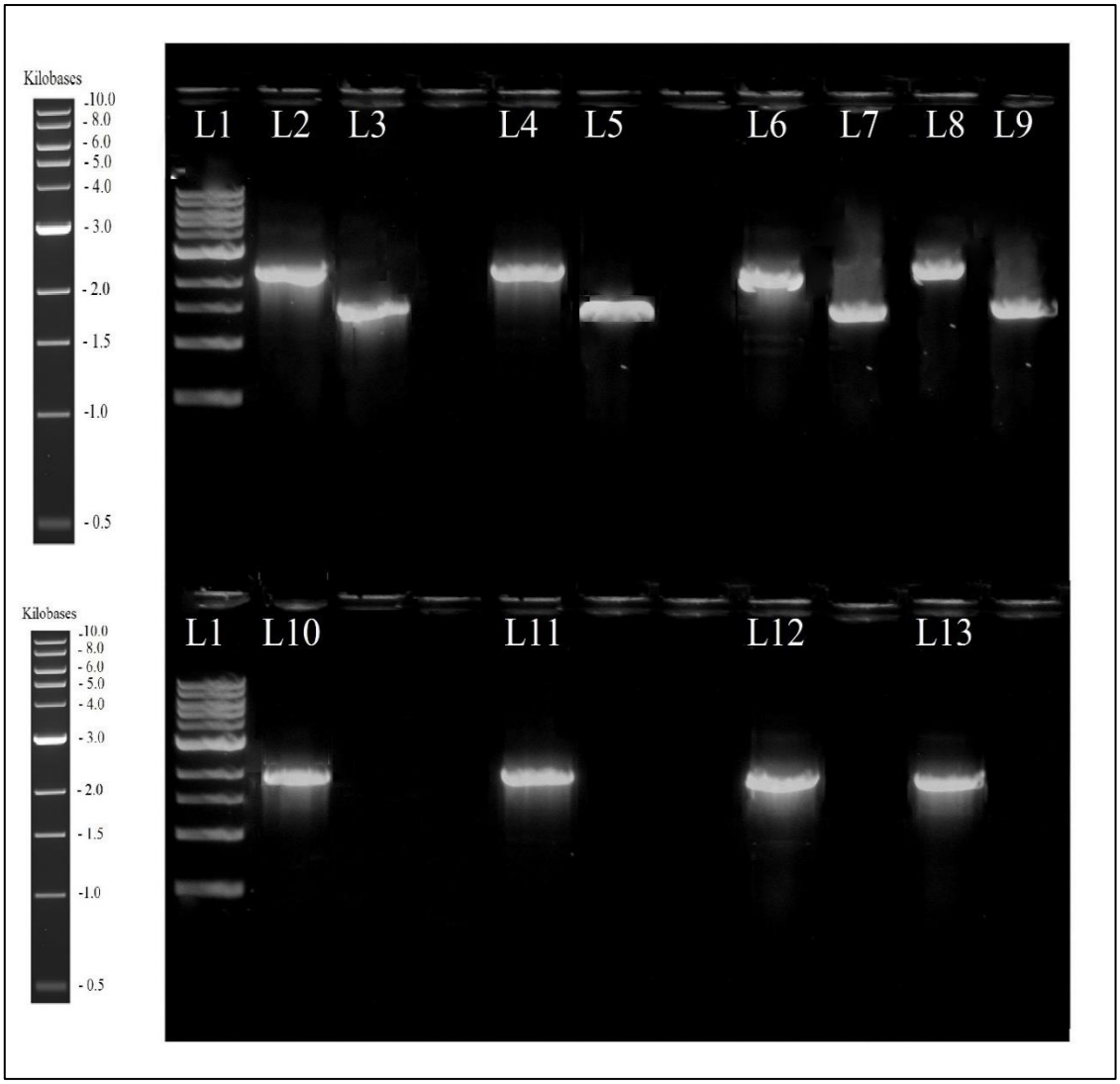

Figure 2.8*: Agarose gel electrophoresis showing the genetic analysis of putative* yneH, ansA, ybiK*, and* KPN_01165 *mutants. PCR products obtained with P1/P6, and P3/P4 primers corresponding to mutant allele, and aph cassette, respectively.* ***L1*** *500 ng 1kb DNA ladder (NEB).* ***L2, 4, 6, and 8*** *represent mutant allele amplicons of* yneH, ansA, ybiK, *and* KPN_01165*, respectively (approximately 2.5 kb).* ***L3, 5, 7, and 9****, represent the amplicons for* aph (3')-II$_{FRT}$*, approximately 1.5 kb, from putative* yneH, ansA, ybiK, *and* KPN_01165 *mutants, respectively.* ***L10, 11, 12, and 13****, (approximately 2.0 kb) amplicons represent the original genomic regions of* yneH, ansA, ybiK, *and* KPN_01165*, respectively, after using P1/P6 primers on wild type KR3167. P1/P6, and P3/P4 primers sequences are listed in Table 2.3.*

2.16.4 Flp-mediated FRT-recombination in *K. pneumoniae*

Insertion of antibiotic markers is sometimes associated with a polar effect due to their impact on downstream expression of genes (Ishikawa and Hori, 2013). The chromosomally integrated antibiotic marker used in this study was flanked by a flippase recognition target FRT site. Flp mediated FRT- site-specific recombination enables curing of resistance markers (Hoang *et al.*, 1998). Flp is provided by the plasmid pFLP2, which includes the *sacB* and *bla* genes (Figure 2.9). The *bla* encodes for ampicillin resistance, while *sacB* is a counter selection marker that is expressed in the presence of 5% (w/v) sucrose (Hoang *et al.*, 1998; van Aartsen and Rajakumar, 2011). Following expression of Flp, a recombination occurs, and the flanked antibiotic resistance cassette is then removed. The removal of the antibiotic resistance cassette allows further genetic manipulations such as double and triple mutant construction to take place (Raynal *et al.*, 2006). This technique of creation of a markerless mutant was previously applied in *K. pneumoniae* (van Aartsen and Rajakumar, 2011). Upon application of the FLP recombinase in *K. pneumoniae*, the central part of the cassette will be removed, leaving an FRT scar of ~ 80-90 bp on the chromosome (van Aartsen and Rajakumar, 2011). The antibiotic cassette was deleted as follows: first, electrocompetent cells from *ΔyneH*::*aph(3')-II*$_{FRT}$, *ΔansA*::*aph(3')-II*$_{FRT}$, *ΔybiK*::*aph(3')-II*$_{FRT}$, and *ΔKPN_01165*::*aph(3')-II*$_{FRT}$, were prepared (section 2.12.1), then 10-20 ng of *sacB*-bearing pFLP2 plasmid was transformed into the strains by electroporation (Figure 2.9A). After non-selective growth at 37 ºC for 1 h, 100 µl of the transformed cultures was plated on LA plates supplemented with 1200 µg/ml ampicillin. Next day, any ampicillin resistant colonies were examined by colony PCR assay. If the transformation was successful, this plasmid would remove *aph* cassette leaving a marker less mutant with FRT scars, as demonstrated in Figure 2.9B.

All tested colonies were should be resistant to 1200 µg/ml of ampicillin, and sensitive to 50 µg/ml kanamycin because of antibiotic cassette excision. This was verified by colony PCR analysis for the markerless *ΔyneH*, *ΔansA*, *ΔybiK*, and *ΔKPN_01165*. A total of 4 gel electrophoresis analyses represent confirmation of markerless *ΔyneH*, *ΔansA*, *ΔybiK*, and *ΔKPN_01165* constructions. (Figure 2.10A, B, C and D, respectively). In each PCR, primer pairs P1/P6, FLP1/FLP2 and P3/P4 were used to confirm the genetic background (left flank and right flank), pFLP2 plasmid presence, and loss of the kanamycin resistance cassette, respectively (Figure 2.10, A, B, C and D). After using P1/P6 primers, the L2 in each gel shows the expected product size for unmarked *ΔyneH* (~983 bp), *ΔansA* (~1013

bp), *ΔybiK* (~ 1039 bp), and *ΔKPN_01165* (~ 1036 bp); and by using FLP1/FLP2, L3 confirms the presence of *sacB* gene of pFLP2, which generates ~ 2.1 kb product. However, using P3/P4 in L4 showed no *aph (3')-II* amplicons, proving its excision.

Next, all colonies were grown on LA supplemented with 5 % (w/v) sucrose at 37ºC to cure pFLP2. The sucrose suppresses the growth of pFLP2 bearing strains, and the plasmid would therefore be cured by the counter selectable marker *sacB* in the pFLP2 backbone, which facilitates its exclusion (Wei *et al.*, 2012, Ishikawa and Hori 2013). Single colonies were genetically screened to confirm pFLP2 and *aph (3')-II*$_{FRT}$ absence (Figure 2.11). The same colonies were also phenotypically tested by patching on LA plates to prove ampicillin, and kanamycin sensitivity. The ampicillin and kanamycin sensitive patches were considered to contain unmarked and cured *ΔyneH*, *ΔansA*, *ΔybiK*, and *ΔKPN_01165*. L3 and L4 in Figure 2.11A, B, C, and D indicated the successful loss of pFLP2 and *aph (3')-II*$_{FRT}$, in *ΔyneH*, *ΔansA*, *ΔybiK*, and *ΔKPN_01165*, respectively, as there were no amplicons. Figure 2.11E shows a positive control in which L2 is an amplicon with 1.5 kb, representing *aph (3')-II*$_{FRT}$, and L3 is 2.1 kb *sacB* PCR product, after using the set of the primers on *yneH*, *ansA*, *ybiK*, and *KPN_01165* (section 2.13.3, and Table 2.5).

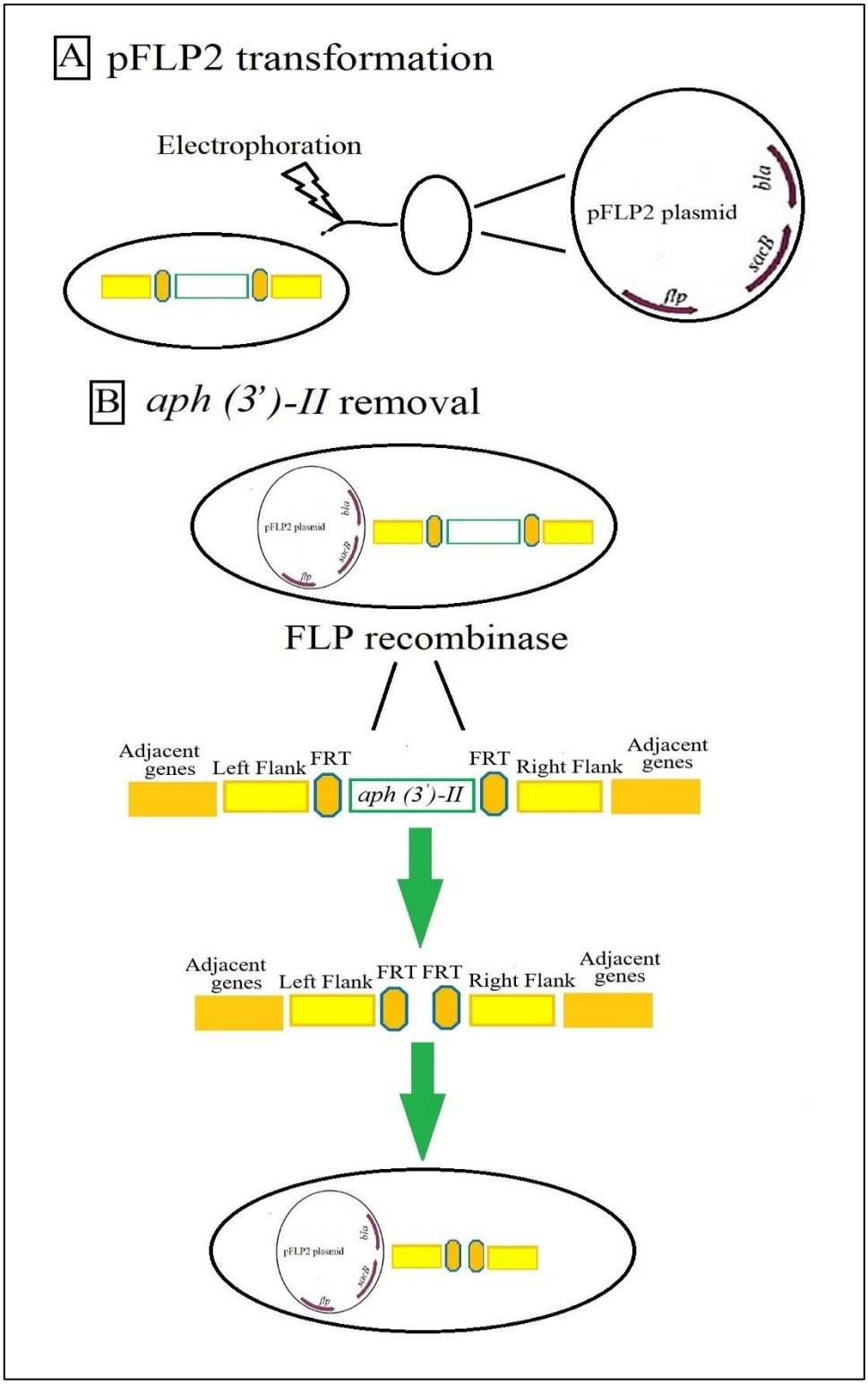

Figure 2.9: *Diagram represents* aph (3')-II$_{FRT}$ *removal by pFLP2. A. This plasmid was transformed by electroporation to* aph (3')-II$_{FRT}$ *bearing strain. In B,* flp *product stimulates FLP recombinase mechanism, leading to excision of* aph (3')-II$_{FRT}$, *leaving FRT scar. FRT stands for Flp Recombinase Target.*

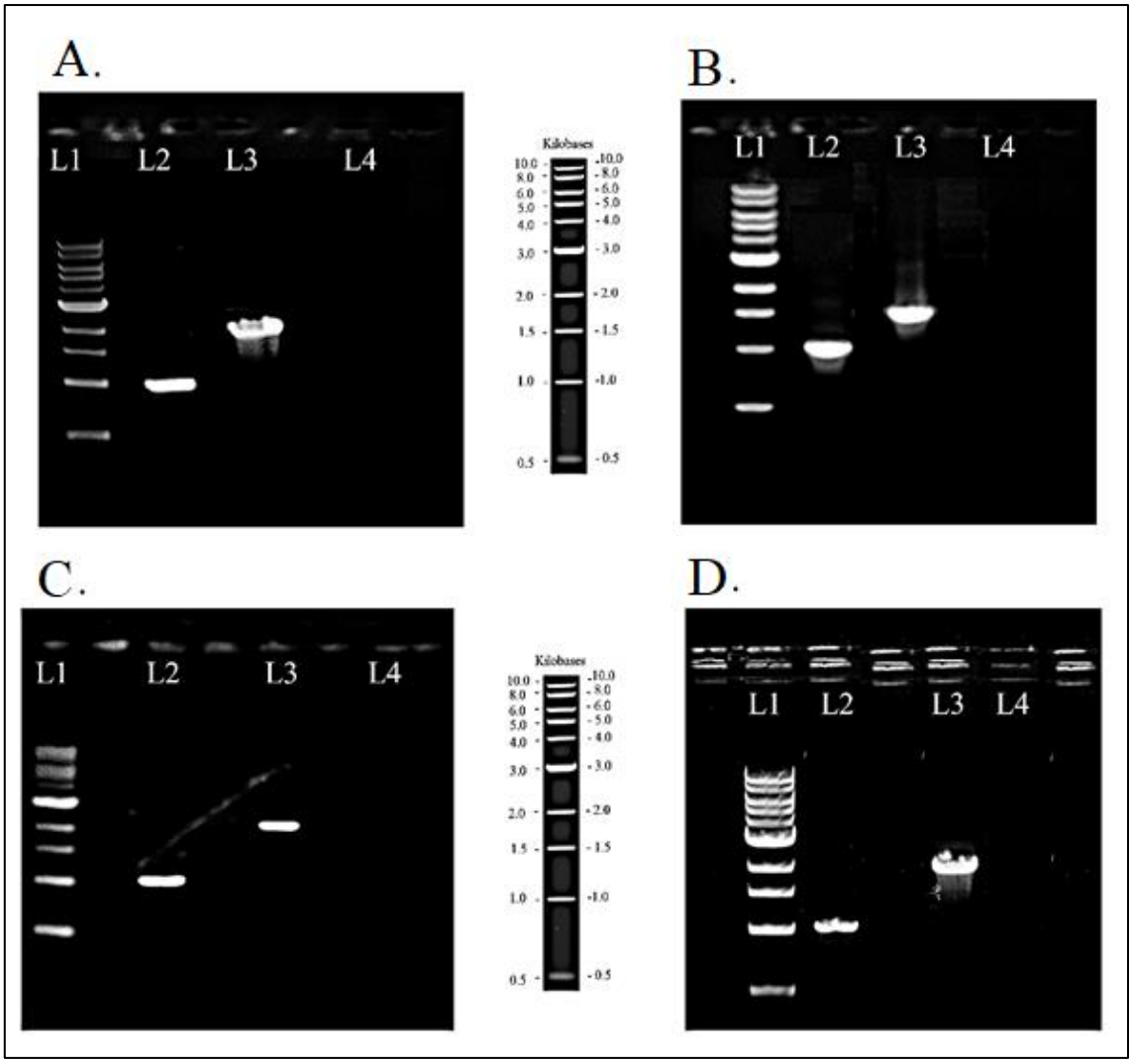

Figure 2.10: *PCR analysis confirmed unmarked mutant construction. The analysis used P1/P6, FLP1/FLP2, and P3/P4 primers. Lane 1 in* ***A***, ***B***, ***C***, *and* ***D*** *is 500 ng of 1kb DNA ladder (NEB). L2 in each gel illustrates the expected size of unmarked asparaginase/glutaminase mutants. L3 indicates the presence of a positive amplicon of* sacB, *amplified using pFLP2 plasmid as a template. L4 has no amplicon, showing the complete removal of kanamycin cassette from* ΔyneH:: aph(3')-II$_{FRT}$, ΔansA::aph(3')-II$_{FRT}$, ΔybiK::aph(3')-II$_{FRT}$, *and* ΔKPN_01165::aph(3')-II$_{FRT}$ *mutants. Full sequences of the primers are listed in Table 2.3 and Table 2.5.*

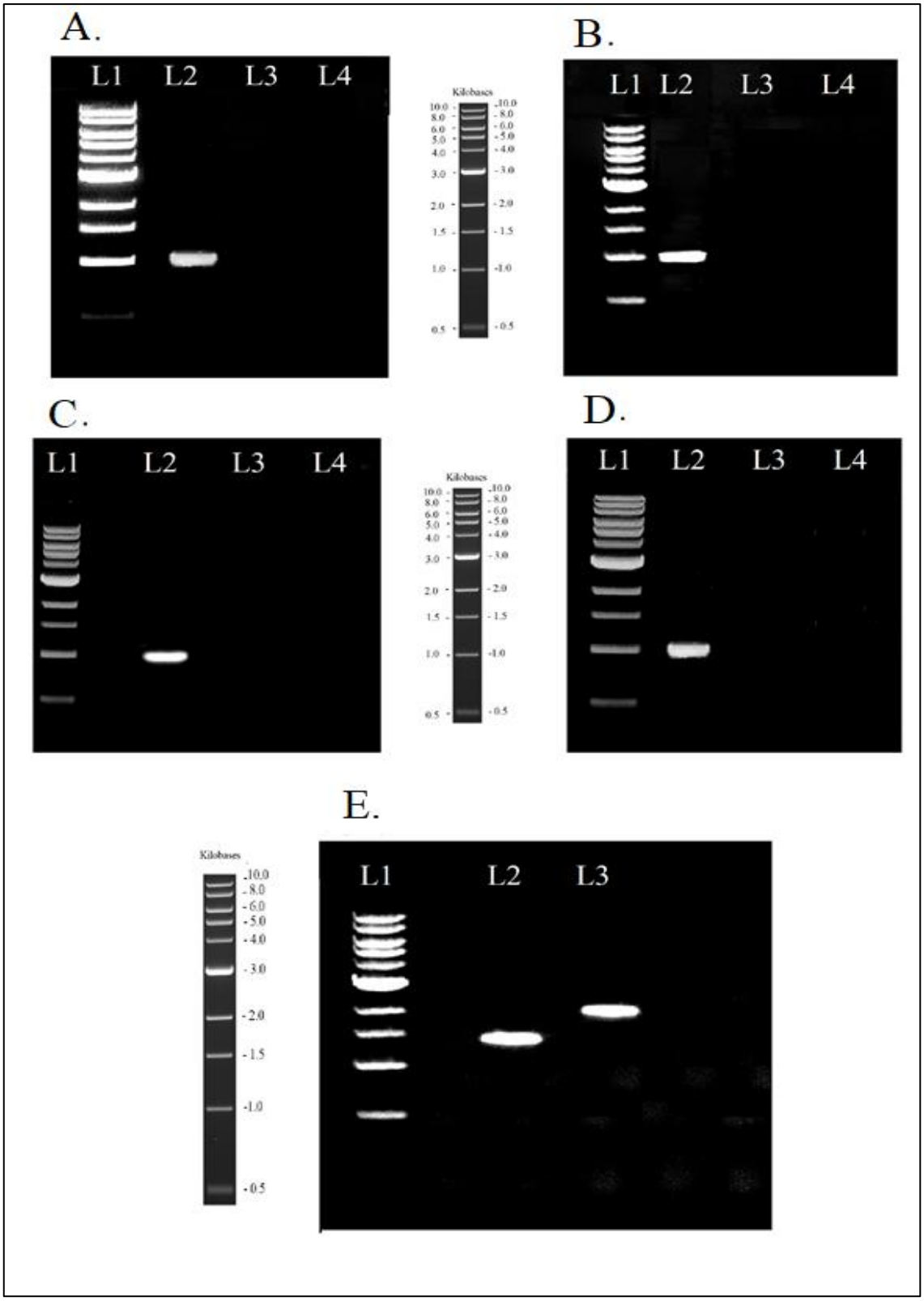

Figure 2.11: *Agarose gel electrophoresis demonstrating the elimination of pFPL2.* ***L1****-500 ng 1kb DNA ladder (NEB);* ***A****,* ***B****,* ***C****, and* ***D*** *show the amplification products representing the sequences around mutated region in* ΔyneH, ΔansA, ΔybiK, *and* ΔKPN_01165 *(right and left flanks), respectively, after losing* aph(3')-II$_{FRT}$ *using P1/P6*

primers. Lanes 3 and 4 represent the absence of aph (3')-II$_{FRT}$ *and* sacB*, using FLP1/FLP2 and P3/P4, respectively. Full sequences of the primers are listed in Table 2.3, and Table2.5, respectively.*

2.16.5 KPN_01165 and *ΔybiK* double mutant construction

Unmarked *ΔybiK* was used to construct a double (*ybiK / KPN_01165*) mutant strain. This double mutation was done to determine whether there is any synergistic impact between *ybiK* and *KPN_01165*. For construction of an unmarked *ybiK/ KPN_01165* mutant, the allele exchange system method was applied again on *ΔybiK* as described in section 2.12. Successful removal of kanamycin cassette *aph (3')-II$_{FRT}$* from marked single mutants allowed the re-use of the same antibiotic cassette for construction of double mutant in the same genetic background. The *KPN_01165* SOEing product was reused and transformed to electrocompetent unmarked *ΔybiK* (section 2.12). Successful SOEing transformation to unmarked *ΔybiK*/ pKOBEG-Apra resulted in construction of a marked double *ΔybiK::ΔKPN_01165::aph(3')-II$_{FRT}$*. *ybiK/ KPN_01165* mutation. This was confirmed by colony PCR as described in section 2.8.2 using P1/P6 primers of *ybiK* and *KPN_01165* (Table 2.3). Lane 2 and 3 in Figure 2.12 show PCR products amplified from marked double *ΔybiK/ΔKPN_01165::aph(3')-II$_{FRT}$* mutant. In L2 P1/P6 in the unmarked *ybiK* is expected to generate a ~ 1039 bp amplicon representing LF (512 bp), plus 527 bp RF. The L3 amplicon represents marked *ΔybiK::ΔKPN_01165::aph(3')-II$_{FRT}$* and this PCR product (2484 bp) consist of 504 bp *ΔKPN_01165* left flank, 1496 bp antibiotic cassette, and 532 bp right flank (after using P1/P6 of *KPN_01165*).

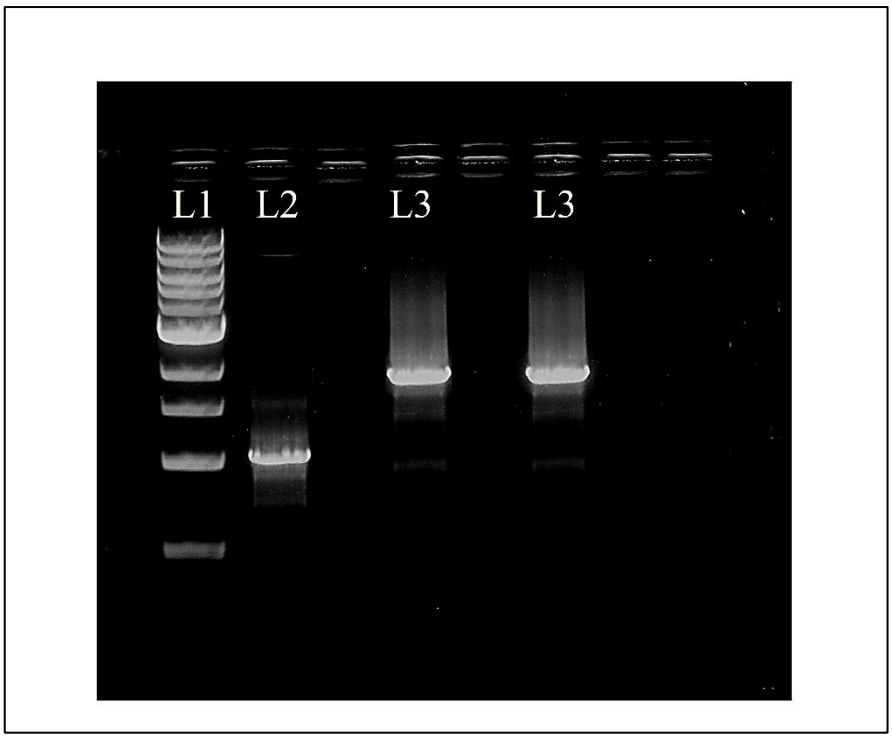

Figure 2.12: *Gel electrophoresis of PCR products to confirm the construction of double asparaginase/glutaminase mutant.* ***L1*** *500 ng of 1 kb DNA ladder (NEB); L2 PCR product of unmarked* ΔybiK, *approximately 1 kb, using P1 (ybiK LF / FP) and P6 (ybiK RF / RP); L3 represents the PCR products for the SOE product in unmarked* ΔybiK *genetic background (approximately 2484 bp) using P1/P6 of* KPN_01165, *which confirm* ΔybiK::ΔKPN_01165::aph(3')-II$_{FRT}$ *creation. Full sequences of the primers are listed in Table 2.3.*

2.16.6 Genetic complementation of mutants

To demonstrate that the phenotypic differences between the wild type and the mutants were due to genuine gene mutations and not polar effects, the mutants were genetically complemented. Polar effects can result after a mutagenesis because of inhibition of downstream gene expression located near the mutated gene, especially if the mutated gene is located at the beginning of an operon (Raynal *et al.*, 2006). The polarity effect can particularly result from insertion of an antibiotic cassette (Ishikawa and Hori, 2013). In this project this phenomenon was resolved through construction of unmarked mutations as described in section 2.16.4.

The *cis*-complementation method was used to genetically complement all unmarked mutant strains, *ΔyneH*, *ΔansA*, *ΔybiK* and *ΔKPN_01165*. This approach of

complementation is applied by re-using the lambda red system to transform the mutated genes back to their native genome loci. SOEing products were constructed, in which asparaginase/glutaminase genes are inserted with the right flank and the antibiotic casetteas described in section 2.13.

SOEing construct for the asparaginase/glutaminase genes were transformed into electrocompetent markerless mutant strain as described in section 2.12. In the second step, the antibiotic cassette was removed by pFLP2 as described in section 2.16.4. The prospective *cis*-complemented strains were PCR screened for confirmation (Figure 2.13, L2-L9). In Figure 2.13, Lane 2-5, it is shown that amplicons were obtained with SC1/P6 primer set for the constructed and transformed SOEing product introduced into *ΔyneH, ΔansA*, *ΔybiK* and *ΔKPN_01165*, respectively. All products had the expected size of approximately 3 kb. This size represents the asparaginase/ glutaminase genes which are approximately 1 kb, 1.5 kb of *aph (3')-II*$_{FRT}$, and 0.5 kb of right flank. The PCR amplicons (expected 2968 bp) in L2 consist of 948 bp *yneH*, plus 1.5 kb *aph (3')-II*$_{FRT}$, and 524 bp right flank. L3 contains approximately 3036 bp product which includes *aph (3')-II*$_{FRT}$, *ansA* coding region, and 520 bp right flank. The DNA band (2965 bp) in L4 resulted from 942 bp *ybiK*, *aph (3')-II*$_{FRT}$ and 527 bp RF. L5 amplicons (3041 bp) belong to *KPN_01165, aph (3')-II*$_{FRT}$, and 532 bp of downstream locus. The amplicons in lane 6, 7, 8, and 9 show the products obtained with the CS1/CS2 (Table 2.3) primer set of *yneH*, *ansA*, *ybiK*, and *KPN_01165*. SC1/SC2 generates amplicons with an expected size of ~ 1 kb, representing the intact copies of these genes, confirming the successful genetic complementation of *ΔyneH*, *ΔansA*, *ΔybiK* and *ΔKPN_01165*.

Figure 2.13: *Agarose gel electrophoresis showing successful cis-complementation of* yneH, ansA, ybiK, *and* KPN_01165 *isogenic mutants. L1 500 ng of 1 kb DNA ladder (NEB). L2, 3, 4, and 5, show PCR products of the inserted SOEing products after using screen SC1/P6 primers (~3 kb) and indicate the right integration of Asparaginase/ Glutaminase genes ~ 1 kb, 1.5 kb* aph (3')-II$_{FRT}$, *and right flank ~ 0.5 kb . Lane 6, 7, 8, and 9, show the products (~1 kb) obtained with SC1/SC2 primers for* yneH, ansA, ybiK, *and* KPN_01165, *respectively. Full sequences of the primers are listed in Table 2.3.*

Section D: Discussion

2.17 Mutagenesis process in *K. pneumoniae* KR3167

K. pneumoniae strains including reference strains *K. pneumoniae* MGH78578 and *K. pneumoniae* NTUH-K2044, are resistant to multiple antibiotics, and have a muco-viscous capsule (Chaves *et al.*, 2001). This has challenges for the Lambda Red mutagenesis system application which is reliant on the use of multiple plasmids each conferring resistance to different antibiotics. Therefore, multiple antibiotic sensitivity is required in the host strain as gene modifications will be constructed in one genetic background. Also, a muco-viscous capsule hinders competent cell preparation, and plasmid transformation by electroporation. These collectively are important compounding factors for genetic manipulations, which led to search for a strain that was less muco-viscous and sensitive to antibiotics conferred by the plasmids used for genetic manipulation. Hence, I utilised *K. pneumoniae* KR3167 to test my hypothesis. During the mutation work it was identified that, pFLP2 transformation was needed for optimization of genetic mutation, as more than 200 colonies were regularly obtained after overnight growth in LA supplemented with ampicillin as described in section 2.16.4. This high number of colonies make a screening procedure a time-consuming process. The screening itself relies on testing colonies for the presence of *sacB* gene of pFLP2, and absence of *aph (3')-II* amplicons. This issue was resolved by altering the different aspects of the experiment, starting by increasing the concentration and amount of pFLP2 before the electroporation process, changing the growth condition of transformed cells through decrease of both the amount of the cells used in the growth assay, and the incubation recovery time. After various attempts, addition of 10 µl of pFLP2 20 ng/ µl to 50 µl electrocompetent cells, followed by plating of 100 µl of those cells after recovery spreaded on a 1200 µg/ml ampicillin LA plate for no more than 18 hours was used. After those modifications, the obtained colonies have reduced from 200 to less than 50 which is more manageable.

Genetic complementation was an important step to confirm that phenotypic variations between the wild type and the mutants had occurred as a result of gene disruption and were not due to a polar effect of the mutation. Previous studies have used *trans*-complementation as preferable method for genetic complementation on *K. pneumoniae* and *E. coli*. This method relies on insertion of a vector like pBAD that carries a desired gene back to the mutant strain (Chen *et al.*, 2002; Frirdich and Whitfield, 2005). The

pBAD have *araC* promoter which induced by L-arabinose, and suppressed by glucose (Guzman *et al.*, 1995). The desired gene expression will be linked with *araC* expression. In this study the application of pBAD was not suitable due to the presence of glucose in M9-medium, which is used for growth experiments. Therefore, all unmarked mutant strains, *ΔyneH*, *ΔansA*, *ΔybiK* and *ΔKPN_01165* were genetically complemented by *cis*-complementation method. This strategy relies on returning those genes back into chromosomal native location.

3 Chapter 3; Phenotypic characterisation of the mutant strains.

Section A: Introduction.

3.1 The role of asparaginases and glutaminases in the biology of *K. pneumoniae*

After reviewing KEGG databases it has been found that the *K. pneumoniae* reference strain contains three enzymes with predicted asparaginase/glutaminase activity, plus an enzyme that is annotated as a glutaminase. All of the three enzymes are type II asparaginase, but the sole glutaminase-specific enzyme is a type A glutaminase gene. The gene *yneH* (KPN_01636) is linked to glutaminase activity by annotation, and *ybiK* (KPN_00861) has been annotated as an L-asparaginase gene. The gene *ansA* (KPN_01203) is listed encoding for a cytoplasmic asparaginase, while the *KPN_01165* gene is annotated as a putative asparaginase/glutaminase.

The main objective of the project is to evaluate the functional significance of the asparaginase/ glutaminase gene in *K. pneumoniae* KR3167 biology and virulence.

After successful creation of *ΔyneH*, *ΔansA*, *ΔybiK*, *ΔKPN_01165* and the double mutant strain *ΔybiK/ ΔKPN_01165* it was necessary to understand the function of each gene, and to confirm the phenotypic characterisation of the mutants.

Section B: Materials and Methods.

3.2 M9 media preparation

The phenotypic characterization of asparaginase/ glutaminase differences was investigated using adaptations of a defined minimal medium called M9. In the original recipe of M9 medium has NH_4Cl as the nitrogen source and glucose as the carbon source (Harwood and Cutting, 1990). In this project the M9 versions were created by changing or removing the nitrogen source and by increasing and decreasing the level of the glucose carbon source. A 5x M9 stock solution was prepared from mixing 200 mM Na_2HPO_4, 100 mM KH_2PO_4, and 50 mM NaCl to 1l of distilled water. All versions of the M9 media were prepared from 1x stock solution plus 0.2 ml of 1M $MgSO_4$ and 0.1 ml of 1M $CaCl_2$. The original version (V1) of M9 will be called full M9 (F M9) with 1x M9 salts solution plus 10 mM NH_4Cl (the original nitrogen source), and 20 mM glucose (carbon source) (Table 3.1). In this project, FM9, was used to prepare *K. pneumoniae* strains for all phenotypic characterisation experiments.

In all other M9 versions, NH_4Cl was removed. As shown in Table 3.1, in V2, V3, and V4 M9, both glucose, and asparagine or glutamine were present in different concentrations. However, in the last version V5, the glucose was removed, and asparagine or glutamine acted as the source for both nitrogen and carbon. Totally 16 media have been created by adding varying concentration of asparagine or glutamine and glucose (Table 3.1) and are referred to as modified M and a number (M X). The M1 and M2 have glucose at 20 mM and asparagine or glutamine at 5 mM concentration (Sonawane *et al*, 2003). Investigation on the effect of glucose addition i.e., the test of carbon catabolite repression, involved varying the amount of glucose and nitrogen source that were added. In the M3 and M4 versions, the glucose was present at 5 mM and both glutamine and asparagine were present at 2 mM. In version 4, M5, M6, M7 and M8; the glucose concentration was the same in all which was 2 mM but the concentration of glutamine was variable 4 mM, 2 mM, 1 mM, and 0.5 mM, respectively. The M9*, M10, M11 and M12 had the glucose concentration at 2 mM in all but variable amount of asparagine in place of glutamine which was 4 mM, 2 mM, 1 mM, and 0.5 mM, respectively. The version 5, M13 and M14 lack the glucose and only had 10 mM glutamine and asparagine, respectively. All M9 media had a pH that was adjusted to 7.4, autoclaved at 121°C for 15 min at 1.5 bar pressure, and left to cool down before addition of any required antibiotics.

T*able 3.1:* *M9 versions used in this project: V2, V3, and V4: NH_4Cl was replaced with glutamine or asparagine in different concentrations, along with variable amounts of glucose. V5: Both NH_4Cl, and glucose were removed and replaced with glutamine or asparagine.*

.

Version	M type	Glucose (mM)	Glutamine (mM)	Asparagine (mM)
V2	M1	20	5	Absent
	M2	20	Absent	5
V3	M3	5	2	Absent
	M4	5	Absent	2
V4	M5	2	4	Absent
	M6	2	2	Absent
	M7	2	1	Absent
	M8	2	0.5	Absent
V4	M9*	2	Absent	4
	M10	2	Absent	2
	M11	2	Absent	1
	M12	2	Absent	0.5
V5	M13	Absent	10	Absent
	M14	Absent	Absent	10

3.3 Preparation of bacteria for the growth experiments

All bacterial growth studies were performed under micro-aerobic conditions. The microaerobic condition was achieved through using most of the space of universal tubes using 30 ml of F M9 medium (the original recipe which has as N source NH_4Cl). Overnight inocula of bacteria were added at 1:100 dilution with the F M9 medium and incubated overnight without shaking at 37°C in a HERA cell, Heraeus incubator. The next day, cultures were centrifuged at 4000 rpm for 10 min at room temperature in an Allegra TM X-22 centrifuge (Beckman Coulter) then the pellet was washed using 50 mM phosphate buffer saline (PBS), pH 7.4. Subsequently, the tubes were centrifuged again at

the same setting, and then the pellet was suspended in 10 ml PBS. One ml of re-suspended material was used to measure the absorbance using a Jenway Spectrophotometer model 6305 (wavelength set to 600 nm). In parallel, a Multiskan GO spectrophotometer (Thermo Scientific) was used to monitor continuously growth at 37 °C, in the different carbon and nitrogen versions of M9 media using a 96 well flat bottom plate. Measurement of growth used turbidity at 600 nm, and microaerophilic conditions were achieved by using in static mode of mixing and a total medium volume of 300 µl. The fitness of the strains was judged by comparing growth rates in the exponential phase and the growth yield of each mutant with wild type; all experiments were performed in at least triplicate and on separate occasions.

The growth rates (µ) were calculated through linear regression of the plots of ln (OD_{600}) versus time during the exponential phase of growth using the following equation (Widdel, 2007):

$$\mu\, h^{-1} = \frac{\ln \mathrm{OD}_2 \text{ or } \mathrm{CFU2} - \ln \mathrm{OD}_1 \text{ or } \mathrm{CFU1}}{(\mathrm{t}_2 - \mathrm{t}_1)}$$

Where: ln is the natural logarithm of a number, t= time; OD2 and OD1 are the cell densities at t2 and t1, respectively. CFU2 and CFU1 are the colony forming units at t2 and t1, respectively.

The growth yield was calculated by measuring the highest turbidity or CFU at the end of bacterial growth.

3.4 Viable counts

To determine the viable plate count (CFU/ml), bacterial cultures were serially diluted in ten-fold steps in a 96-well microplate. The starting dilution point was done by using 20 µl of original bacterial culture into 180 µl PBS (Miles *et al*., 1938). To count viable cells, 20 µl from each dilution was placed on to the surface of LB agar, and left to dry, then incubated at 37°C for 18 h. To calculate the CFU per millilitre, an average of the number of bacterial colonies in 20 µl was multiplied by 50, and the dilution factor using the following formula:

CFU / ml = Average number of colonies for a dilution x 50 x dilution factor.

3.5 Determination of asparaginase–glutaminase activity

This was performed by measuring NH_3, which is a reaction product of glutaminase and asparaginase by Nessler**'s** reagent (Wriston and Yellin, 1973). Glutamine was used as a substrate to measure glutaminase activity and asparagine was used for asparaginase activity. The activities were measured in whole cell extract.

3.5.1 Production of whole cell lysates

The sonication method was used to produce whole cell lysate using previously described protocols(Özbek and Ülgen, 2000). Up to 40 ml of bacterial culture was centrifuged at 4000 rpm for 10 min at room temperature, and the pellet was suspended in 2 ml of 50 mM PBS. Then, the cell suspension was sonicated using a Sanyo Soniprep model 150 for 20 s. This process was repeated six times, and in between each sonication cycle, the samples were allowed to cool for 10 s because the heat from sonication may cause protein denaturation. Later, the lysate was centrifuged at 13000 rpm for 15 min at 4 °C using a Hettich centrifuge model Mikro 22R. The clear cell lysate was kept at –20 °C until required.

3.5.2 Determination of protein concentration

Protein concentrations in whole cell extract was determined using a Bradford assay with Bio-Rad protein reagent (Bio-Rad Laboratories Inc., Hercules, CA) (Bradford, 1976). A standard curve was initially prepared using known concentrations of bovine serum albumin (BSA) (200, 400, 600, 800, 1000 and 1200 µg/ ml). Then, 10 µl of both the standard curve control and the sample plus 190 µl of Bio-Rad reagent were distributed on a 96 well microplate. The concentration of protein in the unknown samples was estimated from the linear equation determined using the optical density of the BSA standards, which were measured at 595 nm using a microplate reader model 680 (Bio-Rad), (Figure 3.1). Afterwards, the protein level in whole cell extract samples was normalised to 1000 µg/ml.

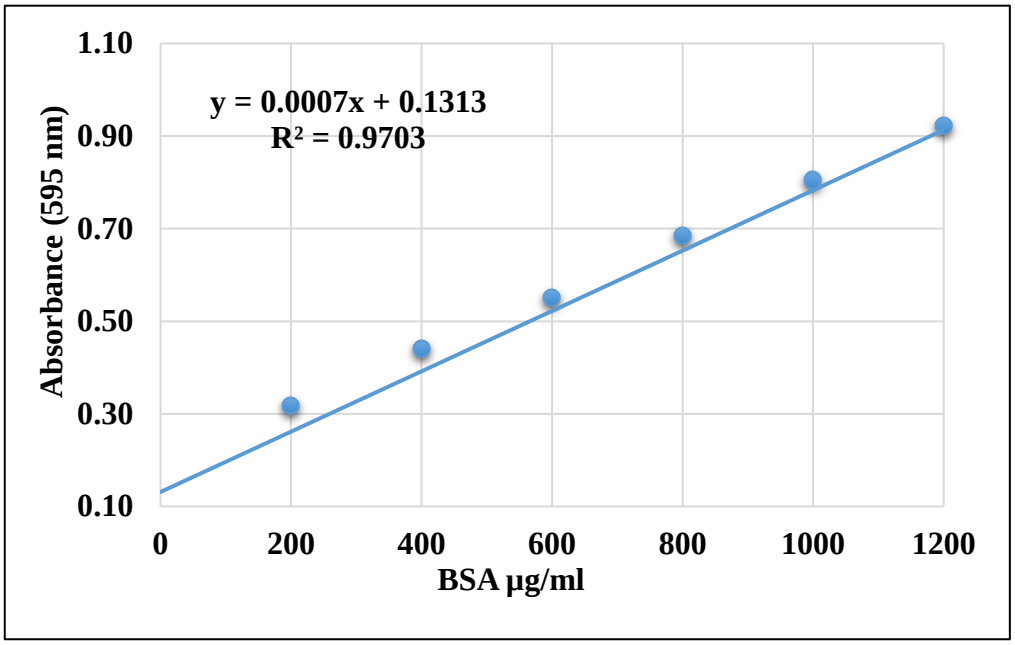

Figure 3.1: *A typical standard curve for measuring unknown protein concentration.*

3.5.3 Preparation of NH_3 standard curve for Nessler's reagent quantification

The standard curve for ammonia release was prepared as described in (Aljewari *et al*, 2010), but this curve contained high concentrations of nitrogen so the nitrogen in the samples which represents the measured activities was not in the range. As a result, several pilot experiments were performed to meet the samples' detection range. Known concentrations of $(NH_4)_2SO_4$ (0, 5, 10, 20, 40, 60 and 80 µg/ml) were prepared. The concentration of ammonium ion in each dilution was calculated. In a 200 µl reaction mixture, 30 µl of each concentration and 20 µl of Nessler's reagent were added. A blank tube was prepared by mixing 30 µl of distilled H_2O and 20 µl of Nessler's reagent. The final volume was made up to 200 µl using distilled water. Both samples and blank were incubated in a water bath at 25 °C for 20 minutes. The absorbance was measured at 450 nm, and then the ammonium standard curve was plotted based on the relationship between absorbance (450 nm) and ammonium ion concentration (µg/ml), as in Figure 3.2.

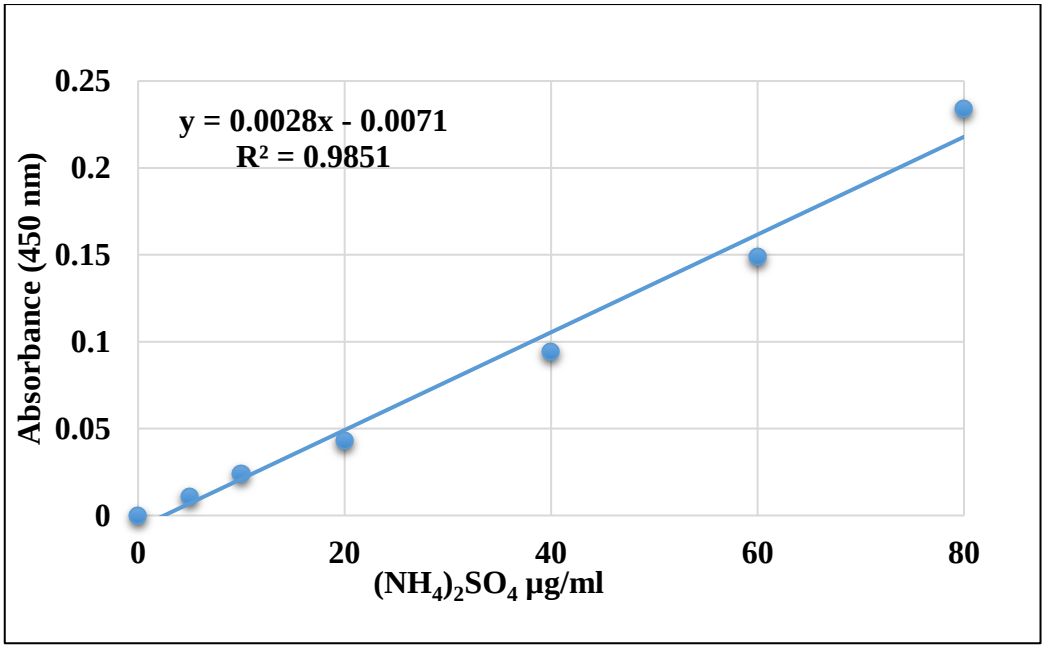

Figure 3.2: *Standard curve for measuring unknown ammonium ion concentration. Known concentrations of* $(NH_4)_2SO_4$ *were incubated with Nessler reagent then the developed colour was recorded under 450 nm.*

3.5.4 Colorimetric determination of ammonium ion by Nessler's reagent

The reaction conditions for glutaminase and asparaginase enzyme activities were optimized from previous protocols (Wriston and Yellin, 1973). In the original Wriston and Yellin article the reaction time was 30 minutes and substrate concentrations were 40 mM of either asparagine or glutamine. In time course assay reactions, the optimization was done by keeping the enzyme concentration fixed and changing either the substrate concentrations (asparagine and glutamine) (from 0 to 8 mM) and recording points (from 0 to 80 minutes with 10-minute recording time increments). The crude extract from wild type bacteria was obtained from cells growing in either glutamine or asparagine (10 mM), and the lysate protein obtained was fixed to 1mg/ml using the Bradford (1976) assay to enable comparison of activity between mutant and wildtype strains.

Asparaginase and glutaminase activities were assayed as follows: a 250 µl reaction mixture containing 50 µl of a range of amino acid concentrations (0, 0.2, 0.5, 1, 2, 3, 4,5,6,7 and 8 mM) of asparagine or glutamine, 50 µl of 0.5 M Tris buffer pH 8.0, 50 µl of enzyme sample and 50 µl distilled water was incubated in a water bath at 37 °C for 50 min. Then, 50 µl of Nessler's reagent (Sigma-Aldrich, UK) was added and the reaction was kept at 25 °C for 20 min, then 50 µl 1.5 M Trichloroacetic acid (Sigma-Aldrich, UK)

was added to stop the reaction before the absorbance at 450 nm was measured. The amount of released ammonia was determined using the prepared NH_3 standard curve (3.5.3), and expressed as μg/ml. Those readings were used in the formula below which calculates enzyme activity levels (Wriston and Yellin, 1973):

Activity in Units = Sample NH_3 concentration in the (μg/ml)/Time of reaction (min)× 4

One Unit (U): is the amount of asparaginase or glutaminase enzyme that liberates 1 μmol of ammonia per minute per ml [μmol/min/ml].

3.6 Over expression and purification of KPN_01165 enzyme

3.6.1 Amplification of *KPN_01165* for cloning:

The pLEICS-01 plasmid (Protex, University of Leicester) was used to express the enzyme encoded by *KPN_01165*. The pLEICS-01 has a promoter operator element from T7 bacteriophages that is recognized by *E. coli* RNA polymerase, which subsequently promotes *in vitro* high expression level. This vector also has 6XHis-tag coding sequence that facilities later affinity purification (Ilghari *et al*, 2009).

For *KPN_01165* cloning process two primers were designed to have 15 nucleotide complementary regions to the cloning site of pLEICS-01 (Table 3.2). Those primers were used to amplify *KPN_01165* from extracted wild type KR367 DNA as described in sections 2.6.1. The PCR reaction was done using Prime STAR HS premix (Takara, Japan) under PCR conditions that are described in Table 2.2. The purified *KPN_01165* along with primers were sent to be cloned in pLEICS-01. The cloning was done by Dr. Yang (PROTEX, Department of Molecular and Cell Biology, University of Leicester). The cloned pLEICS-01 was then extracted from *E. coli* One Shot® TOP10 competent cells using the QIAprep spin Miniprep kit (section 2.6.2).

To eliminate the possibility of any mutations, the plasmid was sent for sequencing at PNACL, University of Leicester. The sequence was done by pLEICS-01 dependent primers (T7 promoter and terminator primers).

Table 3.2: *Primers used for KPN_01165 expression. Bold nucleotides are complementary to the cloning site in pLEICES-01.*

Primers	Sequence (5′----3′)
KPN pro-FP	**TACTTCCAATCCATG**TGACGGTGAAAAGCAACAA
KPN pro-RP	**TATCCACCTTTACTGTCA**GGTCGTTAAGCACCACC

3.6.2 Transformation of pLEICS-01 into *E. coli*

The pLEICS-01 recombinant plasmid was transformed into *E. coli* BL21 (DE3) pLysS which was the strain used for protein expression. In a 1.5 ml centrifuge tube, a thawed 45 µl aliquot of *E. coli* BL21 competent cells was mixed with 5 µl of the extracted pLEICS-01, then the mixture was moved to a prechilled 14 ml BD Falcon polypropylene round bottom tube and kept in ice for 30 minutes. Next, the tube was subjected to heat shock at 42°C for exactly 45 seconds, and immediately transferred back to ice bucket for 2 min. A 450 µl aliquot of LB broth was added to the mixture and incubated for 2 hours at 37°C with shaking set at 200 rpm (New Brunswick Scientific, USA). After incubation, 300 µl of transformation mixture was selected on three (100 µl each) LB agars + ampicillin (100µg/ml), and incubated overnight at 37°C. Next day, to confirm the pLEICS-01 presence, the recombinant bacteria were screened by colony PCR using the primers listed in Table 3.2. From the positive cells 30 % glycerol LB stock was prepared and kept at -80°C until use.

3.6.3 Expression of the recombinant KPN_01165 enzyme

The expression of KPN_01165 was done in both small and large scales. Through the small-scale trial expression, the *E. coli* BL21 (DE3) pLysS strain containing the KPN_01165pLEICS-01 plasmid was grown until OD_{600} reached 0.6. Then to optimise expression different concentrations of isopropyl-β-D-thiogalactopyranoside IPTG (0.1, 0.2, 0.5, and 1 M) were used to induce KPN_01165 expression, as well as growing the cells at different temperatures (18, 30, 37°C). The negative control was achieved by harvesting and extracting the cells before adding IPTG. For large- scale expression the recombinant *E. coli* BL21 (DE3) pLysS was cultured in 10 ml of LB supplemented with 100 µg/ml ampicillin overnight in a shaking incubator at 220 rpm at 37°C. Next day, the overnight culture was added to one liter of fresh LB supplemented with 100 µg/ml

ampicillin. The culture was incubated at 37 ºC with shaking at 220 rpm until the OD_{600} nm reached 0.6 (2 hours), then 1 M IPTG was added. After IPTG addition, the culture was re-incubated at 37ºC for another 8 hours until the OD_{600} reached 1.6. The bacteria were then harvested by centrifugation at 10,000 rpm for 30 min at 4°C in a precooled Avanti J-E centrifuge (Beckman Coulter, USA) and the pellet was kept at -80°C overnight. The frozen pellet was resuspended with 20 ml of binding buffer. This buffer comprised 20 mM Tris, 150 mM NaCl, 10 µl of 10X TURBO DNase Buffer, 2.5 µl of Ambion® TURBOTM DNase (Invitrogen, UK), 5 µl of Proteo Guard TM EDTA-Free protease inhibitor cocktail (Takara Bio Europe, France), pH 7.4. The mixture was then sonicated as described in section 3.5.1. The lysate was centrifuged at 25,000 rpm for 30 min at 4°C using a precooled Avanti J-E centrifuge (Beckman Coulter, USA). To remove the cell debris, the supernatant was filtered through a 0.45µm micro-filter (Fisher Scientific, UK) to remove cell debris.

3.6.4 Purification of KPN_01165:

Metal affinity chromatography using a HisGravi Trap column (GE Healthcare) was used to purify the cloned KPN_01165 which has a histidine-tag in the N-terminus. All buffers were allowed to run through the column by gravity flow. The bottom tip of the His Gravi Trap column was cut off and placed in a column stand. Before adding the protein samples, the column was equilibrated by running 10 ml binding buffer through the column five times to protect the column from running dry during the run. Then in triplicate, the crude extract was passed through the column to allow recombinant protein binding. This step was followed by washing the column 10 times with binding buffer. The column bound protein was eluted with elution buffer treatment (20 mM Tris, 150 mM NaCl, pH 7.45) containing gradually increasing concentrations of imidazole (50, 100, 200, 300 and 500 mM). The eluted protein samples from each concentration were collected and placed in ice before Sodium Dodecyl Sulphate Polyacrylamide Gel Electrophoresis (SDS-PAGE) analysis.

3.6.5 SDS-PAGE Analysis

To monitor expression of the KPN_01165 protein SDS PAGE using 10% acrylamide gels was carried out using a Biorad tetra mingle system according to the recipe by Maniatis et al (1982) (Table 3.3). Protein samples (20 µl) were mixed with 10 µl of 10X SDS protein loading buffer (6.25 ml 0.5 M Tris-HCl pH 6.8, 1 g SDS, 10 mM DTT, 50 mg

bromophenol blue, 10 ml glycerol and 6.25 ml dH_2O). Then samples were heated at 95°C for 1-2 min on a hot plate, allowed to cool and then loaded into the gel. To allow size estimation of proteins, 10 µl protein marker (Precision Plus, Bio-Rad, UK) was loaded into the end wells. The electrophoresis was done at 150 mV until the bromophenol dye front reached the bottom of the gel.

Gel proteins were visualized using Coomassie Brilliant Blue staining solution prepared by mixing 0.4 g of 0.1% w/v Coomassie brilliant blue, 40% v/v methanol, 10% v/v acetic acid, to a volume of 400 ml using distilled H_2O. The gel was left in staining solution for 45 min with gentle shaking. This step was followed by incubation for 1-2 hours with gentle shaking in destaining solution (25% v/v isopropanol, 10% v/v acetic acid, and made up to 400 ml using distilled water), then the gel was washed by dH_2O before scanning using a Chemi Doc touch scanner (Bio-Rad, UK). The KPN_01165 expression was confirmed by protein sequencing at PNACL at University of Leicester.

Table 3.3: *Composition of 10% (w/v) SDS PAGE gel.*

Resolving gel		Stacking gel	
Tris-HCl (1.5M) pH 8.8	3.8ml	Tris-HCl (1M) pH 6.8	630 µl
10%SDS	150µl	10%SDS	50 µl
10% ammonium persulphate (APS), (Bio-Rad, UK)	150µl	10% APS	50 µl
Tetramethyl ethylenediamine (TEMED), (National diagnostics, UK)	6µl	TEMED	5µl
30% acrylamide bis acrylamide	7.5ml	30% acrylamide bis acrylamide	830µl
dH_2O	3.4ml	dH_2O	3.4 ml

3.6.6 KPN_01165 dialysis and quantification

After confirming KPN_01165 identity, Amicon Ultra-15 Centrifugal Filter Units (Millipore, UK) that have filter size of 10 kDa were used to filter and concentrate the

eluted protein. The imidazole concentrated elution buffer plus KPN_01165 (different concentrations) were added to the filter units and centrifuged at 4000 x g at 4°C ten times and each time the centrifugation process continues until approxmatly 1000 µl of protein remained. This step was followed by triplicate washing (under same centrifuge setting) by plain elution buffers (20 mM Tris, 150 mM NaCl, pH 7.45). The concentrated protein was exposed to liquid nitrogen after it was divided into small PCR tubes that have 50 µl aliquot in each, then stored at -80°C until use. The protein concentration then was measured as described in section 3.5.2.

3.6.7 Enzyme kinetic characterisations

The enzyme kinetics for asparaginase and glutaminase activities were done using the recombinant KPN_01165 and wildtype crude extract. Prior to that, the enzymatic reaction time and substrate concentrations (asparagine and glutamine) were optimized using time course assay reactions as described in section 3.5.4.

The crude extract from wild type bacteria and the mutants, *ΔyneH*, *ΔansA*, *ΔybiK*, *ΔKPN_01165*, and *ΔybiK*/ *ΔKPN_01165* were obtained from cells growing in either glutamine or asparagine (10mM) as N source. Extracts were prepared and protein concentration normalised to 1mg/ml using the Bradford (1976) protein concentration measurement method. To determine the kinetic parameters of recombinant KPN_01165 activity 200 µg/ml of recombinant enzyme was used in assays After many trials, I determined that the substrate needed for *Km* determinations would be 0, 0.2, 0.5, 1, 2, 3, 4, 5, and 6 mM of either asparagine or glutamine, and that the optimal assay time of 50 minutes was needed to calculate the kinetic parameters. The reaction mixture was incubated at 37°C for 40 minutes in a microplate reader (Varioskan Flash, Thermo Fisher), and the absorbance was recorded at 450 nm. Each activity test was performed in triplicate. The kinetic curve was calculated by plotting velocity against substrate concentration in a non-linear regression analysis using Prism Graph Pad 7.4 software to determine the enzyme: substrate kinetic *Vmax* and *Km* using the Michaelis Menten model.

3.6.8 Temperature and pH effect on enzyme stability

The purified enzyme was incubated at different temperatures (10, 20, 30, 40, 50 and 60°C) for 30 min., then left to cool down before measuring the activity. The recombinant KPN_01165 protein was also incubated at various pH values ranging between 3.0 – 9.0 for 30 min at 37 ˚C before measuring the activity as described in section 3.5.4. Two

buffers were used: sodium citrate buffer, pH ranged from 3.0 to 6.0, and sodium phosphate buffer, pH ranged from 6.0 to 9.0. The results were expressed as units (U) of asparaginase or glutaminase (Aljewari *et al*, 2010).

3.7 Bacterial phenotypic characterization

Two modified versions of M9 were used to investigate the growth characteristics of mutant vs wild type strains These were called M13 and M14, which did not contain either ammonium or glucose (see section 3.2). M13 was supplemented with 10 mM glutamine and M14 with 10 mM of asparagine. M13 and M14 were used because they only contain glutamine and asparagine the main substrates for asparaginase/glutaminase enzymes. M13 and M14 were also used for other phenotypic characterization, such as the inducibility of genes, and capsule synthesis.

3.8 Real time reverse transcriptase quantitative PCR (qRT-PCR)

This method was used to test the inducibility of asparaginase/glutaminase genes under a condition in which asparagine/glutamine are or are not present.

3.8.1 RNA Extraction

RNA extraction was performed using the TRIzol™ (TRI) (Sigma-Aldrich) extraction method, which was previously described by Stewart et al. (2002). The TRIzol™ is ready to use reagent that designed to isolate total RNA from cells.

The 40 ml FM9 cultures of *K. pneumoniae* strains were incubated statically at 37°C and when OD_{600} reached 0.2 (mid exponential growth) they were centrifuged at 4000 rpm for 10 min in Allegra TM X-22 centrifuge (Beckman Coulter). The bacterial pellets were washed twice by centrifugation under the same condition. Next, wthe wild type, *ΔyneH*, *ΔansA*, *ΔybiK, ΔKPN_01165,* and *ΔybiK/ΔKPN_01165* strains were moved to two versions of M9 in which they were re-incubated statically at 37°C for another two hours. The first M9 (reference condition) had 10 mM NH_4Cl (no glucose added). While the second M9 (treatment condition) had 10 mM of either glutamine or asparagine as sole source of carbon and nitrogen (M13 and M14, respectively). After two hours incubation the cells were centrifuged at 4000 rpm for 10 min, then resuspended in 500 µl of TRI solution. Next, the suspensions were transferred to microcentrifuge tubes and 100 µl chloroform was added followed by 15 seconds vortex. The next step involves moving the mixtures to silica containing tubes (Lysing Matrix B, Hybaid) in which they were

sonicated in Power lyzer™ 24 (MO BIO) which was set at rotor speed of 4000 for 45 seconds, with 15 seconds pause between the two cycles. The tubes were left for 2 min. on ice before centrifugation at 12000 xg for 15 min at 4°C. The upper phase was transferred to 1.5 ml tubes that had 250 µl isopropanol. The samples were mixed by 15 seconds vortex, then 15 min incubation at room temperature, followed by centrifugation at 12000 rpm for 10 min at 4 °C. The supernatants were removed, and the pellet was washed with 75% (v/v) ethanol followed by a second centrifugation at 12000 xg for 5 min, 4 °C. The upper phase was removed, and the pellet was left to dry at room temperature for 15 min. Finally, the pellet was resuspended in 90 µl DNase/RNase free water. The samples were then quantified using a Nano Drop 1000 spectrophotometer (Thermo Scientific).

3.8.2 DNase treatment

DNA contamination in the RNA samples was removed using the DNase reagent kit Ambion TURBO DNA-free™ (Invitrogen). A 20 µl (1.5 µg) amount of RNA was treated with 5 µl of 10X TURBO DNase Buffer, 2 µl of TURBO DNase (2 U/µl) and 23 µl of nuclease-free water. The sample was incubated at room temperature for 5 min, followed by centrifugation at 10000 *g* for 5 min. The upper phase was transferred to a new Eppendorf tube, and the RNA concentration then measured by its absorbance at 260 nm. RNA concentrations were normalized to 1 µg and stored at -80°C until use.

3.8.3 Complementary DNA (cDNA) synthesis

A SuperScript III reverse transcriptase (Invitrogen) kit was used to create the first-strand of cDNA. By following the manufacturer's instructions, 5 µl of DNase-treated RNA (1µg) was mixed with 1 µl of 300 ng random primers (Invitrogen) and 1 µl of 10 mM of dNTP (Promega, UK). This mixture was then heated at 65°C for 5 min, after which 4 µl of 5X First-Strand buffer, 1 µl of 0.1 M dithiothreitol (DTT) and 1 µl (200 U/µl) of SuperScrip III reverse transcriptase was added and made up to 20 µl with nuclease-free water. The mixture was incubated at 25°C for 5 min, and then at 50°C for 45 min. The reaction was finalized by heating at 70°C for 15 min. The cDNA was kept at -20°C until needed. In addition, a second set of reactions was also prepared as described above but without reverse transcriptase, RT-ve, to determine the presence of any DNA contamination.

3.8.4 Transcriptional analysis by qRT-PCR

The SensiMixTM SYBR® Hi-ROX kit (Bioline, UK) was used for performing qRT-PCR. The cDNAs were synthesized from RNA extracted from three independent cultures. The synthesised cDNA was then amplified using a Corbett RG-6000 PCR system (Qiagen) in 40 PCR cycles started by initial denaturation at 95°C for 10 min, then 40 amplification cycles that have: a denaturation step at 95°C for 20 seconds, annealing at 55°C for 30 seconds, and extension at 72°C for 20 seconds at which the fluorescence signal was collected. The primers used in the determination of the expression level of *yneH, ansA, ybiK,* and *KPN_01165* genes are listed in Table 3.4. Transcriptional levels of the asparaginase/glutaminase genes were normalized to the transcriptional level of a housekeeping gene (*rpoD*) (the beta-subunit of RNA polymerase), which was amplified in parallel (Doumith *et al.*, 2009). A 20 µl reaction mixture had 10 µl 2X SensiMix, 2 µl (3 pmol/each) forward and reverse primers, 2 µl (20 ng/µl) cDNA template, and 6 µl nuclease free water. The relative expression for each gene was measured in duplicate after analysing RT-qPCR by the comparative threshold method ($2^{-\Delta\Delta CT}$) as previously described in (Livak and Schmittgen, 2001). Any differences over 2-fold induction were considered significant (Yesilkaya *et al.*, 2007).

Table 3.4: *Primer list for RT-PCR.*

Primers	Sequence (5′----3′)
yneH –FP	TGACGGTGAAAAGCAACAA
yneH –RP	GGTCGTTAAGCACCACCATT
ansA –FP	TTCCACTACTGTTCGCTGGA
ansA –RP	TGGTCATCATCAGGGCATT
ybiK -FP	CGGAGAACAGCATCACTTCA
ybiK -RP	AGCGGTACCGTGAAGAAAAC
KPN_01165 -FP	CGGTGACCGTTGTCAAAGA
KPN_01165 -RP	ATGTGCCATACGTCCTCC
rpoD -FP (Housekeeping gene)	TCTCCGGTACCGTTATCGAC
rpoD -RP (Housekeeping gene)	TGTCGAGCTTCTCAGCTTCA

3.9 Capsule production determination

Capsule production was determined by quantifying glucuronic acid content in extracted capsule from wild type and the mutants *ΔyneH*, *ΔansA*, *ΔybiK*, *ΔKPN_01165* and *ΔybiK/ ΔKPN_01165*. A standard inoculum for each strain was prepared and grown statically in FM9 overnight at 37 ^{o} C. Then, the cultures of *K. pneumoniae* were pelleted by centrifugation at 3500 *g* for 10 min and washed twice in PBS. Next, the pellet was re-suspended in 1 ml PBS, and OD_{600} was adjusted to 0.1, corresponding to 10^6 CFU/ml. These were inoculated at a 1:100 ratio into fresh M13 or M14 media that was supplemented with 10 mM glutamine or 10 mM asparagine, respectively and grown overnight at 37°C. Next day, the cells were harvested by centrifugation at 3500 *g* for 10 min and washed twice in PBS. In each sample the measured glucuronic acid was expressed as micrograms per 10^9 CFU/ml, and the amount prepared by bacteria was quantified using a standard curve prepared with the known concentration of glucuronic acid (0, 10, 20, 40, 60, 80 and 100 µg/ml) (Sigma-Aldrich) (Figure 3.3). This was done by the following carbazole assay as described previously (Cho *et al.*, 2009). Briefly, the bacterial pellets obtained from overnight cultures were suspended with 1 ml of deionized water and added with 200 µl of 1 % (v/v) Zwittergent 3-14 detergent (Sigma-Aldrich, UK) that was dissolved in 100 mM citric acid (pH 2.0). Then, this mixture was incubated at 50°C for 20 min at 250 rpm. Subsequently, the cells were centrifuged at 12,000 xg for 5 min. and 1200 µl of absolute ethanol was added to 300µl of the supernatant. Then, the tubes were centrifuged at 12000 xg for 5 min. After that, the pellet was dissolved in 200 µl of de-ionized water. Finally, 750 µl of 0.025 M sodium tetraborate solution (Borax) in 93 % (v/v) H_2SO_4 (Sigma-Aldrich) was mixed with 125 µl of the dissolved pellet. The mixture was vortexed and incubated at 100°C for 10 min in a shaker hotplate at 250 rpm (Thermo-Shaker). Colour intensity in reaction mixtures was measured by spectrophotometer at 530 nm.

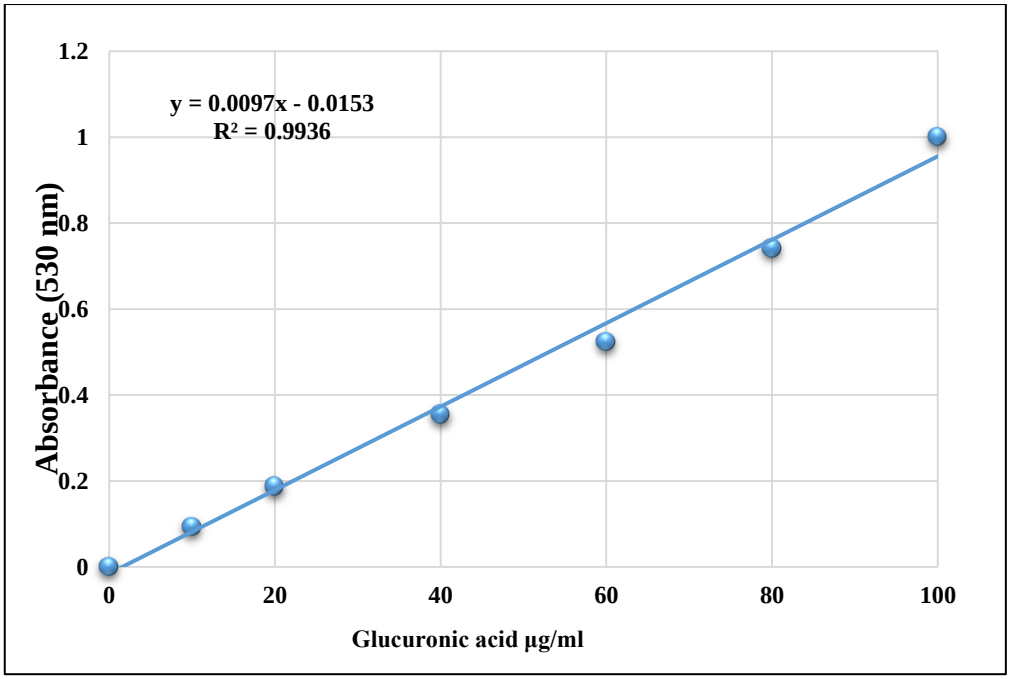

Figure 3.3: *A representative standard curve for quantitative determination of unknown glucuronic acid.*

Section C: Results.

3.10 Growth kinetics

The growth profiles of Wild type, *ΔyneH*, *ΔansA*, *ΔybiK*, *ΔKPN_01165*, and *ΔybiK/ΔKPN_01165* were determined by measuring the absorbance at OD_{600} nm throughout the 20 h incubation time; measurements were done every hour. In all growth parameter data, the growth rate (μ) and yields (Max OD_{600nm}) were obtained from the *K. pneumoniae* strains that were grown micro aerobically in the different M9 versions. Calculated growth rates and yields of mutant strains were compared to wild type KR3167 using one-way ANOVA and Dunnett's multiple comparisons test. The media preparation, growth conditions, results calculation were described in sections 3.2 and 3.3.

3.11 The growth in the original M9 media (F M9)

The first growth experiments were done using original M9 media recipe (F M9). This is defined medium has no glutamine or asparagine addition but has NH_3 in form of 10 mM NH_4Cl. This medium contains high concentrations of glucose and nitrogen, and in this medium no difference was seen in growth profiles between the mutants and wild type. As shown in Figure 3.4 and Table 3.5, the value of growth rates and yields of the mutants and the wild type that had been cultured in a readily assimilated nitrogen source, showed no significant difference in their growth profiles $p>0.05$. So, it can be concluded that the mutations had no significant effect on the growth rate and yield in FM9 (Figure 3.4 and Table 3.5). For this reason, in this project the FM9 media was used as reference media and to prepare mutants for the phenotypic characteristics' assays. The very likely reason for this indifference was that asparaginase and glutaminase enzymes assist in acquiring necessary nitrogen sources when NH_3, the preferable nitrogen source, is below 1 mM, or absent (Sonawane *et al.*, 2003).

Table 3.5: *Growth rate and yields of* K. pneumoniae *strains grown in FM9 that contained 10 mM NH_4Cl and 20 mM glucose. The growth rate and yields are the average of three independent experiments each with three replicates and '±' indicates standard error of means (SEM). The mutant strains were compared to wild type KR3167 by one-way ANOVA and Dunnett's multiple comparisons test (ns) represent no significant difference (p>0.05).*

Strains	Growth parameters in FM9-medium (20 mM glucose plus 10 mM NH_4Cl)	
	Max OD_{600nm}	Growth rate μ (h^{-1})
Wild type	1.11±0.06	0.18± 0.07
ΔyneH	1.03±0.11 (ns)	0.17±0.08 (ns)
ΔansA	1.18±0.08 (ns)	0.20±0.04 (ns)
ΔybiK	1.04±0.13 (ns)	0.18±0.03 (ns)
ΔKPN_01165	1.12±0.01 (ns)	0.16±0.02 (ns)
ΔybiK/ΔKPN_01165	1.08±0.10 (ns)	0.15±0.05 (ns)

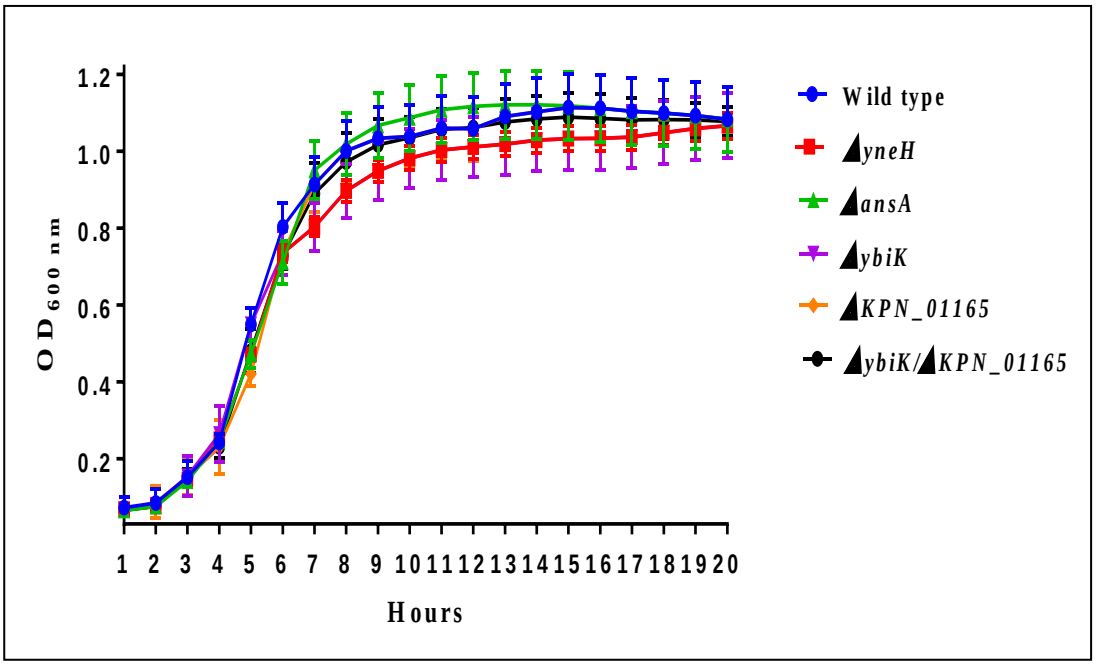

Figure 3.4: *Growth profiles of five mutants along with the wild type in FM9 medium. There is no significance difference in their growth rate and yields (p>0.05) (n=3). Values are average of at least three independent experiments each with three replicates. The vertical bars represent SEM.*

3.12 Effect of high-glucose level on growth of asparaginase/glutaminase mutants

The second growth experiments were done to determine a media composition that would allow phenotypic differences between the mutants and the wild type. Due to the absence of previous studies for the growth of the asparaginase/glutaminase mutants of *K. pneumoniae*, I used different modified M9 media as described in section 3.2. In this section two kinds of M9 are used; M1 and M2. The M1 and M2 were used to characterise *P. aeruginosa* asparaginase (Sonawane *et al.*, 2003). Both M1 and M2 have 20 mM glucose. However, M1 contains glutamine and M2 contains asparagine that replaces the NH_4Cl.

Table 3.6 and Figure 3.5 show the growth rates of all individual strains in M1 (5 mM glutamine and M2 (5 mM asparagine). It can be seen there were no significant differences ($p>0.05$) in either growth rate (μ) growth or yields of the strains ($p>0.05$). According to the Table 3.6, the calculated growth rates for the *ΔyneH*, *ΔansA*, *ΔybiK*, *ΔKPN_01165* and *ΔybiK/ ΔKPN*_01165 were 0.11 h^{-1} ± 0.02, 0.11 h^{-1} ± 0.03, 0.11 h^{-1} ± 0.02, 0.10 h^{-1} ± 0.03, 0.10 h^{-1} ± 0.02, respectively when cultured in M1 medium. Similarly, in M2, which

used asparagine, there was no change in the growth parameters of the strains. Therefore, the composition of nitrogen source is not significant as long as 20 mM glucose is present.

Due to the results of M1 and M2 (Table 3.6), each media component concentration (i.e. glucose, glutamine, and asparagine) and their contribution to the growth needed to be evaluated. So, the following growth profile experiments were carried out with the other M9 versions, as described in section 3.2.

Table 3.6: *Calculated growth rate (μ) and yields of* K. pneumoniae *strains after incubation in M1 and M2 media. The values are the average of three independent experiments with three replicates in each and '±' indicates SEM. The comparison to the wild type done by one-way ANOVA and Dunnett's multiple comparisons test. No significant differences were found between the strains (p>0.05).*

Strains	Growth parameters in M1-medium (20 mM glucose plus 5mM glutamine)		Growth parameters in M2-medium (20 mM glucose plus 5mM asparagine)	
	Max OD_{600nm}	Growth rate μ (h^{-1})	Max OD_{600nm}	Growth rate μ (h^{-1})
Wild type	0.74±0.03	0.11± 0.07	0.62±0.02	0.09±0.01
ΔyneH	0.78±0.05 (ns)	0.11± 0.02 (ns)	0.59±0.01 (ns)	0.08±0.01 (ns)
ΔansA	0.72±0.05 (ns)	0.11± 0.03 (ns)	0.63±0.02 (ns)	0.09±0.05 (ns)
ΔybiK	0.68±0.01 (ns)	0.11± 0.02 (ns)	0.59±0.02 (ns)	0.07±0.02 (ns)
ΔKPN_01165	0.72±0.02 (ns)	0.10± 0.03 (ns)	0.58±0.01 (ns)	0.08±0.01 (ns)
ΔybiK/ΔKPN_01165	0.70±0.03 (ns)	0.10± 0.02 (ns)	0.59±0.03 (ns)	0.07±0.03 (ns)

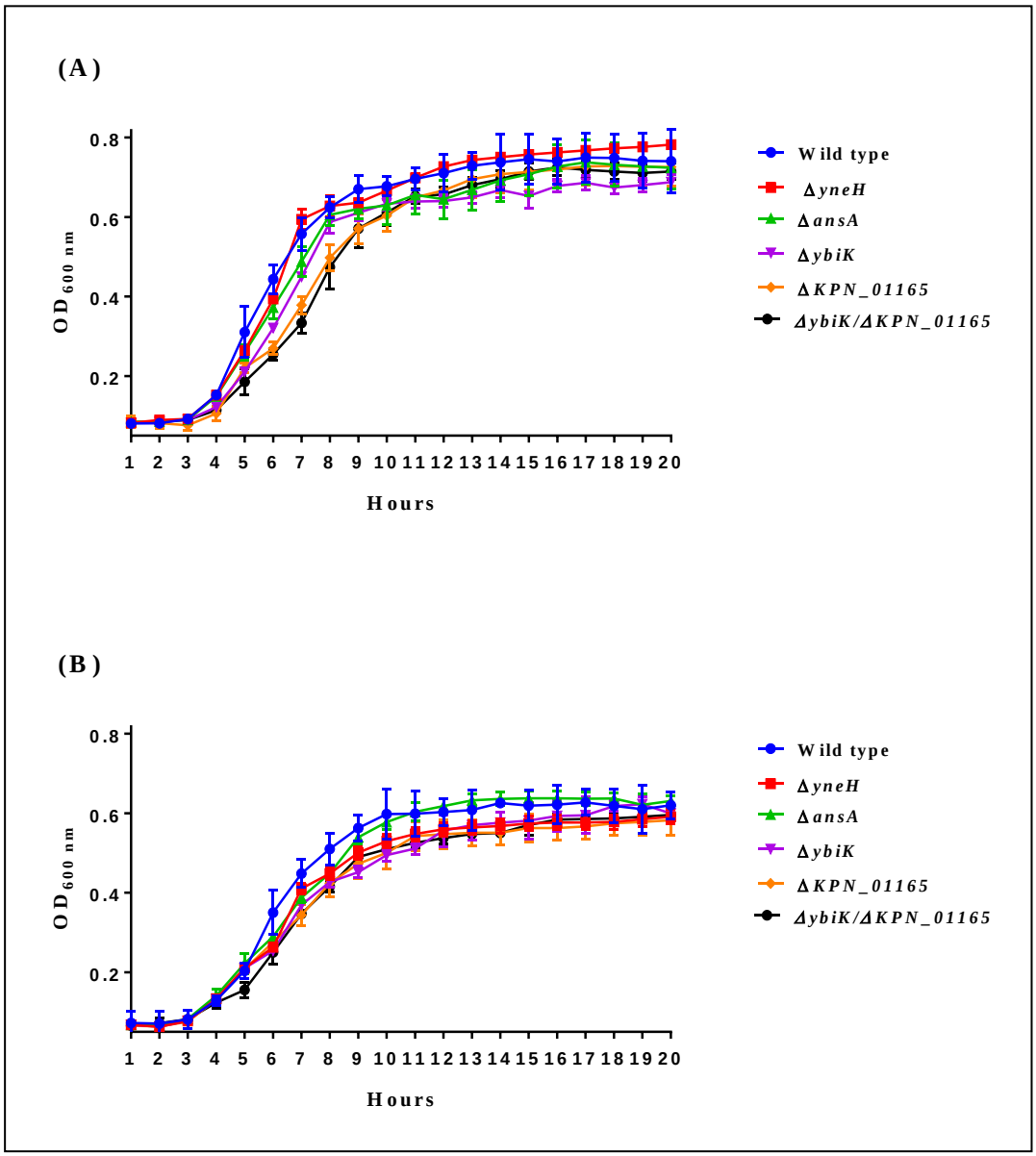

Figure 3.5: *Growth curves of* ΔyneH, ΔansA, ΔybiK, ΔKPN_01165 *and* ΔybiK/ ΔKPN_01165 *along with the wild type in V2 M9 which has fixed concentration of 20 mM glucose.* ***A.*** *had 5mM glutamine addition and* ***B.*** *contains 5mM asparagine as nitrogen source. In both, there is no significance difference in their growth rate and yields (p>0.05) (n=3). The error bars represent SEM.*

3.13 Effect of lowering glucose level on Asparaginase/Glutaminase mutants

At higher concentrations of carbon and nitrogen, 20 mM glucose, and 5mM of either glutamine or asparagine, no difference in growth phenotype between strains could be seen. After reviewing the literature, it was found that glucose availability affects the

dependence on glutamine and asparagine because the TCA cycle can degrade all these substrates (glucose and both glutamine and asparagine) to oxoglutarate and fumarate intermediates. If glucose is high the TCA cycle intermediates will be correspondingly high, therefore the need to utilize glutamine or asparagine will be reduced (Sonawane *et al.*, 2003; Sanches *et al.*, 2007). Consequently, it was decided after a series of trial experiments to lower the amino acid concentrations to 2 mM for glutamine or asparagine, respectively, and reduce the glucose to 5 mM (section 3.2). The growth rates observed in M3 (that have 5 mM glucose plus 2 mM glutamine) for the strains *ΔyneH, ΔansA* (0.08 h^{-1}±0.02 and 0.08 h^{-1}±0.02 (n=3) respectively) were same as the wild type 0.08 h^{-1}±0.01 ($p>0.05$). On the other hand, the strains *ΔKPN_01165* and *ΔybiK/ΔKPN_01165* demonstrated significant alteration in growth rates, which were 0.04±0.01 and 0.03 h^{-1}±0.02, n=3 (both $p<0.01$), respectively (Table 3.7). The growth yield data showed that only *ΔKPN_01165* and *ΔybiK/ΔKPN_01165* were significantly lower ($p<0.05$) (0.34±0.03, and 0.27±0.03, respectively, n=3) compared to wild type (0.55±0.01, n=3) (Table 3.7 and Figure 3.6 A).

According to Table 3.7, the growth rate observed for the wild type strain in the 2 mM asparagine and 5 mM glucose (M4 medium) was 0.06 h^{-1}± 0.02. When this growth rate was compared with the other mutant strains cultured in the same M4 medium, it was found that *ΔyneH, ΔansA* and *ΔybiK* (0.06 h^{-1}± 0.03, 0.05 h^{-1}± 0.02 and 0.05 h^{-1}± 0.02 respectively, n=3) had the same rate as the wild type (0.06 h^{-1}±0.03) ($p>0.05$). While the *ΔKPN_01165* and *ΔybiK/ΔKPN_01165* displayed significant reduction in growth rate (0.03 h^{-1}±0.03, and 0.03 h^{-1}±0.03, respectively, n=3) versus the wild type rate (0.06 h^{-1}±0.03) ($p<0.05$). For the growth yields in M4, a similar trend to the M3 i.e. lower growth yields, was noticed for the affected strains *ΔKPN_01165* and *ΔybiK/ΔKPN_01165* (Table 3.7 and Figure 3.6 B). A possible explanation of *ΔKPN_01165* and *ΔybiK/ΔKPN_01165* behavior in M3 and M4 condition could be due to the inability to utilize the nitrogen source (asparagine and glutamine).

Table 3.7: *Growth parameters after incubation in M3 and M4 (fixed 5 mM glucose plus 2mM glutamine or asparagine, respectively). The 'ns' represent no significant difference ($p>0.05$), * $p<0.05$, and ** $p<0.01$. The growth parameter obtained from three independent experiments each with three replicates. The '±' represent SEM. The mutant strains compared to the wild type by one-way ANOVA and Dunnett's multiple comparisons test.*

Strains	Growth parameters in M3 medium (5 mM glucose plus 2mM glutamine)		Growth parameters in M4-medium (5 mM glucose plus 2mM asparagine)	
	Max OD_{600nm}	Growth rate μ (h^{-1})	Max OD_{600nm}	Growth rate μ (h^{-1})
Wild type	0.55±0.01	0.08±0.01	0.46±0.01	0.06±0.02
ΔyneH	0.53±0.03 (ns)	0.08±0.02 (ns)	0.48±0.03 (ns)	0.06±0.03 (ns)
ΔansA	0.48±0.04 (ns)	0.08±0.02 (ns)	0.47±0.04 (ns)	0.05±0.02 (ns)
ΔybiK	0.44±0.02 (ns)	0.06±0.01 (ns)	0.43±0.02 (ns)	0.05±0.02 (ns)
ΔKPN_01165	0.34±0.03 (*)	0.04±0.01 (**)	0.28±0.03 (*)	0.03±0.03 (*)
ΔybiK/ΔKPN_01165	0.27±0.03 (*)	0.03±0.02 (**)	0.28±0.03 (*)	0.03±0.02 (*)

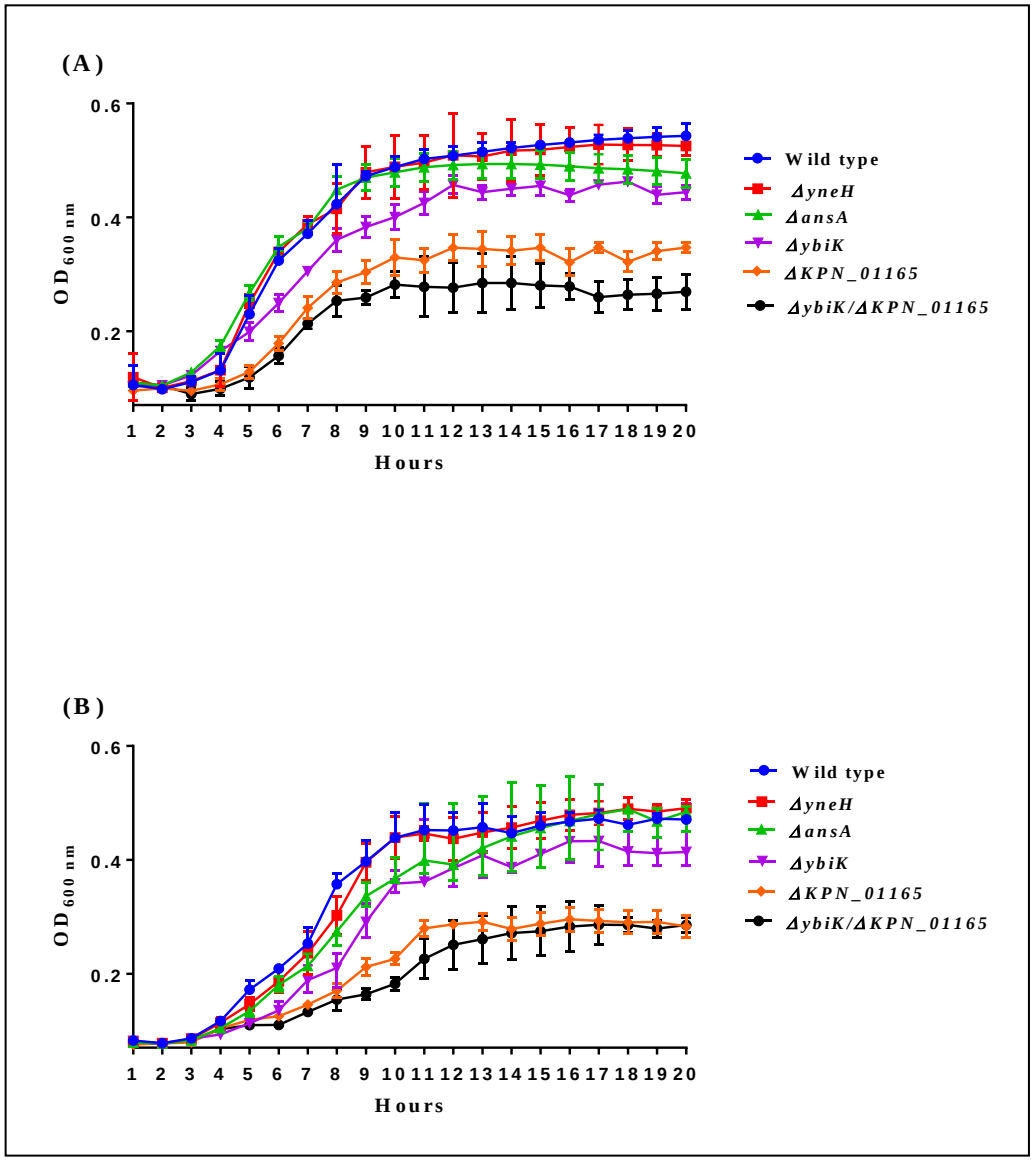

Figure 3.6: *The growth curves of KR3167 in 5mM glucose plus 2mM of either glutamine* ***(A)*** *or asparagine* ***(B)****. In both cases the growth yield is same in case of strains* ΔyneH, ΔansA, *and* ΔybiK *when compared to the wild type, while* ΔKPN_01165 *and* ΔybiK/ΔKPN_01165 *were significantly attenuated in growth yields (p<0.05). Each time point obtained from three independent experiments each with three replicates and the vertical bars represent SEM.*

3.14 Testing *K. pneumoniae* KR3167 strains growth using variable concentrations of glutamine and asparagine

After identifying the phenotype for *ΔKPN_01165* and *ΔybiK/ΔKPN_01165*, I decided to use a range of either glutamine or asparagine while keeping the concentration of glucose to 2 mM. The glutamine concentrations were 4 mM, 2 mM, 1 mM, and 0.5 mM for M5,

M6, M7, and M8, respectively. The other media, M9*, M10, M11, and M12, contained 4 mM, 2 mM, 1 mM, and 0.5 mM asparagine, respectively.

3.14.1 Effect of variable glutamine levels on growth

At 4mM glutamine (M5) *ΔyneH*, *ΔansA*, *ΔybiK*, *ΔKPN_01165* and *ΔybiK/ ΔKPN_01165* grew as well as the wild type in terms of their growth rates and yields ($p>0.05$) (Table 3.8 and Figure 3.7 A). With 2 mM glutamine (M6), the growth rate and yield for the mutants were not significantly different ($p>0.05$) from the wild type except for *ΔKPN_01165*, and *ΔybiK/ΔKPN_01165* ($p<0.05$). For example, the growth rate of *ΔKPN_01165*, and *ΔybiK/ΔKPN_01165* were 0.02 h^{-1}±0.01 and 0.02 h^{-1}±0.02 (n=3) respectively comparing to wild type 0.05 h^{-1}± 0.01 ($p<0.05$) (Table 3.8 and Figure 3.7 B).

The growth yield of the *ΔybiK* (0.31±0.03) (n=3) was thought to be affected due to its low glutaminase but the statistical analysis showed that difference as non-significant comparing to wild type growth yield 0.39±0.03 (n=3) ($p>0.05$) (Table 3.8 and Figure 3.7 B).

Table 3.8: *Growth rate and yields from* K. pneumoniae *grown in M5 and M6 (fixed 2mM glucose plus 4mM or 2mM glutamine, respectively). Data was analysed using one-way ANOVA and Dunnett's multiple comparisons test, 'ns' not significant, * $p<0.05$, (n=3), and '±' indicates SEM.*

Strains	Growth parameters in M5-medium (2 mM glucose plus 4mM glutamine)		Growth parameters in M6-medium (2 mM glucose plus 2mM glutamine)	
	Max OD_{600nm}	Growth rate μ (h^{-1})	Max OD_{600nm}	Growth rate μ (h^{-1})
Wild type	0.46±0.03	0.06±0.02	0.39±0.03	0.05± 0.01
ΔyneH	0.42±0.03 (ns)	0.05±0.02 (ns)	0.38±0.03 (ns)	0.05±0.01 (ns)
ΔansA	041±0.02 (ns)	0.05±0.01 (ns)	0.37±0.01 (ns)	0.04±0.02 (ns)
ΔybiK	0.42±0.03 (ns)	0.04±0.03 (ns)	0.31±0.03 (ns)	0.03± 0.02 (*)
ΔKPN_01165	0.40±0.05 (ns)	0.05±0.03 (ns)	0.24±0.03 (*)	0.02± 0.01 (*)
ΔybiK/ΔKPN_01165	0.41±0.02 (ns)	0.04±0.01 (ns)	0.23±0.02 (*)	0.02± 0.02 (*)

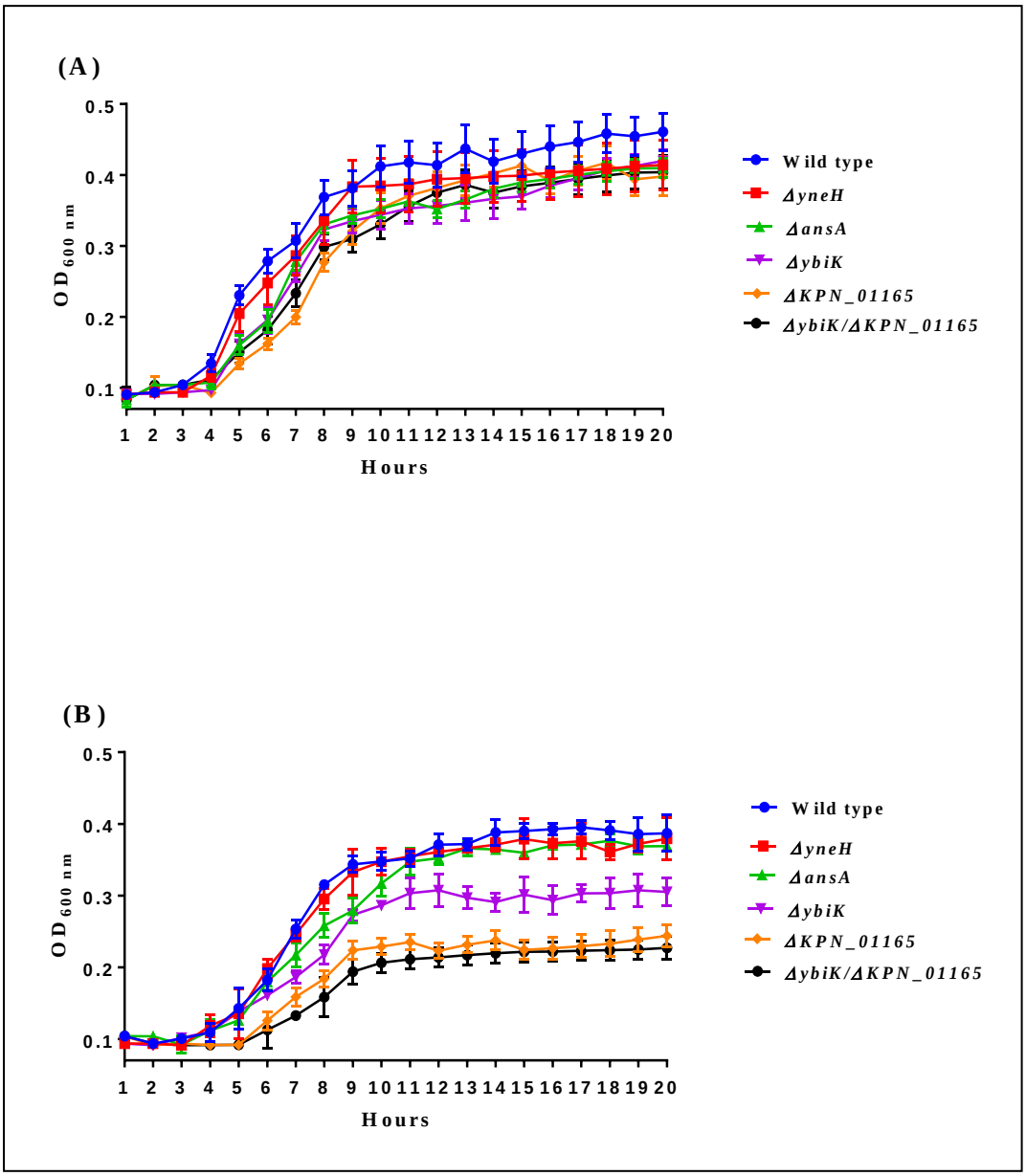

Figure 3.7: *Growth profiles of mutants along with the wild type in M5 and M6 media.* ***A****. The use of 4 mM glutamine does not reveal any phenotypic differences among the strains.* ***B.*** *With 2 mM glutamine* ΔKPN_001165 *and* ΔybiK/ΔKPN_001165 *($p<0.05$) displayed significant differences in growth profiles when compared to the wild type. Each point obtained from three independent experiments each with three replicates and the vertical bars represent SEM.*

Similarly, among strains that were grown in 1 mM glutamine (M7 media), only *ΔKPN_01165* and *ΔybiK/ΔKPN_01165* were significantly attenuated in growth (Figure 3.8 A). In this setting, the growth yield for wild type was 0.38±0.03, while for

ΔKPN_01165 and *ΔybiK/ΔKPN_01165* it was 0.21±0.0, and 0.19±0.02 (both $p<0.01$) (n=3), Table 3.9 and Figure 3.8 A).

Unlike 1 mM glutamine, 0.5 mM glutamine usage led to clear phenotypic differences when *ansA* and *ybiK* were absent. Except for *ΔyneH*, there was a significant difference in growth profiles of all mutant strains compared to wild type strain. For example, the growth yields were 0.36±0.02, 0.20±0.01, 0.18±0.02, 0.14±0.02, 0.16±0.01 for wild type, *ΔansA*, *ΔybiK*, *ΔKPN_001165* and *ΔybiK*/*ΔKPN_001165*, respectively, n=3 ($p<0.05$ for *ΔansA* and *ΔybiK* and $p<0.01$ for *ΔKPN_001165* and *ΔybiK*/*ΔKPN_001165*) (Table 3.9 and Figure 3.8 B). These results may highlight the substantial effect of these gene products in glutamine metabolism. However, the loss of *yneH*, which is a putative glutaminase, had no effect on the ability of *K. pneumoniae* to metabolize glutamine. It seems possible that either *yneH* has no role in glutamine metabolism or the lack of this gene is compensated by the enzymes produced by other glutamine metabolising enzymes.

Table 3.9: K. pneumoniae *growth rate and yield after 20 hours incubation in M7 and M8, containing 2mM glucose plus 1 or 0.5mM glutamine, respectively. The data are average of three independent experiments each in replicates. The comparsion analysis using one-way ANOVA and Dunnett's multiple comparisons test indicate (ns) as not significant, * p<0.05, ** p<0.01, and *** p<0.001 compared to the wild type. The '±' represent SEM.*

Strains	Growth parameters in M7-medium (2 mM glucose plus 1mM glutamine)		Growth parameters in M8 medium (2 mM glucose plus 0.5mM glutamine)	
	Max OD_{600nm}	Growth rate μ (h^{-1})	Max OD_{600nm}	Growth rate μ (h^{-1})
Wild type	0.38±0.03	0.04±0.01	0.36±0.02	0.04± 0.02
ΔyneH	0.35±0.01 (ns)	0.04±0.02 (ns)	0.29±0.03 (ns)	0.03± 0.01 (ns)
ΔansA	034±0.03 (ns)	0.04±0.02 (ns)	0.20±0.01 (*)	0.01± 0.01 (**)
ΔybiK	0.31±0.01 (ns)	0.03±0.02 (ns)	0.18±0.02 (*)	0.01± 0.03 (**)
ΔKPN_01165	0.21±0.01 (**)	0.01±0.03 (**)	0.14±0.02 (**)	0.006± 0.02 (***)
ΔybiK/ΔKPN_01165	0.19±0.02 (**)	0.01±0.02 (**)	0.16±0.01 (**)	0.007± 0.01 (***)

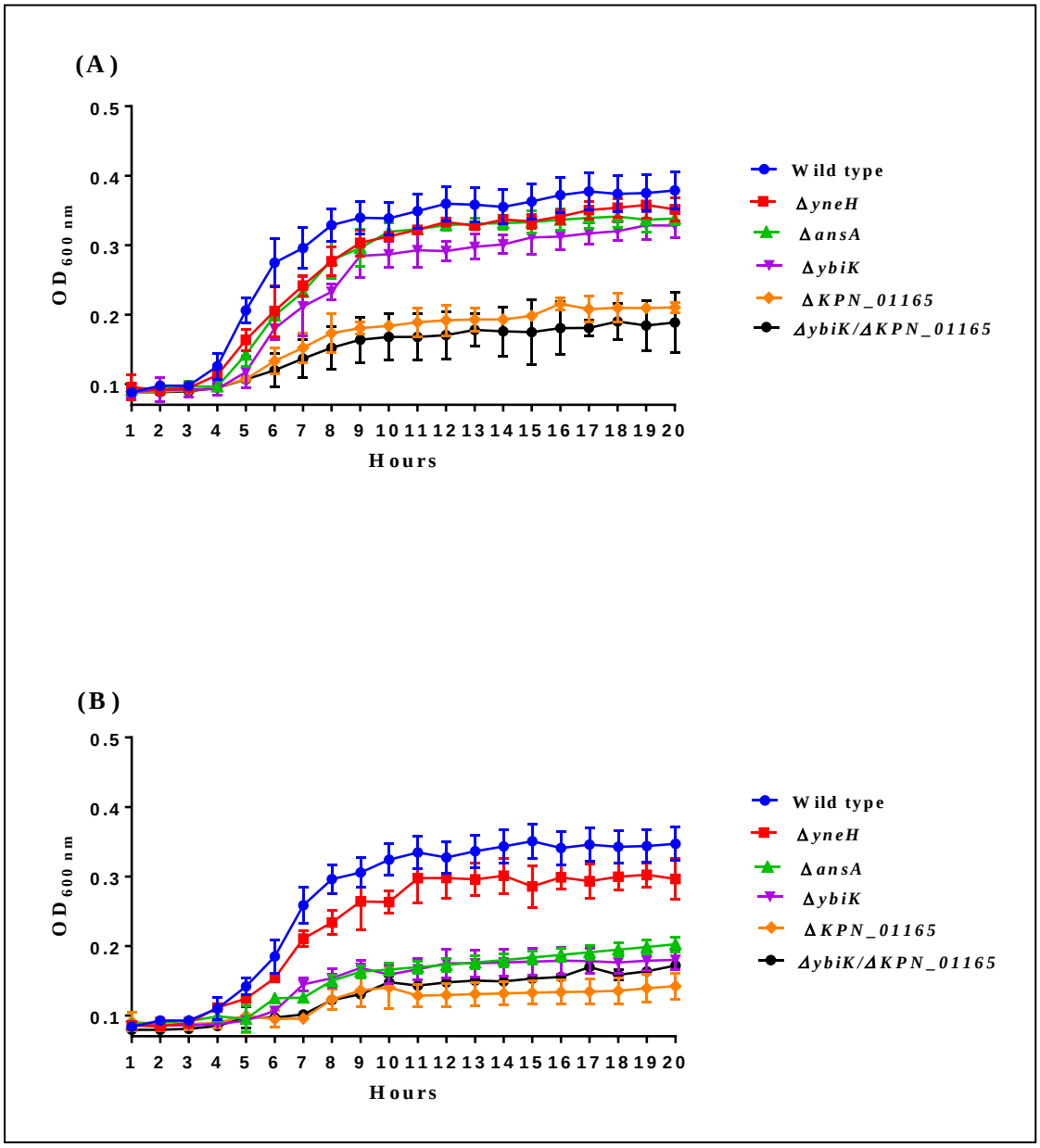

Figure 3.8: *The graphs representing the influence of M7 and M8 media on growth parameters of* ΔyneH, ΔansA, ΔybiK, ΔKPN_001165 *and* ΔybiK/ΔKPN_001165. ***A.*** *Under 1mM glutamine supplement, only* ΔKPN_001165 *and* ΔybiK/ΔKPN_001165 *showed a significant difference in growth rates and yields.* ***B.*** *0.5 mM glutamine leads to the growth attenuation for all mutant strains except* ΔyneH, *relative to the wild type. The resulting curves are average of three independent experiments with three replicates in each. The SEM shown as vertical bars.*

3.14.2 Evaluation of *K. pneumoniae* growth under variable asparagine concentration

The modified M9 medium (M9*) (see section 3.2) contained 4 mM asparagine with 2 mM glucose. The mutant strains did not show any significant growth-related difference compared to the wild type in this medum, either in the growth yield or in the rate ($p>0.05$) (Table 3.10 and Figure 3.9 A). The M10 medium contained 2 mM glucose and 2 mM asparagine and the culture in this medum affected the growth of the *ΔKPN_001165* and *ΔybiK/ΔKPN_001165* mutants whose observed growth rate and yield were significantly different from wild type ($p<0.05$). For example, wild type growth yield was 0.35± 0.01while for *ΔKPN_001165* and *ΔybiK/ΔKPN_001165* the yields were 0.23± 0.02 and 0.21± 0.02, respectively (Table 3.10 and Figure 3.9 B). The *ΔKPN_001165* and *ΔybiK/* behaved similarly toward 2 mM asparagine and 2 mM glutamine supplementation (Figure 3.9 and Figure 3.8, respectively). These results signify the importance of *KPN_01165* in metabolism of both glutamine and asparagine and the growth attenuation may be linked to decrease in asparaginase/glutaminase activity in *ΔKPN_001165* and *ΔybiK/ΔKPN_001165*.

Table 3.10: *The growth rate (μ) and yields of wild type,* ΔyneH, ΔansA, ΔybiK, ΔKPN_01165, ΔybiK/ΔKPN_0116 *in M9* and M10 (contain 2 mM glucose plus 4 or 2 mM asparagine, respectively). The results are the mean of three independent experiments and '±' indicates standard error of means. The results were compared to wild type using ANOVA and Dunnett's multiple comparisons test. 'ns' not significant, * p<0.05.*

Strains	Growth parameters in M9* medium (2 mM glucose plus 4mM asparagine)		Growth parameters in M10 medium (2 mM glucose plus 2mM asparagine)	
	Max OD_{600nm}	Growth rate μ (h^{-1})	Max OD_{600nm}	Growth rate μ (h^{-1})
Wild type	0.37±0.02	0.04± 0.01	0.35±0.01	0.05±0.01
ΔyneH	0.37±0.03 (ns)	0.04± 0.01 (ns)	0.35±0.03 (ns)	0.04± 0.02 (ns)
ΔansA	0.33±0.02 (ns)	0.04± 0.02 (ns)	0.33±0.01 (ns)	0.04± 0.02 (ns)
ΔybiK	0.35±0.03 (ns)	0.04± 0.02 (ns)	0.33±0.03 (ns)	0.03± 0.03 (ns)
ΔKPN_01165	0.34±0.02 (ns)	0.04± 0.01 (ns)	0.23±0.02 (*)	0.02± 0.02 (*)

ΔybiK/ΔKPN_01165	0.33±0.02 (ns)	0.04± 0.02 (ns)	0.21±0.02 (*)	0.02± 0.01 (*)

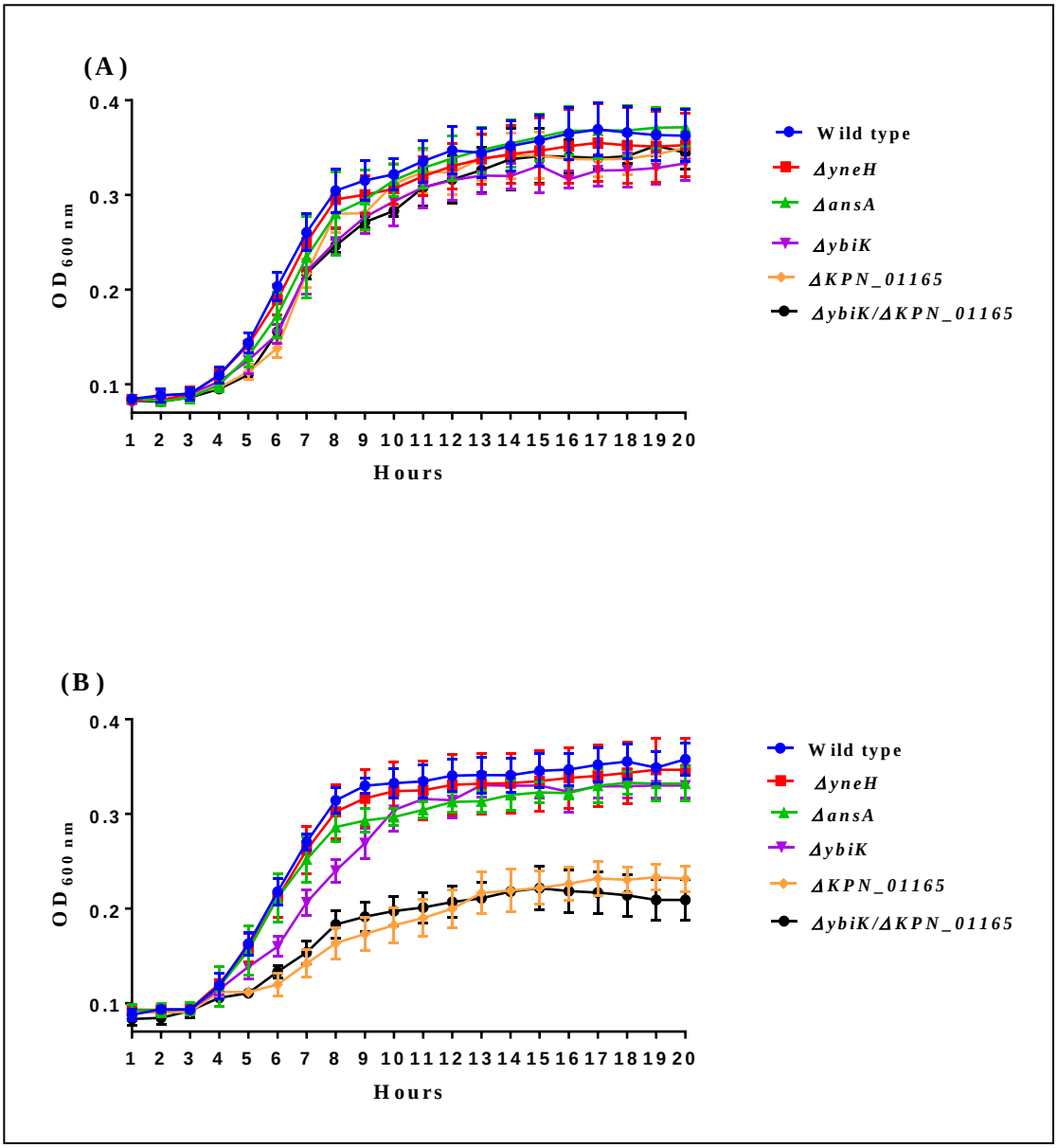

Figure 3.9: *Growth profiles of* K. pneumoniae *strains in* ***M9* and M10 media. A contains*** *4 mM asparagine and no difference in growth among the strains could be observed in this media.* ***B contains*** *2 mM asparagine supplementation.* ΔKPN_001165 *and* ΔybiK/ΔKPN_001165 *showed significance growth attenuation in M10 when compared to the wild type ($p<0.05$) ($n=3$). The growth profiles resulted after three independent experiments with three replicates in each. The vertical bars represent SEM.*

The *ΔyneH* and *ΔansA* growth in M11(that has 2 mM glucose plus 1mM asparagine) was not significantly different from wild type ($p>0.05$) (Table 3.11 and Figure 3.10 A). Furthermore, comparing to the wild type, *ΔKPN_001165* and *ΔybiK/ΔKPN_001165* had significant reduction in growth rate ($p<0.05$) and growth yield ($p<0.01$) (Table 3.11 and Figure 3.10 A). 1 mM asparagine supplementation in M11 caused the *ΔybiK* to produce significant difference in growth rate (0.02 $h^{-1}\pm$ 0.02, n=3) and growth yield (0.20±0.02, n=3) comparing to wild type growth rate and yield (0.04 $h^{-1}\pm$ 0.01 and 0.34±0.03, n=3 respectively) ($p<0.05$) (Table 3.11 and Figure 3.10 A).

No difference between the parent strain and *ΔyneH* could be detected in M12, which had 0.5 mM asparagine and 2 mM glucose ($p>0.05$). The growth rate observed for the wild type was 0.03 $h^{-1}\pm$ 0.01 (n=3) and for *ΔyneH,* it was 0.03 $h^{-1}\pm$ 0.01 ($p>0.05$). On the other hand, all other mutants had an attenuated growth rate and yield compared to wild type. As shown in Table 3.11, the growth rate of *ΔansA,* and *ΔybiK,* were 0.01 $h^{-1}\pm$ 0.02, 0.01 $h^{-1}\pm$ 0.02 (n=3), respectively compared to wild type (0.03 $h^{-1}\pm$ 0.01, n=3) ($p<0.05$). Moreover, the other two strains, *ΔKPN_001165* and *ΔybiK/ΔKPN_001165*, had the growth rate of 0.007 $h^{-1}\pm$ 0.01 and 0.005 $h^{-1}\pm$ 0.02 (n=3), respectively when compared to wild type ($p<0.01$) (Table 3.11 and Figure 3.10 B). A likely explanation of these results that asparaginase activity of *ΔansA, ΔybiK, ΔKPN_001165* and *ΔybiK/ΔKPN_001165* has been affected and 0.5 mM asparagine is not sufficient for supporting the cell growth.

Table 3.11. *Growth profiles of* K. pneumoniae *strains in M11 and M12. The kinetics represented as max growth at* OD_{600nm} *and growth rate* μ (h^{-1}) *which were obtained from three independent experiments each with three replicates. SEM shown as '±'. The values were compered to wild type by one-way ANOVA and Dunnett's multiple comparisons test. 'ns' not significant * p<0.05, and ** p<0.01.*

Strains	Growth parameters in M11 medium (2 mM glucose plus 1mM asparagine)		Growth parameters in M12 medium (2 mM glucose plus 0.5mM asparagine)	
	Max OD_{600nm}	Growth rate μ (h^{-1})	Max OD_{600nm}	Growth rate μ (h^{-1})
Wild type	0.34±0.03	0.04± 0.01	0.28±0.03	0.03± 0.01
ΔyneH	0.33±0.02 (ns)	0.04± 0.01 (ns)	0.28±0.02 (ns)	0.03± 0.0 (ns)
ΔansA	0.32±0.01 (ns)	0.03± 0.02 (ns)	0.19±0.01 (*)	0.01± 0.02 (*)
ΔybiK	0.20±0.02 (*)	0.02± 0.02 (*)	0.18±0.02 (*)	0.01± 0.02 (*)
ΔKPN_01165	0.18±0.02 (*)	0.01± 0.01 (**)	0.14±0.02 (**)	0.007± 0.01 (**)
ΔybiK/ΔKPN_01165	0.18±0.01 (*)	0.01± 0.02 (**)	0.14±0.01 (**)	0.005± 0.02 (**)

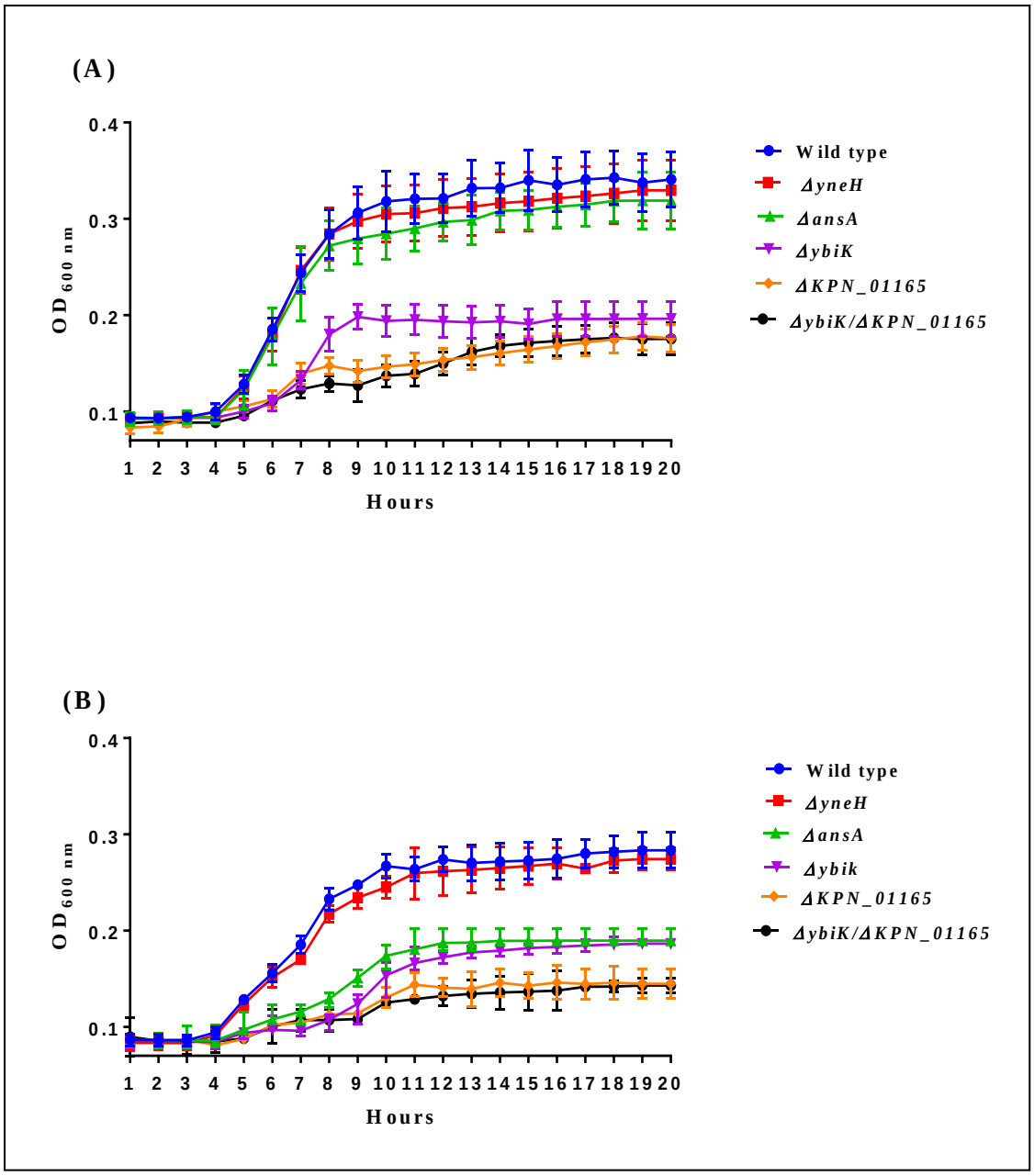

Figure 3.10: *Growth of* K. pneumoniae *KR3167 parent and mutants in M11 and M12.* ***A has*** *1 mM asparagine which cause a growth attenuation in* ΔybiK, ΔKPN_001165 *and* ΔybiK/ΔKPN_001165 *relative to the wild type.* ***B contains*** *0.5 mM asparagine in which all mutants except* ΔyneH *exhibited significance difference in growth profiles when compared to the wild type. The vertical bars represent SEM of three indebdent experiments with triplicate in each.*

3.15 Glutamine and asparagine as sole source of carbon and nitrogen sources for *K. pneumoniae* KR 3167 strains

It has been claimed that *K. pneumoniae* can utilize amino acids as a sole source of carbon and nitrogen (Streicher *et al.*, 1974). To test this, M13 and M14 media were used to test wild type and mutants. M13 and M14 does not have any glucose, and contains 10 mM glutamine and 10 mM asparagine, respectively. In either M13 or M14 media compared to wildtype all the mutants were attenuated in growth rate and yield ($p<0.05$), except *ΔyneH,* which grow similarly to the wild type ($p>0.05$) (Table 3.12 and Figure 3.11 A and B. For example, in M13 the growth rates of *ΔansA ΔybiK, ΔKPN_01165,* and *ΔybiK/ΔKPN_01165* were 0.009 $h^{-1}\pm$ 0.02, 0.009 $h^{-1}\pm$ 0.03, 0.005 $h^{-1}\pm$ 0.02, and 0.005 $h^{-1}\pm$ 0.02, n=3, respectively, were significantly lower than the wild type growth rate (0.014 $h^{-1}\pm$ 0.01, n=3) ($p<0.05$) (Table 3.12 and Figure 3.11 A). Furthermore, the asparagine in M14 did not support *ΔansA, ΔybiK, ΔKPN_01165, ΔybiK/ΔKPN_01165* as the growth yields were 0.12±0.02, 0.12±0.01, 0.11±0.01, and 0.11±0.02, n=3, respectively and that was significantly lower than the wild type growth yields (0.20±0.01, n=3) ($p<0.05$) (Table 3.12 and Figure 3.11 B).

From all growth studies it can be concluded that growth kinetics of *K. pneumoniae* KR3167 strains are highly dependent on media nitrogen composition as well as the concentration of carbon sources. For example, when glucose is present at 20 mM, no difference among the mutants and the wild type could be obtained (Figure 3.5 A and B). However, the mutants' growth profiles are affected when glucose concentration is reduced, and the source of N was limited. This suggests that *ΔansA*, *ΔybiK*, *ΔKPN_001165* and *ΔybiK*/*ΔKPN_001165* have a role in metabolism of asparagine and glutamine for *K. pneumoniae*. To rule out any polar effect of mutation on these observed phenotypes, the genetically complemented strains and wild type were created and cultured in M13 and M14. M13 and M14 were chosen as they have glutamine and asparagine as sole source of carbon and nitrogen. All mutants (except *ΔyneH*) have shown phenotype in those media represented as attenuated growth rates and yields ($p<0.05$) (Table 3.12). The results in Table 3.13 and Figure 3.12 showed that there were no significant differences in calculated growth yields and rates of growth of the *cis* complemented *ΔyneH*, *ΔansA*, *ΔybiK*, and *ΔKPN_01165* mutants when compared with wild type ($p>0.05$) (Table 3.13). In comparison to growth yield of *ΔKPN_001165* in M13 (0.11±0.01, n=3), *cis*-complementation of *KPN_001165* in *ΔKPN_001165* mutant

reconstituted growth yield to 0.20±0.01, n=3, which is almost similar to the wild type growth yield (0.21±0.01) ($p>0.05$) (Table 3.12 and Table 3.13, respectively). Similarly, after the growth in M14 *cis*-complementation of *ansA in ΔansA*, and *ybiK in ΔybiK,* mutant strains restored the growth kinetics to wild type level (0.19±0.02, 0.18±0.01 and 0.19±0.01, n=3, respectively) ($p>0.05$) (Table 3.13, and Figure 3.12 B).

Table 3.12: K. pneumoniae *growth rate and yields in M13 and M14 media. The results were compared to wild type and they are average of three independent experiments each with three replicates. The '±' symbol indicates SEM. The statistical analysis used one-way ANOVA and Dunnett's multiple comparisons test. 'ns', not significant, *p<0.05.*

Strains	Growth parameters in M13 medium (10mM glutamine)		Growth parameters in M14 medium (10mM asparagine)	
	Max OD_{600nm}	Growth rate μ (h^{-1})	Max OD_{600nm}	Growth rate μ (h^{-1})
Wild type	0.21±0.02	0.014± 0.01	0.20±0.01	0.013± 0.01
ΔyneH	0.20±0.02 (ns)	0.014± 0.02 (ns)	0.19±0.01 (ns)	0.013± 0.01 (ns)
ΔansA	0.13±0.02 (ns)	0.009± 0.02 (ns)	0.12±0.02 (*)	0.006± 0.02 (*)
ΔybiK	0.13±0.01 (*)	0.009± 0.03 (ns)	0.12±0.01 (*)	0.005± 0.02 (*)
ΔKPN_01165	0.11±0.01 (*)	0.005± 0.02 (*)	0.11±0.01 (*)	0.004± 0.01 (*)
ΔybiK/ΔKPN_01165	0.11±0.02 (*)	0.004± 0.01 (*)	0.11±0.02 (*)	0.003± 0.02 (*)

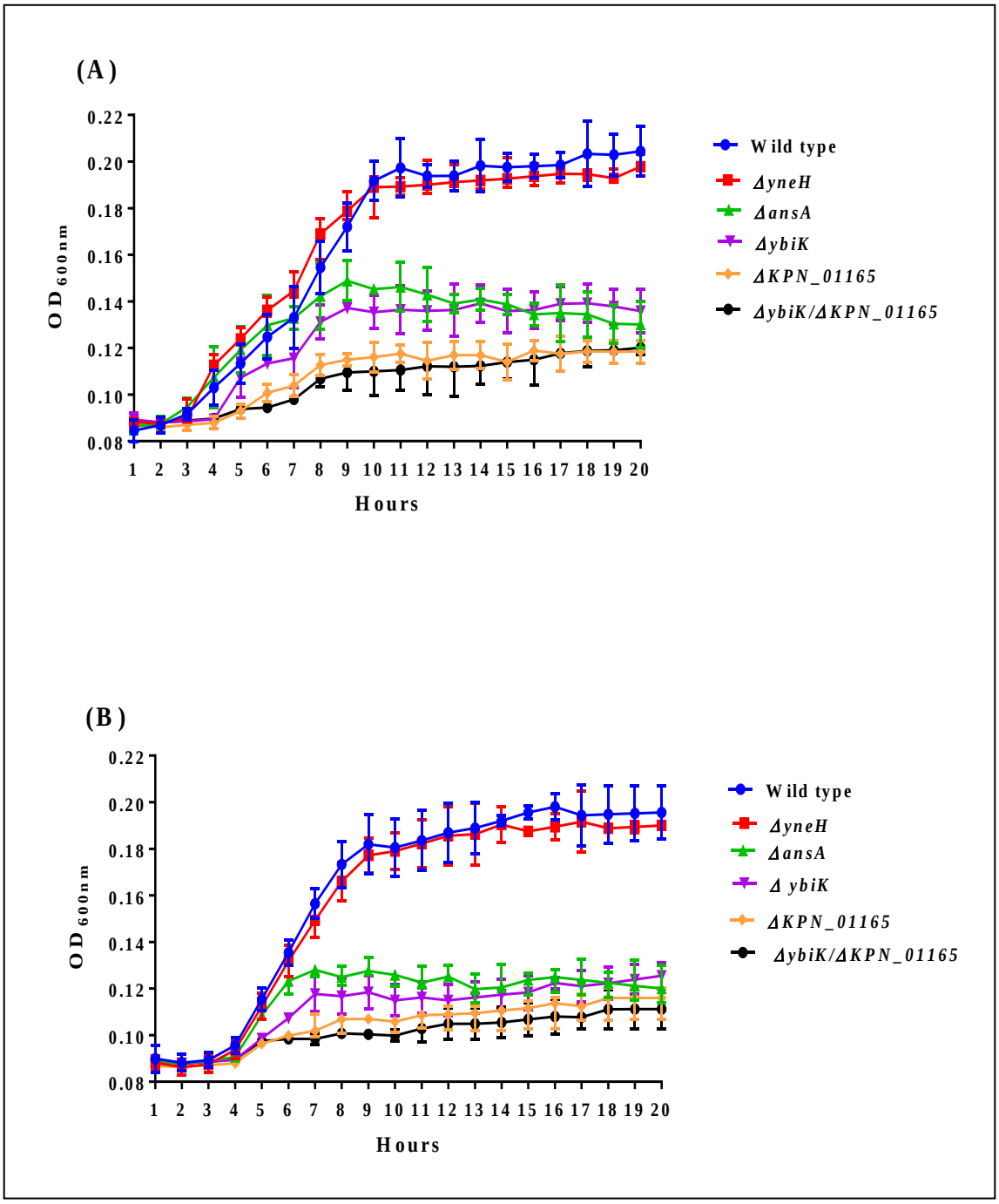

Figure 3.11: *Growth profiles of* K. pneumoniae *strains grown in 10 mM glutamine and 10 mM asparagine in M13 and M14 media, respectively. In both* ***A*** *(M13) and* ***B*** *(M14), all strains, except* ΔyneH, *showed significant difference than the wild type one in their growth profiles (p<0.05) (n=3). The SEM represented as vertical bars.*

Table 3.13: *Calculated growth rate and yields of cis-complemented mutants grown in M13 and M14 media. The results were compared to wild type with one-way ANOVA and Dunnett's multiple comparisons test. The results are average of three independent experiments with three replicates in each and '±' symbol indicates SEM. 'ns', not significant.*

Strains	Growth parameters in M13 medium (10mM glutamine)		Growth parameters in M14 medium (10mM asparagine)	
	Max OD_{600nm}	Growth rate μ (h^{-1})	Max OD_{600nm}	Growth rate μ (h^{-1})
Wild type	0.21±0.01	0.014± 0.01	0.19±0.01	0.013± 0.01
Cis-yneH in *ΔyneH*	0.20±0.01 (ns)	0.014± 0.02 (ns)	0.19±0.01 (ns)	0.013± 0.01 (ns)
Cis-ansA in *ΔansA*	0.20±0.01 (ns)	0.014± 0.02 (ns)	0.19±0.02 (ns)	0.013± 0.02 (ns)
*Cis-ybiK i*n *ΔybiK*	0.19±0.02 (ns)	0.014± 0.03 (ns)	0.18±0.01 (ns)	0.013± 0.02 (ns)
Cis- KPN_01165 in *ΔKPN_01165*	0.20±0.01 (ns)	0.012± 0.02 (ns)	0.19±0.01 (ns)	0.013± 0.01 (ns)

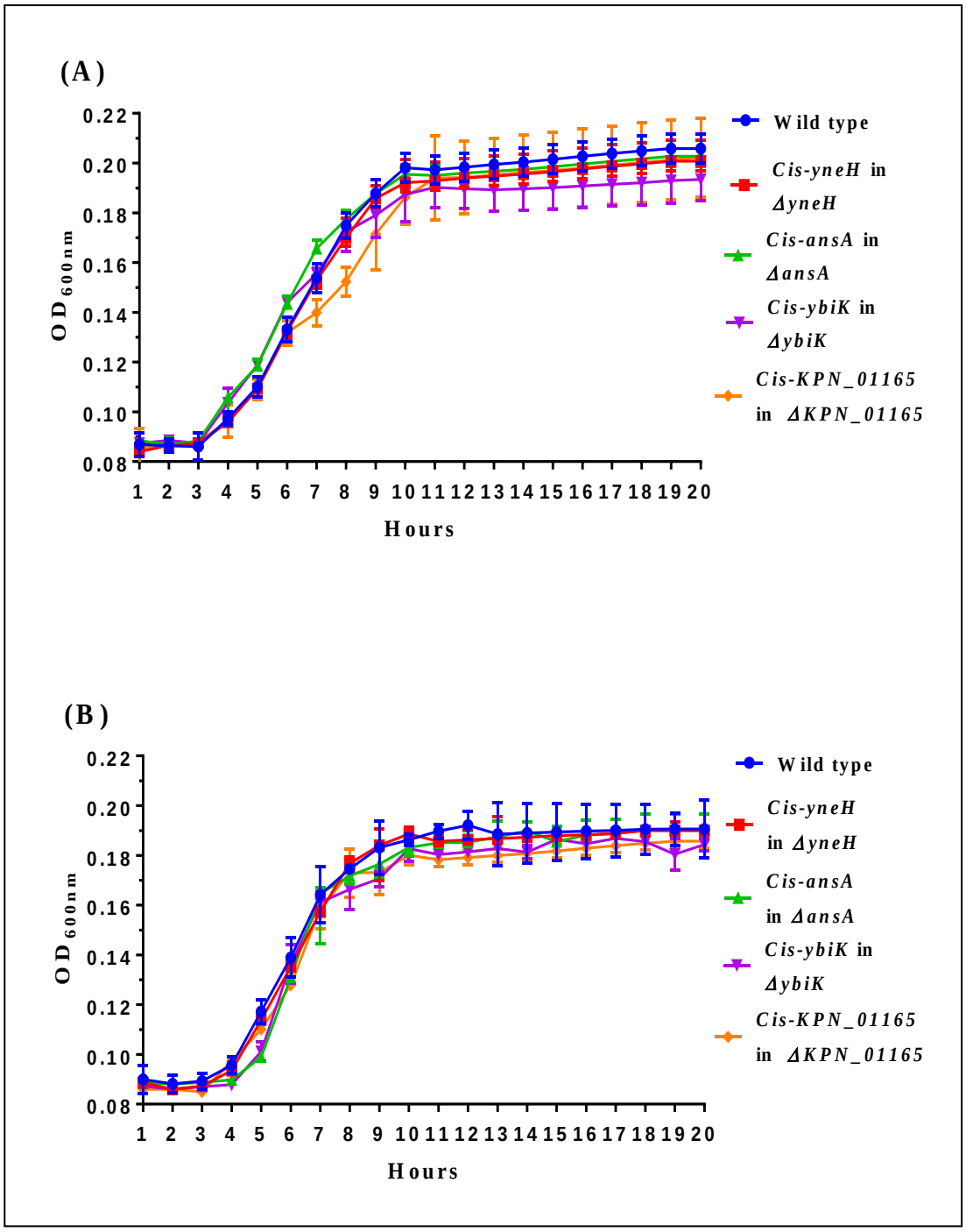

Figure 3.12: *Growth profiles of cis-complemented strains gown in 10 mM glutamine and 10 mM asparagine in M13 and M14, respectively. In both* ***A*** *(M13) and* ***B*** *(M14), all strains showed no significant difference on their growth comparing to wild type growth (p>0.05) (n=3). The curves are produced from three independent experiments with three replicates in each and the vertical bars indicates SEM.*

3.16 Determination of glutaminase and asparaginase activity

Colorimetric determination (Nessler's reagent) of NH_3, which is a reaction product of glutaminase and asparaginase, would give a clear indication of the hydrolysing activity of asparaginase/glutaminase. For this assay, I did a series of optimisation experiments as described below.

3.16.1 Optimization of glutaminase and asparaginase reactions

Glutaminase and asparaginase enzymatic reactions were optimized using wild type crude extract as described in section 3.5.4. The wild type crude extract was obtained from cells grown overnight in 10 mM glutamine or asparagine in which glutaminase and asparaginase activities were measured, respectively. For the glutaminase reaction 0-6 mM glutamine plus wild type crude extract (grown in 10 mM glutamine) were incubated at 37 ^{O}C. At 0 time point a 50 µl aliquot of Nessler's reagent was added and the blank reading at absorbance 450 nm was recorded. Then at 10 minutes intervals up to 80 minutes, the reaction mixtures were incubated at 37 ^{O}C in a microtiter plate. Then, the Nessler's reagent was added at predetermined time periods to record the absorbance at 450 nm using a plate reader. The asparaginase reaction contained asparagine in different concentrations and the crude extracts were obtained from cells grown in 10 mM asparagine. As shown in Figure 3.13.A and B, the optimal recording point was found to be 50 minutes in which the recorded readings plateaued. Furthermore, the maximum glutamine concentration was found to be 4 mM as the readings in the higher concentrations (5 mM, 6 mM, 7 mM and 8 mM) did not increase the total activity. However, 5 mM asparagine was the maximum concentration for the asparaginase (Figure 3.13 B). Following these experiments, I decided to test the mutants in an assay setting that used 0-6 mM of either asparagine or glutamine and 50 min incubation time. The 50 minutes was chosen because the readings (at 450 nm) after this time point have reached a plateau status (Figure 3.13). The enzyme kinetic activities (*Vmax* and *Km*) in the wild type, *ΔyneH*, *ΔansA*, *ΔybiK, ΔKPN_01165, ΔybiK/ΔKPN_01165* were calculated by plotting velocity against substrate concentration in a non-linear regression analysis using the Michaelis Menten model (Prism Graph Pad 7.4).

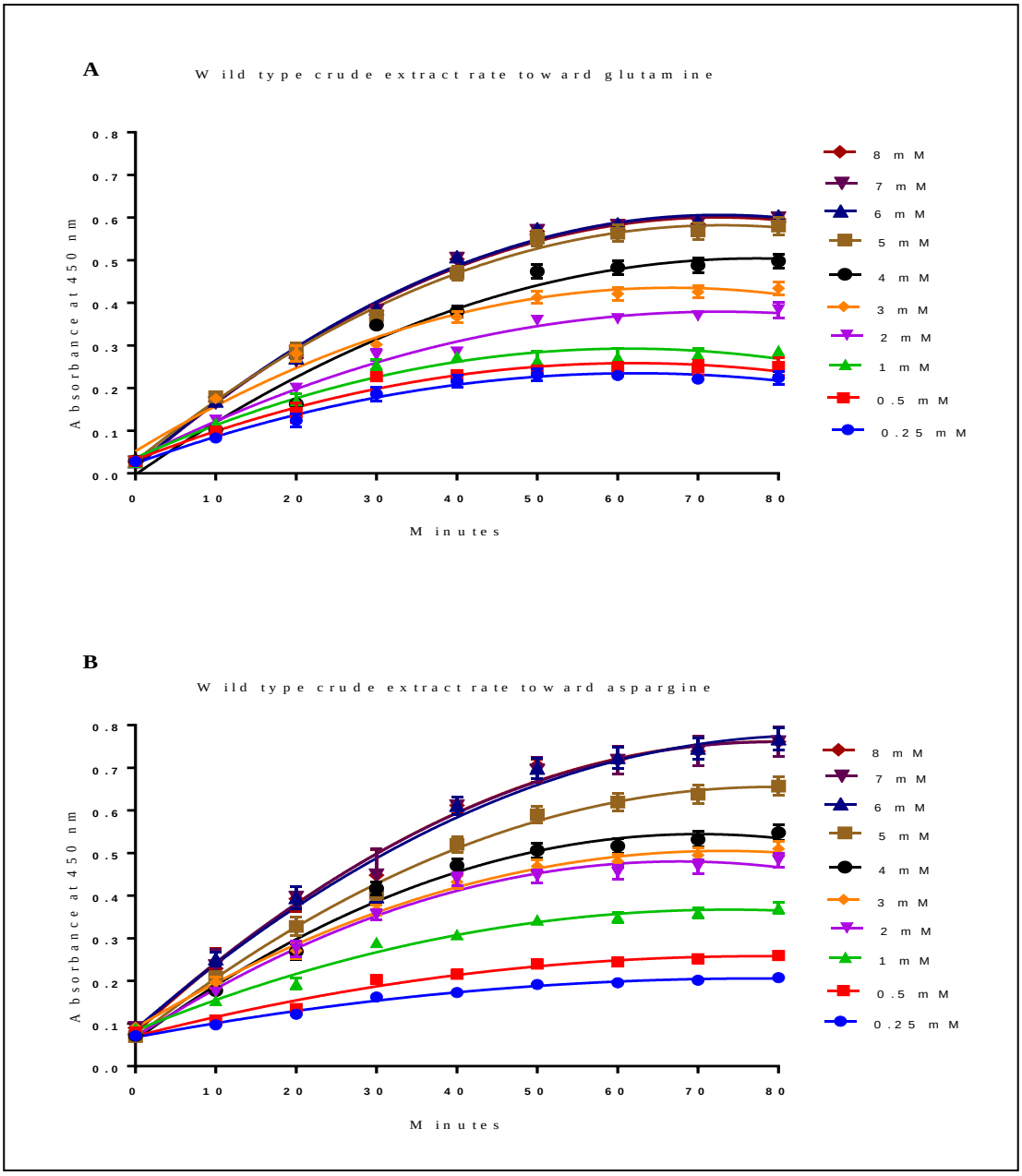

Figure 3.13: *Optimisation of glutaminase* ***(A)*** *and asparaginase enzyme assays* ***(B)****. Nessler's reagent was used to determine* NH_3*. For the assays the crude cell lysates were obtained from cultures grown either in the presence of 10 mM glutamine (A) or 10 mM asparagine (B). The vertical bars represent the standard error of means of three independent experiments with duplicate in each.*

3.16.2 *K. pneumoniae* KR3167 asparaginase and glutaminase activities

The wild type, *ΔyneH*, *ΔansA*, *ΔybiK, ΔKPN_01165, ΔybiK/ΔKPN_01165* were grown overnight in M13 (10 mM glutamine) or M14 (10 mM asparagine) statically at 37 ^{O}C.

Next day the cultures were washed twice with PBS before the sonication step as described in section 3.5.1. The protein concentration in cell lysates was adjusted to 1 mg/ml as described in section 3.5.2. Then in microtiter plate the asparaginase and glutaminase activities were measured by adding asparagine or glutamine as described in section 3.5.4. As shown Figures 3.14 and 3.15, all mutants except *ΔyneH* had attenuated glutaminase and asparaginase activities relative to the wild type ($p>0.05$) (Table 3.14, Figure 3.14, and Figure 3.15). On the other hand, the total glutaminase and asparaginase *Vmax* (maximum velocity) in other mutants was significantly different than the wild type. The *ΔKPN_01165* and *ΔybiK/ΔKPN_01165* mutants had the lowest mean glutaminase activity readings, approximately 8 U, almost a third that of wild type 24 U ($p< 0.05$) (Table 3.14 and Figure 3.14). Furthermore, the crude lysates of *ΔKPN_01165* and *ΔybiK/ΔKPN_01165* showed significantly lower affinity toward glutamine as a substrate as the *Km* values (1.66 mM± 0.34, and 1.96 mM± 0.22 n=3, respectively) were significantly different from in the values observed in the wild type extract, a *Km* value of 0.59 mM ± 0.92 ($p<0.05$) (Table 3.14 and Figure 3.14). However, there was no significant difference in asparaginase *Km* values between *ΔKPN_01165, ΔybiK/ΔKPN_01165* and wild type (1.20 mM± 0.19, and 1.13 mM± 0.16, and 0.69 mM ± 0.09 n=3, respectively) ($p>0.05$) (Table 3.14 and Figure 3.15).

Table 3.14: *Representation of calculated* Vmax *(U) and* Km *(mM) for* K. pneumoniae *KR3167 strains. Glutaminase activity assay used the lysates of cells grown in glutamine containing media and asparaginase activity was calculated using asparagine plus crude extract of cells grown in asparagine. The results were compared to wild type and are average of three independent experiments with three replicates in each. '±' represents SEM. 'ns' not significant, *p<0.05 and **p<0.01.*

Strains	Glutaminase		Asparaginase	
	Vmax (U)	*Km* (mM) glutamine	*Vmax* (U)	*Km* (mM) asparagine
Wild type	24.39±0.88	0.59± 0.92	18.87±0.52	0.69± 0.09
ΔyneH	21.23±1.12 (ns)	0.70± 0.15 (ns)	17.92±0.39 (ns)	0.74± 0.07 (ns)
ΔansA	15.17±0.56 (*)	1.09± 0.14 (ns)	9.52±0.29 (*)	0.92± 0.11 (ns)
ΔybiK	13.94±0.62 (*)	1.41± 0.19 (ns)	10.21±0.39 (*)	0.75± 0.11 (ns)
ΔKPN_01165	8.38±0.54 (**)	1.66± 0.34 (*)	6.93±0.28 (*)	1.20± 0.19 (ns)
ΔybiK/ΔKPN_01165	7.82±0.60 (**)	1.96± 0.22 (*)	8.01±0.36 (*)	1.13± 0.16 (ns)

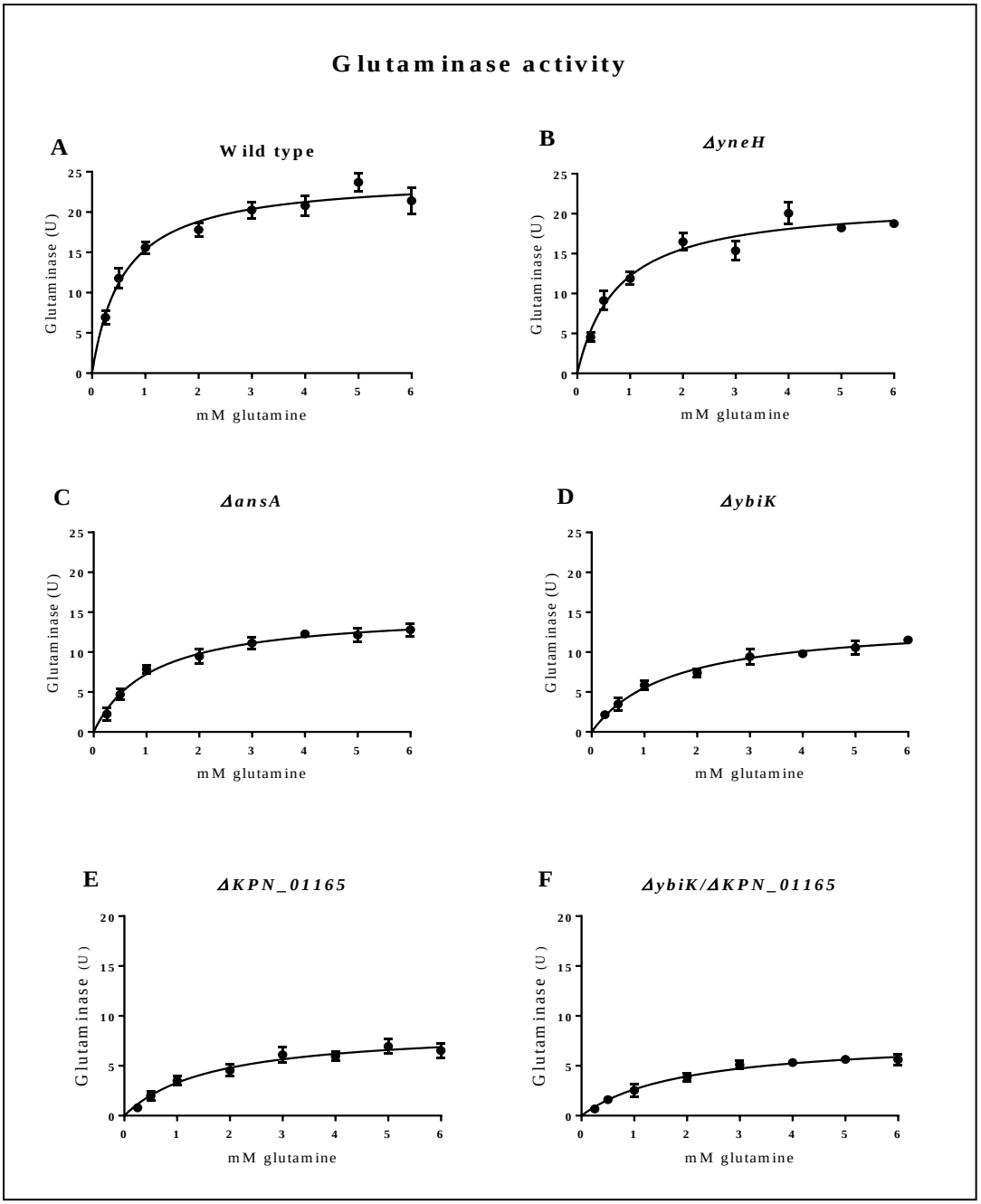

Figure 3.14: *Glutaminase activity determination in wild type,* ΔyneH, ΔansA, ΔybiK, ΔKPN_01165, ΔybiK/ΔKPN_01165 *(A, B, C, D, E, and F, respectively). Each point represents the mean of three independent experiments, each with 3 replicates. From these*

curves, Km *and* Vmax *were calculated using non-linear regression model in GraphPad Prism version 7.4.*

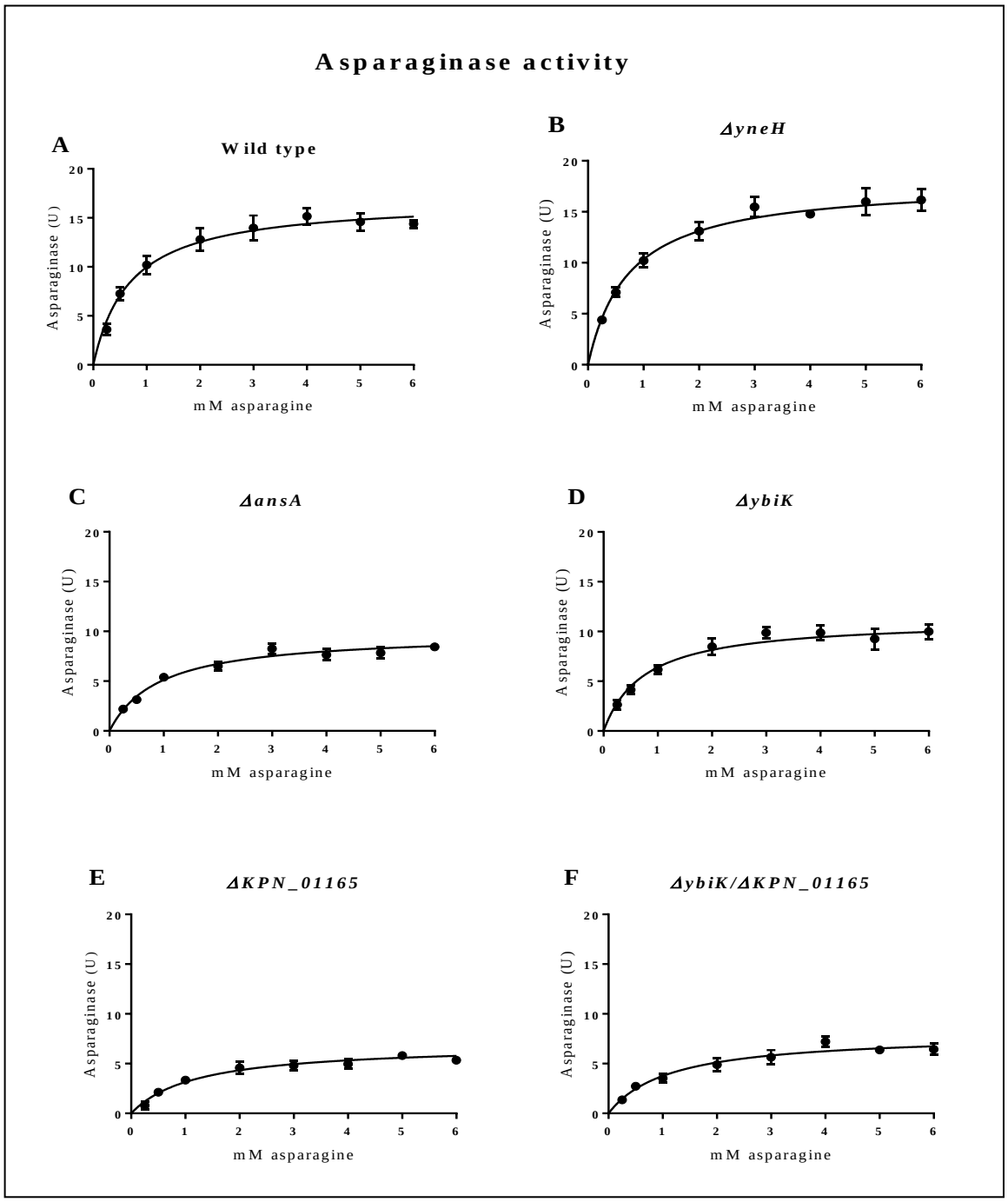

Figure 3.15: *Asparaginase activity determination in wild type,* ΔyneH, ΔansA, ΔybiK, ΔKPN_01165, ΔybiK/ΔKPN_01165 *(A, B, C, D, E, and F, respectively). Each point represents the mean of three independent experiments, each with 3 replicates. From these curves,* Km *and* Vmax *were calculated using non-linear regression model in GraphPad Prism version 7.4.*

3.16.3 Enzyme activity in *cis*-complemented strains

To verify that reduction in asparaginase and glutaminase activity in *ΔansA*, *ΔybiK, ΔKPN_01165, ΔybiK/ΔKPN_01165* did not result from a polar effect of mutation, the glutaminase and asparaginase activities in *cis*-complemented *ΔansA*, *ΔybiK, ΔKPN_01165, ΔybiK/ΔKPN_01165* were also determined. The *cis*-complemented *ΔyneH* was excluded because *ΔyneH* did not show any reduction in asparaginase or glutaminase activity compared to the wild type strain (section 3.16.2). The results in Table 3.15, Figure 3.16 and Figure 3.17 showed that glutaminase and asparaginase (represented in *Vmax* (U) and *Km*) of *Cis-ansA* in *ΔansA*, *Cis-ybiK i*n *ΔybiK*, and *Cis- KPN_01165* in *ΔKPN_01165* were not significantly different from glutaminase and asparaginase activities of the wildtype parent strain ($p>0.05$). This restoration of activity indicates the phenotypes observed were not the result of a polar mutation.

Table 3.15: *Table represents calculated* Vmax *(U) and* Km *(mM) for cis-complemented* K. pneumoniae *KR3167 strains. Glutaminase and asparaginase activities were measured in crude extract of cells grown in either glutamine or asparagine, respectively (M13 and M14, respectively). The results represent the mean of at least 3 experiments, each in triplicates. '±' is SEM. 'ns', not significant (p>0.05).*

Strains	Glutaminase		Glutaminase	
	Vmax (U)	*Km* (mM) glutamine	Vmax (U)	*Km* (mM) asparagine
Wild type	23.87±0.81	0.51± 0.08	17.34±0.59	0.73± 0.12
Cis-ansA in *ΔansA*	22.07±0.95 (ns)	0.57± 0.11 (ns)	18.05±0.63 (ns)	0.86± 0.13 (ns)
*Cis-ybiK i*n *ΔybiK*	20.61±0.85 (ns)	0.64± 0.21 (ns)	16.58±0.62 (ns)	0.69± 0.10 (ns)
Cis- KPN_01165 in *ΔKPN_01165*	23.53±1.23 (ns)	0.75± 0.16 (ns)	20.72±1.12 (ns)	0.80± 0.15 (ns)

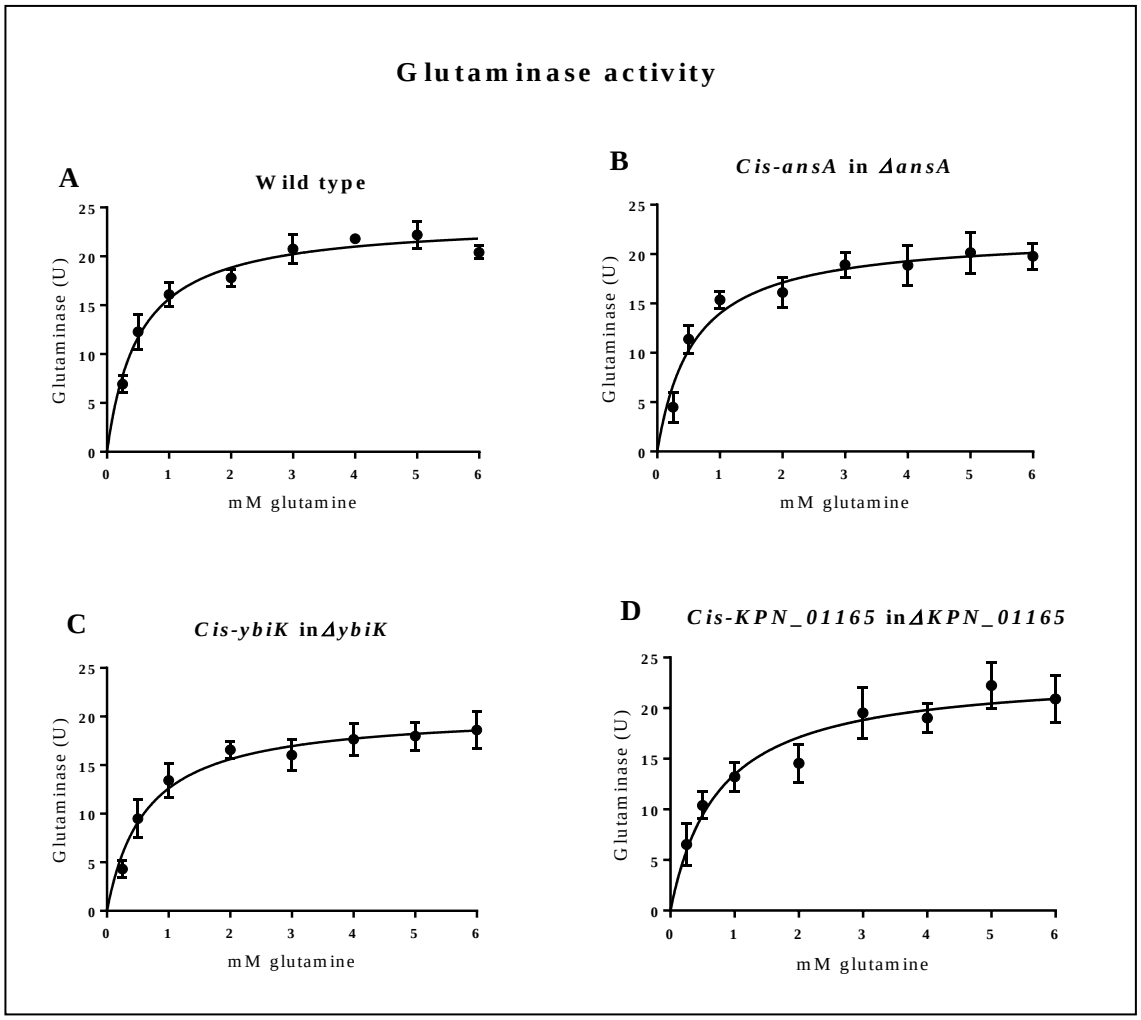

Figure 3.16: *Determination of glutaminase activities in the crude lysates of wild type and cis-complemented strains. The curves represent means of three independent experiments, each in triplicates.*

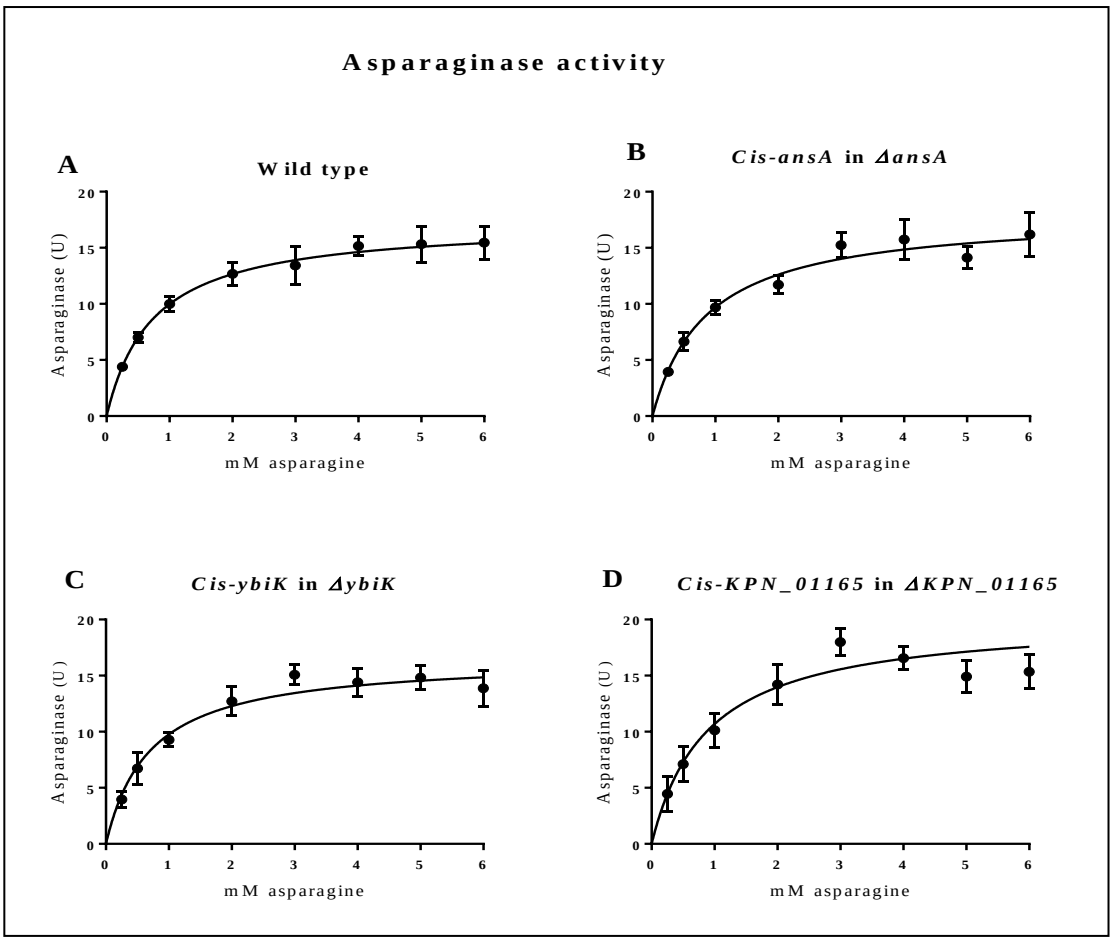

Figure 3.17: *Determination of asparaginase activity for wild type and cis-complemented strains. The curves represent means of three independent experiments, each in triplicates.*

3.17 Overexpression and purification of KPN_01165

The previous results suggested that KPN_01165 coded a protein with asparaginase and glutaminase activities, and it has the largest contribution for total activity. In addition, in its absence, the mutant had the most reduced growth rate and yield. Therefore, I decided to clone and express KPN_01165 to study in isolation its enzyme kinetics.

3.17.1 Construction of a recombinant KPN_01165 strain

The largest reduction in glutaminase and asparaginase activity was observed with *ΔKPN_01165* indicating that KPN_01165 is the main gene coding for glutaminase and asparaginase. Therefore, KPN_01165 was chosen for detailed characterisation, including kinetic analysis and substrate specificity. The cloned plasmid (KPN_01165-pLEICS-01) was extracted from *E. coli* KPN_01165 pLEICS-01-One Shot® TOP10 as described in section 2.6.2 and transformed into *E. coli* BL21 (DE3) pLysS competent cells for protein

expression as described in section 3.6.2. Agarose gel analysis after PCR reaction using the primers in Table 3.2 confirmed the successful KPN_01165 transformation (Figure 3.18). The KPN pro-FP and KPN pro-RP primers set would be expected to produce an approximately 1 kb band. Subsequently, the recombinant vector was isolated and sent to PNACL for sequencing.

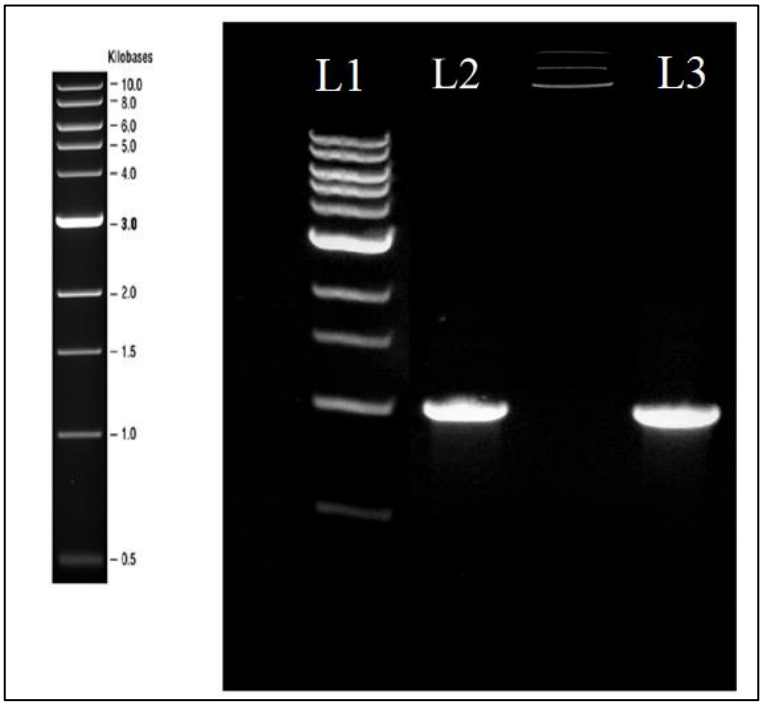

Figure 3.18: *A gel electrophoresis representing a successful transformation of the recombinant plasmid (KPN_01165-pLEICS-01) to* E. coli *BL21 (DE3) pLysS competent cells. L1 500 ng 1 kb DNA ladder (NEB); L2 and L3 (~ 1 kb) that represent* KPN_01165*, the lanes contained between 40-100 ng DNA. Full primer sequences are listed in Table 3.2.*

3.17.2 Expression and purification of KPN_01165

In small scale expression it was determined that the optimal incubation temperature is 37°C, and the optimal IPTG concentration is 1 mM as described in section 3.6.3. For large scale expression, triplicate 1l LB media were inoculated with positive KPN_01165pLEICS-01*E. coli* BL21 and grown until OD_{600} reached 0.6. Then 1 mM IPTG was added and the cultures were re-incubated at 37ºC for another 8 hours until the OD_{600} reached 1.6. Subsequently, the steps in section 3.6.4 were followed and the cell extracts were eluted with different concentrations of imidazole buffer, 50, 100, 200, 300, and 500 mM (Figure 3.19 A L2, L3, L4, L5, and L6, respectively). The purified protein

was analysed by SDS-PAGE, and the gel was stained with Coomassie Blue. The Figure 3.19 A demonstrated that KPN_01165 was expressed in a soluble state and purified with 300 mM and 500 mM of imidazole elution buffer L5 and L6, respectively. The SDS-PAGE analysis showed the expected size for the KPN_01165 protein which had an expected molecular weight of approximately 38.6 kDa (Figure 3.19 A L5, and L6, respectively). The size of the fusion enzyme was more than the expected size of the enzyme. This was due to the fusion of the C-terminal His tag (840 Da) and TEV (Tobacco Etch Virus) cleavage site (957 Da) of the pLEICS-01 vector (Figure 3.19 A L5, and L6, respectively). Afterward, to remove any remaining imidazole the recombinant protein was dialysed against the elution buffers treatment (20 mM Tris, 150 mM NaCl, pH 7.45) buffer (Section 3.6.6) and KPN_01165 was concentrated and visualised using SDS-PAGE (Figure 3.19 B L2 and L3).

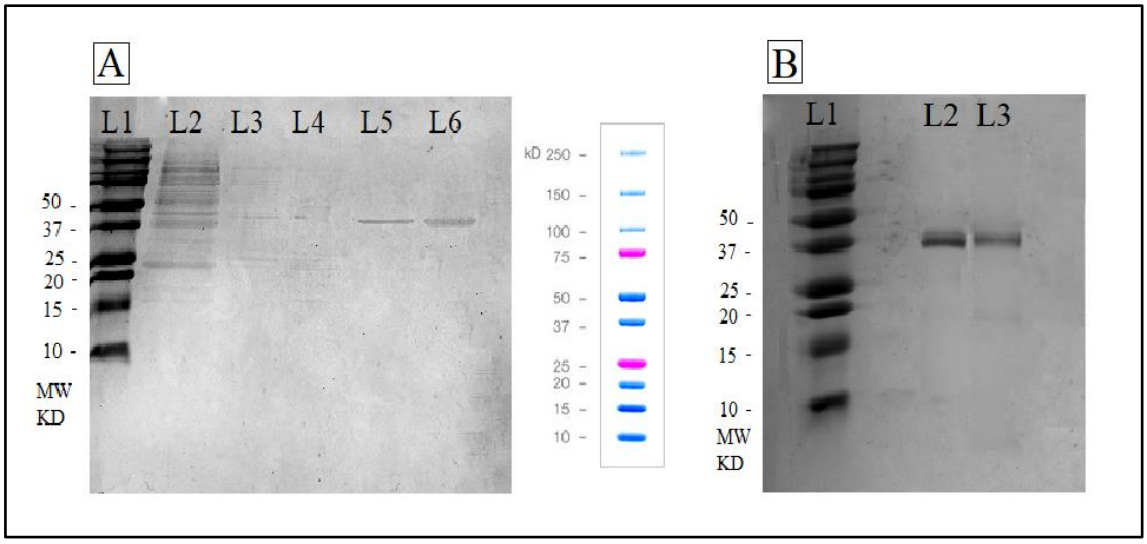

Figure 3.19: A. *SDS-PAGE analysis showing the purified fractions of* E. coli *BL21. A. The cell lysates were eluted with increasing concentrations of imidazole 50, 100, 200, 300, and 500 mM, Lanes 2-6 respectively. Lanes 5 and 6 represent KPN_01165 (38.6 kDa) after elution with 300 mM and 500 mM imidazole (respectively); L1 protein molecular weight marker (Bio-Rad, UK).* ***B*** *SDS-PAGE analysis showing the dialyzed and concentrated purified KPN_01165 (38.86 kDa) (Lane 2 and 3). Gel was stained with Coomassie brilliant blue.*

3.17.3 Kinetic characterisation of recombinant KPN_01165

The optimal pH and temperature for measuring the enzyme activity of the KPN_01165 protein was determined as described in section 3.6.8. Briefly, the enzyme (200 µg/ml

KPN_01165) was incubated for 30 min in pH values ranging from 3.0 to 9.0 before measuring the activity.Also, it was incubated for 30 min at different temperatures starting from 10 to 60°C for the activity measurement. Glutamine (5 mM) was used as a substrate to measure glutaminase activity, and asparagine (5 mM) was used for asparaginase activity and the reaction was carried out as described in section 3.5.4.

With increasing pH, the activity also gradually increased and both glutaminase and asparaginase activity peaked at pH 6 (Figure 3.20 A). The maximum glutaminase and asparaginase activities were 152.26±10.32 U/mg and 100.95±9.22 U/mg, respectively (n=3). With further increases in pH values, both activities declined. For example, at pH 9 glutaminase activity was 60.46±5.90 which is significantly different ($p<0.01$) compared to pH 6 (Figure 3.20 A). Furthermore, the lowest recorded values were obtained at pH 3.0, in which the glutaminase activity was 9.59±2.63 U/mg and asparaginase was 3.92±1.37 U/mg. The optimal temperature for the purified KPN_01165 was 40 ^{o}C (Figure 3.20 B). At this temperature the glutaminase and asparaginase activities peaked, 162.40±5.62 U/mg and 122.67±6.36 U/mg, respectively (n=3). However, the high temperature 60 ^{o}C decreased the activities to 63.97±9.84 U/mg for glutaminase and 41.26±8.31 U/mg for asparaginase. These readings were significantly different from what was recorded at 40 ^{o}C ($p<0.01$). At low temperature, for example at 10 ^{o}C, glutaminase and asparaginase activities of the recombinant protein decreased 11.26±0.45 U/mg and 8.32±2.79 U/mg, respectively (n=3) (Figure 3.20 B).

After the optimal pH and temperature were identified, *Vmax* and *Km* were determined as described in section 3.6.7. The asparaginase and glutaminase activity was used to determine Michaelis Menten kinetics of recombinant 200 µg/ml recombinant KPN_01165 (Figure 3.21 A and B). The recorded *Vmax* and *Km* for KPN_01165 glutaminase were 146.54±7.79 U/mg and 0.69±0.13 mM, respectively, and KPN_01165 asparaginase *Vmax* and *Km* values were 108.42±3.93 U/mg and 0.59±0.08 mM, respectively (Figure 3.21 A and B, respectively). The 5mM lysine and valine were used to test substrate specificity of recombinant KPN_01165. However, no detectable NH_3 could be detected using Nessler reaction, confirming the preference of KPN_01165 toward asparagine and glutamine.

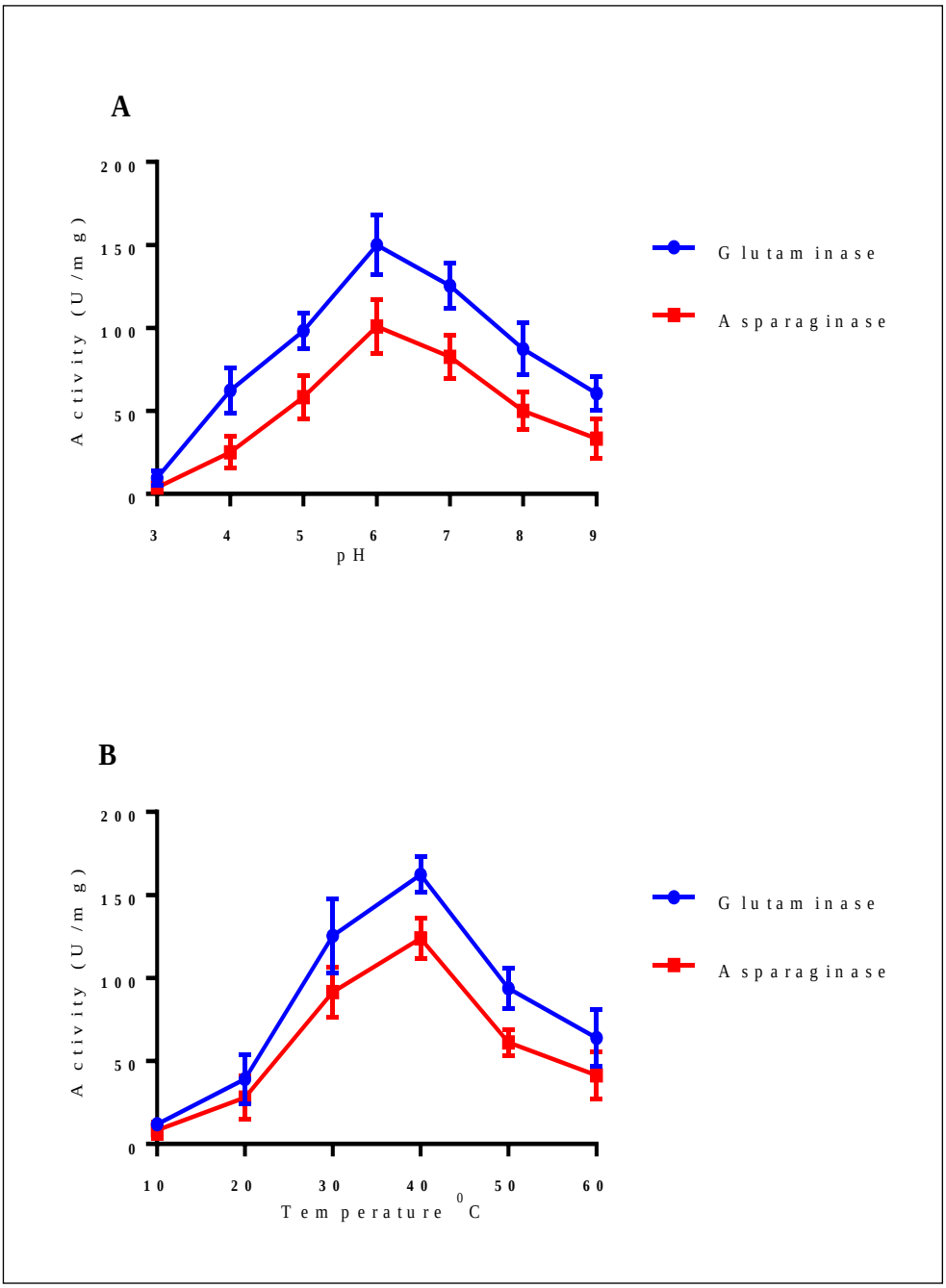

Figure 3.20: *Determination of optimal pH and temperature for recombinant KPN_01165.* ***A.*** *Total glutaminase and asparaginase activities were determined at different pH. Sodium citrate buffer was used for pH values from 3.0 to 6.0 and sodium phosphate buffer was used to obtain pH that ranged from 6.0 to 9.0.* ***B.*** *KPN_01165 glutaminase and asparaginase at increasing temperature from 10 ^{o}C to 60 ^{o}C with 10 increments. Optimal activities were recorded at 40 ^{o}C.*

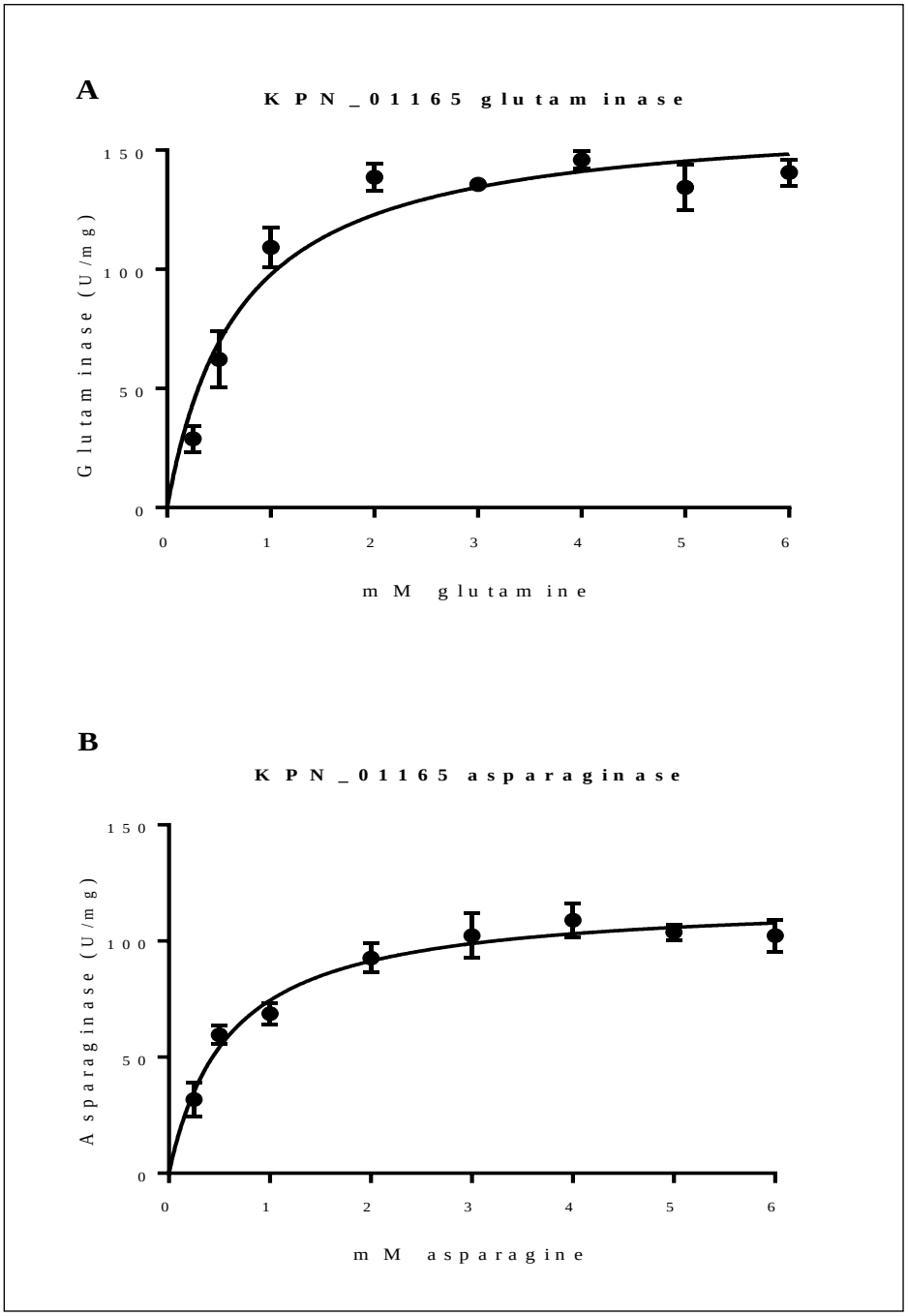

Figure 3.21: *KPN_01165 kinetic parameters (*Km *and* Vmax*) were calculated by nonlinear regression analysis. Plot of glutaminase* ***(A)*** *and asparaginase* ***(B)*** *reaction velocities Each datum point represents the mean activity calculated from two independent experiments each with triplicates.*

3.18 Transcriptional analysis of asparaginase/glutaminase genes

The expression of asparaginase/glutaminase genes was quantified *in vitro* to determine, first, whether the exposure to glutamine and asparagine relative to NH_4Cl would influence

the expression of these genes, and second, to assess whether the mutation of one gene would be compensated by changes in expression of the other asparaginase/glutaminase genes.

3.18.1 Inducibility of asparaginase/glutaminase genes

The aim was to find if there were differences in the transcription levels of the asparaginase/glutaminase genes in wild type *Klebsiella* when grown in different N containing conditions. As described in section 3.8, the wild type was grown in M9 media supplemented either with NH_4Cl or glutamine or asparagine. The qRTPCR data was analysed by $C_T 2^{-\Delta\Delta CT}$ method to quantify fold differences in gene expression between the two conditions as described in section 3.8.4. Differences in expression of two-fold or greater were considered significant (Yesilkaya *et al.*, 2007). The results (Figure 3.22 A, and B) (n=3), show that in the presence of glutamine (Figure 3.22 A), *ybiK* and *KPN_01165* expression increased significantly, by 3.84 ± 0.35 and 10.79 ± 2.53-fold (n=3), respectively. However, under the same condition the expression of *yneH* and *ansA* did not change significantly. The M9 supplemented with asparagine (Figure 3.22 B), led to the expression of *ansA*, *ybiK* and *KPN_01165* increase by 3.09 ± 0.69, 3.99 ± 0.10 and 6.38 ± 1.54-fold (n=3), respectively, while *yneH* expression was not affected significantly. It can be concluded that *KPN_01165* and *ybiK* are inducible in both treatment conditions. However, *ansA* expression was induced after only asparagine treatment. The fold differences were relative to their expression when the bacteria were grown on M9 media containing NH_4Cl, and this supports the involvement of the proteins encoded these genes in cleavage and utilization of glutamine and asparagine.

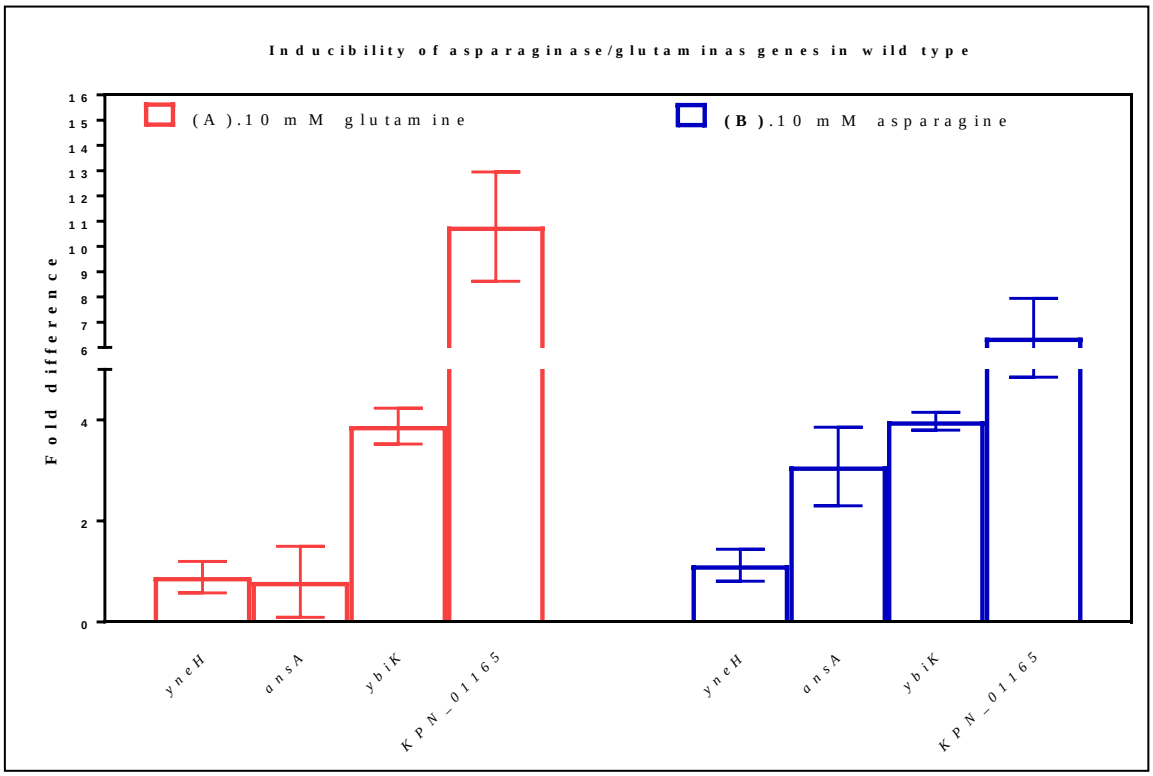

Figure 3.22: Inducibility of asparaginase/glutaminase genes in wild type *K. pneumoniae* grown micro-aerobically in M9 supplemented with 10 mM of glutamine or asparagine. The expression level is relative to the wild type exposed to NH_4Cl.Values are average of three independent experiments each with replicates. '±' indicates standard error of means (SEM).

3.18.2 Evaluation of compensatory effect of asparaginase/glutaminase genes

The transcription level of *yneH*, *ansA*, *ybiK*, and *KPN_01165* were analysed in *ΔyneH*, *ΔansA*, *ΔybiK, ΔKPN_01165, ΔybiK/ΔKPN_01165* backgrounds to investigate the regulatory interactions among these genes.

Figure 4.23 A and B shows the difference in expression level of asparaginase/glutaminase genes exposed to glutamine or asparagine relative to the exposure to NH_4Cl. The figure shows that *KPN_01165* could compensate for the absence of other asparaginase/glutaminase genes as both glutamine and asparagine induce expression of this gene (Figure 3.23 A and B, respectively). The expression of *KPN_01165* was up-regulated by (in fold) by 4.53 ± 0.67, 3.33 ± 0.34, and 2.89 ± 0.72 after glutamine exposure, and with exposure to asparagine its expression went up by 4.53 ± 0.67, 2.83 ±

0.67, and 3.90 ± 0.72 in *ΔyneH*, *ΔansA*, and *ΔybiK*, respectively (Figure 3.23 A and B, respectively) relative to its expression in wild type (n=3).

It was found that M9 supplemented with glutamine down regulated the expression of *ansA* and *yneH* by 3.21 ±0.45 and 4.86 ±0.61, respectively, in *ΔyneH* and *ΔansA,* respectively, relative to the wild type (n=3). This result indicates that *yneH* and *ansA* could affect each other's expression as the mutation in one of them down regulate the expression of other. Comparing to the wild type in the presence of glutamine, the expression of *ybiK* did not change in *ΔansA* and *ΔKPN_01165*, which indicate that *ybiK* does not compensate the absence of *ansA* or *KPN_01165* (Figure 3.23 A). However, *ybiK* compensates the lack of *yneH* in *ΔyneH* as its expression level went up 5.81±1.09 fold compared to its expression in the wild type (Figure 3.23 A) (n=3).

However, after exposure to asparagine the expression levels of *yneH* in *ΔansA*, *ΔybiK, ΔKPN_01165, ΔybiK/ΔKPN_01165* was not affected significantly relative to the wild type (Figure 3.23 B). This indicates that there is no compensatory effect by *yneH.* Under the same condition i.e. asparagine exposure, the expression of *ansA* did not change in in *ΔyneH*, *ΔybiK, ΔKPN_01165, ΔybiK/ΔKPN_01165* relative to the wild type (Figure 3.23 B). The results also show that absence of *ybiK* or *KPN_01165* cannot be compensated by *ansA* (Figure 3.23 A and B).

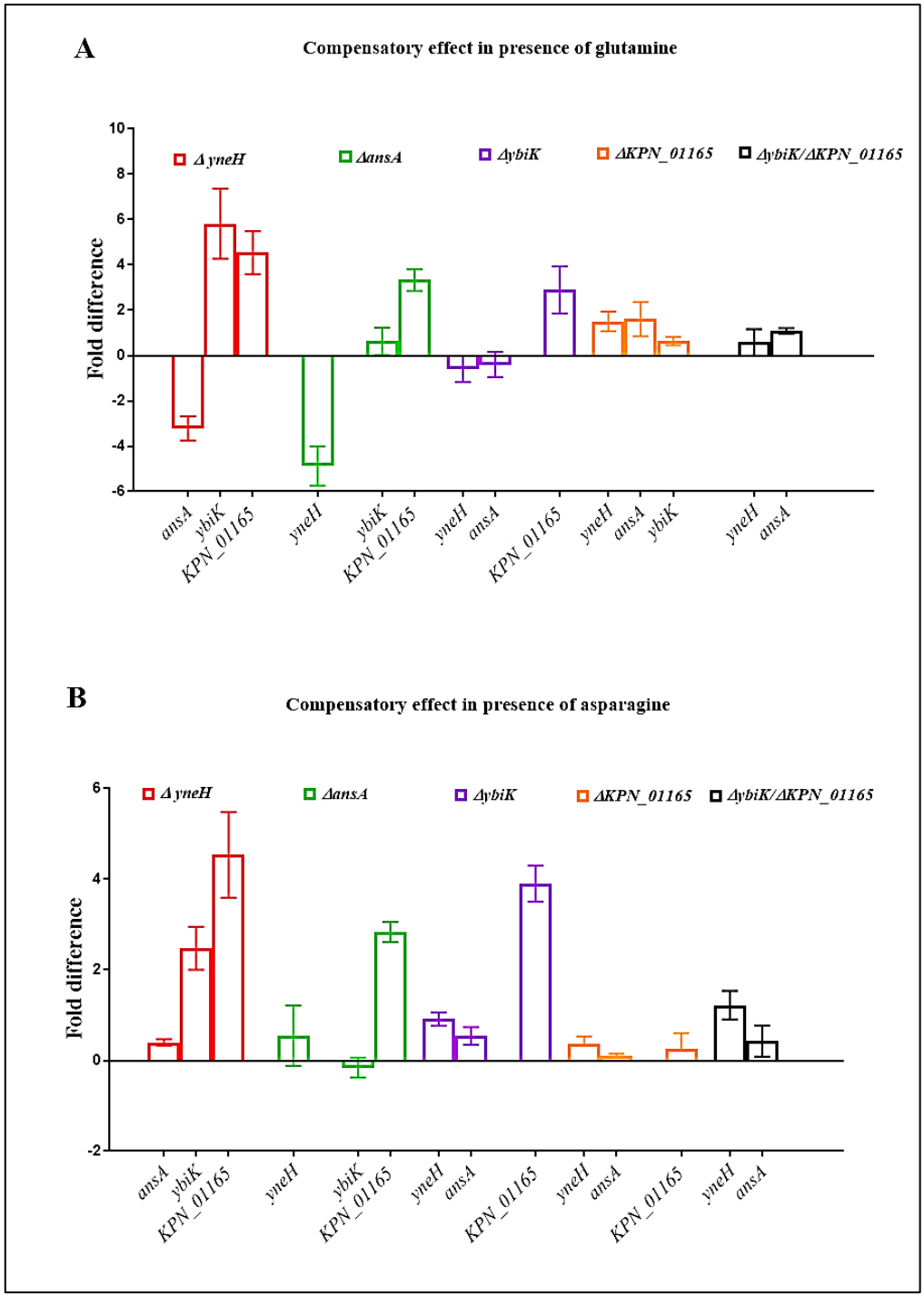

Figure 3.23: *The expression of putative asparaginase/glutamines genes in the presence of glutamine* ***(A)*** *and asparagine* ***(B)*** *in mutants relative to the wild type. The expression levels are compared to their expression after exposure to NH_4Cl. Columns represent fold difference of target genes and vertical bars indicate standard error of mean of three independent experiments in duplicate. 2-fold difference was considered to be significant.*

3.19 *ΔKPN_01165* capsule phenotype

3.19.1 Effect of *KPN_01165* mutation on colony morphology

Other aspects relevant to *Klebsiella* biology were also investigated. After an overnight growth at 37 ^{o}C on LB agar, differences in colony morphology between the wild type, *ΔKPN_01165* and *ΔybiK/ΔKPN_01165* were observed. Comparing to wild type colonies, *KPN_01165* mutants' colonies were found to be more viscous, smaller in size, and contained less white pigmentation (Figure 3.24 A, B and C, respectively). It was hypothesized that these changes happened due to the impact on capsule synthesis in *ΔKPN_01165* and *ΔybiK/ΔKPN_01165*. However, the capsule morphology of *ΔyneH*, *ΔansA*, and *ΔybiK* were not different from the wild type (results not shown).

It can be conculalated that the apparent variation in capsusule size between the wild type and both *ΔKPN_01165* and *ΔybiK/ΔKPN_01165* is not due to inability of those mutants to acquire nutrients (glucose, glutamine and asparagine). Because all strains (wild type, *ΔKPN_01165* and *ΔybiK/ΔKPN_01165*) were growin in LB agar which is a nutrant rich media that have high quantity of glucose, glutamine and asparagine. According to Sezonov et al (2007), the content of the free glutamine and asparagine in 1 L of LB can reach 19.1 and 7.3 mM, respectively. Also, it has been found that LB have around 0.04% glucose (2.22 mM) (Cote, 1999). Accordin to my results, the modified M9 media (M5 and M9*) (see section 3.14) contain 4 mM glutamine or 4 mM asparagine, respectively, with 2 mM glucose. The mutant strains (*ΔKPN_01165* and *ΔybiK/ΔKPN_01165*) did not show any significant growth-related difference compared to the wild type ($p>0.05$) (Figure 3.7 A and Figure 3.9 A).

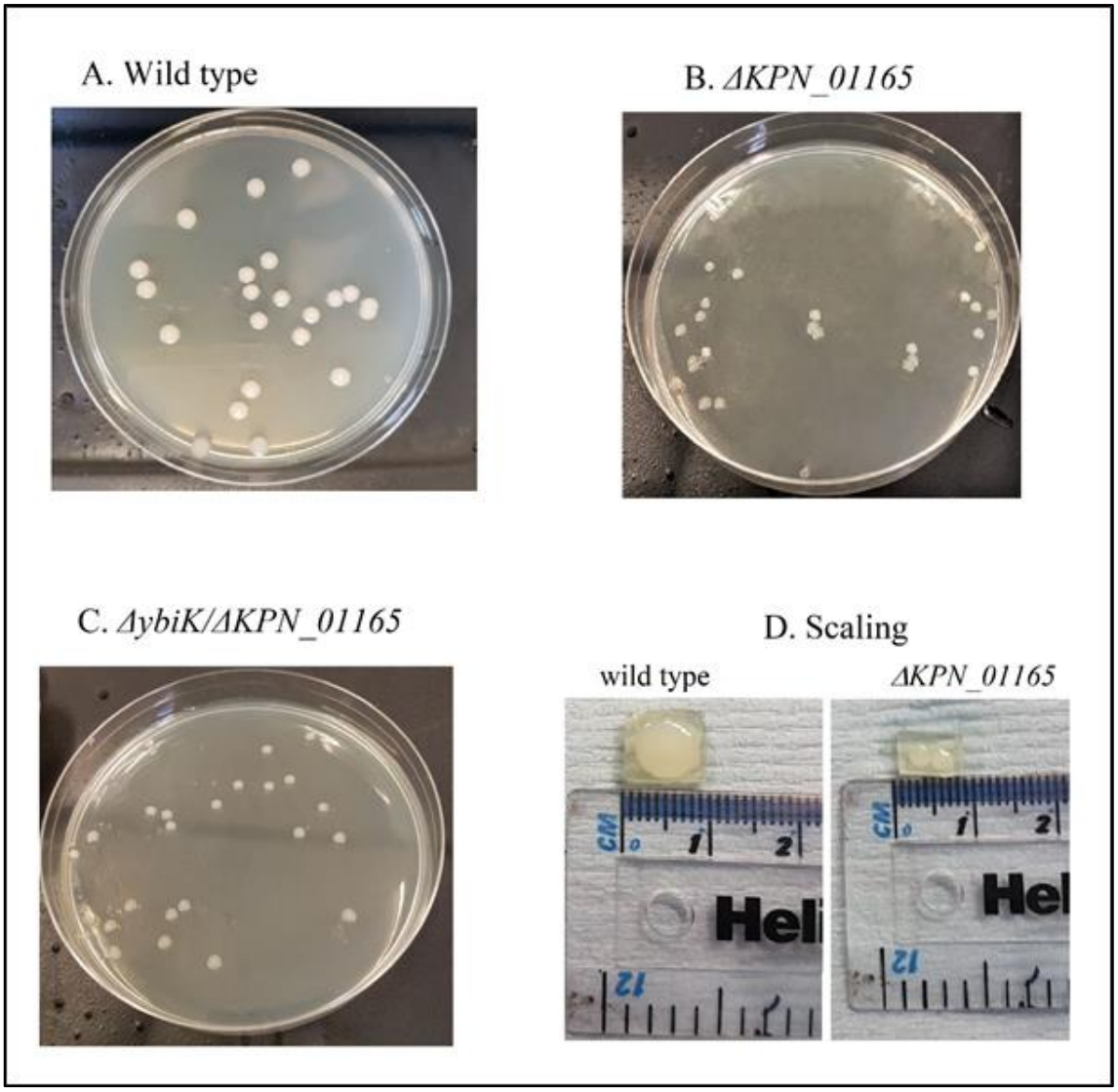

Figure 3.24: *Pictures representing the phenotypic appearance of* Klebsiella pneumoniae *colonies after overnight incubation on LB agar* ***A.*** *Wild type* ***B.*** ΔKPN_01165 *and* ***C.*** ΔybiK/ΔKPN_01165. *Wild type colonies (A) are bigger comparing to* ΔKPN_01165 *and* ΔybiK/ΔKPN_01165 *colonies (B and C, respectively).*

3.19.2 Effect of asparaginase/glutaminase mutation on *Klebsiella* colony size

The colony sizes of wild type *Klebsiella* and the, *ΔyneH*, *ΔansA*, *ΔybiK, ΔKPN_01165,* and *ΔybiK/ΔKPN_01165* mutants were determined. Initially, overnight LB broth cultures of mutants and wild type were harvested by centrifugation and washed with PBS after which the culture turbidity was adjusted to OD_{600} 0.1. Next, 100 µl of these cells were cultured by spreading on LB agar overnight at 37 ^{o}C. Next day, colony size was measured using Nikon light microscope equipped with graded eyepiece (10X) (Figure 3.25 A). Each line in the graded lens represents 0.1 mm. In total, 20 well-isolated colonies from each of

wild type, *ΔyneH*, *ΔansA*, *ΔybiK, ΔKPN_01165,* and *ΔybiK/ΔKPN_01165* were measured (Figure 3.25 A 1, 2,3,4,5, and 6, respectively). The mean colony size of each mutant was statistically compared to the wild type using one-way ANOVA and Dunnett's multiple comparisons test (Figure 3.25 B). The results showed that there were no significant variations between colony size of wild type *K. pneumoniae* (0.84 cm ±0.02), and colony size of *ΔyneH*, *ΔansA*, *ΔybiK* mutants (0.86 cm ±0.03, 0.70 cm ±0.03 and 0.73 cm ±0.02, n=20, respectively) ($p>0.05$) (Figure 3.25 B). However, *ΔKPN_01165,* and *ΔybiK/ΔKPN_01165* mutants, had a significantly reduced colony size (0.36 cm ±0.01 and 0.30 cm ±0.02, n=20, respectively), compared to the wild type (0.84 cm ±0.02), ($p \leq 0.001$) (Figure 3.25 B). Therefore, it was concluded that KPN_01165 plays a key role in maintenance of colony size on LB agar medium. It has been reported that the colony morphology in *K. pneumoniae* CG43 and capsule synthesis were linked. Unlike wild type *K. pneumoniae* CG43, the colonies that resulted from *ΔrmpA2* (a gene that enhance CPS synthesis) were completely unmucoid (Lai *et al*., 2003). For this the next step was measuring capsule synthesis in *K. pneumoniae* KR3167 strains.

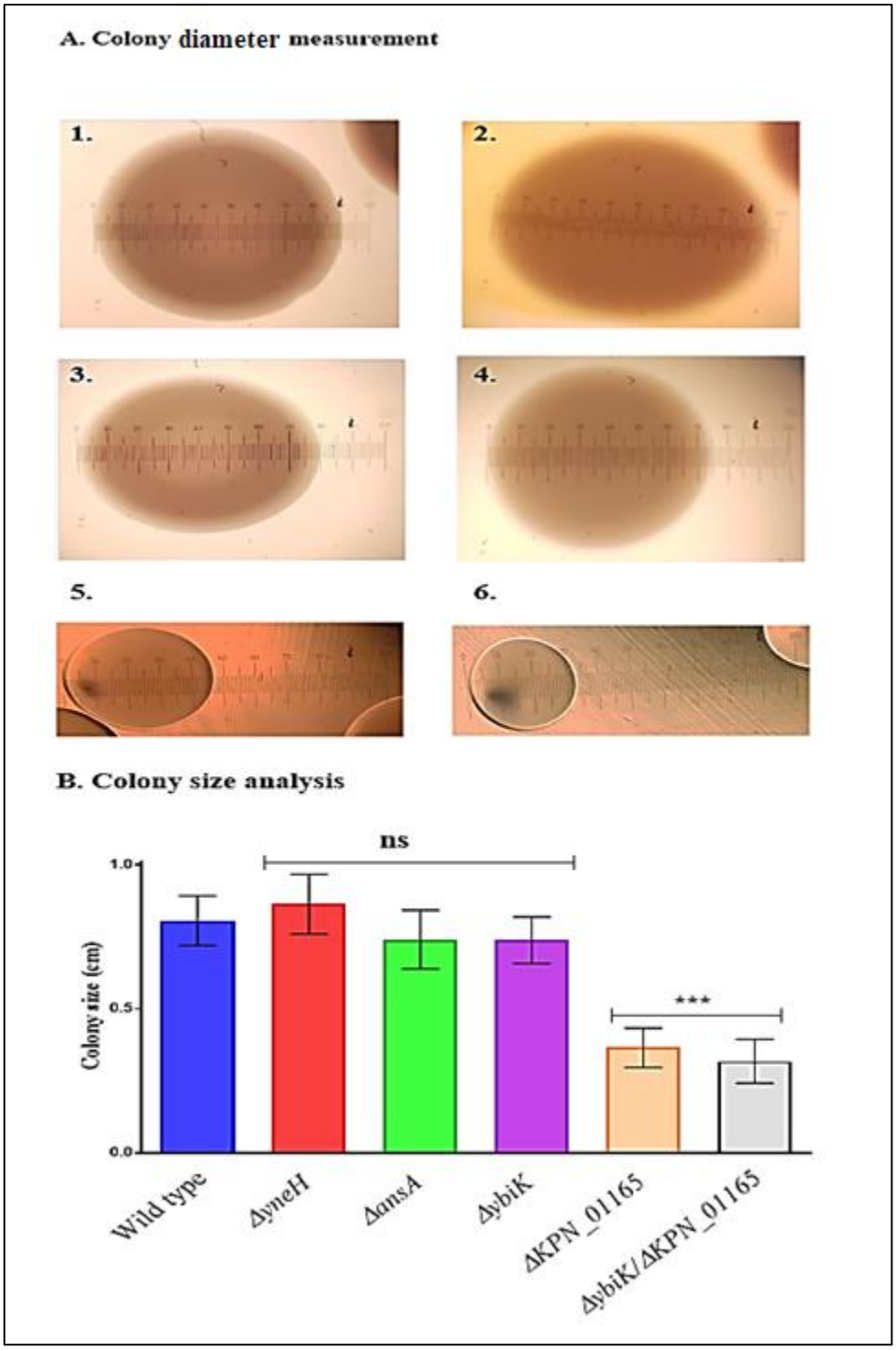

Figure 3.25. *Colony size measurement/analysis of the mutants and wild type* K. pneumoniae. *Strains were grown overnight at 37◦C on LB agar plate,* ***(A)*** *The size of individual colonies of* K. pneumoniae *strains under 10X magnification (Nikon) is shown.* ***(1)*** *Wild type* ***(2)*** ΔyneH ***(3)*** ΔansA ***(4)*** ΔybiK ***(5)*** ΔKPN_01165 ***(6)*** ΔybiK/ΔKPN_01165. ***(B)*** *Each column represents the mean size of 20 well-isolated colonies. Data were analysed using ANOVA and Dunnett's multiple comparisons test, ***p≤0.001.*

3.19.3 Effect of asparaginase/glutaminase on *Klebsiella* capsule production

The *Klebsiella* genus expresses two different types of antigens on their surface. The O antigen is a component of the lipopolysaccharide layer while the K antigen is a capsular polysaccharide. The capsule plays an important role in the infection process by inhibition of phagocytosis, and opsonization (including the complement system) (Shankar-Sinha *et al*., 2009).

Glucuronic acid is a capsule sugar that has uronic acid as the acidic component. D–glucuronic acid, D-galactose, D-mannose and L-rhamnose are the components of *Klebsiella* K2 capsular polysaccharide (Cho *et al*., 2009). Therefore, glucuronic acid quantification is considered an important indicator of capsule synthesis (Lai *et al*, 2003). Glucuronic acid was quantified by measuring uronic acid concentration in extracted capsular polysaccharide. The measured uronic acid was expressed as micrograms per 10^9 CFU of bacteria using a standard curve of glucuronic acid. Glucuronic acid quantification of cultures done by following the carbazole assay that was described previously (section 3.9).

To determine whether asparaginase/glutaminase would affect capsule synthesis, glucuronic acid in extracted capsule from wild type, *ΔyneH*, *ΔansA*, *ΔybiK*, *ΔKPN_01165* and *ΔybiK/ΔKPN_01165* was determined. The quantification was done in three independent trials with triplicate samples in each. The cells were harvested after overnight incubation at 37°C in M13 (10 mM glutamine) or M14 (10 mM asparagine) media.

The results indicate that glucuronic acid levels from cells grown in either glutamine (M13) or asparagine (M14) did not vary significantly between the wild type *K. pneumoniae* KR3167 and *ΔyneH*, *ΔansA*, and *ΔybiK*. The glucuronic acid in wild type after growth in glutamine (M13) was 152.76 ±5.01 µg/10^9 CFU, while in *ΔyneH*, *ΔansA*, and *ΔybiK* it was 150.63±5.92, 156.54±8.48 and 159.56±6.07 µg/10^9 CFU, (n=3), respectively ($p>0.05$) (Figure 3.26). On the other hand, after growth in M13 (that has 10 mM glutamine) and M14 (that has 10 mM asparagine), *ΔKPN_01165* and *ΔybiK/ΔKPN_01165* had significantly lower glucuronic acid content compared to the wild type ($p\leq0.001$). The glucuronic acid content after M13 growth were 73.28±7.07, and 76.88±4.30 µg/10^9 CFU (n=3), in *ΔKPN_01165* and *ΔybiK/ΔKPN_01165*, respectively while wild type produced significantly higher glucuronic acid 152.76 ±5.01 µg/10^9 CFU, n=3 ($p\leq0.001$) (Figure 3.26). Also, the measured glucuronic acid of wild type,

ΔKPN_01165 and *ΔybiK/ΔKPN_01165* after growth on asparagine (M14) were 112.20±3.57, 69.07±1.58, and 50.52±1.60 µg/10^9 CFU n=3, respectively ($p \leq 0.001$) (Figure 3.26). Together, results suggested there is an association between glucuronic acid content and KPN_01165.

The results also show the role of glutamine and asparagine as substrates in glucuronic acid production. For example, wild type *ΔansA* and *ΔybiK* produced more glucuronic acid, 152.76 ±5.01, 156.54±8.48 and 159.56±6.07 µg/10^9 CFU, n=3, respectively in the presence of glutamine than the growth in the presence of asparagine: glucuronic acid content for wild type *ΔansA* and *ΔybiK* was, 118.83±2.35 and 110.09± 6.27µg/10^9 CFU (n=3), respectively ($p \leq 0.01$) (Figure 3.26). The M13 (that has 10 mM glutamine) and M14 (that has 10 mM asparagine) are nutrient limited media. As Vu et al. (2009) mentioned quantity and composition of exo-polysaccharide of the capsule vary among bacteria and are influenced by many factors including concentration of oxygen, nitrogen, and temperature. It seems that glutamine is more supportive for capsule synthesis than asparagine in term of capsule synthesis in *K.pneumoniae*.

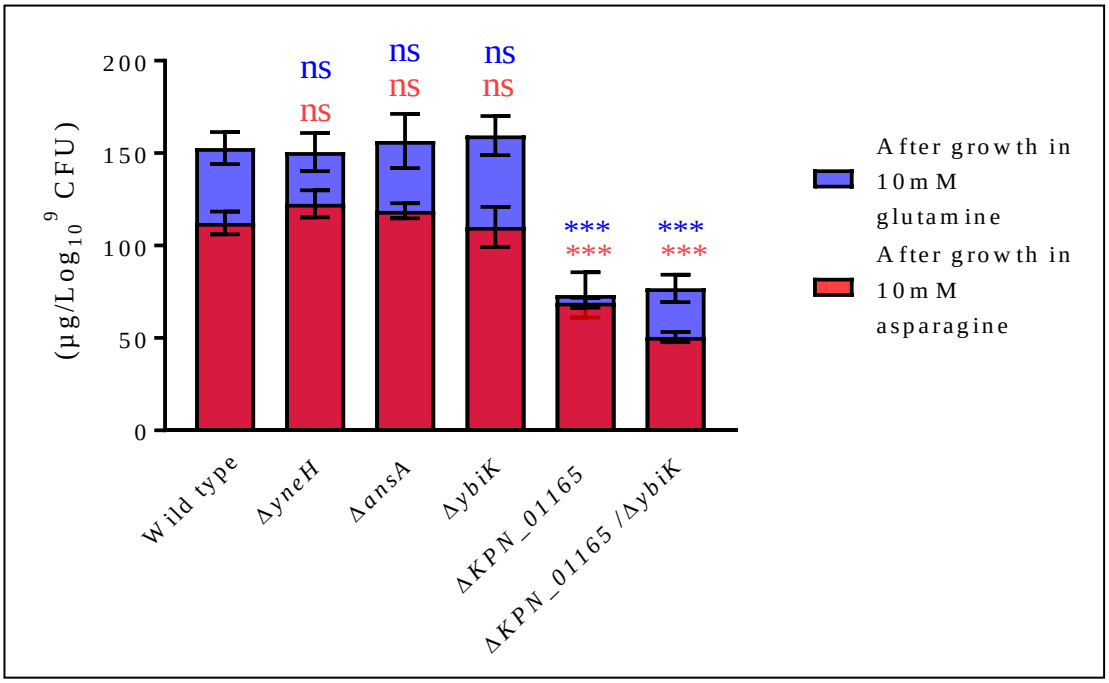

Figure 3.26. *Glucuronic acid concentration of capsular polysaccharide was quantified using carbazole assay and expressed as µg (Glucuronic acid) /Log_{10}^9 CFU. Data are means of three independent experiments, each in triplicates. P-value was determined by*

*one-way ANOVA and Dunnett's multiple comparisons test comparing to wild type, ***$p \leq 0.001$.*

3.19.4 *Cis*-complementation reconstitutes colony characteristics

As there were no significant colony variations between the wild type and *ΔyneH*, *ΔansA*, *ΔybiK*, only *cis*-complemented *KPN_01165* in *ΔKPN_01165* was studied to rule out any polar effect of KPN_01165 mutation on the observed phenotypes. Initially, the genetically complemented strain and wild type were cultured on LB-agar media. Comparing to wild colonies, *cis*-complemented *KPN_01165* colonies were morphologically similar, and this included both the pigmentation intensity and the size (Figure 3.27 A 1 and 2). The size measurement was also done as described above. The Figure 3.27 C indicate that *cis*-complementation of *KPN_01165* in *ΔKPN_01165* restores the colony size to a wild type level (0.82 cm ±0.02 and 0.78 cm ±0.04, n=20, respectively) ($p>0.05$). Restoration of colony morphology and size of the complemented strain indicate reversible phenotypic features that occur due to the absence of KPN_01165 activity.

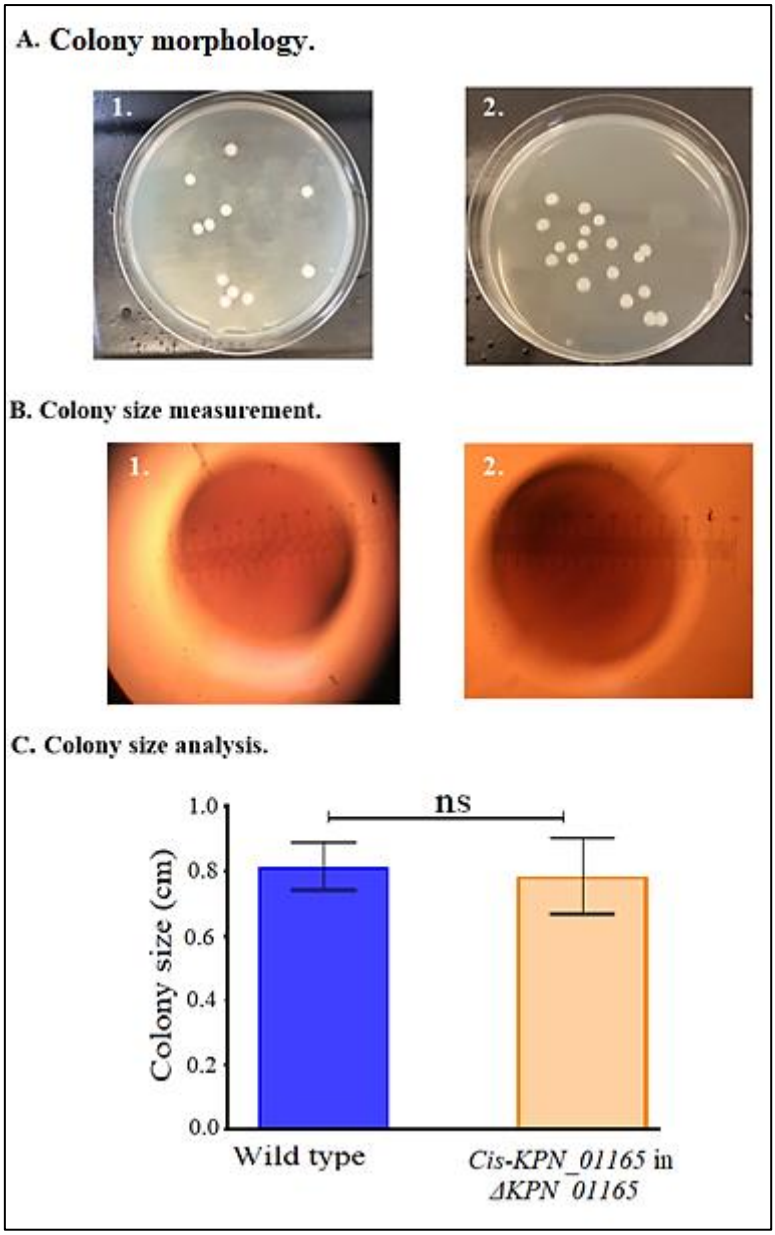

Figure 3.27. *Representation of colony morphology and size of wild type and cis-complemented strain.* ***(A)*** *Overnight cultures of* K. pneumoniae *strains were prepared, then diluted, and plated on LB-agar* ***(1).*** *Wild type* ***(2).*** cis-KPN_01165 *in* Δ KPN_01165 ***(B)****. After overnight incubation at 37◦C, colony size was measured using Nikon light microscope 10X* ***(1).*** *Wild type* ***(2).*** cis-KPN_01165 in Δ KPN_01165 ***(C).*** *The columns represent mean size of 20 well-isolated colonies with standard error of mean shown as vertical bars. No significant difference in colony size (ns) p>0.05 between wild type and* cis-KPN_01165 *in* Δ KPN_01165.

Section D: Results summary and discussion

3.20 *K. pneumoniae* KR3167 asparagine and glutamine metabolism

The presented results support my hypothesis regarding the importance of *K. pneumoniae* asparaginase and glutaminase in utilisation of nitrogen. Based on gene annotation and enzyme activity assays it was found that *ansA*, *ybiK* and *KPN_01165* code for type II asparaginases. Sanches et al. (2007) suggested that asparaginase II enzymes have more affinity toward asparagine than glutamine. Regardless of their substrate specificity, these enzymes provide a nitrogen source (NH_3) from either glutamine or asparagine when NH_3 is absent or below 1 mM. The cellular location of these enzymes is also believed to be different (Srikhanta *et al*., 2013), indicating that their function *in vivo* may be different too. AnsA is predicted to be in cytoplasmic space, and the others in periplasmic space. *E. coli* has a homologous protein that has been described as a type I asparaginase (Srikhanta *et al*., 2013).

Growth assays in different M9 media, asparaginase and glutaminase enzymatic activity were done and compared to the wild type. M9 media that have either asparagine or glutamine were used to determine the other characteristics. The reason for using asparagine and glutamine were to study effects of nitrogen metabolism on inducibility of asparaginase/glutaminase genes, capsule formation and morphology. As *ΔKPN_01165* was the most attenuated strain, KPN_01165 enzyme was cloned and expressed, and the enzyme kinetics were determined

Based on my work, mutation of *ansA*, *ybiK*, and *KPN_01165* adversely affected the growth yield of *K. pneumoniae*.

The mutant KPN_01165 coded protein which has asparaginase and glutaminase activities. It is apparent from my results that this was the most essential enzyme as the mutant strain suffered the most reduced growth rates and yields and had the lowest asparaginase/ glutaminase activities. Also, *ΔKPN_01165* showed morphological differences to wild type, such as size and capsule synthesis. Based on these observations, I hypothesise that these changes will reflect on host response to *K. pneumoniae*, for example through its effect on serum resistance, which therefore was investigated.

Even though all these genes are annotated to be important in asparagine and glutamine metabolism, it was found in this report that when asparagine or glutamine was used as

sole nitrogen source, the *ΔyneH* mutant growth and enzyme activity was similar to that of wild type. This may be either due to compensation by other asparaginases, or the protein coded by this gene is not important in asparagine or glutamine metabolism. the transcriptional analysis by qRT-PCR indicate that *ybiK*, and *KPN_01165* may substitute the presence of *yneH*. The mean C_T values of *ybiK* and *KPN_01165* in *ΔyneH* were 5.81±1.09 and 4.53±0.670, respectively.

3.21 Optimizing glucose concentrations

In order to detect the contribution of putative asparaginase and glutaminase genes in *K. pneumoniae* growth, the conditions had to be optimized. For example, in this study, when the asparaginase and glutaminase mutants were cultured in medium containing high concentrations of both carbon and nitrogen, 20 mM glucose, and 5mM either from either glutamine or asparagine, no difference in phenotype in the mutants relative to the wild type could be seen. The glucose concentration affects the dependence on nitrogen because bacteria can use it as the preferred source of carbon to produce energy in a process known as carbon catabolite repression (Sonawane *et al.*, 2003). During this process, many carboxylic acids are produced, including 2-oxaloglutarate, and the presence of these compounds in high concentration decreases the need to utilise amino acids (Sanches *et al*., 2007; Sonawane *et al*., 2003). In my study, it was found that 2 mM glucose supplement is the optimal concentration, where the difference between the wild type and the mutant strains could be detected for phenotypic characterisation of mutants. Hence the glucose concentration was lowered to 2 mM glucose, and 0.5 mM asparagine or glutamine were used.

3.22 Optimizing glutamine and asparagine concentration

Sonawane et al. (2003) used 5 and 10 mM of both glutamine and asparagine as the sole source of both carbon and nitrogen in their enzymatic studies. In my project 10 mM was the optimal concentration as at 5 mM level of the amino acids, no growth could be detected either with the wild type or with the mutants (results not included). Furthermore, increasing concentration to 15mM had a negative impact on the yield (results not included). According to Yan (2007) adding glutamine in a percentage higher than the biosynthetic requirement leads to glutamate accumulation inside the cell. Subsequently, this accumulation affects the osmolarity status and K+ transmission, which may play a role in cell viability.

Depending on the obtained results from the *in vitro* growth experments it can be suggested that the effect from the attenuated strains during *in vivo* infections could be complemeneted. This could be done through injecting the infected host for example with extracellular 5 mM glucose plus 0.5 mM glutamine. This claim can be supported by the fact that besides glutaminase *k.pneumoniae* also has other nitrogenase enzymes like glutamate dehydrogenase and glutamine synthesis that can fulfill the bacterial nitrogen need. The glutamate dehydrogenase and glutamine assimilate NH_4^+ into glutamate and glutamine respectively. However, the affinity toward NH_4^+ is different in which it is high (1 mM) in glutamate dehydrogenase and low in glutamine synthesis (Stewart *et al*., 1980). The involvement of those enzymes on my mutants can be included in future work by using an animal model both control and supplemented (with glucose and glutamine). In this project, it was shown by the growth experiments that 0.5 mM glutamine plus 2 mM glucose supplementation was enough to show the phenotype of all mutant strains (except *ΔyneH*). Moreover, this project also showed that asparaginase and glutaminase might have other roles beside nitrogen assimilation which was shown in *ΔKPN_01165* that has affected capsule synthesis.

3.23 KPN_01165 kinetic characterisations

In this project, I determined the optimal pH of KPN_01165 asparaginase and glutaminase as pH 6.0 (Figure 3.21 A). In other bacteria like *Vibrio succinogenes* the optimal pH for asparaginase II was found to be 7.0. The microbial L-glutaminase/asparaginases have a broad variation in their optimal pH range, as illustrated in figure (3.20). Results of KPN_01165 pH stability has shown that the enzyme is stable at pH 7 as the enzyme kept around 90% of its activity.

Sodium phosphate buffer was used to obtain pH that ranged from 6.0 to 9.0 and sodium citrate buffer was used for pH values from 3.0 to 6.0. Many studies have evaluated asparaginase and glutaminase activities using those two buffer systems (Ferrara *et al.*, 2004; Aljewari *et al.*, 2010; Kebeish *et al.*, 2016). However, it seems that this system has many disadvantages. For example, the use of phosphate buffer may affect the total glutaminas activity. It has been known that phosphate can activate mammalian glutaminase activity (O'donovan and Lotspeich, 1966). The other disadvantage is related to citrate which is a TCA cycle intermediate that can feed-back to asparaginase or glutaminase (Kornberg, 2000). As a result, and to overcome any result interference, future

work should include other buffers that don't have phosphate or citrate like HEPES; which is a zwitterionic organic buffering agent.

Next the thermal stability of KPN_01165 was investigated. After exposure to the temperature values that ranged from 10 ^{o}C to 60 ^{o}C, it was found that KPN_01165 asparaginase and glutaminase activities are stable at 30 ^{o}C and 40 ^{o}C. However lower (10 ^{o}C and 20 ^{o}C) and higher temperatures (50 ^{o}C and 60 ^{o}C) reduced the KPN_01165 asparaginase and glutaminase activity (Figure 3.20). These results indicate that KPN_01165 is active under the host physiological condition rather than the environmental existence of *K. pneumoniae*, supporting the view that these enzymes are involved in the infection process.

4 Chapter -4: Serum bactericidal activities against *K. pneumoniae*

Section A: Introduction.

4.1 Overview

In the previous chapter, it was clear from the growth assays and enzyme activity assays that the mutations in asparaginase/glutaminase genes affect *K. pneumoniae* fitness especially *KPN_01165* mutants being the least fit. Also, *ΔKPN_01165* has shown some morphological differences regarding the capsule production compared to the wild type as described in sections 3.19. Based on these observations, I hypothesized that the metabolic and morphological changes due to the lack of asparaginase/glutaminase activities would affect the microbe's interaction with host. To test this hypothesis, I studied the impact of mutations on the deposition of complement, which is part of the innate immune system.

One important characteristic of *K. pneumoniae* is its ability to evade the host immune system, which is considered as an important virulence factor. It was hypothesized that the *Klebsiella* capsule plays an important role in inhibiting both phagocytosis and opsonization (including the complement system) (Shankar *et al*., 2004). In this chapter, I will present my data showing the sensitivity of *K. pneumoniae* toward the bactericidal activity of bovine and murine serum in relation to presence and absence of asparaginase and glutaminase enzymes. In the beginning, I will provide some background information for immune response to *K. pneumoniae*, focusing particularly on the complement system in clearance of microbe. Then the relevant methodology and the results will be presented.

4.2 Immune response

Innate immune and adaptive immune responses are the two pillars of immune response that work collectively to protect the body from invading pathogens and all other potentially harmful substances (Abbas *et al*., 2014). The former response is a non-specific, immediate, primary, yet essential, defense that recognizes and clears invasive bodies, without keeping specific memory i.e. previous exposure does not change the response. However, the latter is an adaptive response that can form a specific response to, for example, a specific infectious microbe and at the same time develop an immunological memory for it. The memory function is carried out by specific T and B cells (Abbas et

al., 2014; Borghesi and Milcarek, 2007). The regulation of innate and the adaptive responses occurs through communication between cellular and humoral elements. The cellular part of innate immunity includes haematopoietic and non-haematopoietic cells. Neutrophils, eosinophils, macrophages, dendritic cells, mast cells, NK cells, and NK T cells are haematopoietic cells, while epithelial cells are an example of the non-hematopoietic cells (Turvey and Broide, 2010). Complement system proteins, cytokines, interferon, chemokines and coagulation factors are the humoral elements (Ali *et al*., 2012).

4.3 Complement system

The complement system is an effector branch of the humoral immune system. In the 1890s, by using sheep antiserum, Jules Bordet found that the lysis of *Vibrio cholerae* was due to this system because, upon heating, the bacteriolytic activity was lost (Kindt *et al*., 2007). The bacteriolytic activity was restored upon fresh serum addition. This led to the conclusion that bacteriolytic activity is dependent on a heat-sensitive component that causes lytic activity. The heat-sensitive component was called "complement" after another similar experiment was done by Paul Ehrlich. The name was given upon observing that the activity of blood serum is needed to complete the action of antibody in the blood. Later, it was discovered that complement is the interaction of a large and complex group of proteins (Kindt *et al*., 2007; Dunkel *et al*., 2010).

Researchers have discovered that there are about 30 soluble and cell-bound proteins involved in the complement system. Complement proteins are usually present in their inactive form. This system affects both innate and acquired immune system, far beyond the original observation, which was limited to lysis of bacteria and red blood cells. Complement proteins also carry out other functions like opsonization, which promotes phagocytosis, and antigen binding that triggers specific cell functions, inflammation, and secretion of immunoregulatory molecules. Immune clearance is another function that removes immune complexes from the circulation and transports them to the spleen and liver. Activation of complement can lead to release of anaphylatoxins that mediate cellular activation, B-cell differentiation, and chemotaxis related to the adaptive immune response. All of what is mentioned above shows that the complement system is a highly developed part of the immune system (Kindt *et al*, 2007; Turvey and Broide, 2010; Ali *et al*, 2012)

4.4 Complement system activation

There are three pathways that mediate complement system activation; classical pathway (CP), alternative pathway (AP), and lectin pathway (LP) (Kindt *et al.*, 2007; Kennedy, 2010). The complement system can opsonize the microbe and directs phagocytes to the site of infection and also kills the microbe directly. A proteolytic cascade occurs during activation which alters an inactive precursor enzyme, called a zymogen. The zymogen is cleaved and becomes an active protease which also cleaves its downstream effectors. This enzymatic cascade causes amplification of the signal to a large extent. Before this cascade is initiated, the molecule or virulence factors must be recognized on the microbial surface. The interaction between pattern recognition receptors (PRRs) like mannose receptors, and specific pathogen associated molecular patterns (PAMPs) is key to activate the complement system. Unlike the other pathways, CP is mostly activated by the first subcomponent C1q binding to fragment crystallizable region (FC) of immunoglobulin antibodies of IgG 1, 2, and 3 classes, (but not IgG4), and IgM (antibody-dependent). LP is initiated after binding to the pattern recognition molecules, mannan-binding lectin (MBL), ficolins and collectin (collectin-11). The AP is also antibody-independent and mainly four serum proteins, C3, factor B, factor D and properdin, are involved in its operation. This pathway is activated by C3b binding to foreign particles which is protease independent (Schwaeble *et al.*, 1995; Kindt *et al.*, 2007; Wallis *et al.*, 2010; Ali *et al.*, 2012).

The membrane attack complex (MAC) is the end product of all the three pathways, and it is formed due to collaboration of terminal complement activated molecules, which include C5b, C6, C7, C8 and C9. The MAC causes disruption of the membrane integrity and lysis of the cell (Kindt *et al.*, 2007; Delves and Roitt, 2011; Abbas *et al*., 2014) (Figure 4.1).

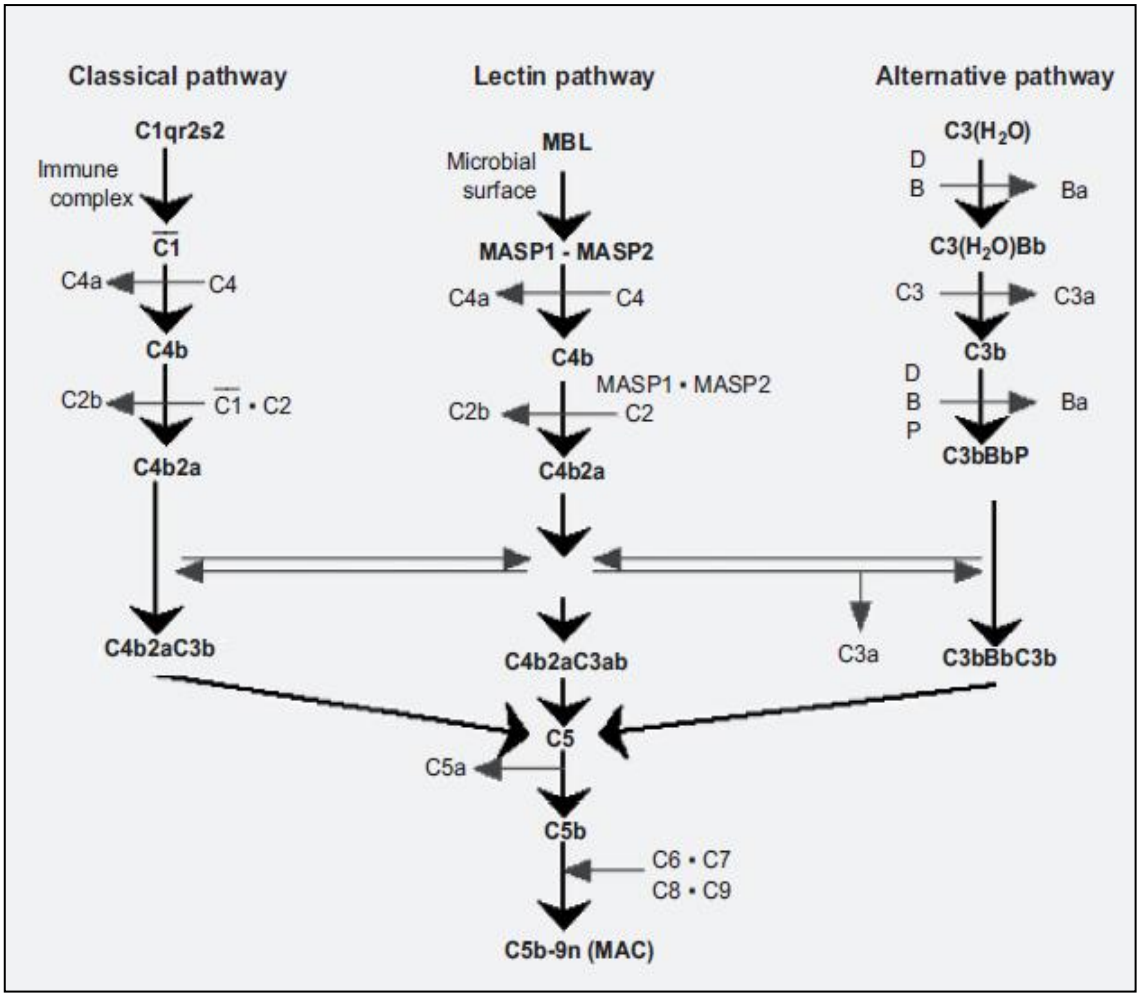

Figure 4.1: *Schematic acquired from (Fujita, 2013), representing the complement system activation. CP, LP, and AP are three pathways that can activate the complement cascade that lead to C3 convertase formation (CP and LP (C4b2a), and AP (C3bBb)), then C5 convertase and MAC formation.*

4.4.1 Classical pathway

The CP is initiated after recognition of soluble immune complex, i.e. antigen-antibody complex or binding with an antibody such as IgG and IgM bound to an antigen like microbial surface. The complex formation occurs on the Fc regions of antibodies. In general, during complement activation two types of complement fragments are formed; small fragments released into blood stream, such as C3a, and a large fragment such as C3b, which is usually attached to a pathogen surface. C1 is composed of three parts: C1q and two molecules each of C1r and C1s (Kindt *et al.*, 2007; Ali *et al.*, 2012; Abbas *et al.*, 2014). After binding of the C1q molecule, a conformational change occurs in C1r and it activates C1s by cleaving it. Furthermore, C1r can be active in the absence of Ca^{+2},

whereas C1s is Ca^{+2} dependent (Villiers *et al.*, 1985). C1s acts on two of its substrates: C4 and C2. C4 is a glycoprotein and upon hydrolyzation, it produces two fragments: C4a, small fragment and C4b, a large fragment. The C4b part gets attached to C1 and C2 gets attached to the exposed binding site of C4b, and C2 is cleaved by the C1s. This cleavage causes diffusion of C2b fragment. C4b2a is a C3 convertase that acts on C3 and turns it into an active form. The C3 component also produces a smaller fragment (C3a) that diffuses away and a larger fragment (C3b). The C3 convertase is an amplifier of the signal which can produce C3b in large quantities. The C3b molecule then binds to the C4b2a and forms a C4b2a3b complex which acts as C5 convertase. The C5 convertase acts on C5 and produces analogous molecular fragments i.e., C5a that diffuses away and C5b which binds to C6 and initiates the formation of membrane attack complex (MAC). The smaller fragments (C4a, C3a and C5a) are anaphylatoxins i.e., inflammation mediators (Kindt *et al.*, 2007) (Figure 4.1).

4.4.2 Alternative pathway

AP is antibody-independent, and it activation occurs by involvement of four serum proteins, which are C3, factor B, factor D and properdin. This pathway is activated upon recognition of foreign particles such as the cell wall of bacteria. The pathway does not require specific recognition molecules as it is activated by binding of C3b to foreign particles which is protease independent (Walsh *et al.*, 2005). Frank (2010) found that antibodies involved in activation of classical pathway, can make AP function more effective.

Briefly, this is how AP is activated. The hydrolysis of the unstable thioester bond of serum C3 by a process called the tick-over mechanism causes the production of C3a and C3b. C3b bound to a foreign particle then binds with a serum protein called factor B and the complex is stabilized by Mg^{2+} binding. After binding with C3b, the complex is exposed to factor B that serves as the binding site for factor D. Factor D can mediate the proteolytic cleavage and release of a small fragment from factor B, leaving, C3bBb (the C3 convertase). Then C3 convertase catalyzes cleavage of C3 and produces C3b as an active component, which then amplifies the signal. The C3b then forms a C3Bb3b complex (C5 convertase). The Bb component of the C5 convertase generates C5a and C5b from C5 molecules, and C5b binds to the pathogen surface and forms MAC (Schwaeble and Reid, 1999; Quin *et al.*, 2005; Frank, 2010) (Figure 4.1).

4.4.3 Lectin pathway

This pathway is also known as mannan-binding lectin pathway or MBL pathway. A lectin is a protein that has a capability to bind to sugar (Weis *et al*., 1998). LP can initiate complement by recognition of PAMPs such as mannose residues which are present in the bacterial surface. Mannose residues are present as glycoproteins or carbohydrates of the bacterial surface. MBL is an acute phase protein produced during inflammatory responses and act in the similar way to C1q.

The LP initiates the complement cascade upon binding of LP recognition molecules (MBL, Cl-11, and ficolins) to the targeted cell surface (Schwaeble *et al*., 2011). Once these carbohydrate pattern recognition molecules attach to a microbial surface, they initiate activation of MBL-associated serine proteases (MASPs). The active complex causes cleavage and activates C4 and C2 (in similar way to C1 complex of the CP). After activation of C2-C4, C3 convertase is formed (C4b2a), which cleave C3 to C3a and C3b. The C3b combined with C3 convertase form C5 convertase (C4b2aC3b) and ultimately the formation of MAC (Gadjeva *et al.*, 2001; Matsushita *et al.*, 2002; Walsh *et al.*, 2005) (Figure 4.1).

4.4.3.1 Mannose-binding lectin and ficolin

MBL is the first described recognition subcomponent of LP and it is a sugar-binding plasma protein that binds mannan/mannose, fucose and N-acetylglucosamine. MBL is a serum protein, produced in the liver, and has subunits of identical polypeptide chains. A single polypeptide chain consists of four domains: N-terminal composed of cysteine-rich amino acid, collagen-like domain with 59 amino acids, hydrophobic coil neck domain of 30 amino acid, and C-terminal domain that recognizes carbohydrate in presence of calcium (C-type lectins) (Takahashi and Ezekowitz, 2005)

Ficolin belongs to the family of oligomeric proteins, which has an N-terminal and C-terminal domain. The N-terminal domain has functional similarity with collagen-like domain and the C-terminal with the fibrinogen-like domain that favorably binds to acetylated molecules and this is what makes ficolins different from MBL and CL-11. Ficolin also recognizes compounds that have N-acetyl groups, such as N-acetylglucosamine (GlcNAc), and bacterial cell wall components (Matsushita and Fujita, 2002; Yongqing *et al.*, 2012)

Ficolin can interact with MASPs and play a role in activation of lectin pathway. When lectin pathway recognition complexes, comprising one of the carbohydrate recognition components (e.g. MBL or a ficolin) and MASPs bind to a PAMP, the MASPs becomes active and consequently activate complement. There are three forms of ficolins in humans: L, M and H ficolin. These forms are different in tissue expression, protein location site, and bacteria recognition. Ficolins are mainly expressed by monocytes, and macrophages in the lungs and the spleen (Matsushita and Fujita, 2002; Fujita, *et al.*, 2004; Endo *et al.*, 2011).

Ficolins in rodents are different. While man has L-, M- and H-ficolins, rodents have only two ficolins: ficolin A, resembling to L-ficolin, and ficolin-B. The former is synthesized in the liver and mainly found in serum, and the latter is mainly found in the bone marrow (Runza *et al.*, 2008).

Lipopolysaccharides (LPS) on the surface of Gram negative bacteria can bind and then activate MBL. However, lipoteichoic acid found in cell wall of Gram positive bacteria, can be recognized by L-ficolin, which initiates the LP of complement activation (Lynch *et al*., 2004). The three ficolins L, H and M have different properties to activate the LP in which the most important carbohydrate recognition molecule in human is H-ficolin, and both L-ficolin and MBL have similar activity, while, M-ficolin appears to have lower activity (Matsushita, 2010).

4.4.3.2 Collectin-11

Collectin has a property of binding to microorganisms directly and can promote neutralization and agglutination. CL-11 or Collectin kidney (CL-K1) belongs to the collectin family and was first described by Keshi and his colleagues (Keshi *et al.*, 2006). CL-11 is a calcium-dependent carbohydrate recognition molecule. It is composed of a globular head, a neck region, collagenous domain, which is located at cysteine-rich N-terminal, and carbohydrate recognition C-type lectin domain (Takahashi *et al.*, 2010; Schwaeble *et al.*, 2011). The collagenous region has the affinity to bind with MBL-associated serine proteases, MASP-1, MASP-2, and MASP-3, which act as a initiator of the complement cascade. CL-11 is present in serum and it is encoded by *COLEC11*, which belongs to soluble C type lectin family that is involved in pattern recognition (Hansen *et al.*, 2010; Farrar *et al*, 2016). The main function of CL-11 is directing the innate immune response against a pathogen, which invades locally. More recent work by

Ali *et al.* (2012) demonstrated that CL-11 also binds to MASP-2 and activates LP in a MASP-2 dependent fashion.

4.4.3.3 MASPs of the LP

There are three MBL-associated serine proteases (MASP), and two related non-enzymatic proteins. The enzymes are MASP-1, -2 and -3, while other proteins are Map19, and Map44, which are alternative splice products of *MASP2* and *MASP1*, respectively (Kjaer *et al.*, 2013). MBL and ficolins form complexes with MASPs. The MASP-1 and MASP-2 were first thought to have structural and functional similarity with C1r and C1s (Wallis *et al.*, 2007). However, MASP-2 can activate complement in absence of MASP-1 and MASP-3 (Thiel *et al.*, 1997). Moreover, MASP-2 form an active complex that cleaves C4 and C4 bound C2. Subsequently when the lectin pathway subcomponents MBL or CL-11 or ficolins bind to the surface of pathogens, auto-activation of MASP-2 can occur or direct cleavage of MASP-2 by MASP-1 can also occur, which leads to formation of C3 convertase (Heja *et al.*, 2012).

MASP-1 can cleave C2 but it is not efficient. MASP-3 is the only protein that cleaves zymogen complement factor D and it is an essential component of the alternative pathway. It has recently been reported that MASP-1 can cleave C3, which may lead to complement activation. However, this cleavage was reported to be too low to be physiologically important (Selander *et al.*, 2006). The need for MASP-1 in activating the LP is unclear, as MASP-2 can auto-activate itself. Additionally, MASP-1 can perform other biological functions, for example, it has the ability to cleave the coagulation factor XIII and fibrinogen, can promote coagulation factor-like activity, and it induces several signaling pathways through a protease-activated receptor in the endothelial cells, such as NF-kB, and p38 MAPK pathway (Heja *et al.*, 2012). Previous studies showed that MASP-3 is unable to cleave C2, C3 or C4, while more recent reports show that MASP-1/MASP-3 are important to convert a proenzymatic component of the alternative pathway's factor D into its enzymatically active form. Activated factor D is essential to convert C3-bound factor B into Ba and the enzymatically active component Bb (Takahashi *et al.*, 2010; Iwaki *et al.*, 2011).

4.5 Host response to *K. pneumoniae*

Klebsiella pneumoniae, upon entry, interacts first with the mucosal barrier and then humoral and cellular innate immune defence barriers. Humoral response relies mainly on

opsonization of the microbe by secreting a wide range of factors that have bactericidal and bacteriostatic effect. These factors are activated after recognition of the bacterial surface components by antibody and complement (Groisman, 2001). *K. pneumoniae* strains isolated from clinical specimens are differentiated from other enterobacteria by consistent production of surface polysaccharide capsule and lipopolysaccharide (Ciurana and Tomas, 1987). The complement system is an example of humoral defense that helps in eliminating the bacteria. Complement C3b binding to the bacterial surface is an essential factor that helps in recognition and the opsonization process. Complement system ultimately forms MAC that causes pore formation in bacterial membrane, and lysis. The C3b surface binding to resistant *K. pneumoniae* strains occurs in the longest polysaccharide side chains. Thus phagocytosis, not MAC formations is considered as the main protection mechanism against *K. pneumoniae* (Merle *et al*., 2015; Albert *et al*., 1996). Also, the complement system can produce proinflammatory mediators and chemoattractants to activate and recruit immune cells upon recognition of virulence factors of bacteria.

The immune control of *K. pneumoniae* is achieved by the activity of the innate immune system alone or in combination with humoral response. The alveolar macrophages cause amplification of the immune response by secreting chemokines and cytokines. In an established infection, recruitment of neutrophils occurs by releasing of cytokines and chemokines. Interleukin-8 (IL-8), leukotriene B4 and complement proteins are examples of chemokines. In clearance of *K. pneumoniae*, neutrophils have greater phagocytic and killing properties than macrophages. Optimal clearance of *K. pneumoniae* is dependent on neutrophils and/or CCR2+ monocytes (Hirche *et al*., 2005; Xiong *et al*., 2015).

Section B: Material and Methods.

I am grateful for Dr. Nicholas J Lynch, University of Leicester for his help regarding experiments designing, and providing both different deficient mouse sera and chemicals. His readiness was essential in finishing this chapter.

4.6 *K. pneumoniae* preparation for serum sensitivity assays

K. pneumoniae strains were grown over night at 37°C in 5 ml LB. Then from this culture, a fresh 5 ml LB was inoculated in 1/100 dilution, and bacteria were left to grow for 3-4 hours at 37°C. The pellet was harvested in the exponential phase (OD_{600nm} 0.6–0.8) by centrifugation at 2,500 g for 10 min at room temperature. Using the same setting, the pellet was washed twice with PBS. Then cells were resuspended in different barbital buffered saline solutions and the turbidity at 600 nm was adjusted to approximately OD_{600nm} of 1.0. From this dilution the cell numbers were adjusted to approximately 1×10^5 CFU/ml.

4.7 Preparation of sera

The foetal bovine serum (Sigma, UK) was stored at -80˚C until use, and the C57BL/6 mouse serum was collected from whole blood supplied by a commercial provider (Envigo, UK). The mouse blood was extracted from 6-8 weeks naive mouse and it was clotted on ice for 3 hours to prevent complement activation. Then the blood was spun down using a refrigerated centrifuge at 5000 xg for 7 minutes. The serum was separated and stored at -80˚C until use.

4.8 Serum bactericidal assays

The sensitivity of the mutant and wildtype strains toward 25% (v/v) foetal bovine serum and 50% (v/v) C57BL/6 mouse serum was assessed as previously described (Estabrook *et al*., 1997). The bacterial strains and serum were suspended in barbital buffered saline (BBS; pH 7.4). The BBS contains; 4 mM barbital, 145 mM NaCl, 2 mM $CaCl_2$, 1 mM $MgCl_2$, pH 7.4. The additions of 2 mM $CaCl_2$ or 1 mM $MgCl_2$ was used to assess *K. pneumoniae* sensitivity toward CP, LP, and, AP. The lone AP involvement was investigated by adding the chelation agent ethylene glycol-bis (b-aminoethyl ether)-*N, N, N9, N9*-tetraacetic acid (8 mM EGTA) plus 5 mM $MgCl_2$, and removing the 2 mM $CaCl_2$ and 1 mM $MgCl_2$ from the BBS. The chelation agent inhibits both classical and lectin pathways. All pathways were inactivated by heating the bovine and murine serum at 56

^{o}C for 30 min. The role of LP was further examined by using complement deficient serum isolated from MBL deficient mice, Ficolin A deficient serum, and CL-11 deficient serum that were provided by Dr. Nicholas J Lynch.

For the serum sensitivity assays, the reaction mixture (1×10^5 CFU/ml plus serum) was then incubated at 37^{o}C, with shaking at 220 rpm for 120 minutes. In three independent trials with duplicate tubes in each, samples were taken at 0, 30, 60, 90 and 120 minutes post incubation to determine CFU/ml by serial dilution and plating onto LB agar media.

4.9 C3 deposition assays

Complement C3 deposition assays were carried out by enzyme-linked immunosorbent assay (ELISA). This assay was done by following the protocols mentioned in Lynch et al. (2004). Unless otherwise stated, all chemicals used in this study were purchased from Sigma Aldrich.

4.9.1 *K. pneumoniae* fixation for ELISA assay

K. pneumoniae was grown in LB overnight at 37°C. The following day, bacterial growth was centrifuged for 10 minutes at 4000xg. Then, the cell pellet was washed three times in phosphate-buffered saline (PBS). Subsequently, the OD_{600nm} was adjusted to 1.0 and fixed by adding 0.5% formalin in PBS, which was then kept for 60 minutes at room temperature followed by twice-washing with plain PBS. To confirm fixation, fixed bacteria were plated and incubated at 37°C overnight (no growth should appear). The fixed bacterial suspension was kept at 4°C until usage.

4.9.2 Coating ELISA

The microtiter ELISA plates (Maxisorb, Nunc) were coated with 100 µl/well of coating buffer containing formalin-fixed *K. pneumoniae* (diluted to an adjusted OD_{600nm} value of 0.1). The coating buffer (15 mM Na_2CO_3, 35 mM $NaHCO_3$, 0.02% sodium azide, pH 9.6) was also used for preparation and coating the positive control (10 µg/ml Zymosan). Coated plates were then kept at 4°C overnight. The next day, the residual binding sites were blocked for two hours at room temperature by addition of 250 µl blocking buffer (PBS with 1% w/v Bovine Serum Albumin). Then, the triplicate washing step was done with 250 µl of washing buffer (PBS+ tween 20 0.1%).

4.9.3 Binding ELISA

After performing the steps in the previous section, the C3 binding was performed under CP and LP condition after 1hour incubation at 37 ^{o}C. in BBS. This BBS contain; 4 mM barbital, 145 mM NaCl, 2 mM $CaCl_2$, 1 mM $MgCl_2$, pH 7.4, with seven fold diluted (initial dilution 1/40) serum (the wild type and deficient murine sera are included) The AP is undetectable under these conditions, because the serum concentration is too low (Lynch *et al.*, 2004). Deposition via the AP was measured using 4 mM barbital, 145 mM NaCl, 5 mM $MgCl_2$, 8 mM EGTA, pH 7.4. EGTA preferentially chelates calcium, which is required for the classical and lectin pathways, but not the AP. The other conditions were the same as described above, but the starting dilution was 1/5. In both conditions, 10 µg/ml zymosan (Sigma) was used as positive control, and for negative control the wells contained only BBS buffer without any serum. Following the 1hour incubation (in both conditions), the plates were washed three times, using the washing buffer. The bound C3b was targeted using the primary antibody (rabbit anti-C3c (Dako)) (diluted 1/5000 in the washing buffer) (kindly provided by Dr. Nicholas J Lynch, University of Leicester, UK) 100 µl/well was added then the plates were incubated for 90 minutes at room temperature. Then, the solution was washed three times with washing buffer, as previously done. Next, a 100 µl/well aliquot of the secondary antibodies (goat α- rabbit IgG-alkaline phosphatase conjugate and goat α-mouse IgG-alkaline phosphatase conjugate) (diluted 1/10000) was added to the plates and incubated at same setting. Plates were washed again, and the degree of C3b deposition on wild type, *ΔyneH*, *ΔansA*, *ΔybiK*, *ΔKPN_01165*, and *ΔybiK*/*ΔKPN_01165* was determined by adding 100 µl/well of colorimetric substrate p-nitrophenyle phosphate (pNPP) (Sigma) that detects the presence of alkaline phosphatase. After incubation at room temperature, absorbance was measured at 405 nm using BioRad micro-titer plate reader.

4.10 Glutamine level determination

The Glutamine/Glutamate Determination Kit (Sigma-Ardrich) was used to determine the glutamine level in sera. The principle of the assay is based on spectrophotometric measurement of L-glutamine in liquid samples. The measurement is done in two steps: (A) The available L-glutamine is converted to L-glutamate by the action of the provided glutaminase enzyme (B) The glutamate dehydrogenase will degrade the resulting L-glutamate to α-ketoglutarate accompanied by reduction of NAD+ to NADH. The conversion gives colored product that is measured spectrophotometrically at 340 nm and

it is proportional to the amount of the glutamine in the sample. By following the kit protocol the amount of glutamine in each sample was estimated using a standard curve prepared from known concentrations of kit provided glutamine (0 to 0.5 mM). Then from linear equation of standard curve, the quantity of glutamine in unknown samples was determined (Figure 4.2).

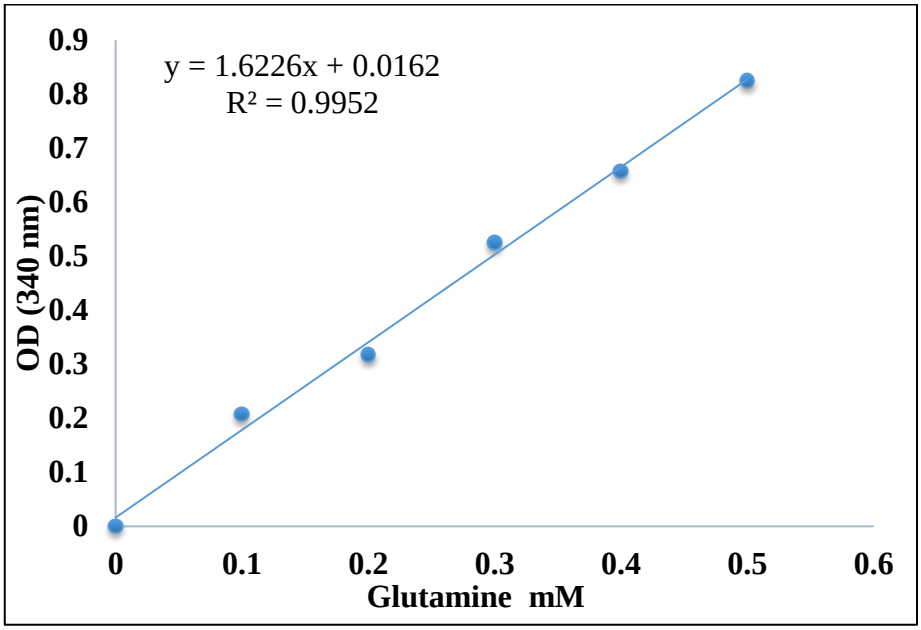

Figure 4.2: *A representative standard curve for quantitative measurement of glutamine.*

Section C: Results.

4.11 Serum bacteriolytic activity

Bactericidal activity here is defined as the change in bacterial viable counts following incubation in serum (Estabrook *et al*., 1997). This test will assess the bacteriolytic activity of the three pathways of complement system as described in section 4.8. The growth of wild type, *ΔyneH*, *ΔansA*, *ΔybiK*, *ΔKPN_01165*, and *ΔybiK*/*ΔKPN_01165* will be challenged by 25% bovine serum and 50% C57BL/6 murine serum.

4.11.1 Bacteriolytic activity of bovine serum

The mutant strains' sensitivity toward the serum was compared to the wild type sensitivity (as described in section 4.8). Initially, the bovine serum was used to assess the growth profiles of strains. In each tested strain, the cell counts were adjusted to approximately 1×10^5 CFU/ml, and then, the strains were incubated with 25% bovine serum at 37^{o}C for 120 minutes, during which samples were taken at 0, 30, 60, 90- and 120-minutes post incubation. In BBS with 25% serum (diluted with BBS that had 2 mM $CaCl_2$, 1 mM $MgCl_2$), and all complement pathways (CP, LP, and AP) are preserved. The bactericidal activity of the serum against~ 1×10^5 CFU/ml of wild type, *ΔyneH*, *ΔansA*, *ΔybiK*, *ΔKPN_01165*, and *ΔybiK*/*ΔKPN_01165* was statistically compared to wild type growth yield and rate by Dunnett's test. The results indicate that only the growth yields and rates of *ΔKPN_01165*, and *ΔybiK*/*ΔKPN_01165* (growth yield: Log_{10} 4.56±0.21 and 4.43±0.15, n=3, respectively, growth rate: -0.48 h^{-1} ±0.01; and -0.43 h^{-1} ±0.03, n=3, respectively), were significantly lower in compare to the wild type strain yield (Log_{10} 6.75 ±0.02, n=3), ($p\leq0.01$), and rate (1.08 h^{-1} ±0.01, n=3) ($p<0.001$) (Table 4.1, Figure 4.3). However, the growth yields and rates of *Δ yneH*, *Δ ansA*, and *ΔybiK* were not affected by the serum relative to the wild type ($p>0.05$) (Table 4.1, Figure 4.3 A).

Under the alternative pathway (AP) specific condition (by adding 8 mM EGTA and 5 mM $MgCl_2$ to serum) as described in section 4.8, there were no significant differences between the growth yields and rates of *ΔyneH*, *ΔansA*, *ΔybiK*, *ΔKPN_01165*, and *ΔybiK*/*ΔKPN_01165* relative to wild type growth yield and rate (Log_{10} 6.54±0.09, and 1.15 h^{-1} ± 0.03, n=3, respectively) ($p>0.05$) (Table 4.2, Figure 4.3B). These results indicate that AP has no bacteriolytic activity against the study strains and highlight the role of CP and LP in reducing the bacterial numbers of *ΔKPN_01165*, and *ΔybiK*/*ΔKPN_01165*.

Similarly, the growth of *ΔyneH*, *ΔansA*, *ΔybiK*, *ΔKPN_01165*, *ΔybiK/ΔKPN_01165* and wild type in heated inactivated serum was similar (p>0.05) (Table 4.2, Figure 4.3C). This heating condition was a negative control to confirm that the bacterial cells number reduction was due to serum mediated killing not due to growth condition.

In summary, the results highlight the important of asparaginase and glutaminase (*ΔyneH*, *ΔansA*, and *ΔybiK*) in serum resistance as the loss of *KPN_01165* has made the *K. pneumoniae* more vulnerable to bovine serum killing. As the results showed this killing was mainly mediated by CP and LP (CP role may consider minimum as the serum used is foetal serum that lack antibody against *k. pneumoniae*).

Table 4.1: *Maximum growth yield (Log_{10} CFU/ml) and growth rate μ (h^{-1}) of mutants and wild type* K. pneumoniae *after 120 minutes incubation in bovine serum with $CaCl_2$ and $MgCl_2$ addition. Each value represents the mean of three independent experiments, each in duplicate, with their standard error of mean, '±' represents the standard error of mean. The significant differences are shown with stars: ** p<0.01, *** p<0.001.*

Strains	Growth parameters in bovine serum plus $CaCl_2$ and $MgCl_2$	
	Max growth Log_{10} CFU/ ml	Growth rate μ (h^{-1})
Wild type	6.75±0.02	1.13±0.01
ΔyneH	6.46±0.01 (ns)	1.08±0.01 (ns)
ΔansA	6.33±0.02 (ns)	0.76±0.05 (ns)
ΔybiK	6.26±0.02 (ns)	0.73±0.02 (ns)
ΔKPN_01165	4.56±0.21 (**)	(-)0.48±0.01 (***)
ΔybiK/ΔKPN_01165	4.43±0.15 (**)	(-)0.43±0.03 (***)

Table 4.2. *The effect of bovine serum that have EGTA and $MgCl_2$ and heat inactivated bovine serum on growth yield (Log_{10} CFU/ml) and growth rate μ (h^{-1}) of mutants and wild type* K. pneumoniae *after 120 minutes incubation. Each value represents the mean of three independent experiments, each in duplicate, with their standard error of mean. The non-significant differences are shown as (ns) p>0.05.*

Strains	Growth parameters in bovine serum plus EGTA and $MgCl_2$		Growth parameters in heat inactivated bovine serum	
	Max growth Log_{10} CFU/ ml	Growth rate μ (h^{-1})	Max growth Log_{10} CFU/ ml	Growth rate μ (h^{-1})
Wild type	6.54±0.09	1.15± 0.03	6.59±0.14	1.19±0.12
ΔyneH	6.48±0.08 (ns)	1.10± 0.03 (ns)	6.56±0.09 (ns)	1.08±0.03 (ns)
ΔansA	6.38±0.11 (ns)	1.02± 0.04 (ns)	6.63±0.08 (ns)	1.10±0.05 (ns)
ΔybiK	6.33±0.16 (ns)	0.92± 0.05 (ns)	6.62±0.04 (ns)	1.03±0.09 (ns)
ΔKPN_01165	6.10±0.17 (ns)	0.93± 0.05 (ns)	6.48±0.15 (ns)	0.88±0.20 (ns)
ΔybiK/ΔKPN_01165	6.01±0.03 (ns)	0.90± 0.10 (ns)	6.58±0.28 (ns)	0.83±0.13 (ns)

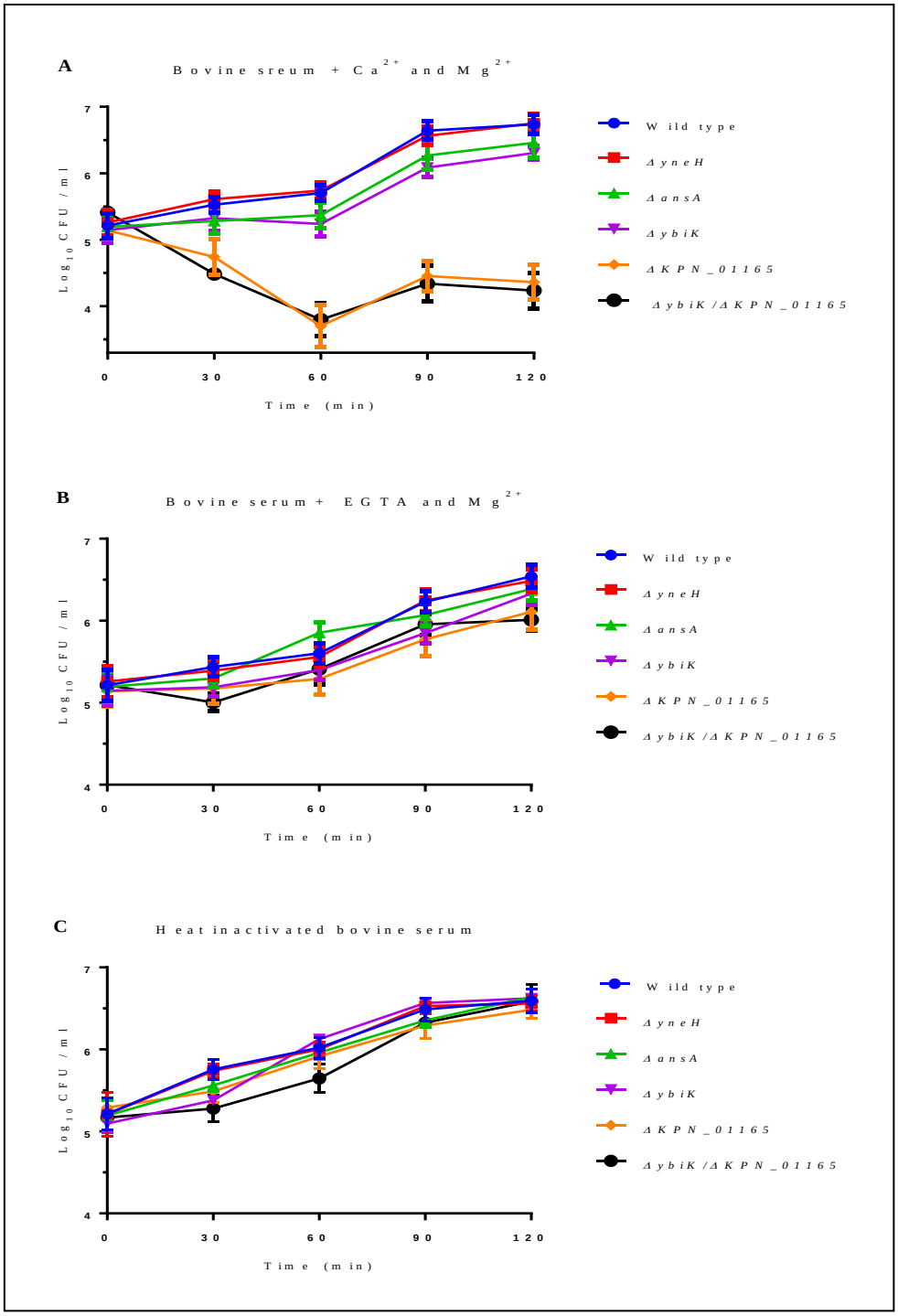

Figure 4.3: *Growth profiles of* K. pneumoniae *wild type and mutants grown in 25% v/v bovine serum. Viable counts were determined at different time intervals. The strains were grown aerobically (220 rpm) at 37°C. (A) The growth profiles in 25% bovine serum plus* $CaCl_2$ *and* $MgCl_2$ *addition. (B) Growth profiles in bovine serum plus EGTA and* $MgCl_2$ *(C) Growth profiles in heat inactivated bovine serum. Each curve represents the mean of three experiments each in duplicate. Vertical bars represent standard error of the mean.*

4.11.2 Bactericidal activity of wild type mouse serum

The bacteriolytic activity of 50% v/v mouse serum against wild type, *ΔansA*, *ΔybiK*, *ΔKPN_01165*, and *ΔybiK*/*ΔKPN_01165* was determined. The serum was extracted from C57BL/6 naive mouse as described in section 4.8. The *ΔyneH* was excluded since it showed growth patterns that is similar to the wild type in the bovine serum. The wild type murine serum was used due to the availability of other different transgenic mice lines that are deficient in one or more of complement pathways. The transgenic murine sera were used to specifically determine which subcomponents of the three complement pathways is responsible for the complement-mediated killing.

Like the bovine serum results, only *ΔKPN_01165*, and *ΔybiK*/*ΔKPN_01165* were sensitive to murine bacteriolytic activity. As shown in Figure 4.4A, and Table 4.3, the usage of 50% murine serum (that has $CaCl_2$ and $MgCl_2$) resulted in non-significant difference in both growth yields and rates of *ΔansA* and *ΔybiK* relative to the wild type ($p>0.05$). However, the growth parameters of *ΔKPN_01165*, and *ΔybiK*/*ΔKPN_01165* were affected. As shown in Figure 4.4A, the onset of the serum bactericidal activity started 30 minutes post-incubation. Furthermore, this effect continued until the end of the incubation period as the growth yield of *ΔKPN_01165*, and *ΔybiK*/*ΔKPN_01165* were Log_{10} 4.88±0.06 and 4.85±0.13, n=3, respectively comparing to wild type growth yield (Log_{10} 5.74±0.05, n=3) ($P<0.05$). The growth rates were also affected for *ΔKPN_01165*, and *ΔybiK*/*ΔKPN_01165* (0.25 h^{-1} ±0.11; and 0.28 h^{-1} ±0.05, n=3, respectively) relative to wild type growth rate (0.69 h^{-1} ±0.08, n=3) ($p<0.05$) (Figure 4.4A, and Table 4.3). These results further confirm the involvement of LP in the clearance as the used serum is naïve (6-8 weeks mouse serum and probably does not have specific antibody to activate CP). The LP carbohydrate recognition molecules to the targeted cell surface through the carbohydrate-recognition domains, is Ca^{+2} dependent (Takahashi and Ezekowitz, 2005).

On the other hand, under the AP specific condition (through 8 mM EGTA and 5 mM $MgCl_2$ addition), there was no difference in clearance level between wild type and the other mutants (Figure 4.4A, B, and C). The bactericidal activity of AP against ~ 1×10^5 CFU/ml of wild type, *ΔansA*, *ΔybiK*, *ΔKPN_01165*, and *ΔybiK*/*ΔKPN_01165* was statistically not significant ($p>0.05$) as the growth yields were (Log_{10} 5.54±0.16, 5.59±0.14, 5.52±0.11, 5.15±0.15, and 5.27±0.06, n=3, respectively), and rates were (0.63 h^{-1} ±0.10, 0.70 h^{-1} ±0.05, 0.52 h^{-1} ±0.04, 0.45 h^{-1} ±0.05, and 0.50 h^{-1} ±0.03, n=3,

respectively) (Figure 4.4B, and Table 4.4). The negative control, which was carried out using heated inactivated C57BL/6 serum, showed no significant difference in the growth yields and rates between all used strains which confirms that the reduction in CFU/ml of *ΔKPN_01165*, and *ΔybiK*/*ΔKPN_01165* during the incubation period was due to the complement mediated reduction ($p>0.05$) (Figure 4.4C, and Table 4.4).

The results in the section 4.11 confirm my hypothesis of sensitivity of *KPN_01165* mutant strains toward the complement deposition activity hence the lack of *KPN_01165* causes the *K. pneumoniae* to be less capsulated and that more likely make it more vulnerable to complement deposition. The demonstrated bacteriolytic activity against *KPN_01165* did not result in massive clearance of the CFU/ml. My result indicted that complement lytic attack against *ΔKPN_01165*, and *ΔybiK*/*ΔKPN_01165* has resulted at the most in approximately one log difference from the start inoculum. For example, the C57BL/6 serum bactericidal activity at 30 minutes post-incubation against Δ*KPN_01165*, and Δ*ybiK*/ Δ*KPN_01165* were Log_{10} 4.36±0.17 and 4.24±0.08, n=3, respectively, relative to the wild type (Log_{10} 4.93±0.15, n=3 which was not different from the start inoculum Log_{10} 5.21±0.13) (Figure 4.4 A). A possible explanation of this result may relate to *Klebsiella* (like most bacteria) are not thought to be susceptible to complement lysis, but are cleared mainly though opsonophagocytic mechanisms (Groisman, 2001).

Table 4.3: *Growth yield (Log_{10} CFU/ml) and growth rate μ (h^{-1}) of mutants and wild type grown in C57BL/6J serum with $CaCl_2$ plus $MgCl_2$ addition. Each value represents the mean of three independent experiments, each in duplicate, with their standard error of mean, '±' represents the standard error of mean. The significant differences resulted from one-way ANOVA and Dunnett's multiple comparisons are shown with star: (*) p <0.05.*

Strains	Growth parameters in murine serum plus $CaCl_2$ and $MgCl_2$	
	Max growth Log_{10} CFU/ ml	Growth rate μ (h^{-1})
Wild type	5.74±0.05	0.69±0.04
ΔansA	5.55±0.07 (ns)	0.60±0.05 (ns)
ΔybiK	5.52±0.08 (ns)	0.53±0.04 (ns)
ΔKPN_01165	4.88±0.06 (*)	0.25±0.11 (*)
ΔybiK/ΔKPN_01165	4.85±0.13 (*)	0.28±0.05 (*)

Table 4.4: *The effect of C57BL/6J serum that have EGTA and $MgCl_2$ and heat inactivated C57BL/6J serum on growth yield (Log_{10} CFU/ml) and growth rate μ (h^{-1}) of mutants and wild type* K. pneumoniae *after 120 minutes incubation. Each value represents the mean of three independent experiments, each in duplicate, with their standard error of mean. This table showing no significant differences between the growth yields and rates of the wild type and the other mutants that are represented as (ns) p>0.05.*

Strains	Growth parameters in murine serum plus EGTA and $MgCl_2$		Growth parameters in heat inactivated murine serum	
	Max growth Log_{10} CFU/ ml	Growth rate μ (h^{-1})	Max growth Log_{10} CFU/ ml	Growth rate μ (h^{-1})
Wild type	5.54±0.16	0.63± 0.10	5.86±0.12	0.53±0.08
ΔansA	5.59±0.14 (ns)	0.70± 0.05 (ns)	5.75±0.12 (ns)	0.40±0.04 (ns)
ΔybiK	5.52±0.11 (ns)	0.52± 0.04 (ns)	5.77±0.08 (ns)	0.41±0.07 (ns)
ΔKPN_01165	5.15±0.15 (ns)	0.45± 0.05 (ns)	5.76±0.06 (ns)	0.46±0.10 (ns)
ΔybiK/ΔKPN_01165	5.27±0.06 (ns)	0.50± 0.03 (ns)	5.76±0.05 (ns)	0.57±0.06 (ns)

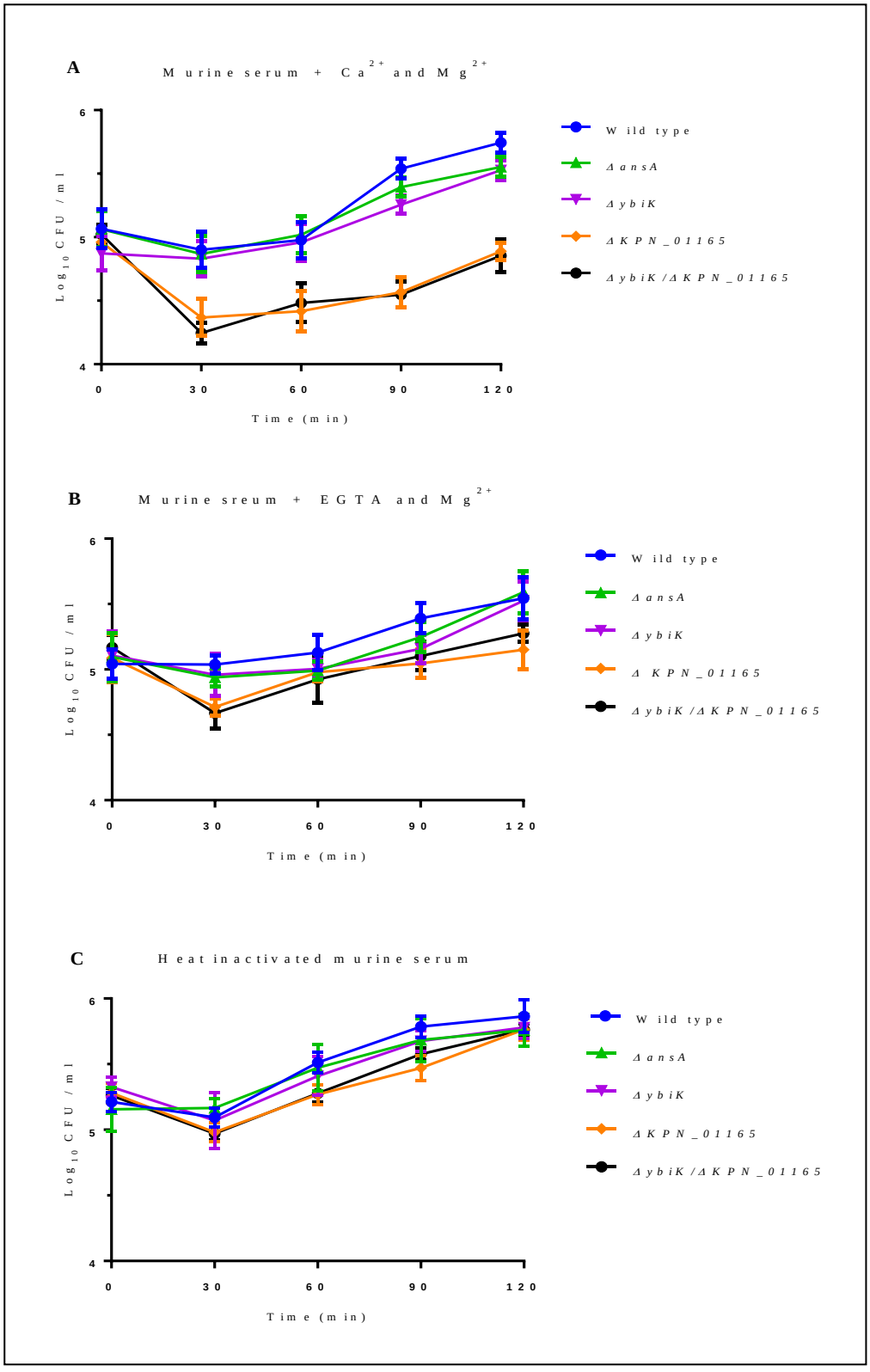

Figure 4.4: *Growth curves of mutants and wild type K. pneumoniae representing their sensitivity to 50% murine serum. CFU was done every 30 minutes after the strains were grown at 37 ^{O}C in a shaker incubator.* ***(A)*** *Shows growth curves after adding Ca^{+2} and*

*Mg^{2+} to a 50 % murine serum. (**B**) Represents the growth profile in murine serum plus both EGTA and Mg^{2+} and there were no significant differences between the growth yields and rates of the wild type and the other mutants p>0.05. (**C**) Growth profiles after heat inactivating the serum which are showing no significant difference in the growth yields and rates between all used strains p>0.05. Each curve represents the mean of three experiments each in duplicate. Vertical bars represent the standard error of the mean.*

4.12 C3 deposition using C57BL/6J serum

C3 activation and C3b surface binding is the central step of the complement system. This binding opsonises the pathogen to support its clearance by neutrophils and macrophages and it could participate in formation of C5 convertase that creates MAC, which may kill the pathogen (Albert *et al*., 1996).

After serum bacteriolytic assays, and by following the protocols described in section 4.9, C3 deposition experiments were done. The aims of these assays were to investigate the ability of the formalin fixed *K. pneumoniae* in initiation of LP and AP pathways by using different dilutions of the mouse serum. C3 cleavage was followed by measuring the amount of C3b deposited on *K. pneumoniae*. Under the assay condition C3b deposition is expected to be via either the LP or AP pathway as the used serum is non-immunized serum. For statistical analysis, I used the OD_{405nm} readings (C3 deposition) that resulted from serum dilution points (2.5% serum in LP and 25% serum in AP) then by the one-way ANOVA and Dunnett's multiple comparisons test the values were compared against the wild type readings. Under AP condition, the OD_{405nm} readings show that C3 deposition on *K. pneumoniae* KR3167 was not detectable with the exception of the OD_{405nm} readings of zymosan (the positive control) (Figure 4.5 A). The C3 deposition of wild type, *ΔansA*, *ΔybiK*, *ΔKPN_01165*, and *ΔybiK*/ *ΔKPN_01165* were not significantly different (p>0.05) (0.21±0.01, 0.17±0.01, 0.16±0.02, 0.21±0.01, and 0.20±0.02, n=3, respectively) (Figure 4.5A). This result confirms that AP is not involved in opsonisation of KR3167 and this is consistent with the serum bacteriolytic results. However, under LP condition, I observed an increase of C3 deposition on all used *K. pneumoniae* strains comparing to their deposition under AP condition which suggests involvement of LP in the deposition (Figure 4.5 B). Interestingly, by comparison to OD_{405nm} reading of wild type (0.60±0.04, n=3), the C3 deposited on *ΔKPN_01165*, and *ΔybiK*/*ΔKPN_01165* (0.91±0.02, and 0.88±0.02, n=3, respectively) were not significantly different (p >0.05)

(Figure 4.5B) through the LP. Furthermore, the C3 deposition results on *ΔKPN_01165*, and *ΔybiK/ ΔKPN_01165* are more than the deposition on zymosan but that was not significantly different $p>0.05$.

The results confirm that wild type, *ΔansA*, *ΔybiK*, *ΔKPN_01165,* and *ΔybiK/ΔKPN_01165* are positively opsonized by LP. Although there was no significant difference in the deposition between all tested strains, the C3 deposition on the less capsulated *ΔKPN_01165*, and *ΔybiK/ ΔKPN_01165* has made them more susceptible to complement attack than the other strains (which was shown in section 4.11). Also, as there was no significant different between *ΔKPN_01165*, and *ΔybiK/ ΔKPN_01165*, this confirms that *ybiK* has no effect on resistance against C3 deposition. In all, the resultshowing that *KPN_01165* deficiency renders the *Klebsiella* susceptible to complement mediated killing.

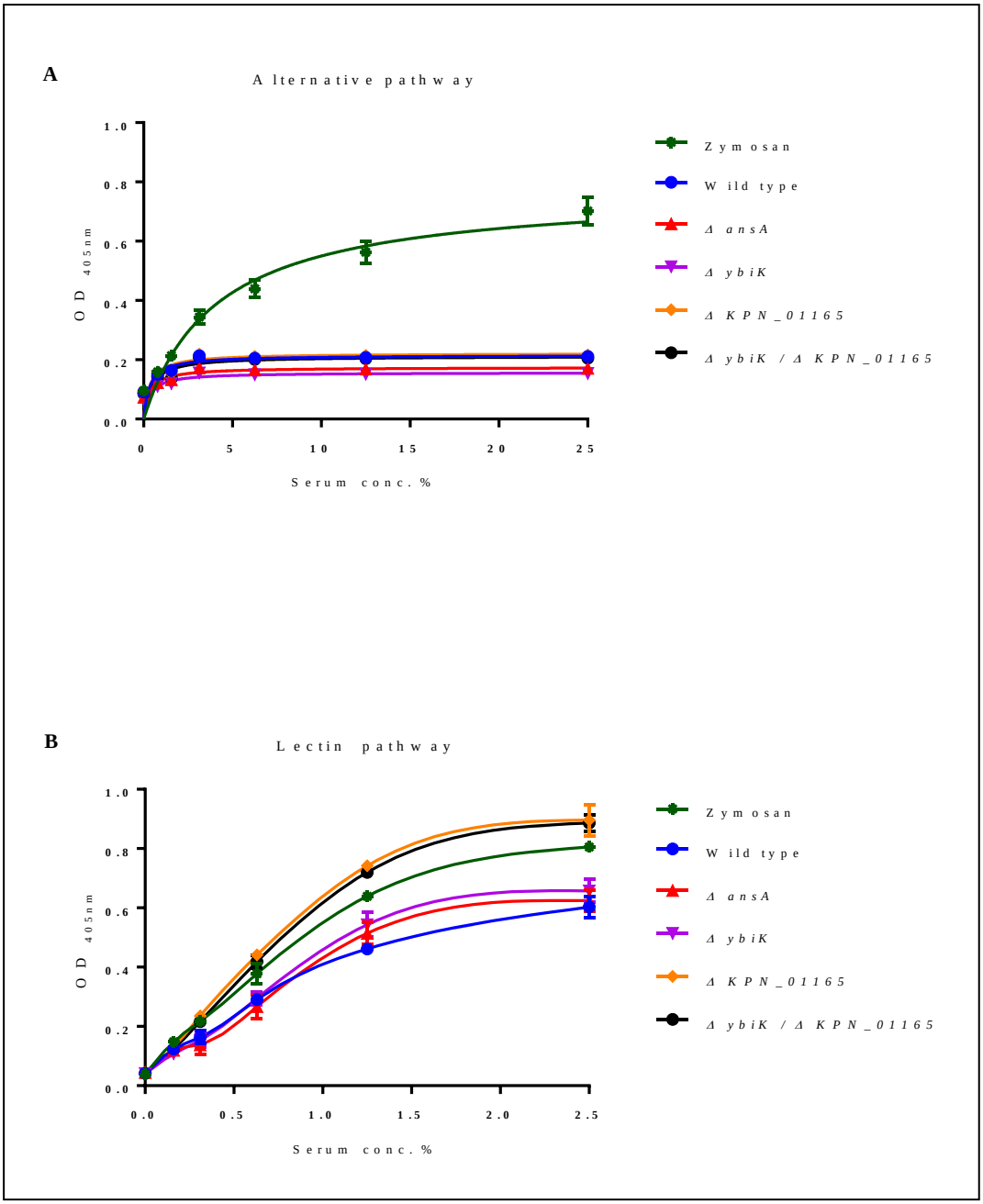

Figure 4.5: *Deposition of C3 fragment products on* K. pneumoniae *measured in ELISA plates.* ***A.*** *The C3 deposition under AP pathway, no detectable absorption is detected in* K. pneumoniae *and there was no significant difference in the C3 deposition levels between all used strains p>0.05* ***B.*** *Lectin pathway mediates activation of complement system on* K. pneumoniae. *The C3 deposited on tstestd stains was not significantly different p>0.05. Zymosan was used as a positive control. The results represent triplicate independent with duplicate for each. Each curve of each strain showing the relative OD values that are expressed as the standard error of the means.*

4.13 Activation of the lectin pathway on *ΔKPN_01165*

In the following experiments, *ΔansA* and *ΔybiK* will be excluded since they didn't show any phenotypes comparing to the wild type. Furthermore, *ΔybiK*/*ΔKPN_01165* will also excluded because it behaved similarly to *ΔKPN_01165*. The previous results have demonstrated the clear role of LP against *ΔKPN_01165*. In mouse, activation of the lectin pathway is mediated by different carbohydrate recognition molecules (MBL-A, MBL-C, ficolin-A and CL-11) (Schwaeble *et al*., 2011). This part of this project aimed to identify which of the murine carbohydrate recognition molecules of the lectin pathway binds to the *ΔKPN_01165*. The role of each of these recognition molecules will be assessed individually through using different transgenic mouse sera.

The used sera were deficient in C3/ MASP-2, MBL-A/C, Ficolin A, and CL-11. All sera were used to compare sensitivity of *ΔKPN_01165* against the wild type. The first deficient serum C3/ MASP-2 $^{-/-}$ was used as negative control (without need for the heating). This serum doesn't have the C3 component along with MASP-2 which is a LP key component hence a deficiency of MASP-2 has leads to a complete loss of lectin pathway C3 convertase complex (Schwaeble *et al*., 2011). The bacteriolytic activity results (with 2 mM $CaCl_2$ and 1 mM $MgCl_2$ addition) in Figure 4.6 A and B show a healthy growth i.e. no bactericidal effect toward both the wild type and Δ*KPN_01165*. The growth of wild type and *ΔKPN_01165* start with Log_{10} 5.06±0.16, and Log_{10} 5.12±0.10, respectively, and continue growing exponentially until the end of the experiment (2 hours) in which the CFU/ml were Log_{10} 6.31±0.14, and 6.19±0.14, n=2, respectively ($p>0.05$) (Table 4.5). Similarly, there was no bacteriolytic activity in the presence of the CL-11 deficient serum as there was no significant differences between the wild type and *ΔKPN_01165* in the growth yields (Log_{10} 5.86±0.01, and 5.72±0.05, n=3, respectively), and rates (0.46 h^{-1} ±0.04, and 0.55 h^{-1} ±0.06, n=3, respectively) ($p>0.05$) (Figure 4.6 A and B, and Table 4.5). The CL-11$^{-/-}$ results highlight the importance of CL-11 as designated recognition molecule, since both MBL (A and C) and Ficolin A are intact, and that do not produce a significant bacteriolytic effect against *ΔKPN_01165* (Figure 4.6 B). The importance of CL-11 was further supported because in the MBL- null serum the bacteriolytic activity was at its maximum. The MBL-A/C$^{-/-}$ serum significantly affected only the growth yield of *ΔKPN_01165* (Log_{10} 5.47±0.12) comparing to the wild type growth yield (Log_{10} 6.13±0.03) ($p<0.05$) (Table 4.5 and Figure 4.6 A and B). Furthermore, it seems that the CL-11 function was better supported in the presence of Ficolin A because in the Ficolin

$A^{-/-}$ serum (both CL-11 and MBLs are present), the effect on *ΔKPN_01165* was only a bacteriostatic effect that last only for one hour then the growth proceeds for the other hour to give growth yield that is not significantly different from the wild type (Log_{10} 5.85±0.05, and 5.77±0.03, n=3, respectively) ($p>0.05$) (Figure 4.6 A and B, and Table 4.5). The CFU/ml of Δ*KPN_01165* at 60 minutes point was Log_{10} 5.10±0.03, and for the wild type it was Log_{10} 5.58 ±0.10 (Figure 4.6 A and B).

Under LP condition (BBS containing; 4 mM barbital, 145 mM NaCl, 2 mM $CaCl_2$, 1 mM $MgCl_2$, pH 7.4), C3 deposition assay was done, on same set of deficient sera. The data analysis was done with one-way ANOVA and Dunnett's multiple comparisons against the wild type. There was no detectable level of C3 in C3/MASP-$2^{-/-}$ serum (Figure 4.7 A). The other results represented in Figure 4.7 further confirm that CL-11 is likely to be the carbohydrate recognition molecule that can initiate the LP complement activation upon binding to the surface of *ΔKPN_01165*. As shown in Figure 4.7 B, the C3 in MBL-A/$C^{-/-}$ serum binds to *ΔKPN_01165* significantly more than the wild type (0.81±0.01, and 0.45±0.01, n=3, respectively) ($p<0.05$) (Figure 4.7 B). However, Ficolin-$A^{-/-}$ and CL-$11^{-/-}$ usage did not lead to any significant C3 deposition difference between the wild type and *ΔKPN_01165* (0.50±0.02, and 0.66±0.01, n=3, respectively) for Ficolin-$A^{-/-}$, and for CL-$11^{-/-}$. The values were 0.48±0.01, and 0.50±0.01, n=3, respectively, ($p>0.05$) (Figure 4.7 C and D, respectively).

Table 4.6: *The effect of C3/ MASP-2, MBL-A/C, Ficolin-A, and CL-11 deficient sera on wild type and* ΔKPN_01165 *on growth yield (*Log_{10} *CFU/ml) and growth rate* μ *(*h^{-1}*) after 120 minutes incubation. Each value represents the mean of triplicate independent experiments, each in duplicate, with their standard error of mean. The significant differences resulted from one-way ANOVA and Dunnett's multiple comparisons against the wild type and the differences are shown with stars, *, p<0.05.*

Strains	Growth parameters in C3/ MASP-2 $^{-/-}$		Growth parameters in CL-11$^{-/-}$	
	Max growth Log_{10} CFU/ ml	Growth rate μ (h^{-1})	Max growth Log_{10} CFU/ ml	Growth rate μ (h^{-1})
Wild type	6.31±0.14	0.72± 0.11	5.86±0.01 (ns)	0.46±0.04 (ns)
ΔKPN_01165	6.19±0.14 (ns)	0.53± 0.05 (ns)	5.72±0.05 (ns)	0.55±0.06 (ns)
Strains	Growth parameters in MBL-A/C$^{-/-}$		Growth parameters in Ficolin-A $^{-/-}$	
	Max growth Log_{10} CFU/ ml	Growth rate μ (h^{-1})	Max growth Log_{10} CFU/ ml	Growth rate μ (h^{-1})
Wild type	6.13±0.03	0.62±0.04	5.85±0.05 (ns)	0.46± 0.01 (ns)
ΔKPN_01165	5.47±0.12 (*)	0.73±0.04 (ns)	5.77±0.03 (ns)	0.62± 0.03 (ns)

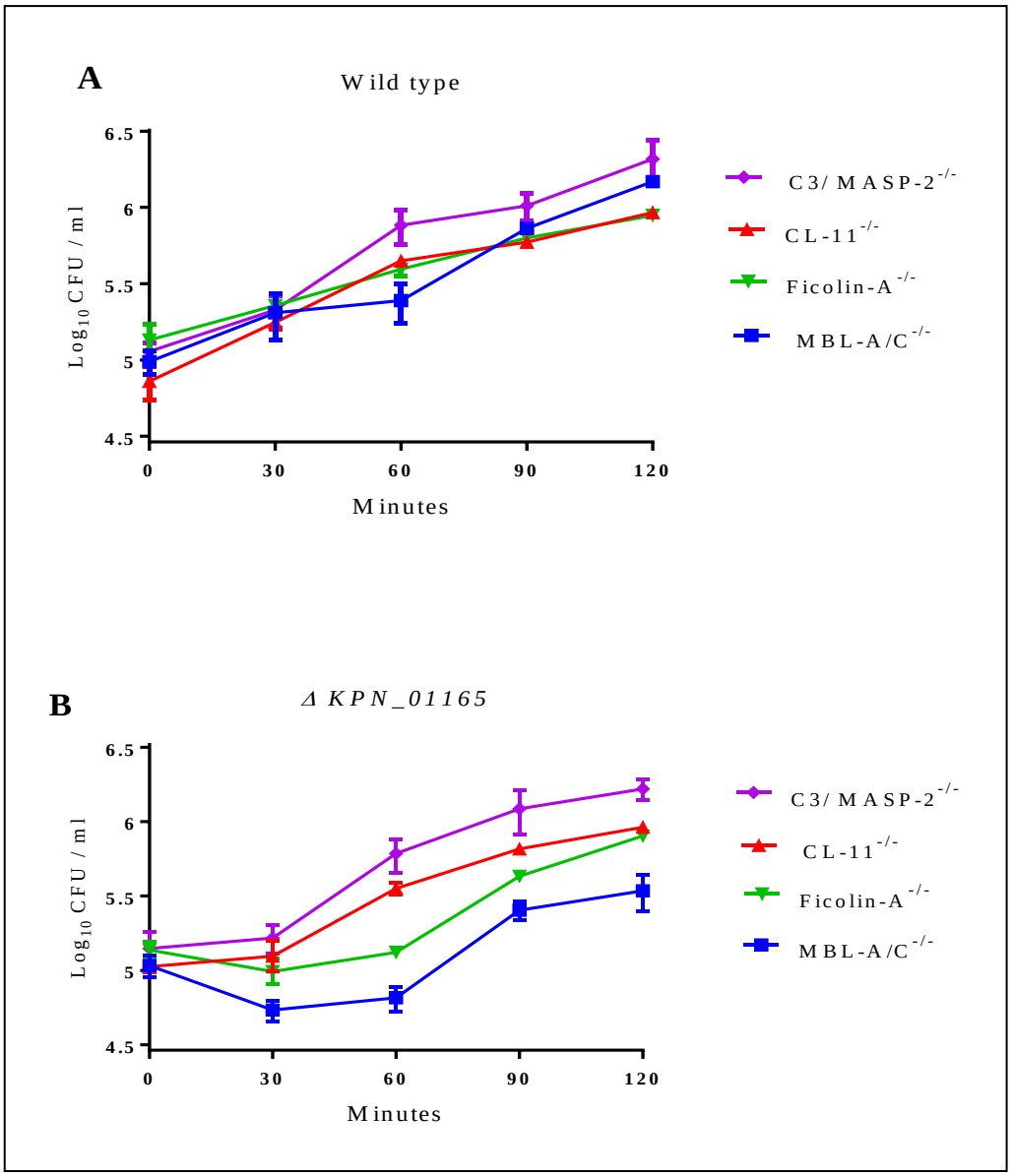

Figure 4.6: *Growth profiles of wild type and* ΔKPN_01165 *that represent their sensitivity to 50% deficient sera shown as curves ranged from top to bottom C3/ MASP-2$^{-/-}$ MBL-A/C$^{-/-}$, Ficolin-A$^{-/-}$, and CL-11$^{-/-}$. Each curve represents the connected points of the mean CFU that was done every 30 minutes after the strains were grown at 37 C^{O} in a shaker incubator. Vertical bars represent the standard error of mean of three experiments each in duplicate. (**A**) The sensitivity of the wild type toward the chosen sera. (**B**) Shows that* ΔKPN_01165 *is sensitive to MBL-A/C$^{-/-}$ serum.*

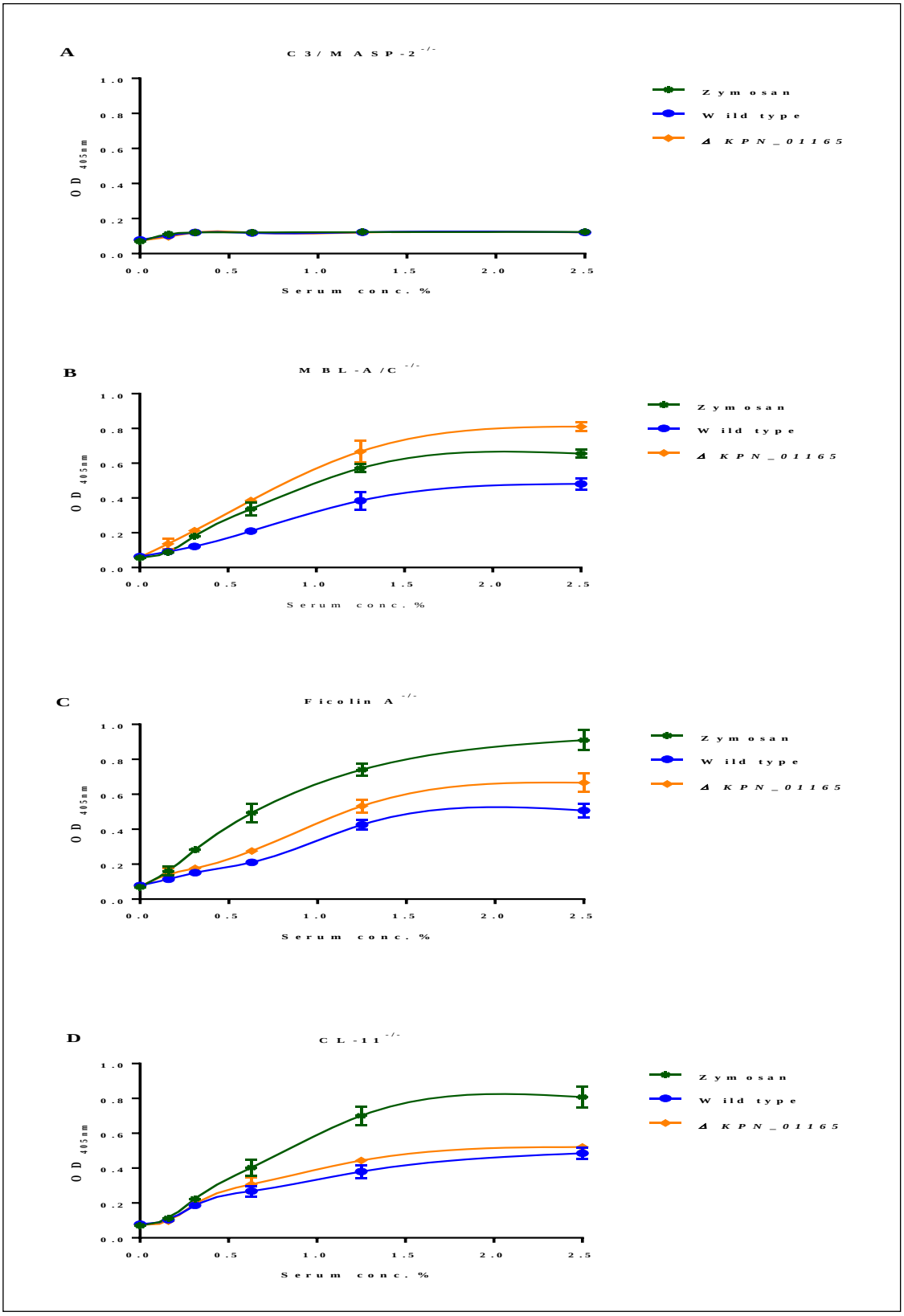

Figure 4.7: *Graphs representing ELISA determination of the deposited C3 fragments on wild type and* ΔKPN_01165 *after incubation with different serially diluted (0 to 2.5 %)*

deficient sera that involve all the carbohydrate recognition molecules of the LP. All C3 depositions done under LP condition. ***A.*** *The negative control condition, as this serum does not have the C3 component along with MASP-2, no detectable absorption was detected in K. pneumoniae and there was no significant dfiierence on the detected C3 levels p>0.05.* ***B.*** *MBL-A/C$^{-/-}$ causes significantly higher C3 deposition on* ΔKPN_01165 *p<0.05, and this could be attributed to the involvement of the CL-11, and in less degree the Ficolin A in K. pneumoniae capsule recognition.* ***C.*** *Graph shows the detectable C3 deposition after using Ficolin A$^{-/-}$ serum which lead to no significant C3 deposition difference between the wild type and* ΔKPN_01165 *p>0.05.* ***D.*** *similar C3 deposition level on wild type and* ΔKPN_01165 *(p>0.05) after using the CL-11$^{-/-}$ serum. This experiment done in three independent occasions with duplicate in each. Each curve has OD values that increased proportionally with serum concentrations and each point expressed as the standard error of the means shown as vertical bars.*

4.14 Murine sera glutamine level

The level of glutamine in the murine sera used here was measured to determine that decreased CFU/ml of *ΔKPN_01165* was not due to inability of acquiring nutrition as *KPN_01165* mutation produced the greatest effects on *K. pneumoniae* biology which hinders its ability in acquiring glutamine (as shown in chapter 3). By using a commercial kit, the glutamine level in tested sera was measured (as described in section 4.10). This kit is indirect method that determines the available glutamine in biological fluids (Kung *et al*., 2011). Human serum has a glutamine level that can reach up to 0.5 mM, and this level drops in infections, burns, and after surgery cases (Haber *et al*., 2017). In two independent trials, with duplicate in each, 50 µl of undiluted serum was used in the enzymatic reactions that yields color change proportional to amount of glutamine because of reduction of NAD+ to NADH by the glutamate dehydrogenase. As shown in Figure 4.8, the one-way ANOVA and Dunnett's multiple comparisons indicate that there were no significant differences between glutamine levels of C57BL/6J serum, C3/MASP-2$^{-/-}$, MBL-A/C$^{-/-}$, Ficolin-A$^{-/-}$, and CL-11$^{-/-}$ which was expressed as mmol glutamine/ml (219.72±9.35,206.1±16.65, 227.9±15.53, 208.00±17.86, and 225.3±11.78, n=2, respectively) (p>0.05). This result confirms the sensitivity to serum shown by *KPN_01165* mutants was due to the serum bactericidal activity not due to glutamine shortage.

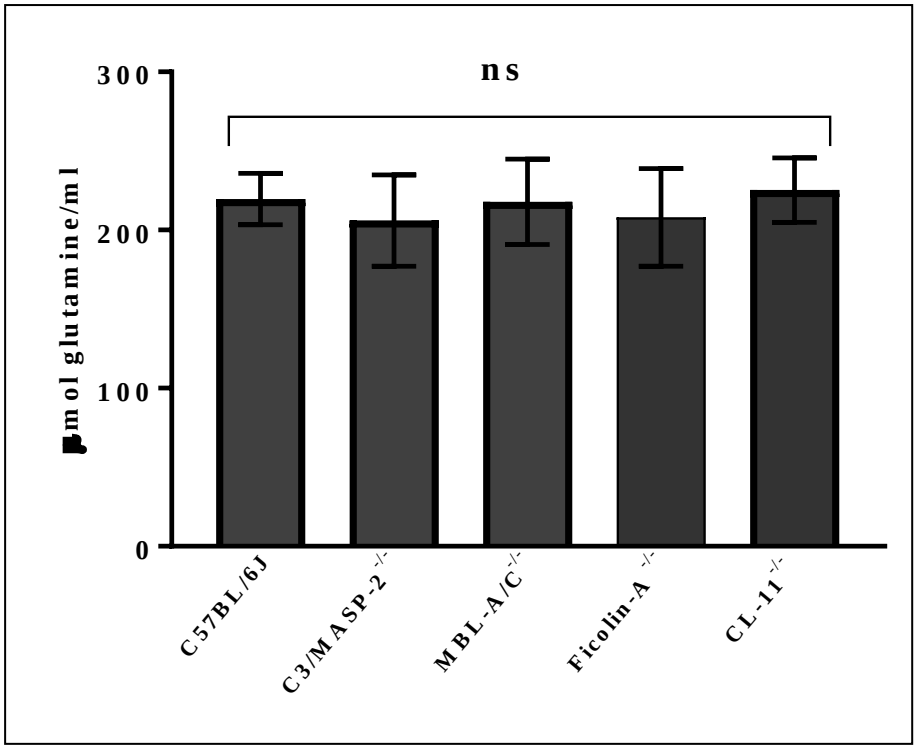

Figure 4.8: *Glutamine content measurement in wild type C57BL/6J serum, and the deficient sera in C3/MASP-2, MBL-A/C, Ficolin-A, and CL-11 murine serum using glutamine assay. The data is average of two independent experiments, each with duplicate. Error bars indicate standard error of the mean.*

Section D: Results summary and discussion

4.15 *K. pneumoniae* response to complement mediated killing

K. pneumoniae causes infection after inhibiting phagocytosis, complement activation, and lysis by antimicrobial peptides. Capsule and lipopolysaccharides (LPS) help in resistance against complement-mediated lysis (Lawlor *et al*., 2006; Clements *et al.*, 2008). Activation of complement pathways on *K. pneumoniae* surface could lead to opsonic proteins deposition like the C3b and potentially formation of MAC, that may damage bacterial membrane resulting in cell death (Albert *et al*., 1996). The capsule is a polysaccharide matrix representing a cell coat for the bacteria, as the acapsular bacteria show less virulence than the bacteria with the capsule (Podschun and Ullmann, 1998). Complement system activated upon recognition of *K. pneumoniae* and the activation of the pathway is varied across *K. pneumoniae* strains. In the previuos chapter, It has been confirmed that the mutant strains in *KPN_01165* is a less capsulated strain and that it is more sensitive to complement attack than the wild type and other strains.

It has been suggested that LPS also serves to protect from the complement system. LPS is a component of the cell membrane of Gram-negative bacteria known also as endotoxin. The component of LPS includes O antigen, core oligosaccharide, and lipid A. There is 9 different O-antigens present in the capsule: O1 is the most common (Merino *et al.*, 2000; Frirdich and Whitfield, 2005; Raetz *et al.*, 2009; De Majumdar *et al.*, 2015). When LPS is “smooth” i.e., it contains the full-length O antigen it can provide the complement protection. However, when the O chain is absent or in shortened form (due to mutation), it is termed as “rough LPS” and then becomes susceptible for complement-mediated recognition as well as killing of the bacteria, even though the capsule is present (Merino *et al.*, 1992). However, other researchers have indicated that O antigens production (endotoxin) can activate the complement system but does not get killed by it. The reason behind this is the capsule binding to C3b. The C3b and MAC proteins bind to the capsule which remain far away from the bacterial membrane and thus avoid from pore formation (Merino *et al.*, 1992; Albertí *et al.*, 1993). My hypotheses is that due to impaired capsule production in *KPN_01165* mutant strains, it led LPS O side chain to be more exposed to complement attack. Future work needs to be done investigate this.

It was demonstrated in a previous study that in *K. pneumoniae* the O side chain of the LPS, is the major deposition site of C3b (Albert *et al*., 1996). The activation of the

complement was reported to be host dependent. In immune hosts, both CP and LP participate in the activation (Ciurana and Tomas, 1987). My results represent CL-11 of the lectin pathway as a major player in recognnition of *K. pneumoniae* KR3167.

The growth profile in different bovine and murine sera point out that the complement system may have significant bactericidal role as the differences in yields between *KPN_01165* mutants and wild type diminished when the serum was heated, and this emphasises the role of asparaginase/ glutaminase enzyme in *K. pneumoniae* biology.

My results point out that LP of the complement system may have a role in recognition of *K. pneumoniae* KR3167. The investigation processes were first established through the bacteriolytic assays using bovine and wild type murine sera (sections 4.11). Only *KPN_01165* mutants have demonstrated a sensitivity toward the bacteriolytic activity of both sera. It seems that the loos of *KPN_01165* has made *K. pneumoniae* KR3167 more sensitive for complement mediated lysis. The bactericidal effect against *K. pneumoniae* is believed to be mediated by opsonic protein deposition like C3b on microbial surfaces (Albert *et al*., 1996). The results of the C3b binding assays clearly showed that *K. pneumoniae* KR3167 can be recognised by the LP carbohydrate recognition molecules. These results also indicate the importance of the asparaginase and glutaminase in *K. pneumoniae* biology as the loss of KPN_01165 has made KR3167 strain a serum-sensitive strain.

Different transgenic mouse sera that were deficient in MBL-A/C, Ficolin A, and CL-11 were used to identify which of the murine carbohydrate recognition molecules of the lectin pathway binds to the *ΔKPN_01165*. The bacteriolytic activities and C3b depositions results using those sera indicate that CL-11 may form complexes with MASPs enzymes and initiate the LP complement activation on the surface of *K. pneumoniae* KR3167.

The role of CP in all experiments was present but this role may be reduced as the used sera are naïve. Classical pathway is primarily activated after the binding of C1q to immune complexes on the surface of targeted cells. However, C1q has also been reported to activate the classical pathway through binding directly to bacterial lipopolysaccharides (Ali *et al*., 2012). For this reason, the future experiments should be designed toeleminate any invovment of CP. This can be done by using transgenic mouse sera deficient in C1q.

5 Chapter -5: *In vivo* virulence studies

Section A: An overview on *Galleria mellonella* usage

5.1 Use of a *Galleria mellonella* larvae as a model of infection

Asparaginase and glutaminase enzymes are involved in the nutritional aspect of microbial life. Factors important for nutrient metabolism are inherently linked to fitness. To determine the role of asparaginase and glutaminase in *K. pneumoniae* virulence, I utilised a *Galleria mellonella* infection model. Unlike purely *in vitro* studies, *in vivo* models of infection are a key investigation tool that reveals the tangible behaviours of mutants without any involvement of any external factors. Struve and Krogfelt, (2003) emphasised the necessity of *in vivo* studies after finding out that *in vitro* results were not sufficient to justify the signficace of bacterial virulence factors, as *in vitro* models cannot truly mimic bacterial behaviour *in vivo*.

Mammalian infection models such as the mouse are generally used for assaying *K. pneumoniae* survival and virulence within a host. However, many published data have reported that mouse infection models are strain dependent and there are variation in susceptibility of mouse strains to *K. pneumoniae* infections (Berendt *et al.*, 1977; Nishi and Tsuchiya, 1980; Domenico *et al.*, 1982; Iizawa *et al.*, 1991). Furthermore, in a mouse model there are many external factors that can confound the results, such as inoculum preparation, inoculum administration route, as well as host relevant factors including mouse strain, age, weight, and sex (Nishi and Tsuchiya, 1980). For instance, different results were obtained when *K. pneumoniae* was administered intranasally or via generation of aerosols (Lawlor *et al.*, 2005). Moreover, mouse models require a high level of experimenter training and experience, and mice colonies are expensive to maintain. On the other hand, insect models are cheaper, and it is easier to maintain insects. The implication of this, is that to detect small differences in fitness, a large number of insects can be used to reach statistical significance. Moreover, the results obtained with insect models have been reported to be consistent with those obtained with the mouse models for various bacterial species (Wand *et al.*, 2013; Insua *et al.*, 2013). Because of the several advantages of insect models, in this study I used an insect model.

The insect used in this study is *Galleria mellonella,* also called the wax moth or honeycomb moth, which is from the order Lepidoptera and the family Pyralidae (Scoble, 1991). Its 'caterpillar' larvae stage is used as a model not the adult moth. Compared to a mouse model, which is ethically questionable, *G. mellonella* is cheaper as large number of worms can be used in each experiment without a need for special accommodation and food. *G. mellonella* are easy to handle regarding infection dose delivery and post infection monitoring, there is also less inter assay variation due to the host's biology or genetic background. The results obtained from *G.mellonella* are clear and easy to interpret which relies on assessment of movement, and the skin colour change, which increases until the worm eventually dies (Joyce and Gahan, 2010; Scorzoni *et al.*, 2013; Harding *et al.*, 2013). Additional advantages of using *G. mellonella* as a virulence model include the possibility of incubating them in different temperatures including the biologically significant 37 ^{o}C, which is also the preferred incubation temperature of the bacterial strains in this study (Scorzoni *et al.*, 2013). In recent years, *G. mellonella* have been widely adapted to study microbial infections, and evaluate a newly discovered antimicrobial agents due to the similarity of their innate immune system to the one found in vertebrates (Joyce and Gahan, 2010; Scorzoni *et al.*, 2013; Harding *et al.*, 2013; Insua *et al.*, 2013; Tsai *et al.*, 2016).

5.2 *G. mellonella* innate immunity and melanisation

Cellular and humoral immune responses are two pillars of the *G. mellonella* immune system. The cellular response is represented by larvae hemolymph, which resembles mammalian blood as the hemolymph cells like haemocytes mediate phagocytosis and clotting. The larval humoral responses include complement- proteins such as melanin, and antimicrobial peptides that opsonise or kill foreign particles (Schmit and Ratcliffe, 1977; Boman and Hultmark, 1987; Pech and Strand, 1996). It has been found that the phagocytosis process in *G. mellonella* and mammals are close to each other in terms of expressed proteins and post phagocytosis mechanisms. For example, haemocytes express a protein that has a great homology to calreticulin, a protein expressed by human neutrophils (Scorzoni *et al.*, 2013). Haemocytes also produce superoxide which is a reactive oxygen species that forms part of the oxidative burst to kill the phagocytosed pathogens (Boman and Hultmark, 1987; Tojo *et al.*, 2000; Scorzoni *et al.*, 2013). The melanisation response to infection is a process that results from melanin deposition on an

invading pathogen as a way of encapsulating it. This opsonization process is followed by phagocytosis by hemolymph cells (Tsai *et al.*, 2016).

5.3 *Galleria mellonella* as a model for *K. pneumoniae* infections

A number of studies have reported the suitability of *G. mellonella* as a model for *K. pneumoniae* infections. Insua et al. (2013) used *G. mellonella* to study the capsule related pathogenicity in different *Klebsiella* strains including the pathogenic and non-pathogenic ones. Similarly, another study that used 50 *Klebsiella* clinical strains and compared them against reference strains reported parallel responses with mouse models regarding survival rate after using a challenge dose of 10^5 CFU/ml, and cell damage (melanisation in the larvae) which was measured using lactate dehydrogenase as a marker (Wand *et al.*, 2013).

Section B: Material and Methods.

Unless otherwise stated, the methods regarding using *G. mellonella* as infection model were done by following protocols published by Insua et al. (2013). I am also grateful for Professor Jose Bengoechea School of Medicine, Dentistry and Biomedical Sciences, Queen's University Belfast, for providing the training in use of *G. mellonella* as an infection model.

5.4 *G. mellonella* selection and incubation conditions

The insects were purchased from Live Foods UK, and on arrival, they were kept in the dark in an incubator (INCU-Line IL 10, VWR International) set at 12°C, using the plastic containers that permit air exchange, and have padding of wood chips. *G. mellonella* larvae were used within 3 days of receipt. On the experiment day, or the night before, larvae selection was done using the criteria of 2 -3 cm long, and 300 – 350 mg weight. All inactive larvae, or with dark exterior skin pigmentation were discarded. In each experiment, a replicate group of 10 larvae were selected, plus 20 larvae as control group, divided as follows:10 with no injection, and the other 10 were injected with PBS (Insua *et al.*, 2013). The larvae stage used represents the 6^{th} stage of *G. mellonella* life cycle in which it can remain for around two weeks without nutrients before moving to next stage (pupating) (Harding *et al.*, 2013).

5.5 Inoculum preparation and dosage delivery for *G. mellonella* infection

Each tested *K. pneumoniae* strain was grown over night at 37ºC in 5 ml LB, then from this culture, a fresh 5 ml LB culture was inoculated using a 1/100 dilution of the overnight culture, and bacteria were left to grow for 3-4 hours at 37 ºC. The bacteria were harvested in the exponential phase (OD_{600nm} 0.6–0.8) by centrifugation at 2,500 xg for 10 min at room temperature. Using the same centrifugation setting, the bacterial pellet was washed twice with PBS. Then cells were resuspended in PBS and the turbidity at 600 nm was adjusted to give an OD_{600nm} of approximately 1.0. From previous investigations, when *K. pneumoniae* KR3167 reach OD_{600} 1, the viable cell count is approximately 10^9 CFU/ml. Based on this knowledge, five dilutions with approximate cell numbers of 1×10^8, 1×10^7, 1×10^6, 1×10^5, and 1×10^4 CFU/ml, were made. These dilutions were used to determine 50% lethal dose (LD_{50}), and in the other infection experiments only 1×10^6 CFU/ml dilution was used. From each prepared dilution, a 100 µl aliquot was plated on LA plates

for precise CFU counting, and a vial of the same PBS that was used for dilution preparation was used for injection control.

In each experiment, 70% ethanol (vol/vol) was used as the larval surface disinfectant. Subsequently, 10 individual disinfected insects were injected with 10 µl of relevant bacterial suspension, into the last proleg (not the head side). The doses were delivered accurately using 10µl capacity Hamilton syringe attached with a fine 26-gauge needle. This glass needle if it is used correctly is optimal for delivering accurate volumes with accuracy of ±1%, as it was designed with a plunger that prevents acquiring excess volumes and limits air disruptions. Moreover, the Hamilton syringe has been used in experiments that require precise sample dispensing such as in column liquid chromatograph experiments (Bavister *et al.,* 1988).

5.6 Lethal dose 50 (LD_{50}) determination

5.6.1 *in vivo* bacterial load determination

This dose response assay was done to detect the bacterial cell number that caused the death of half the tested *G. mellonella* population during an assessment period (Akhila *et al.,* 2007). The lethal dose assay for each strain was performed using PBS alone as control or PBS dilutions containing approximate number of 1×10^8, 1×10^7, 1×10^6, 1×10^5, and 1×10^4 CFU/ml (10^x) *K. pneumoniae* (the precise injected dose for each infection experiment was determined using plate counts). These dilutions were injected into groups of 16 larvae three independent times and the larvae were monitored for three days.

For each group of 16 infected larvae, at 0 h time point, the accuracy of dosage delivery was confirmed in six insects. These six insects were removed randomly among 16 larvae, and they were distributed in groups of two's into 3 sterile Petri-dishes. Immediately after infection, these insects were dissected from the last proleg, then approximately 30 µl of hemolymph was directly transferred to a sterile microcentrifuge tube containing 20 µl 1 mg/ml N-phenylthiourea (Sigma, UK) dissolved in H_2O to prevent melanisation. Then, to determine bacterial count, the lysates were serially diluted and plated into LA to confirm the exact number of CFU/larvae. The remaining 10 infected insects were placed in a Petri dish, then incubated at 37 ^oC, in the dark for only 3 days to avoid pupa stage formation (Insua *et al.,* 2013). The signs of disease were assessed periodically.

5.6.2 Lethal dose calculation

The aim of this experiment was to discover the wild type bacterial cell numbers that would kill all infected larvae within a set period of time. This dose could then be used for comparative mutant testing. The larvae infected by the wild type and mutants were monitored to record the dead and live insects for each bacterial dilution of known CFU/larvae. The median of the lethal dose LD_{50} data was taken as obtained after 24 hours of infection. From this LD50 was calculated after fitting Boltzmann sigmoidal curve and the results were expressed as $Log_{10}\,LD_{50}$, as described in Sanchez et al. (2011). The non-linear sigmoid correlations were calculated in GraphPad Prism 7.4 software through the logarithmic trend line:

$$y = a + (b - a) / (1+10^{\wedge (x\text{-}\log LD50)})$$

a = log number the least deadly dose in a tested group.

b = log number that represents highest deadly dose.

Linear and non-linear correlations were calculated with the GraphPad Prism 7.4 software. LD50 was calculated by fitting a Boltzmann sigmoidal function to the data.

5.7 Determination of *K. pneumoniae* mutant *in vivo* survival and disease score

From the exponentially growing wild type, *ΔyneH*, *ΔansA*, *ΔybiK*, *ΔKPN_01165*, and *ΔybiK/ΔKPN_01165*, approximately 10^6 bacterial cells in 10 µl PBS were deliver to *G. mellonella*. When needed 10 mM glutamine, the main substrate for asparaginase and glutamines enzymes, was also injected. Ten insects for each cohort were used and each experiment was repeated on three independent occasions. Following injection, at predetermined time points (0, 3, 6, 9, and 12 hours post-infection), six insects were collected for the triplicate CFU calculation as described in section 5.6.1 (Insua *et al.*, 2013). The insects were also individually examined at 6, 12, 18, and 24 hours post-infection, for both pigmentation production (melanisation), and mortality. The insects were considered to be dead if they were unresponsive to physical stimuli combined with advance melanisation; usually third and fourth stage as shown in Figure 5.4.

Section C: Results.

5.8 Assessing the fitness of *Klebsiella pneumoniae* using a *G. mellonella* infection model

5.8.1 *K. pneumoniae* KR3167 kills *G. mellonella* in a dose dependent manner

To determine the virulence properties of the *K. pneumoniae* strains, *G. mellonella* was infected by *K. pneumoniae* KR3167 wild type and asparaginase and glutaminase mutant strains. In the beginning, the lethality of the strains was evaluated by injecting the larvae with different inoculum doses containing~ 1×10^8,~ 1×10^7,~ 1×10^6,~ 1×10^5, and~ 1×10^4 CFU/ml as described in section 5.6.1. Insects were kept at 37 ^{O}C and were monitored over 72 h (Figure 5.1 A–F). After the initial experiment, 1×10^8 CFU/larvae was excluded for all strains as the tested larvae could not tolerate this high number of bacteria, and demonstrated rapid and deep melanisation followed by death in less than 24 h. In each experiment, the negative control included groups of 10 larvae that were inoculated with PBS alone. In these groups, no mortality was recorded (Figure 5.1 A–F).

The mean survival percentages of mutants were compared to the wild type with one-way ANOVA and Dunnett's multiple comparisons test. The *G. mellonella* survival percentages in insects that received~1×10^7CFU/ larvae of wild type and *ΔyneH* were not significantly different ($p>0.05$). At 24 h the survival percentages were 7.2 % ± 5.1 and 6.4 % ± 4.6, respectively, and after 48 h the wild type and *ΔyneH* killed 100% of insects. However, the other mutants produced a significantly higher survival rates comparing to the wild type. For example, after 24 h, the survival percentage of *G. mellonella* that received ~1×10^7CFU/ larvae of *ΔansA*, *ΔybiK*, *ΔKPN_01165*, and *ΔybiK/Δ KPN_01165* were 31.3 % ± 6.3, 26.5 % ± 5.7, 51.2 % ± 4.7, and 49 % ± 6.2, respectively, and these numbers were significantly higher than the survival ratio produced by the wild type infection (7.2 % ± 5.1) ($p<0.01$ for *Δ ansA* and *Δ ybiK*) and ($p<0.001$ for *ΔKPN_01165*, and *ΔybiK/Δ KPN_01165*) (Figure 5.1 A–F). Similarly, at 48 h, the larvae infected with ~ 1×10^7CFU/ larvae of *ΔansA*, *ΔybiK*, *ΔKPN_01165*, and *ΔybiK/ΔKPN_01165* continue to produce significantly higher survival percentages (13.4 % ± 6.2, 8.5 % ± 2.5, 21.4 % ± 3.5, and 23.5 % ± 3.5, respectively) than the wild type (0 %) ($p<0.05$ for *ΔansA* and *ΔybiK* and $p<0.01$ for *ΔKPN_01165*, and *ΔybiK/Δ KPN_01165*) (Figure 5.1 A–F). In the third day of infection, the~1×10^7CFU/ larvae from *ΔansA* and *ΔybiK* resulted in complete death of tested larvae, which was similar to the wild type infected larvae (0 % at 72 h)

($p>0.05$) (Figure 5.1 A, C and D, respectively). However, at same time point (72 h), this high dose (~1×10^7CFU/ larvae) from *ΔKPN_01165*, and *ΔybiK/Δ KPN_01165* did not kill all tested insects as the survival percentages were 7.7 % ± 1.8 and 9.5 % ± 4.5, respectively, comparing to wild type survival ratio (0%) ($p<0.05$) (Figure 5.1 A, E and F, respectively).

The surviving larvae after 24 h of infection by~1×10^6 CFU/ larvae of wild type and *ΔyneH* were 36.3 % ± 6.1 and 38.4 % ± 3.4, respectively ($p>0.05$) (Figure 5.1 A and B, respectively). However, at 48 h and 72 h time points, this dose (~1×10^6 CFU/ larvae) in all mutants, except *ΔyneH,* produced significantly higher survival rates than the wild type. For example, the percentage survival of *ΔansA*, *ΔybiK*, *ΔKPN_01165*, and *ΔybiK/Δ KPN_01165* infected larvae at 72 h were 14.3 % ± 2.3, 28.0 % ± 4.3, 42.4 % ± 2.7 and 45.5 % ± 7.4, respectively, which are significantly higher than the wild type infected cohort, in which none survived ($p<0.05$ for *ΔybiK* and $p<0.001$ for *ΔansA*, *ΔKPN_01165*, and *ΔybiK/ΔKPN_01165*).

At 24h and 48 h post-infection, the recorded survival percentages of larvae infected with approximately 1×10^5 CFU/larvae from wild type and *ΔyneH* was not significantly different ($p>0.05$) (Figure 5.1 A and B, respectively). However, under same conditions, the recorded survival levels of *ΔansA*, *ΔybiK*, *ΔKPN_01165*, and *ΔybiK/ΔKPN_01165* infected cohorts were higher than the wild type infected group. For example, the percentage survival after 48 h for *ΔansA*, *ΔybiK*, *ΔKPN_01165*, and *ΔybiK/Δ KPN_01165* infected groups were 65.3 % ± 5.4, 55.5 % ± 3.3, 79.5 % ± 2.5 and 79.4 % ± 2.4, respectively, and the survival levels were significantly higher than the wild type infected cohort, 32% ± 2.7 ($p<0.01$). However, at 72 h post-infection, there was no significant difference in the survival rate between the wild type, *ΔyneH* and *ΔybiK* infected cohorts ($p>0.05$), while the survival rates of cohorts infected with *ΔansA*, *Δ KPN_01165*, and *Δ ybiK/Δ KPN_01165* were higher than the wild type infected larvae (45.0 % ± 5.2, 59.3 % ± 4.0 and 56.5 % ± 6.2, respectively) (Figure 5.1 A-F).

Infection with approximately 1×10^4 CFU/larvae led to 96.4 % ± 2.5 and 97.4 % ± 2.5 survival after 24 h for *ΔKPN_01165* and *ΔybiK/Δ KPN_01165* and this was significantly higher than the survival ratio obtained with the wild type infection (84.5% ± 3.5) ($p<0.05$). On the other hand, the survival ratio of other cohorts infected with *ΔyneH*, *ΔansA*, and *ΔybiK* was similar to the wild type infected cohort ($p>0.05$) (Figure 5.1 A-F).

However, at 48 and 72 h post infection, the survival ratios of larvae infected with all other strains, except *ΔyneH,* was significantly higher than the wild type infected cohort (Figure 5.1 A-F).

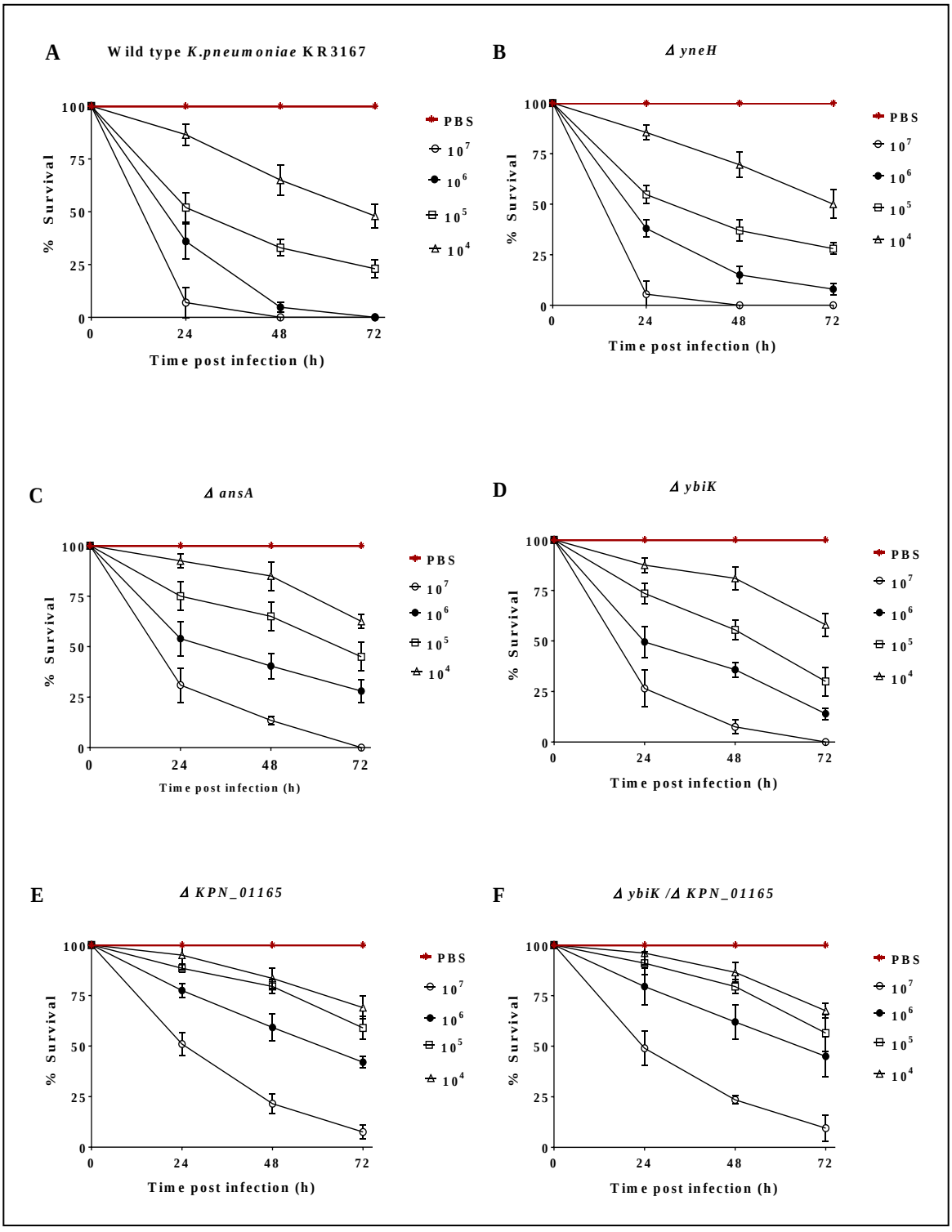

Figure 5.1: K. pneumoniae *KR3167 infection of* G. mellonella *to test the dose-dependent killing. For each bacterial strain, 10 µl from different dilutions of bacterial stock (~*

1×10^7,~1×10^6,~1×10^5, and~1×10^4 CFU/ml) was injected to a group of 16 G. mellonella. *Larvae survival was monitored every 24 h post infection for 72 h. Larvae survival after injection with (A) wild type* K. pneumoniae *KR3167, (B)* Δ yneH, *(C)* Δ ansA, *(D)* Δ ybiK, *(E)* Δ KPN_01165 *and (F)* Δ ybiK/ Δ KPN_01165. *PBS injection was used as assay control. Error bars show the standard error of mean for three individual experiments using one-way ANOVA and Dunnett's multiple comparisons test.*

5.8.2 Lethal dose 50 (LD_{50}) determination

From the same data of the dose–response experiments (section 5.8.1), the lethal dose 50 (LD_{50}) of each strain was determined as described in section 5.6.2. LD_{50} is the dose required to kill half the members of a test group after a specified test duration (Trevan, 1927). My aims were to determine the susceptibility of *G. mellonella* to *K. pneumoniae* KR3167 wildtype and asparaginase/glutaminase deficient strains, and to discover a baseline of bacterial cell number in which the lethality of the mutant strains could be compared against the wild type.

The LD_{50} was calculated for each strain at 24 h post-infection (Figure 5.2 A–F). Unlike 48 h and 72 h time points, at 24 h post infection, the highest dose for all study strains, 1×10^7 CFU/larvae, did not kill all the larvae (Figure 5.1 A–F). The exact LD_{50} of all strains was calculated by recording the number of dead insects and expressed as Log_{10} LD_{50} (as described in section 5.6.2). The results showed no significant difference between Log_{10} LD_{50} of *ΔyneH* and *ΔybiK* (Log_{10} LD_{50} 5.59±0.06 and Log_{10} LD_{50}5.86±0.11, CFU/larvae, n=30, respectively) compared to the wild type ($LD_{50}Log_{10}$ 5.65±0.14, CFU/larvae, n=30) ($p>0.05$) (Figure 5.2 A-F). However, approximately one log increase was recorded in the LD_{50} of *ΔKPN_01165*, and *ΔybiK/ ΔKPN_01165*S (Log_{10} LD_{50} 6.55±0.04 and Log_{10} LD_{50}6.43±0.14, CFU/larvae, n=30, respectively) comparing to wild type LD_{50} ($LD_{50}Log_{10}$ 5.65±0.14, CFU/larvae, n=3) ($p<0.05$). A significant difference in Log_{10} LD_{50} was also recorded in the strain lacking *ansA* (Log_{10} LD_{50} 6.09±0.08, CFU/ larvae, n=30) ($p<0.05$) (Figure 5.2 A-F).

Collectively, those results suggest that Asparaginase and Glutaminase genes are important in maintenance of *K. pneumoniae* KR3167 in *G. mellonella* tissues, and this insect is susceptible to *K. pneumoniae* infection.

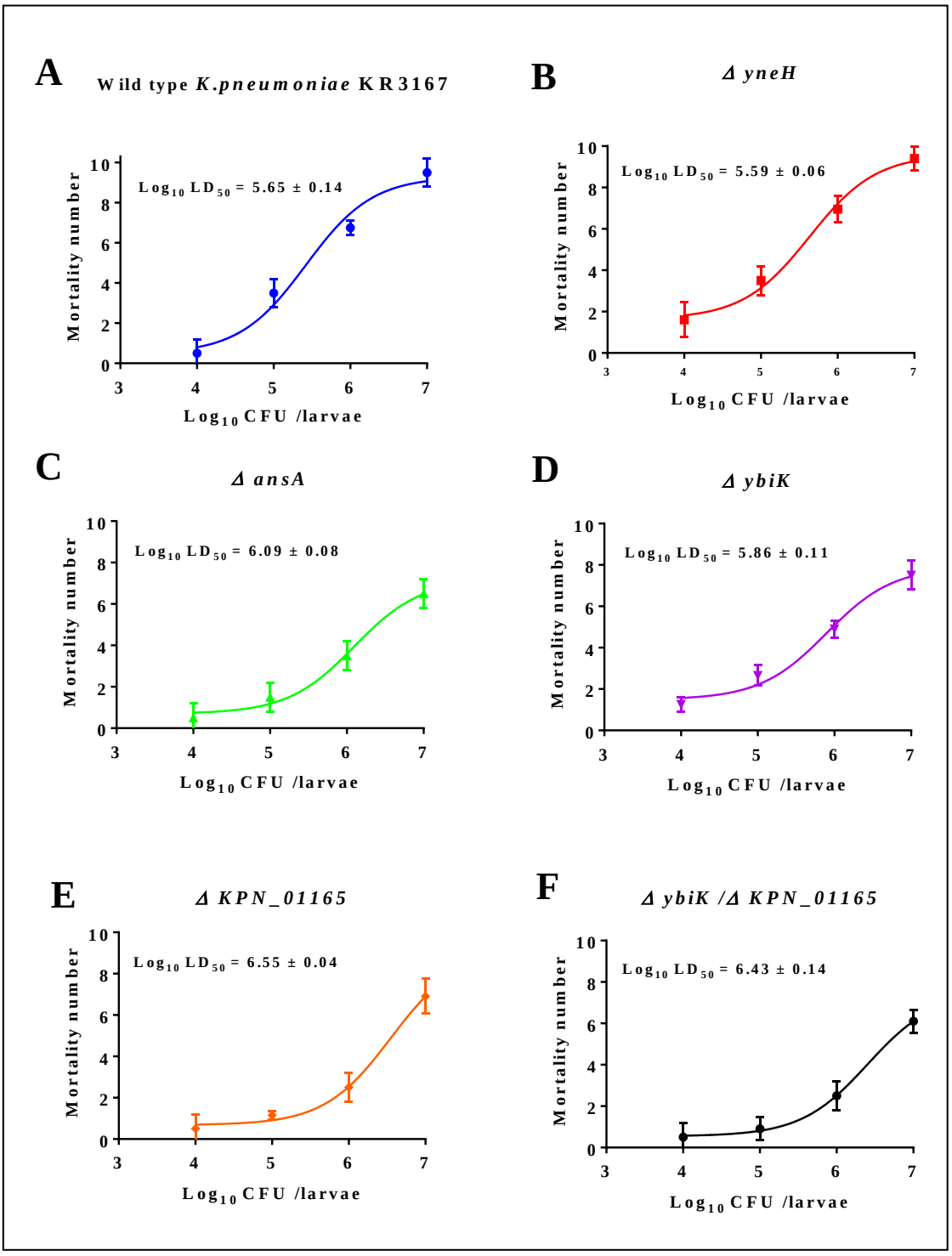

Figure 5.2: *Plots represent the calculated LD_{50} for different* K. pneumoniae *strains after 24 h post infection.* G. mellonella *were injected with 10 µl PBS containing ~ 1×10^7, ~ 1×10^6, ~ 1×10^5, and ~ 1×10^4 CFU/ml of* K. pneumoniae *KR3167 strains. No significant difference was found ($p>0.05$) in $log_{10}LD_{50}$ of* ΔyneH *and* ΔybiK *(B and D, respectively), comparing to the log_{10} LD_{50} of wild type strain (A), while there were significant differences between the* Δ ansA, Δ KPN_01165, *and* Δ ybiK/ Δ KPN_01165 *(C, E, and*

F, respectively) and the wild type. Error bars represent the standard error of mean of triplicate experiments (10 insects per each).

5.9 Assessment of *Klebsiella pneumoniae* strain survival during *G. mellonella* infection

I demonstrated the susceptibility of *G. mellonella* to *K. pneumoniae* strains as some of these strains killed the larvae with different LD_{50}, which suggested a reduction in the pathogenicity of asparaginase and glutaminase mutants. Next, I hypothesised that the reduction of virulence is linked to microbial growth attenuation *in vivo*. Hence, I assessed the growth of each strain during infection. Larvae were infected with~1×10^6 CFU/ml with or without 10 mM glutamine for each strain. In these infections, glutamine was used to determine its impact on *K. pneumoniae* growth *in vivo*. PBS injections (plain and with 10 mM glutamine) were used as assay control. Those two set of experiments (i.e with glutamine addition and without glutamine addition) were doneseparately in three independents trials with 10 insects in each. After infection, the bacterial growth was monitored over 12 h. The viable bacterial count determination was done as described in section 5.7. After delivering 10^6 CFU/ml at 0 h time point, bacterial loads in the 6 larvae for different cohorts were determined. Also, at 0 h time point, the glutamine level in the hemolymph was measured but no results were obtained and that may due to glutamine level being below the kit detection limit (section 4.10). The results showed no significant difference among different groups, illustrating the accuracy of inoculation ($p>0.05$) (Table 5.1, and Table 5.2, respectively), (Figure 5.3. A and B, respectively). At 12 h post-infection, the growth yield and rate of *ΔyneH* infected larvae (growth yield: Log_{10} 7.87±0.13, CFU/larvae, and growth rate: 0.32 h^{-1} ± 0.05, n=6) were not significantly different from that of wild type (growth yield: Log_{10} 7.89±0.08, CFU/larvae, and rate 0.39 h^{-1} ± 0.03, n=6) ($p>0.05$). However, at 12 h post-infection, less than one log reduction was recorded in *ΔansA*, *ΔybiK* counts (Log_{10} 6.70±0.18, and Log_{10} 6.81±0.10, CFU/larvae, n=6, respectively) comparing to wild type numbers (Log_{10} 7.89±0.08, CFU/larvae, n=6), and a significant growth attenuation, around log_{10} 1.5 CFU/larvae relative to the starter inoculum, was recorded in *ΔKPN_01165*, and *ΔybiK/ΔKPN_01165* (Log_{10} 4.60±0.15, and Log_{10} 4.28±0.20, CFU/larvae, n=6, respectively) ($p<0.001$) comparing to the wild type which was able to thrive and grow inside *G. mellonella* tissues as the recorded log_{10} bacterial numbers at 12 h post infection were 7.89±0.08 comparing to starter inoculum log_{10} 6.25±0.20 (Table 5.1 and Figure 5.3 A).

When the dose was administered in the presence of glutamine, there was no significant difference between *ΔyneH* and wild type growth parameters as the recorded growth yields were Log_{10} 7.07±0.12 CFU/larvae and Log_{10} 7.18±0.20, respectively and growth rates were 0.19 h^{-1} ± 0.03 and 0.23 h^{-1} ± 0.04, respectively, (p>0.05) (Table 5.2 and Figure 5.3 B). However, the addition of glutamine changes the growth parameters of other strains. What can be clearly seen in Table 5.2 and Figure 5.3 B is that both *K. pneumoniae* and *G. mellonella* behave differently when the bacterial dose is given in the presence of glutamine. This addition reverses the microbial phenotype by improving the survival of *ΔansA* and *ΔybiK*. The results indicate that the growth yields and rates of *ΔansA* and *ΔybiK* (growth yield: Log_{10} 6.89±0.31 CFU/larvae and 7.07±0.25 CFU/larvae, n=6, respectively, and growth rate: 0.21 h^{-1} ±0.02; and 0.22 h^{-1} ±0.03, n=6, respectively), were not affected by *G. mellonella* clearance mechanism relative the wild type strain yield (Log_{10} 7.18±0.20 CFU/larvae, n=6), (P>0.05), and rate (0.23 h^{-1} ±0.04, n=6) (P>0.05) (Table 5.2, Figure 5.3 B). However, glutamine addition did not support the growth of *ΔKPN_01165*, and *ΔybiK/ ΔKPN_01165* since *G. mellonella* started clearing the infection as early as 3 h post-infection (Table 4.2 and Figure 5.3 B). A good illustration of this clearance can be seen with the growth yield in which there was significant difference, around 2 log_{10} CFU /larvae, between the wild type and both *ΔKPN_01165*, and *ΔybiK/ ΔKPN_01165* (Log_{10} 7.18±0.20, Log_{10} 4.84±0.24, and Log_{10} 4.91±0.09, CFU/larvae, n=6, respectively) (p<0.001) (Table 5.2, Figure 5.3 B). Interestingly, at 6 h post-infection the *ΔansA* numbers (Log_{10} 5.66±0.20, CFU/larvae, n=6) were significantly lower than the wild type log_{10} numbers (Log_{10} 6.50±0.17, CFU/larvae, n=6) (p<0.05) (Figure 5.3 B). Overall, these results indicate that *ansA*, *ybiK*, and *KPN-01165*, are essential in maintenance of *K. pneumoniae* KR3167 in *G. mellonella* tissues.

Table 5.1: *Growth yield (Log_{10} CFU/larvae) and growth rate μ (h^{-1}) of mutants and wild type* K. pneumoniae *after delivering 1×10^6 CFU /larvae (without glutamine addition). At three independent trials and at different time intervals six larvae were dissected and haemolymphs were collected. Then the viable plate counts were obtained, and Log_{10} CFU /larvae was determined. Data are the mean of triplicate experiments. Six larvae were used for each time point, '±' represents the standard error of mean. The significant differences are shown with stars: (*) p< 0.05, (***) P<0.001 relative to the wild type. 'ns' not significant p>0.05. 0 h: time zero, and (h) is a symbol of hours.*

Strains	0 h	Growth rate μ (h^{-1})	Max growth Log_{10} CFU/larvae
Wild type	6.25±0.20	0.39± 0.03	7.89±0.08
ΔyneH	6.30±0.16 (ns)	0.32± 0.05 (ns)	7.87±0.13(ns)
ΔansA	6.16±0.09 (ns)	0.15± 0.03 (*)	6.70±0.18 (*)
ΔybiK	6.13±0.22 (ns)	0.20± 0.04 (*)	6.81±0.02 (*)
ΔKPN-01165	6.22±0.06 (ns)	(-)0.14± 0.03 (***)	4.60±0.21 (***)
ΔybiK/ΔKPN-01165	6.14±0.14 (ns)	(-)0.17± 0.02 (***)	4.28±0.15 (***)

Table 5.2: *The impact of adding 10 mM glutamine to* K. pneumoniae *maximum growth yield (Log_{10} CFU/larvae) and growth rate μ (h^{-1}) in* G. mellonella. *In three independent trials ten insects were administered with 10 μl PBS dosages containing 1×10^6 CFU / ml bacterial loads plus 10 mM glutamine. Data are the mean of triplicate experiments. Six larvae were used for each time point, '±' represents the standard error of mean. *** P<0.001 relative to the wild type. 'ns' not significant p>0.05. 0 h: time zero, and (h) is a symbol of hours.*

Strains	0 h	Growth rate μ (h^{-1})	Max growth Log10 CFU/larvae
Wild type	6.14±0.11	0.23± 0.04	7.18±0.20
ΔyneH	6.22±0.06 (ns)	0.19± 0.03 (ns)	7.07±0.12 (ns)
ΔansA	6.19±0.09 (ns)	0.21± 0.02 (ns)	6.89±0.31 (ns)
ΔybiK	6.06±0.04 (ns)	0.22± 0.03 (ns)	7.07±0.25 (ns)
ΔKPN-01165	6.19±0.26 (ns)	0.06± 0.01 (***)	4.84±0.24 (***)
ΔybiK/ΔKPN-01165	6.25±0.07 (ns)	0.03± 0.01 (***)	4.91±0.09 (***)

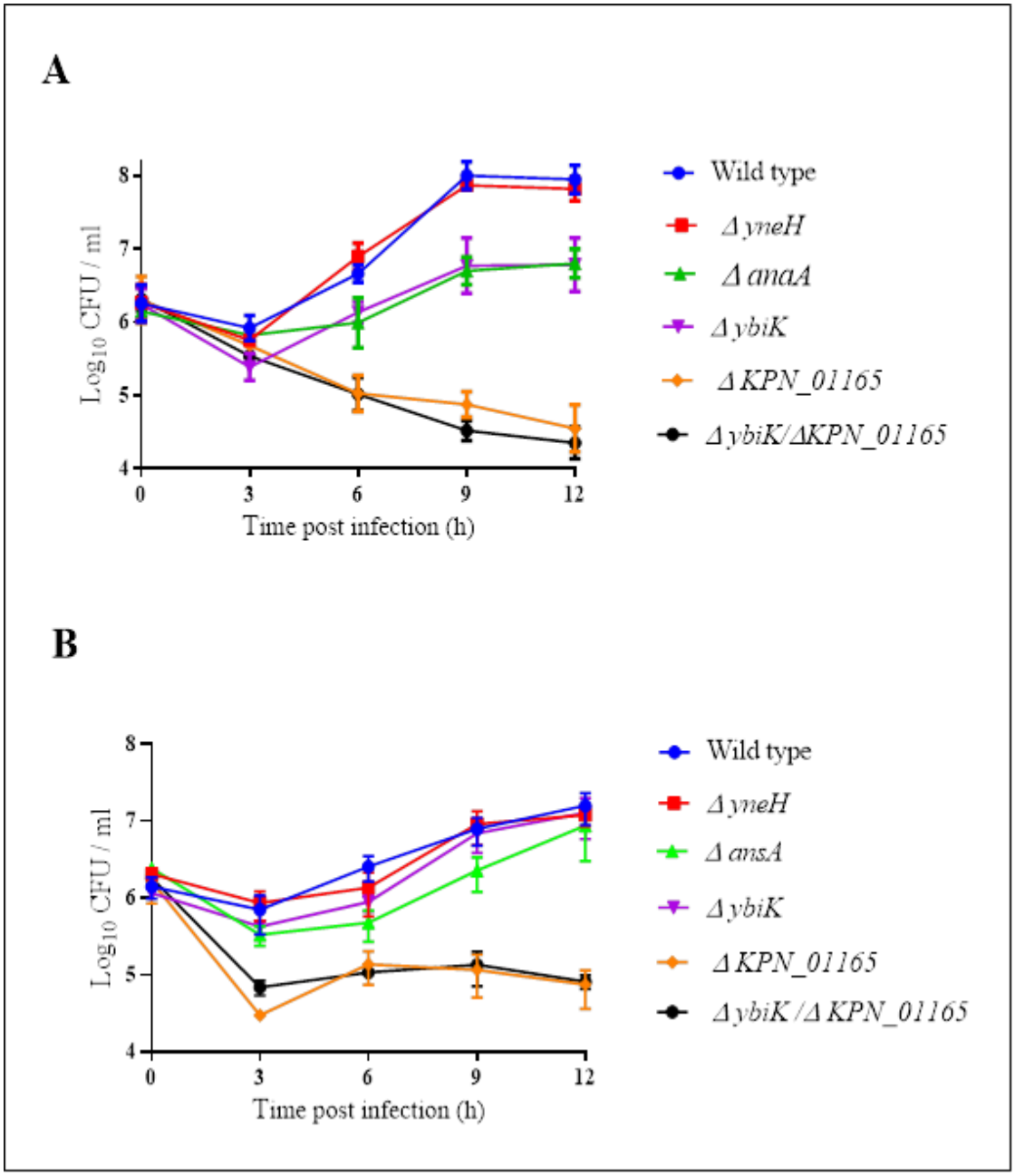

Figure 5.3: *Survival of mutants and wild type* K. pneumoniae *KR3167 strains in* G. mellonella *tissues after injection of 1 ×10^6 CFU / larvae in 10 µl PBS only (A) or 10 µl PBS supplemented with 10 mM glutamine (B). The bacterial load (Log$_{10}$ CFU / larvae) was determined at several time points as described in section 5.6. Each point represents the mean Log$_{10}$ CFU /larvae derived from triplicate experiments in 6 larvae and the bars represent the standard error of mean.*

5.10 *G. mellonella* response to infection by *K. pneumoniae* KR3167

An obvious advantage of using *G. mellonella* as a model is the infection process can be visualised in real time. This infection associated phenotype is defined as melanisation, which was described in section 5.2. Melanisation is a disease sign that results from increased melanin production to encapsulate foreign bodies. Usually these pigment formations are the result of microbial peptide production, and coagulation of haemolymph. This process can be visualised after infection as the larvae skin start changing to black and can be used as the indicator of infection progress and larvae tissue damage (Tsai *et al.*, 2016).

In the experiments in sections 5.8 and 5.9, I observed that infected larvae signs (skin colour and movement) varied depending on the bacterial strains used for infection. As a result, the objective of this experiment was to quantify disease signs that resulted from infection with each *K. pneumoniae* strain. Several reports have illustrated the melanisation stages during infection. The healthy stage is characterised by a white creamy colour, while in diseased stage the melanisation increases gradually (Insua *et al.*, 2013; Harding *et al.*, 2013; Scorzoni *et al.*, 2013; Tsai *et al.*, 2016). In my work on *G. mellonella*, I categorized the melanisation stages that caused by *K. pneumoniae* KR3167 strain infections by periodically monitoring the infected larvae at 6, 12, 18, and 24 h post infection and recording the stages and the number of larvae for each stage (Figure 5.5A). From these observations I was able to categorise the infection progression into five stages depending on the melanisation development (Figure 5.4). Stage zero represented the healthy active larvae that are creamy in colour with no pigmentation. Stage one defined as primary melanisation stage in which a clear black line stretching from tail to head will appear on examined larvae. At stage two, larvae are no longer creamy but develop slightly brown pigmentation, and comparing to stage one the black line now is thicker and intensely black. The next phase is stage three, the larvae are severely ill and sometimes dead, and if they are live they will be slow in motion with completely dark brown skin, and the black line in this stage becomes integrated with the skin. The last stage is stage four, when most larvae are dead with totally black hard texture. At all stages I have recorded the mortality rates that caused by each strain (Figure 5.5 B).

The assessment of melanisation stages and mortality assay were done in parallel with survival monitoring of KR3167 strains during *G. mellonella* infection (section 5.8). After

recording the melanisation stages that resulted for each strain infection at 6, 12, 18, and 24 hours, I was able to produce an overall disease scores to ease the interpretation of results. The results were expressed as a percentage of disease relative to wild type score (Figure 5.5 A). At each time point i.e. 6, 12, 18, and 24 hours, from each tested strain, the percentage of overall disease score was calculated by adding the numbers of larvae that are in different stages, such as stage 1, 2, 3, and 4 (Figure 5.4 and Figure 5.5 A). The repeated-measures that assess *G. mellonella* response against each study strain were statically analysed by two-way ANOVA and Dunnett's multiple comparisons test. It can be seen from Figure 5.5 A, that the disease score percentages of *ΔyneH* infected insects was not significantly different to that of the wild type throughout the infection process ($p>0.05$) (Figure 5.5 A). For example, at 6 h and 12 h post infection *G. mellonella* infected with approximately 1×10^6 CFU/ larvae of a strain lacking *yneH* had recorded disease scores (29.3 % ± 6.3 and 41.4 % ± 4.4, respectively) that were not significantly different ($p>0.05$) from wild type infected larvae scores for the same time points (27.5 % ± 4.3 at 6 h and 44.0 % ± 3.5 at 12 h) (Figure 5.5 A). Also, at these two points (at 6 h and 12 h), the disease scores recorded for *ΔansA* and *ΔybiK* were not significantly different form the wild type scores. A clear demonstration can be seen at the 12 h recording point as the mean percentages of the overall melanisation stages recorded for *ΔansA* and *ΔybiK* infections were 36.5 % ± 3.4 and 41.8% ± 5.6, respectively, and these were not significantly different form the wild type result, 44.0 % ± 3.5 ($p>0.05$) (Figure 5.5 A). However, at the other time points (18 h and 24 h), *ΔansA* and *ΔybiK* showed a significant reduction in disease score compared to wild type ($p<0.001$). However, compared to the wild type, the *ΔKPN_01165,* and *ΔybiK/ ΔKPN_01165* mutant infected larvae at all-time points (6, 12, 18, and 24 hours) showed significantly lower disease scores ($p<0.01$ at 6h and $p<0.001$ at 12- 24 h). A clear illustration for the lower disease scores in *ΔKPN_01165*, and *ΔybiK/ ΔKPN_01165* infected larvae is shown at 18 h post-infection. The recorded *ΔKPN_01165,* and *ΔybiK/ Δ KPN_01165* scores at 18 h were 31.5 % ± 4.9 and 38.4 % ± 3.6, respectively, and the wild type score was 69.5 % ± 7.0 ($p<0.001$) (Figure 5.5 A).

This result highlights the important role of asparaginase and glutaminases in infection process since as the melanin deposition on larvae body was varied among the tested strains. For example, the statistical analysis of 18 h post-infection data point showed significant difference in the number of stage 3 larvae carrying *ΔansA*, *ΔKPN_01165,* and

ΔybiK/ ΔKPN_01165 infection compared to wild type ($p<0.05$) for *ΔansA*, and ($p<0.01$) for *ΔKPN_01165*, and *ΔybiK/ ΔKPN_01165*.

In addition to recording the disease sign scores, I also assessed the *Galleria* mortality during the course of infection. Comparing to the other strains, the collected data at 6 h post infection, showed that only larvae infected with the wild type and *ΔyneH* had mortality, 4% ± 0.72, and 3 % ± 1.41 dead larvae respectively (Figure 5.5 B). This result highlights the importance of the role of asparaginase and glutaminase enzymes in the infection process since the other larvae infected by the other mutants were not dead at the 6 h time point, (Figure 5.5 B). At 12h, all the infected larvae displayed increasing signs of mortality. At 12 h post infection, the mortality rate due to infection with the *ΔansA*, *ΔKPN_01165*, and *ΔybiK/ ΔKPN_01165* mutants were 9.5% ±2.2,4.5% ±0.8, and 3.5% ± 1.7, respectively, which was significantly lower than the mortality inflicted by the wild type at 19.5% ± 3.5 ($p<0.05$ for *Δ ansA*) and ($p<0.001$ for *ΔKPN_01165*, and *ΔybiK/ ΔKPN_01165*) (Figure 5.5 B). At 18 h post-infection, the higher levels of mortality in wild type (37.5% ± 3.5) infected larvae contrast strongly with the less pathogenic *ΔansA*, *ΔybiK*, *ΔKPN_01165*, and *ΔybiK/ Δ KPN_01165* mutants ($p< 0.01$ for *ΔansA*, and *ΔybiK*) and ($p<0.001$ for *Δ KPN_01165*, and *Δ ybiK/ Δ KPN_01165*) (Figure 5.5 B). At the last time point (24 h), the mortality rates due to the wild type infections were always higher (64.5% ±3.7) than the mortality rates due to the mutants) ($p<0.001$) (Figure 5.5 B).

In summary, except *Δ yneH*, all tested asparaginase/glutaminase mutants attenuated in growth and virulence significantly in *G. mellonella* infection model.

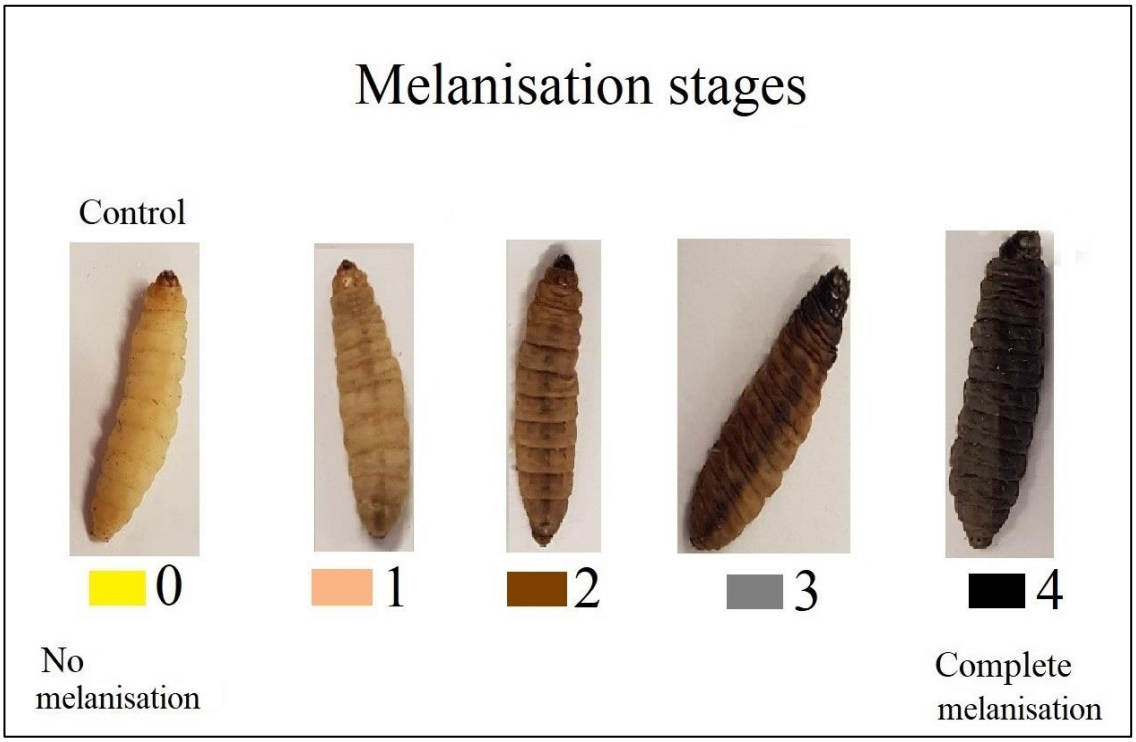

Figure 5.4. *Pictures of* G. mellonella *representing the scoring strategy that was followed to assess the progression of infection. Intensity of melanisation and mobility were the criteria for differentiating one stage from the other. The control stage is indicated with (0), healthy mobile larvae with cream skin colour. As infection progresses larvae are melanised with reduced mobility. As the infection progresses melanisation rate increases, and insects become progressively less mobile (stages of 2 and 3), and at the final stage the insect does not move, and insect is seen as black (stage 4).*

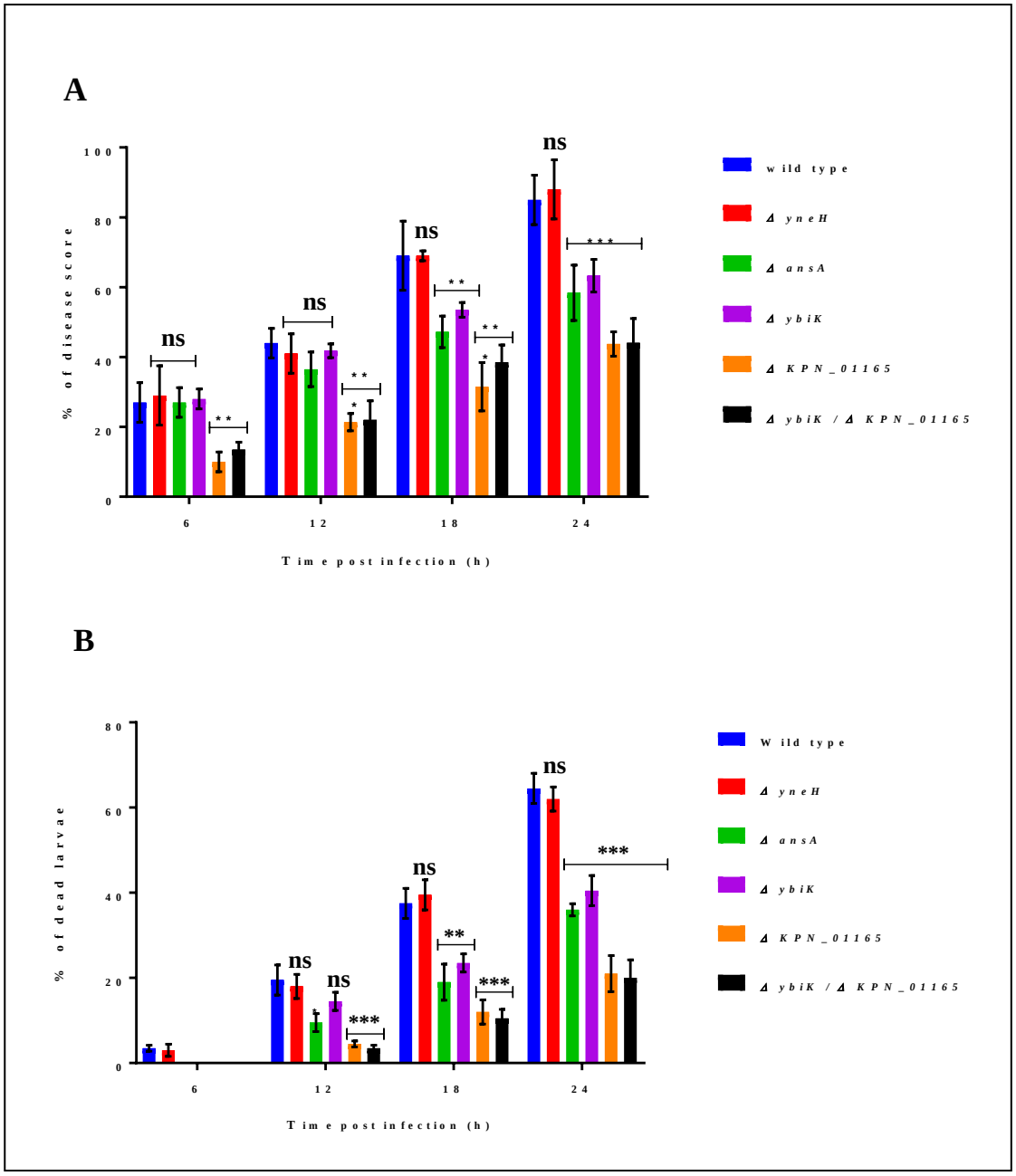

Figure 5.5. *Virulence assessment of* K. pneumoniae *strains in* G. mellonella *infection model* ***A.*** *Graph represents the percentage disease sign scores for* G. mellonella *infected with approximately 1 ×10^6 CFU/larvae* K.pneumoniae *strains. Each column represents the mean percentages of the added melanisation stages at 6, 12, 18, and 24 h post infection with* K. pneumoniae *strains.* ***B****. Graph showing* G. mellonella *percentage mortality during a 24 h infection course with approximately1 ×10^6 CFU/larvae* K.pneumoniae *strains. As shown only wild type, and* ΔyneH *were able to kill at 6 h post-infection, whereas the other mutants were not. The columns represent the mean percentage killing and data were derived from triplicate experiments, each used 10*

*larvae. The vertical bars represent the standard error of mean. Data were analysed using two-way ANOVA and Dunnett's multiple comparisons test. 'ns' not significant p> 0.05, *p< 0.05, **p<0.01, and *** p<0.001 relative to the wild type infected cohort for corresponding time points.*

Section D: Results summary and discussion.

5.11 The role of asparaginase and glutaminase enzymes in virulence of *K.pneumoniae* KR3167

This project has focused on whether there is a role of asparaginase and glutaminase enzymes in *Klebsiella pneumoniae* virulence. To test this theory *G. mellonella* larvae were infected with *K.pneumoniae* KR3167 wild type and asparaginase and glutaminase mutant strains. *G. mellonella* is a suitable model for *K.pneumoniae* as it has an innate immune response that is closely related to mammalian organisms, and in comparison infection studies give survival rates post infection that are a close parallel with mouse infection models (Wand *et al.*, 2013). However, the results of using *G. mellonella* as *in vivo* infection model support the hypothesis that impaired nutrition acquisition (nitrogen and carbon) processes can weaken *K. pneumoniae* pathogenesis, as the asparaginase and glutaminase mutant strains (excepting ***Δ****yneH*) showed decreased virulence compared to the wild type (Figure 5.1 A–F). In all *in vitro* experiments, ***Δ****yneH* was not significantly different ($p>0.05$) from the wild type. This suggests that the asparaginase and glutaminase activities or cellular roles in ***Δ****yneH* are not different from the wild type. Furthermore, the transcriptional analysis by qRT-PCR indicated that *ybiK*, and *KPN_01165* may substitute the presence of *yneH*. Also, another possible theory of the similarity in wild type and ***Δ****yneH* behaviour *in vivo* may relate to the over expression of *ybiK* and *KPN_01165* in both strains (section 3.18).

A comparison of the infection scores of the *ΔansA*, *ΔKPN_01165*, and *ΔybiK/ΔKPN_01165* showed around a log difference in Log_{10} LD_{50} compared to wild type as the recorded Log_{10} LD_{50} after 24 h post-infection ($p<0.05$). At 24 h the *ΔybiK* mutant did not show a significant difference in LD_{50} (5.86±0.11) compared to the wild type LD_{50} (5.65±0.14) ($p>0.05$). However, in the other infection experiments *ΔybiK* was attenuated. For example, in the *in vivo* survival experiment which last for 12 hours the Log_{10} CFU/larvae of *ΔybiK* after 12h post-infection was 6.81±0.02 comparing to wild type Log_{10} 7.89±0.08, CFU/larvae, n=6 ($p<0.05$).

There are two possible explanations for the *ΔansA* and *ΔybiK* different behaviour. It seems possible that *ΔansA in vivo* produces lower asparaginase and glutaminase activity comparing to *ΔybiK* and this decreases *ΔansA's* ability to utilise available asparagine and glutamine. The second theory related to *yneH* expression. The qRTPCR indicate that the

expression of *yneH* was different in *ΔansA* and *ΔybiK*. The expression of *yneH* in *ΔybiK* after glutamine exposure was not affected significantly. However, *yneH* in *ΔansA* was down regulated by 4.86 ±0.61 (Figure 3.23 A). The down regulation of *yneH* in *ΔansA* may contribute to its weak pathogenesis and this suggests that *yneH* may have a role in *in vivo* colonization. It seems possible that this reduction in virulence is due to the importance of asparaginase and glutaminase and their substrate nutrient sources (asparagine and glutamine) during infection process, for both *K.pneumoniae* and the larvae. Also it is possible that the mutants were not able to acquire sufficient nutrients inside their host and this give *G. mellonella* the upper hand in using the nutrient which leads to a reduction in the bacterial load. Another possible explanation that may be related to *G. mellonella* nutrient composition that include glucose, asparagine, and glutamine i.e. the *in vivo* has given the optimal condition that evaluate the real fitness of each strain regarding the ability to acquire those nutrients.

The glutamine effect on infection process was investigated by adding 10 mM glutamine with the bacterial inoculum as described in section 5.9. In eukaryotes and prokaryotes, glutamine uptake is required to fulfil the requirement of protein synthesis, and nitrogen source. Interruption in amino acid uptake mechanisms can also affect bacterial virulence, and colonisation (Leduc *et al.*, 2010).

Considering the absence of any study regarding glutamine level in *G. mellonella* and the role of glutaminase and asparaginase in the pathogenicity of *K. pneumoniae*, glutamine addition would test two hypotheses. First, that the pathogenicity of asparaginase and glutaminase mutant strains would be reduced due to their inability to metabolise asparagine and glutamine within their host, and the addition of glutamine may complement this need. Second, the excess glutamine may help *G. mellonella* in clearance of *K. pneumoniae* infection. Ding and Li. (2003) showed the significance of glutamine as a fuel for rapidly dividing immune cells, and for the maintenance of the integrity of intestinal mucosal tissues. Also, when glutamine was peritoneally injected into experimental rats, bacterial translocation in intestinal tract was reduced due to the elevation in immune response supported by healthier mucosal tissues. What can be concluded from glutamine addition experiment is that glutamine has enhanced the survival of *ΔansA* and *ΔybiK* in *G. mellonella* and this enhancement has supported my hypothesis regarding nutrient availability's importance during infection process.

However, the presence of glutamine did not reverse the attenuated phenotype of *ΔKPN_01165*, and *ΔybiK/ ΔKPN_01165*.

The last *in vivo* experiments in *G. mellonella*, have showed that the disease sign scores and mortality rate were statistically less from infection with *ΔansA*, *ΔybiK*, *ΔKPN_01165*, and *ΔybiK/ ΔKPN_01165* compared to the wild type. Interestingly the *ΔansA* and *ΔybiK* mutants were not attenuated in virulence at the early stages of infection. However, these strains manifested a statistically significant reduction in virulence at the later stages of infection (at 18 h and 24 h post infection). A possible theory for this could be that in the beginning of the infection (6 h and 12 h), *ΔansA* and *ΔybiK* were not metabolically different from wild type in their ability to acquire nutrients. At 18 h and 24 h post infection, *ΔansA* and *ΔybiK* may became unable to acquire glutamine and asparagine and this starvation situation made the bacteria enter lag phase. As the bacteria were not able to increase in numbers this may have allowed *G. mellonella* a better clearing window.

Those results also suggest KPN_01165 is the most important asparaginase and glutaminase enzyme *in vivo* as the mutants of this gene were the most attenuated strains. It was shown in the previous chapter that there is sensitivity of *ΔKPN_01165* toward the complement system attack. *G. mellonella* shows similarity in their innate immune system to the one found in vertebrates (Joyce and Gahan, 2010). Therefore, it is possible that the clearance of *ΔKPN_01165* and *ΔybiK/ΔKPN_01165* was more effective due to the attenuation of capsule production, which may have enhanced complement mediated clearance. It is known in other encapsulated bacterial species, such as *Streptococcus pneumoniae*, that the absence or attenuation of capsule production leads to increase in complement deposition, which then leads to effective phagocytosis (Ali *et al*., 2012).

In summary, my results further support the idea that asparaginase/glutaminase enzymes are important in infection process, except the one coded by *yneH*.

6 Chapter-6: General discussion and future work

Chapter-6: Discussion.

6.1 Overview

A report published by World Health Organization (WHO) in 2014, indicated that the top antibiotic resistant pathogens are *E. coli*, *K. pneumoniae*, and *S. aureus* and their infections can happen in hospital setting and in the community (Gelband *et al*., 2015). Antibiotic resistance ability of *K. pneumoniae* combined with production of extended-spectrum beta-lactamases (ESBLs) that act as a reservoir for most plasmid harbouring resistance in Gram-negative bacteria are what make it hard to treat the resulting infections (Podschun and Ullmann, 1998). *K. pneumoniae* is a causative agent of several nosocomial and community acquired infections including pneumonia, urinary tract infection, and pyogenic liver abscesses. *Klebsiella* are widely spread in the environment and can be isolated from water, soil, plants, industrial waste, and food (Fouts *et al*., 2008, Podschun *et al*., 2001). The widespread distribution of the microbe in the environment and human microbiome complicates the control of *K. pneumoniae* nosocomial outbreaks and also suggests that the microbe has efficient mechanisms to adapt to diverse environments.

Klebsiella infections are generally observed in individuals with compromised immune systems and the most common disease caused by *Klebsiella* in such patients is pneumonia with death rates up to 50%. *Klebsiella* can also cause less serious urinary and soft tissue infections (Hickman-Davis *et al*., 2002). What controls *K. pneumoniae* virulence is incompletely understood. It has been suggested that efficient acquisition and metabolism of host nutrients in the sites of infection are important for the microbe's ability to cause infections (Broberg *et al*., 2014). *Klebsiella* is metabolically adaptive and can use a wide range of amino acids as both nitrogen and carbon sources (Resnick and Magasanik, 1976). In other genuses, such as *Pseudomonas*, glutamine and asparagine are more favoured than the other amino acids (Sonawane *et al*., 2003).

Elusive virulence mechanisms, numerous infection sites, highly resistant strains and difficult to control outbreaks are the reasons to investigate *K. pneumoniae* further. This study hypothesis was that degradation of nitrogen-containing materials (like amino acids) is an important factor for *K. pneumoniae* colonisation and virulence. The main objective

of my project was to evaluate the role of asparaginase and glutaminase in *K. pneumoniae* biology and virulence.

In recent years, several studies have linked asparaginase and glutaminase enzymes with virulence in several microorganisms such as *Helicobacter pylori, Salmonella typhimurium,* and *Campylobacter jejuni* (Srikhanta *et al*., 2013). These results showed the importance of nitrogen metabolism and in particular key role of asparaginase in the virulence of pathogenic bacteria. Bacteria that are defective in the production of asparaginase and glutaminase show reduced virulence (Washington *et al*.,2013), however, nothing has been known about these enzymes' contribution to *K. pneumoniae* virulence. Therefore, I hypothesise that the asparaginase and glutaminase enzymes are important for *K. pneumoniae* nitrogen metabolism, and *in vivo* survival.

6.2 The effect of asparaginase/glutaminase mutation on *K. pneumoniae*

The objective of this study was to identify if there are nutrient related influences on *K. pneumoniae* virulence, such as the role asparaginases and glutaminases. To investigate the functional role of putative asparaginase/glutaminase genes, the deletion of these genes was needed. Different types of mutagenesis systems are available for *K. pneumoniae*. In this project, Lambda red-mediated gene replacement mutagenesis technique was applied. This method allows deletion of the gene of interest and insertion of antibiotic resistance marker (Murphy, 1998). SOEing PCR mutagenesis allows insertion-deletion mutagenesis by relying on site directed mutagenesis. It requires the construction of mutant allele by several steps of PCR. SOEing PCR mutagenesis has low margin of error (Horton *et al*., 1990). To rule out polar effect of mutations, wild type restoration of these genes in the mutant strains was done by genetic complementation. My results point out that mutation of each putative asparaginase/glutaminase gene (except *yneH*) adversely affected the growth yield and asparaginase/glutaminase activity of *K. pneumoniae*.

6.3 The interaction between carbon and nitrogen metabolism

Klebsiella has a high capability of metabolizing different sources of nitrogen. For example, *Klebsiella* is able to fix atmospheric nitrogen i.e., they can convert atmospheric nitrogen into ammonium. Genomic analysis indicated that all sequenced *K. pneumoniae* strains contained the homologues of putative asparaginase and glutaminase genes, *yneH, ansA, ybiK,* and *KPN_01165*. These enzymes are responsible for the hydrolysis of asparagine and glutamine, leading the production of aspartate and glutamate,

respectively, and NH_3 (Pokrovskii *et al*., 2013). It is, however, not completely understood why the microbes evolved to possess multiple types of asparaginase and glutaminase isozymes with relatively similar structures and different affinities. For example, in *E. coli*, there are two types of L-asparaginase. Type I asparaginase more specific to asparagine and is constitutively expressed whereas the type II (asparagine and glutamine dual activities) is expressed under induced conditions (Cedar and Schwart, 1967). The *Km* values of type 1 and type 2 asparaginase toward asparagine are 3.5×10^{-3} M and 1.2×10^{-5} M, respectively (Sanches *et al*., 2007). Also, in *E. coli*, there are two glutaminases (A and B) and both are specific to glutamine. The affinity (*Km*) of glutaminase for glutamine varies from 1.5 to 9.5 mM (Brown *et al*., 2009).

Generally, the availability of macronutrients is what controls the bacterial metabolism. Bacterial metabolic processes work collectively to ensure that carbon and nitrogen are always available. The intercellular carbon and nitrogen balance are highly regulated processes (Magasanik, 1960). In *K. pneumoniae*, carbon availability plays a role in nitrogen metabolism regulation. In carbon limited environment the carbon stress response (CAP-cAMP) system regulates the expression of the genes that are involved in glutamine metabolism. The CAP-cAMP activate glutamine synthase and glutamate dehydrogenase and represses glutamate synthetase and glutaminase (Tian *et al*., 2001). Furthermore, nitrogen limitation may define as amino acid limitation as nitrogen availability inside the cell sensed by the concentration of glutamine (Leduc *et al*., 2010). Depending on what was mentioned it seem that glutamine is the key nutrient that may balance carbon/nitrogen pool.

For this, the growth experiments involved both carbon intervention conditions that were mediated by glucose addition and purely substrate challenge mediated by solo addition of glutamine or asparagine. In all experiments ammonia was excluded because these enzymes produce ammonia as an end product. After the growth experiments, asparaginase and glutaminase activities were measured in crude extracts of each strain

According to my results, *K. pneumoniae* KR3167 was able to acquire as little as 2 mM glucose and 0.5 mM of either asparagine or glutamine, and could grow. In comparison, Sonawane et al. (2003) have used glucose at 20 mM and asparagine or glutamine at 5 mM to show the phenotypes from *Pseudomonads* mutants. For example, the OD_{600} for the strains after 20 h incubation in media that had 2 mM glucose and 0.5 mM glutamine were

0.36±0.02, 0.20±0.01, 0.18±0.02, 0.14±0.02, 0.16±0.01 for wild type, *ΔansA*, *ΔybiK*, *ΔKPN_001165* and *ΔybiK*/*ΔKPN_001165*, respectively , n=3 ($p<0.05$ for *ΔansA* and *ΔybiK* and $p<0.01$ for *ΔKPN_001165* and *ΔybiK*/*ΔKPN_001165*) (Table 3.8 and Figure 3.8 B). These results indicate that *K. pneumoniae* have highly adaptive asparaginase and glutaminase system that can tolerate the limited carbon and nitrogen condition.

6.4 Why *yneH* showed no detectable phenotype

According to NCBI database, *yneH* was annotated as glutaminase A, which indicates a specificity toward glutamine. My results showed that the absence of *yneH* had little to no effect on asparaginase/ glutaminase activities hence the mutant strain showed no difference in all chosen assays. A possible explanation is that *Klebsiella* is a designed organism in terms of asparagine and glutamine metabolism beside *yneH* there are *ansA*, *ybiK*, and *KPN_001165* that can hydrolyze both glutamine and asparagine. My findings indicate that asparaginase II may have higher glutaminase activity than asparaginase. For example, the recombinant KPN_01165 has a total glutaminase activity of 152.26 U ±10.32 and asparaginase of 100.95 U ±9.22. Furthermore, the transcriptional analysis by qRT-PCR indicate that *ybiK*, and *KPN_01165* may substitute the presence of *yneH*.

6.5 The connection between capsule production and asparaginase enzymes

The evidence from this study suggests a possible connection between *KPN_01165* and capsule production as *ΔKPN_01165* displayed morphological differences regarding the capsule compared to the wild type. These variations were confirmed by various tests as described in section 3.19. Very little is found in the literature on the connection between asparaginase and capsule synthesis. However, I found two examples that may explain the reduced capsule production in *ΔKPN_01165*. The first example was on *Shigella flexneri* which is a dangerous pathogen responsible for the endemic outbreak of shigellosis. Proteomic analysis of the asparaginase mutants revealed that OmpA (an outer membrane protein) is up regulated in the mutant which is required for bacterial pathogenesis (George *et al*., 2014). This suggests that asaparaginases in different microbial species have also functions other than enzymatic dissimilation of asparagine and not specific to *K. pneumoniae*. Currently, we do not know what these additional functions may be but it is reasonable to assume that the products generated by the activity of asparaginase may be utilised by several biosynthetic pathways such the production of OmpA and capsule.

Future studies are required to determine the mechanistic details of such biosynthetic processes.

Another possible explanation of the reduced capsule belongs to asparaginase impact on-cAMP. Srikhanta et al, (2013) indicated that asparaginase II expression requires activation by the c-AMP receptor protein (CRP). Lin et al, (2013), showed a connection between capsule production and c-AMP proteins. For example deletion of *crp* in *K.pneumoniae* increases CPS production. Similarly, deletion of cAMP phosphodiesterase (cpdA) decreases CPS production. Future work needs to be done to investigate the connection between *KPN_01165* and c-AMP proteins in *K. pneumoniae*.

KPN_01165 coded protein has asparaginase and glutaminase activities, and it seems that this was the most essential enzyme as the mutant strain suffered the most reduced growth rates and yields and had the lowest asparaginase and glutaminase activities. According to KEGG database, *KPN_01165* is located in the periplasmic space. This location may enhance the physiological importance of *KPN_01165* as it may enable it to encounter its substrates before the cytoplasmic asparaginase/glutaminase enzymes.

In Gram negative bacteria, the periplasmic space has enzymes and proteins that respond to environmental changes, acquire nutrients to the cell, and accommodates the enzymes that hydrolyse and remove harmful compounds (Madigan *et al*. 2003). Furthermore, Kullas et al, (2012), suggest that the cytoplasmic asparaginase ansA degrade asparagine after it accumulated to an appropriate intracellular concentration.

Based on my results, I hypothesise that *KPN_01165* plays an important role in initial enzymatic breakdown of asparagine and glutamine then transfer the hydrolysed products to cytoplasm. This hypothesis may explain why the mutation of the *KPN_01165* had the largest impact on the growth parameters even under conditions of relatively high (2 mM) extracellular glutamine or asparagine supplementation. On the other hand 2 mM glutamine or asparagine supplementation were enough to the support *ΔansA* and *ΔybiK* growth to wild type level (section 3.14). Also, the constitutive expression of *KPN_01165* in all tested strains is another support for the significance of this protein in glutamine and asparagine metabolism (section 3.18). Because of its significant biological importance recombinant KPN_01165 was produced.

6.6 The connection between virulence and asparaginase

Bacteria have various strategies to enhance their virulence and evade their host's immune system. One important example of this phenomena is the production of certain products like, endotoxin and type III secretion system that can affect host cell. The effect of such enzymes is clear, and it may result in hydrolysis of cell membrane . There are other enzymes involved in metabolism that may produce very moderate changes, but these modifications can be important for the pathogenesis and control of the host cell mechanism. One such enzymatic reaction is asparaginase deamination. This reaction is irreversible, and it produces a substrate that cannot be used by the host (Washington *et al*., 2013).

This project has focused on the relative contribution of asparaginase and glutaminase on *Klebsiella* virulence. This was done through testing my strains' sensitivity to serum killing and their *in vivo* survival inside *G. mellonella*.

The application of *G. mellonella* model has many limitations. For example, it is not yet a well establish model like fruit fly as the use of this larva in infections just started last decade. It does not have a complete genome sequence and it will not replace the use of the animal models because they have complex systems like nervous system (Tsai *et al*.,2016). In this project the main limitation of using *G. mellonella* was that the glutamine and asparagine concentration in the larva is not known. I used the Glutamine/Glutamate Determination Kit (Sigma-Ardrich) (section 4.10), to determine larvae hemolymph glutamine level. However, no detectable glutamine could be detected very likely due to larvae glutamine level was lower than the kit determination level.

In Chapter 5, I demonstrated that the attenuation in virulence in *ΔansA, ΔybiK, ΔKPN_01165,* and *ΔybiK /ΔKPN_01165* could be due to the inability to acquire glutamine and asparagine in *G. mellonella*. Here I will provide another possible explanation for attenuation in virulence.

Virulence assay results may indicate that asparaginase and glutaminase may have a role beyond hydrolysing aspartate and glutamate to produce ammonia. This is supported by the observation that the loss of KPN_01165 rendered *K. pneumoniae* strain serum-sensitive. This is very likely due to reduction of capsule synthesis and increase in complement deposition in the mutant strain. The pathogenicity assays via *G. mellonella*

also showed that *ansA*, *ybiK*, and *KPN_01165* are important in *Klebsiella* survival inside *G. mellonella* as the mutants showed lower survival rates comparing to the wild type.

The growth profile in different bovine and murine sera point out that lectin pathway of the complement system may have a significant bactericidal role as the differences in yields between *KPN_01165* mutants and wild type diminished when the serum was heated. This emphasises the role of asparaginase/ glutaminase enzyme in *K. pneumoniae* biology. Also, this may draw a picture of these mutant strains' behaviour, if they are tested in an animal model through intravenous mode of infection. It is expected that after intra venous administration, these mutants will be cleared faster than the wild type. The behaviour of *ΔansA* and *ΔybiK* toward the serum bacteriolytic activity was not different from the wild type. This behaviour may occur because these strains did not show any difference in capsule production from the wild type. Thus, the production and the size of the capsule may likely contribute to *K. pneumoniae* serum resistance.

Klebsiella capsule is thought to play an important role in infection through inhibition of phagocytosis and complement activation (Highsmith and Jarvis, 1985; Lawlor *et al*., 2006). O antigen is believed to provide the complement production while K virulent antigen attaches to the host cell membrane and alters the bacterial cell surface thereby hindering phagocytosis (Highsmith and Jarvis, 1985; Frirdich and Whitfield, 2005; Lawlor *et al*., 2006; De Majumdar *et al.,* 2015). However, when *ΔansA*, *ΔybiK* infected into *G. mellonella* they were less virulent than the wild type. It seems possible that these results are due to the weak asparaginase and glutaminase activities that are presented by these two strains. My hypothesis to explain the attenuated virulence of *ΔansA*, *ΔybiK* and *ΔKPN_01165* is that during survival in *G. mellonella Klebsiella* secrete asparaginase and glutaminase to help in nutrition acquirement and supress the immune response of their host. As *ΔansA*, *ΔybiK* and *ΔKPN_01165* are attenuated in both asparaginase and glutaminase their colonisation process will be also weak comparing to wild type and *ΔyneH* that have higher asparaginase and glutaminase. Geckil et al. (2005), stated that asparaginase is a secretory protein. Moreover, an asparaginase in *E. coli* that is encoded by *ansB*, is found to be a high affinity secreted enzyme with a role in virulence (Jennings and Beacham, 1990). Washington et al. (2013) reported *E. coli* asparaginase as a cytotoxic secreted enzyme by testing their harmful effect against U937 cells. The asparaginase toxicity could be a contributing factor as to why wild type and *ΔyneH* are more virulent than the mutants. It is also possible that asparaginase toxicity may interfere with

complement system proteins and contribute to wild type resistance to serum killing. Future work is needed to investigate toxicity of *Klebsiella* asparaginase toward complement proteins and *G. mellonella*. This can be done with the cloned KPN_01165. This protein can be inoculated into different cell lines, and the effect can be monitored, or it can be injected to *G. mellonella* or it can be added to the serum during the bacteriolytic assays.

6.7 Final remarks

In this study the roles of *K. pneumoniae* asparaginase and glutaminase in glutamine and asparagine metabolism, capsule synthesis, complement activation, and infection / persistence in *G. mellonella* tissues were examined. The main function of these enzymes is to provide the NH_3 after hydrolysing asparagine and glutamine. This function is found to be affected by many factors including carbon (glucose) and nitrogen (NH_3) availability and as a result these enzymes are involved in both *K. pneumoniae* carbon and nitrogen metabolism. All mutants displayed a healthy growth which was not different from the wild type when high concentrations of glucose and NH_3 were provided. Both asparagine and glutamine were considered as important sources for carbon and nitrogen as they are gluconeogenic amino acids and their ultimate metabolism will serve as precursor for gluconeogenesis (Paul and Cooksey 1981). After many growth experiments, the catabolic repression effect was minimized after decreasing the glucose to 2 mM and this effect was eliminated by removing glucose from the media and supplemented with high concentrations (10 mM) of either glutamine or asparagine. This project started with the hypothesis that all tested asparaginase and glutaminase genes may contribute in biology and virulence of *K. pneumoniae*. The results demonstrate that *ansA*, *ybiK*, and *KPN_01165* contribute to the total asparaginase and glutaminase activities. However, *yenH* mutation did not yield any phenotype, and this may be due to the incorrect gene annotation (sole glutaminase) or the compensatory impact of the other enzymes (KPN_01165 and YbiK). The enzyme coded by *KPN_01165* is the most essential asparaginase and glutaminase. The expression of this enzyme was constitutive.

Expression of *KPN_01165* was required for the normal growth, colony size, and complement resistance of *K. pneumoniae*. Moreover, *KPN_01165* contribution to these functions support its importance specifically for *K. pneumoniae* biology and housekeeping. The contribution of asparaginase and glutaminase enzymes to virulence

was investigated using *G. mellonella* as infection model. The *in vivo* tests revealed that wild type and *yneH* were more virulent than *ansA*, *ybiK*, and *KPN_01165* mutant strains. The results obtained from this study provide a new insight for the role of asparaginase and glutaminase beyond their metabolic role and clearly demonstrate an unexplored link between metabolism and virulence.

6.8 Future work

The significance of asparaginase and glutaminase in *K. pneumoniae* biology and virulence was shown in this project by many *in-vivo* and *in-vitro* assays. However, the contribution of these enzymes to the other aspects of *K. pneumoniae* biology need to be investigated extensively. The further work is required to fully understand how asparaginase and glutaminase contributes to bacterial physiology. One clear example of contribution of asparaginase and glutaminase to *K. pneumoniae* physiology was the attenuated capsule production in *ΔKPN_01165*. There was no clear explanation for how asparaginase and glutaminase contribute to capsule synthesis. Another future expermrnt may be on the impact of these enzymes on proteome profiles of mutant strains. This analysis can reveal wider functional roles of these enzymes on *K. pneumoniae* biology. This analysis can be combined with the chromatography analysis of the total carbohydrate content of the wild type and *ΔKPN_01165*. Other work may include real time reverse transcriptase PCR assays to test the impact of asparaginase and glutaminase on the transcription of capsule locus genes of *K. pneumoniae*. The other aspect that can be further investigated is related to the impact of asparaginase and glutaminase on attachment of *K. pneumoniae*. Periplasmic L-asparaginase mutants in *Shigella* show reduced adherence to epithelial tissue suggesting that asparaginase plays a major role in the colonization of the pathogen (George *et al*., 2014). The percentage of *K. pneumoniae* attachment to mammalian cells might be assessed using wild type and mutant strains. This experiment could be done via an epithelial cell line. A monolayer of the epithelial cells could be mixed with the bacterial suspension then the level of attachment will be determined via viable counts of attached cells.

Another area of research is to determine how my mutants will behave in a mouse model of *K. pneumoniae* infection. The involvement of asparaginase in microbial pathogenesis has been shown in recent studies in organisms like *Helicobacter*, *Salmonella*, and *Shigella* (Scotti *et al*., 2010; Kullas *et al*., 2012; George *et al*., 2014). Collectively, these examples

suggest that asparaginase is important in bacterial colonisation and virulence. The examples above clearly show that the microbes inhabiting diverse tissue sites require asparaginase and glutaminase for their virulence. Given that *K. pneumoniae* inhabit diverse tissues, and glutamine is high in the mammalian lung, and blood stream, it is justified to further test my *K. pnumoniae* mutant strains in mouse model of infection. These infections can be done through intranasal and intravenous routes to reveal the importance of these enzymes in survival of *K. pneumoniae* in these tissues. Lau. (2007) reported that animal models are essential to determine *K. pneumoniae* interactions with the host during infection. Mouse infections will provide more insight about the role of asparaginase and glutaminase in virulence. For example, many studies suggest that *K. pneumoniae* colonise the respiratory tracts during chronic pneumonia. To mimic the natural route of infection, *K. pneumoniae* needs to be administered into the nostrils of the tested animal (Borna and Theodore, 1999). The other mode of infection would be through intravenous route and that can be combined with the use of my recombinant KPN_01165. The addition of KPN_01165 would further limit *K. pnumoniae* access to the available glutamine and asparagine and this may make *K. pnumoniae* more vulnerable for host immune clearance. However, due to the possible toxicity of KPN_01165 for the host, its addition needs to be optimised before use. This approach may allow using asparaginase as novel antibiotic treatment. Although this is the expected result, the use of recombinant KPN_01165 during infection may increase the severity of infection by increasing the availability of ammonia.

It is also noteworthy to develop an antibody against KPN_01165. This antibody can be used first for localization experiments through the Western blot technique to investigate KPN_01165's cellular localisation. Also, it will be beneficial to investigate the uptake level of glutamine and asparagine by *yneH, ansA, ybiK*, and *KPN_01165* mutants. This experiment can be done by using ^{14}C-labelled glutamine and asparagine, then the uptake levels will be measured in wild type *ΔyneH, ΔansA, ΔybiK, ΔKPN_01165,* and *ΔybiK /ΔKPN_01165*. This assay may provide an insight into which enzyme is more involved in uptake and metabolism of asparagine and glutamine.

In vitro studies showed that CL-11 activates the LP on the surface of *K. pneumoniae*. This can be confirmed by using CL-11$^{-/-}$ mice as *in vivo* model. This experiment should include WT control mice to compare the resulted survival rates and to know the severity of the infection in a reduced complement activation environment.

Further future work can include investigating the antitumor activity of KPN_01165. Bacterial asparaginase enzyme is used among others as antileukemic treatment to deplete the circulating pools of asparagine, which leads to destruction of tumour cells (Savitri and Azmi, 2003). Normal cells are protected from asparagine starvation due to their ability to synthesize asparagine.

Appendix 1

DNA sequencing of pLEICS-01 constructs carrying the intact copy of KPN_01165 The sequence was done by dependent primers (T7 promoter and terminator primers).

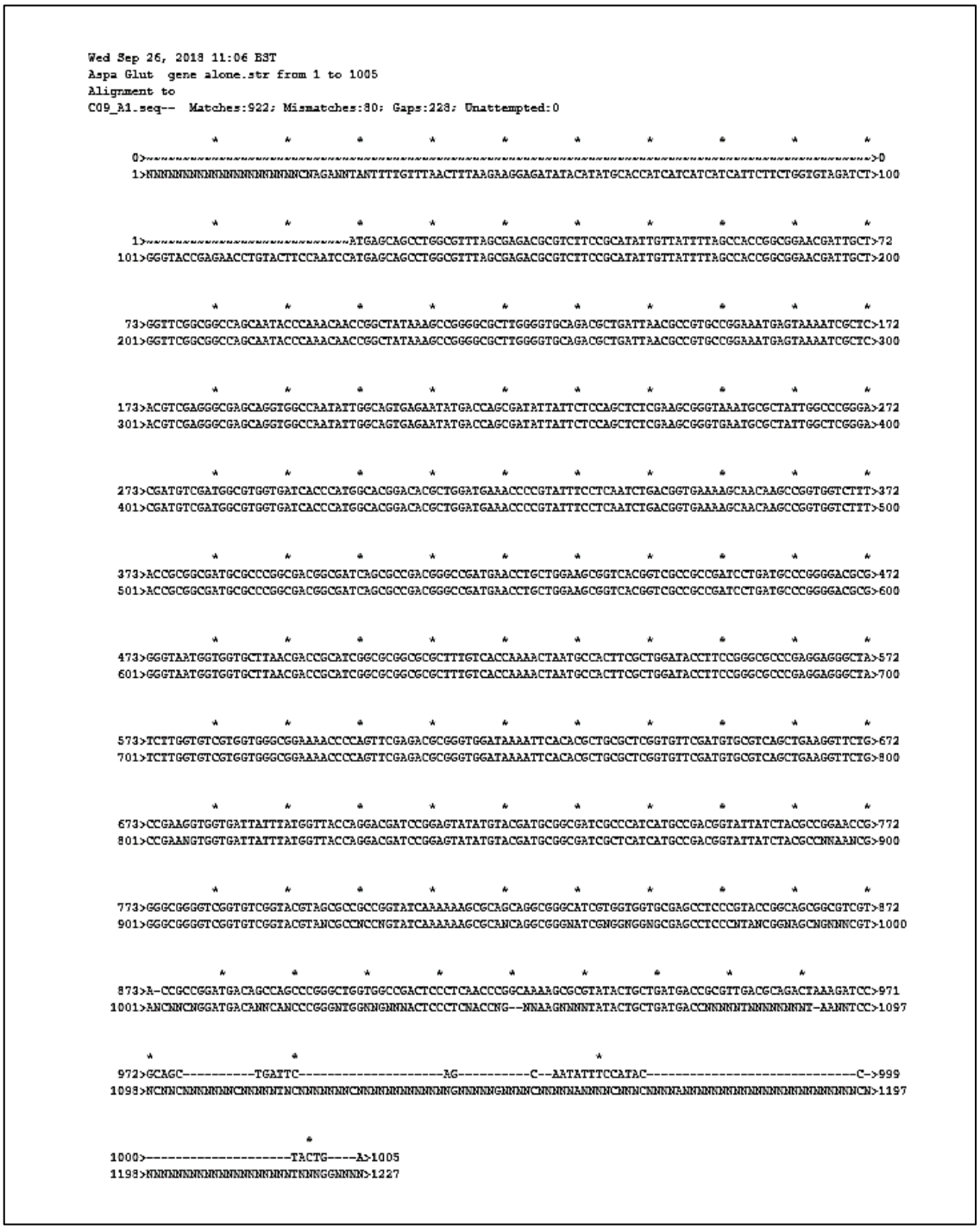

Appendix 2

MALDI-TOF mass spectrometry confirming the identity of KPN_01165 recombinant protein.

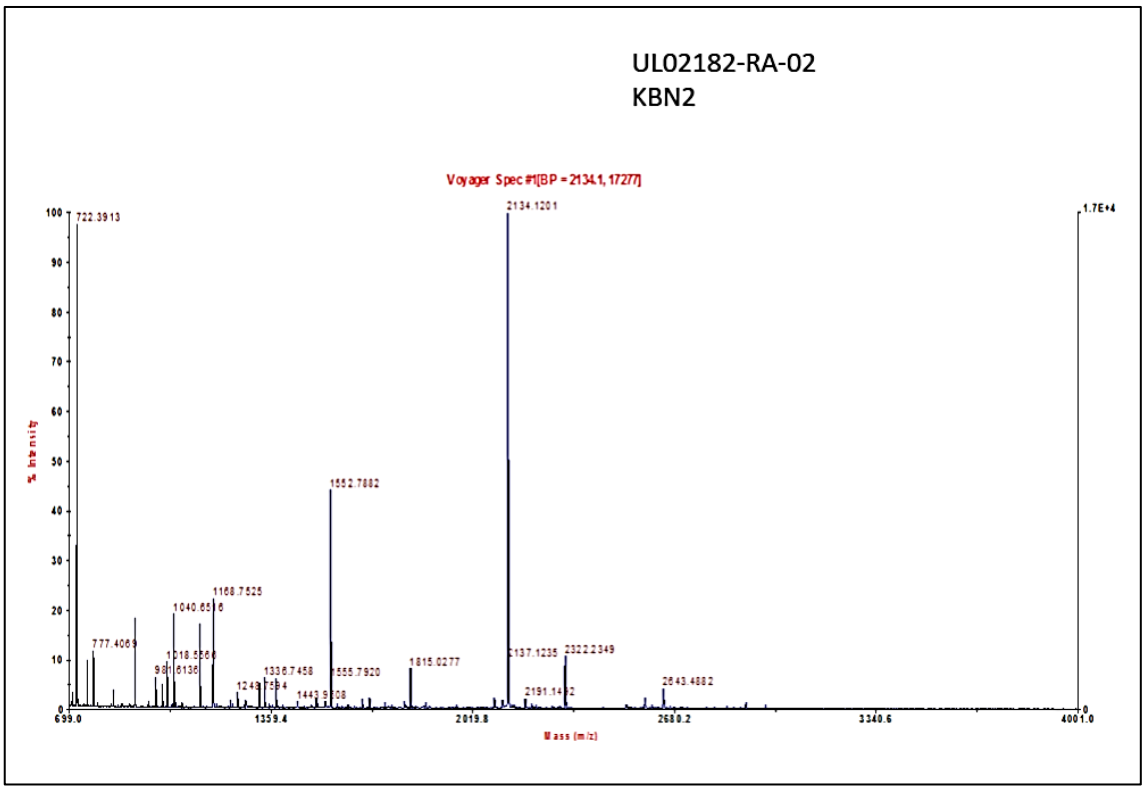

References

Abbas, A., Lichtman, A., Pillai, S. (2014). Cellular and molecular immunology E-book Elsevier Health Sciences.

Ako, H. & Nip, W. (2012). Enzyme Classification and Nomenclature. Food Biochemistry and Food Processing, 109.

Albertí, S., Alvarez, D., Merino, S., Casado, M., Vivanco, F., Tomás, J. and Benedí, V.J., 1996. Analysis of complement C3 deposition and degradation on *Klebsiella pneumoniae*. *Infection and immunity*, *64*(11), pp.4726-4732.

Ali, Y., Lynch, N., Haleem, K., Fujita, T., Endo, Y., Hansen, S… Dudler, T. (2012). The lectin pathway of complement activation is a critical component of the innate immune response to pneumococcal infection. PLoS Pathogens, 8(7), e1002793.

Aljewari, H., Nader, M., Alfaisal, A. (2010) 'High efficiency, selectivity against cancer cell line of purified L-Asparaginase from pathogenic Escherichia coli,' *World Academy of Science, Engineering and Technology, International Journal of Medical, Health, Biomedical, Bioengineering and Pharmaceutical Engineering,* 4(5), pp. 199-204.

Altman, B., Stine, Z. and Dang, C. (2016). From Krebs to clinic: glutamine metabolism to cancer therapy. Nature Reviews Cancer, 16(10), pp.619-634.

Arakawa, Y., Ohta, M., Wacharotayankun, R., Mori, M., Kido, N., Ito, H., Komatsu, T., Sugiyama, T. and Kato, N., 1991. Biosynthesis of Klebsiella K2 capsular polysaccharide in Escherichia coli HB101 requires the functions of rmpA and the chromosomal cps gene cluster of the virulent strain *Klebsiella pneumoniae* Chedid (O1: K2). *Infection and immunity*, *59*(6), pp.2043-2050.

Asselin, B. (1999). 'The three asparaginases. Comparative pharmacology and optimal use in childhood leukemia,' *Advances in experimental medicine and biology*, 457, pp. 621–9. Available at: http://www.ncbi.nlm.nih.gov/pubmed/10500842 (Accessed: 18 April 2018).

Avramis, V. I. and Panosyan, E. (2005) 'Pharmacokinetic/Pharmacodynamic Relationships of Asparaginase Formulations,' *Clinical Pharmacokinetics*, 44(4), pp. 367–393. doi: 10.2165/00003088-200544040-00003.

Bachman, M., Lenio, S., Schmidt, L., Oyler, J. and Weiser, J.N., 2012. Interaction of lipocalin 2, transferrin, and siderophores determines the replicative niche of *Klebsiella pneumoniae* during pneumonia. *MBio*, *3*(6), pp.e00224-11.

Bassler, B. (1999). How bacteria talk to each other: regulation of gene expression by quorum sensing. Current Opinion in Microbiology, 2(6), pp.582-587.

Batt, T. and Brown, D. (1974). The influence of inorganic nitrogen supply on carbohydrate and related metabolism in the blue-green alga, Anabaena cylindricaLemm. Planta, 116(3), pp.197-206.

Bavister, D., Gerrity, B. and Kopf, G. (1988) In vitro fertilization and embryo transfer: a manual of basic techniques. Springer Science & Business Media.

Bender, D. (2012). Nitrogen Metabolism. Amino Acid Metabolism, Third Edition, 1-65.

Bender, R. (2010). A NAC for regulating metabolism: the nitrogen assimilation control protein (NAC) from *Klebsiella pneumoniae*. Journal of bacteriology, 192(19), 4801-4811.

Berendt, R., Long, G., Abeles, F., Canonico, P., Elwell, M. and Powanda, M. (1977) 'Pathogenesis of respiratory *Klebsiella pneumoniae* infection in rats: bacteriological and histological findings and metabolic alterations.' Infection and immunity, 15(2), pp. 586-593.

Boman, H. and Hultmark, D. (1987) 'Cell-free immunity in insects,' Annual Reviews in Microbiology, 41(1), pp. 103-126.

Borghesi, L. & Milcarek, C. (2007). Innate versus adaptive immunity: A paradigm past its prime? Cancer Research, 67(9), 3989-3993.

Brabb, A., Suckow, M., Stevens, K. and Wilson, R., eds., 2012. *The laboratory rabbit, guinea pig, hamster, and other rodents*. Academic Press.

Bradford, M. (1976) 'A rapid and sensitive method for the quantitation of microgram quantities of protein utilizing the principle of protein-dye binding,' *Analytical Biochemistry*, 72(1-2), pp. 248-254.

Branger, J., Knapp, S., Weijer, S., Leemans, J., Pater, J., Speelman, P., Florquin, S. and van der Poll, T., 2004. Role of Toll-like receptor 4 in gram-positive and gram-negative pneumonia in mice. *Infection and immunity*, *72*(2), pp.788-794.

Broberg, C., Palacios, M. & Miller, L. (2014). *Klebsiella: a long way to go towards understanding this enigmatic jet-setter*. F1000prime reports, 6.

Brooks, G., Janet, S. & Stephan, A., 2001. *Medical microbiology.*, Lange medical Books/ McGraw-Hill.

Brown, G., Singer, A., Proudfoot, M., Skarina, T., Kim, Y., Chang, C. & Yakunin, A. (2008). Functional and Structural Characterization of Four Glutaminases from *Escherichia coli* and *Bacillus subtilis*. *Biochemistry*, *47*(21), 5724-5735.

Budu, C., Luengpailin, J., Reyes, G., Doyle, R. and Cowan, M. (2003). Virulence factors of Porphyromonasgingivalis are modified by polyphenol oxidase and asparaginase. Oral Microbiology and Immunology, 18(5), pp.313-317.

Bullen, J., Rogers, H. and Griffiths, E. (1972) 'Iron binding proteins and infection.' *British journal of haematology*, 23(4), pp. 389–92.

Cedar, H. and Schwartz, J. H. (1967) 'Localization of the two-L-asparaginases in anaerobically grown Escherichia coli,' *The Journal of biological chemistry*, 242(16), pp. 3753–5. Available at: http://www.ncbi.nlm.nih.gov/pubmed/4962587 (Accessed: 18 April 2018).

Cho, S., Law, J. and Ng, C. (2009) 'Effect of Growth at Sub-lethal Concentrations of Kanamycin on the Cell Membrane Integrity and Amount of Capsular Glucuronic Acid in Wild-type Escherichia coli and Strain with a cpsB Mutation,'

J.Exp.Microbiol.Immunol, 13, pp. 29-35.Ciurana, B., & Tomas, J. (1987). Role of lipopolysaccharide and complement in susceptibility of *Klebsiella pneumoniae* to nonimmune serum. Infection and Immunity, 55(11), 2741-2746.

Clarissa, G.; Lewinski, K.; LaCount, M.W.; Roberts, J. and Lebioda, L. (1997). Ion binding induces closed conformation in Pseudomonas 7A glutaminase-asparaginase (PGA): crystal structure of the PGA-SO4(2-) NH4+ complex at 1.7 A resolution J.Biochem, 36(4):P.923-31.

Cote. 1999. Media composition, microbial, laboratory scale. In Flicker and Drew (ed.), Encyclopedia of bio process technology: fermentation, biocatalysis, and bioseparation. John Wiley & Sons, Inc., New York.

David S. (2005). The Molecular Perspective: L-Asparaginase. The Oncologist;10:P.238–239.

de Bruijn, F. and Ausubel, F. (1983). *The cloning and characterization of the glnF (ntrA) gene of Klebsiella pneumoniae: Role of glnF (ntrA) in the regulation of nitrogen fixation (nif) and other nitrogen assimilation genes*. Molecular and General Genetics MGG, 192(3), pp.342-353.

De Majumdar, S., Yu, J., Fookes, M., McAteer, S., Llobet, E., Finn, S., Spence, S., Monaghan, A., Kissenpfennig, A., Ingram, R. and Bengoechea, J., 2015. Elucidation of the RamA regulon in*Klebsiella pneumoniae* reveals a role in LPS regulation. *PLoS pathogens*, *11*(1), p.e1004627.

Deutscher, J., 2008. The mechanisms of carbon catabolite repression in bacteria. *Current opinion in microbiology*, *11*(2), pp.87-93.

Ding, L. and Li, J. (2003) 'Effects of glutamine on intestinal permeability and bacterial translocation in TPN-rats with endotoxemia', World journal of gastroenterology: WJG, 9(6), pp. 1327.

Distasio, J., Salazar, A., Nadji, M. and Durden, D. (1982). Glutaminase-free asparaginase from Vibro succinogenes: an antilymphoma enzyme lacking hepatotoxicify. nt. J. Cancer. 30: P.343 347.

Domenico, P., Johanson, W. and Straus, D. (1982) 'Lobar pneumonia in rats produced by clinical isolates of *Klebsiella pneumoniae*.' Infection and immunity, 37(1), pp. 327-335.

Dominika, B., Karolina, M., Krzysztof, B., Agnieszka, K., Jan, P., David, T., Daniel, Kr., Jacek O. and Mariusz, J. (2004). Expression, purification and catalytic activity of Lupinus luteus asparagine βamidohydrolase and its Escherichia coli homolog, J.Biochem.,271(15):P. 3215–3226.

Doumith, M., Ellington, M., Livermore, D. and Woodford, N. (2009) 'Molecular mechanisms disrupting porin expression in ertapenem-resistant Klebsiella and Enterobacter spp. clinical isolates from the UK,' *Journal of Antimicrobial Chemotherapy*, 63(4), pp. 659-667.

Endo, Y., Matsushita, M., Fujita, T. (2011). The role of ficolins in the lectin pathway of innate immunity. The International Journal of Biochemistry & Cell Biology, 43(5), 705-712.

Estabrook, M., Griffiss, J., Jarvis, G. (1997). Sialylation of neisseria meningitidis lipooligosaccharide inhibits serum bactericidal activity by masking lacto-N-neotetraose. Infection and Immunity, 65(11), 4436-4444.

Fang, C., Chuang, Y., Shun, C., Chang, S. and Wang, J., 2004. A novel virulence gene in *Klebsiella pneumoniae* strains causing primary liver abscess and septic metastatic complications. *Journal of Experimental Medicine*, *199*(5), pp.697-705.

Farrar, C., Tran, D., Li, K., Wu, W., Peng, Q., Schwaeble, W., . . . Sacks, S. (2016). Collectin-11 detects stress-induced L-fucose pattern to trigger renal epithelial injury. The Journal of Clinical Investigation, 126(5), 1911-1925.

Ferrara, M. A., Mattoso, J. M., Bon, E. P., & Pereira, N. (2004). Kinetics of asparaginase II fermentation in Saccharomyces cerevisiae ure2dal80 mutant. *Applied biochemistry and biotechnology*, *113*(1-3), 299-305.

Feehily, C. and Karatzas, K. A. G. (2013) 'Role of glutamate metabolism in bacterial responses towards acid and other stresses.' *Journal of Applied Microbiology*, 114(1), pp. 11–24. doi: 10.1111/j.1365-2672.2012.05434.x.

Fouts, D., Tyler, H., Deboy, R., Daugherty, S., Ren, Q., Durkin, A., Huot, H., Shrivastava, S., Kothari, S. & Dodson, R. (2008). Complete genome sequence of the N 2-fixing broad host range endophyte *Klebsiella pneumoniae* 342 and virulence predictions verified in mice. PLoS Genet, 4, e1000141.

Frank, M. (2010). Complement disorders and hereditary angioedema. Journal of Allergy and Clinical Immunology, 125(2), S271.

Fujita, T. (2013). Extra-immunological role of complement activation in diabetic nephropathy. OA Nephrology, 1(2).

Fujita, T., Matsushita, M. and Endo, Y. (2004). The lectin complement pathway–its role in innate immunity and evolution. *Immunological Reviews*, 198(1), 185-202.

Gadjeva, M., Thiel, S., Jensenius, J. C. (2001). The mannan-binding-lectin pathway of the innate immune response. Current Opinion in Immunology, 13(1), 74-78.

Geckil, H., Ates, B., Gencer, S., Uckun, M. and Yilmaz, I., 2005. Membrane permeabilization of gram-negative bacteria with a potassium phosphate/hexane aqueous phase system for the release of L-asparaginase: an enzyme used in cancer therapy. *Process Biochemistry*, *40*(2), pp.573-579.

Gelband, H., Sumanth, J., Devra, B., Andera, W., Ramanan, L. & 2015. The state of worlds antibiotics. in*:* CENTER FOR DISEASE DYNAMICS, E. P. (ed.).

George, D., Mathesius, U., Behm, C. and Verma, N. (2014). The Periplasmic Enzyme, AnsB, of Shigella flexneri Modulates Bacterial Adherence to Host Epithelial Cells. PLoS ONE, 9(4), p.e94954.

Glöer, J., Thummer, R., Ullrich, H. & Schmitz, R. (2008). Towards understanding the nitrogen signal transduction for nif gene expression in *Klebsiella pneumoniae*. Febs Journal, 275(24), 6281-6294.

Goodsell, D. S. (2005). The molecular perspective: L-asparaginase. The oncologist, 10(3), 238-239.

Goss, T., Perez-Matos, A. & Bender, R. (2001). Roles of glutamate synthase, gltBD, and gltF in nitrogen metabolism of Escherichia coli and Klebsiella aerogenes. *Journal of bacteriology*, 183(22), 6607-6619.

Gosset G (2005) Improvement of *Escherichia coli* production strains by modification of the phosphoenol pyruvate: sugar phosphotransferase system. *Microb Cell Fact* 4:14–2.

Gottschalk, G. (2012). *Bacterial metabolism*. Springer Science & Business Media.

Groisman, E. (2001). Principles of bacterial pathogenesis Academic Press.

Hajela, K., Kojima, M., Ambrus, G., Wong, K., Moffatt, B., Ferluga, J., . . . Sim, R. (2002). The biological functions of MBL-associated serine proteases (MASPs). Immunobiology, 205(4-5), 467-475.

Haber, A., Friedman, S., Lobel, L., Burg-Golani, T., Sigal, N., Rose, J., Livnat-Levanon, N., Lewinson, O. and Herskovits, A. (2017). L-glutamine Induces Expression of *Listeria monocytogenes* Virulence Genes. *PLoS pathogens*, *13*(1), p.e1006161.

Hansen, D., Mestre, F., Albertí, S., Hernández-Allés, S., Álvarez, D., Doménech-Sánchez, A., Gil, J., Merino, S., Tomás, J. and Benedí, V.J., 1999. *Klebsiella pneumoniae* lipopolysaccharide O typing: revision of prototype strains and O-group distribution among clinical isolates from different sources and countries. *Journal of clinical microbiology*, *37*(1), pp.56-62.

Hansen, S., Selman, L., Palaniyar, N., Ziegler, K., Brandt, J., Kliem, A., . . . Hartshorn, K. (2010). Collectin 11 (CL-11, CL-K1) is a MASP-1/3–Associated plasma collectin with microbial-binding activity. *The Journal of Immunology*, 185(10), 6096-6104.

Harper, C., Hayward, D., Kidd, M., Wiid, I. & Van Helden, P. (2010). Glutamate dehydrogenase and glutamine synthetase are regulated in response to nitrogen availability in Myocbacterium smegmatis. BMC microbiology, 10(1), 138.

Harwood, C. and Cutting, S. (1990) *Molecular biological methods for Bacillus.* Wiley.

Harding, C., Schroeder, G., Collins, J. and Frankel, G. (2013) 'Use of Galleria mellonella as a model organism to study Legionella pneumophila infection,' Journal of visualized experiments: JoVE, (81).

Heckman, K. L., & Pease, L. R. (2007). Gene splicing and mutagenesis by PCR-driven overlap extension. *Nature protocols*, *2*(4), 924.

Heja, D., Kocsis, A., Dobe, J., Szilugyi, K., Szasz, R., Zavodszky, P., Gal, P. (2012). Revised mechanism of complement lectin-pathway activation revealing the role of serine protease MASP-1 as the exclusive activator of MASP-2. Proceedings of the National Academy of Sciences, 109(26), 10498-10503.

Hickman-Davis, J. O'Reilly, P., Davis, I., Peti-Peterdi, J., Davis, G., Young, K. & Matalon, S. (2002). Killing of *Klebsiella pneumoniae* by human alveolar macrophages. *American Journal of Physiology-Lung Cellular and Molecular Physiology*, 282(5), 944-956.

Highsmith, A. and Jarvis, W. (1985). *Klebsiella pneumoniae: Selected Virulence Factors that Contribute to Pathogenicity*. Infection Control, 6(02), pp.75-77.

Hirche, T., Gaut, J., Heinecke, J. & Belaaouaj, A. (2005). Myeloperoxidase plays critical roles in killing *Klebsiella pneumoniae* and inactivating neutrophil elastase: Effects on host defense. The Journal of Immunology, 174(3), 1557-1565.

Hirokawa, T., Boon-Chieng, S. and Mitaku, S., 1998. SOSUI: classification and secondary structure prediction system for membrane proteins. *Bioinformatics (Oxford, England)*, *14*(4), pp.378-379.

Horton, R., Cai, Z., Ho, S. & Pease, L. 1990. Gene splicing by overlap extension: tailor-made genes using the polymerase chain reaction. Biotechniques, 8, 528-35.

Hüser, A, Klöppner, U and RöhmK. (1999). Cloning, sequence analysis, and expression of ansB from Pseudomonas fluorescens, encoding periplasmic glutaminase/asparaginase, FEMS Microbiol Lets., 178(2):P.P.327–335.

Lai, Y. C., Peng, H. L., & Chang, H. Y. (2003). RmpA2, an activator of capsule biosynthesis in Klebsiella pneumoniae CG43, regulates K2 cps gene expression at the transcriptional level. *Journal of bacteriology*, *185*(3), 788-800.

Iizawa, Y., Nishi, T., Kondo, M. and Imada, A. (1991) 'Examination of host defense factors responsible for experimental chronic respiratory tract infection caused by *Klebsiella pneumoniae* in mice', Microbiology and immunology, 35(8), pp. 615-622.

Ilghari, D., Waters, L., Veverka, V., Muskett, F. and Carr, M., 2009. 15 N, 13 C and 1 H resonance assignments and secondary structure determination of the Mycobacterium tuberculosis Rv0287–Rv0288 protein complex. *Biomolecular NMR assignments*, *3*(2), p.171.

Insua, J., Llobet, E., Moranta, D., Pérez-Gutiérrez, C., Tomás, A., Garmendia, J. and Bengoechea, J., 2013. Modelling *Klebsiella pneumoniae* pathogenesis by infecting the wax moth Galleria mellonella. *Infection and immunity*, pp.IAI-0039.

Iwaki, D., Kanno, K., Takahashi, M., Endo, Y., Matsushita, M. & Fujita, T. (2011). The role of mannose-binding lectin-associated serine protease-3 in activation of the alternative complement pathway. *The Journal of Immunology*, 187(7), 3751-3758.

Jennings, M. and Beacham, I. (1990). Analysis of the Escherichia coli gene encoding L-asparaginase II, ansB, and its regulation by cyclic AMP receptor and FNR proteins. *Journal of Bacteriology*, 172(3), pp.1491-1498.

Ji, X., Nie, Z., Huang, H., Ren, L., Peng, C. and Ouyang, P. (2010). Elimination of carbon catabolite repression in Klebsiella oxytoca for efficient 2,3-butanediol production from glucose–xylose mixtures. Applied Microbiology and Biotechnology, 89(4), pp.1119-1125.

Joyce, S. and Gahan, C. (2010) 'Molecular pathogenesis of Listeria monocytogenes in the alternative model host Galleria mellonella,' Microbiology, 156(11), pp. 3456-3468.

Kebeish, R., El-Sayed, A., Fahmy, H., & Abdel-Ghany, A. (2016). Molecular cloning, biochemical characterization, and antitumor properties of a novel L-asparaginase from Synechococcus elongatus PCC6803. *Biochemistry (Moscow), 81*(10), 1173-1181.

Kennedy, M. A. (2010). A brief review of the basics of immunology: The innate and adaptive response. Veterinary Clinics: Small Animal Practice, 40(3), 369-379.

Keshi, H., Sakamoto, T., Kawai, T., Ohtani, K., Katoh, T., Jang, S., and Koyama, S. (2006). Identification and characterization of a novel human collectin CL-K1. Microbiology and Immunology, 50(12), 1001-1013.

Khushoo, A., Pal, Y., Singh, B. and Mukherjee, K. (2004). Extracellular expression and single step purification of recombinant Escherichia coli L-Asparaginase II. Protein Expression and Purification., 38(1):P. 29–36.

Kindt, T., Goldsby, R., Osborne, B., & Kuby, J. (2007). Kuby immunology Macmillan.

Kjaer, T., Thiel, S., Andersen, G. (2013). Toward a structure-based comprehension of the lectin pathway of complement. Molecular Immunology, 56(4), 413-422.

Knockdown of asparagine synthetase A renders Trypanosome brucei auxotrophic to asparagine. PloS *neglected tropical diseases*, 7(12), e2578.

Koneman, E.W. and Allen, S., 2008. *Koneman. DiagnosticoMicrobiologico/Microbiological diagnosis: Texto Y Atlas EnColor/Text and Color Atlas*. Ed. MédicaPanamericana.

Kornberg, H., 2000. Krebs and his trinity of cycles. *Nature Reviews Molecular Cell Biology*, *1*(3), p.225.

Kozak, M., Borek, D., Janowski, R. & Jaskolski, M., (2002). Crystallization and preliminary

Crystallographic studies of five crystal forms of Escherichia coli L-asparaginase II (Asp90Glu mutant). ActaCrystallographica Section D: Biological Crystallography, 58(1), 130-132.

Kullas, A., McClelland, M., Yang, H., Tam, J., Torres, A., Porwollik, S. & van der Velden, A., (2012). L-Asparaginase II Produced by Salmonella Typhimurium Inhibits T Cell Responses and Mediates Virulence. Cell host & microbe, 12(6), 791-798.

Kung, H., Marks, J. and Chi, J., 2011. Glutamine synthetase is a genetic determinant of cell type–specific glutamine independence in breast epithelia. *PLoSgenetics*, *7*(8), p.e1002229.

Labow, B. and Souba, W. (2000) 'Glutamine,'World journal of surgery, 24(12), pp. 1503-1513.

Lawlor, M., Handley, S. and Miller, V. (2006) ‘Comparison of the Host Responses to Wild-Type and cpsB Mutant *Klebsiella pneumoniae* Infections,’ *Infection and Immunity*, 74(9), pp. 5402–5407. doi: 10.1128/IAI.00244-06.

Lamarche, M., Wanner, B., Crépin, S. and Harel, J. (2008). The phosphate regulon and bacterial virulence: a regulatory network connecting phosphate homeostasis and pathogenesis. *FEMS Microbiology Reviews*, 32(3), pp.461-473.

Lawlor, M., Hsu, J., Rick, P. and Miller, V. (2005) 'Identification of *Klebsiella pneumoniae* virulence determinants using an intranasal infection model,' Molecular microbiology, 58(4), pp. 1054-1073.

Lebioda, L.; Zhang, E.; Lewinski, K.; and Brewer, J. (1993).Fluoride inhibition of yeast enolase: crystal structure of the enolase-Mg(2+)-F(-)-Pi complex at 2.6 A resolution. J.Proteins 16:P.219-225

Leduc, D., Gallaud, J., Stingl, K. and de Reuse, H. (2010) 'Coupled amino acid deamidase-transport systems essential for Helicobacter pylori colonization,' Infection and immunity, 78(6), pp. 2782-2792.

Lesic, B. and Rahme, L. (2008) 'Use of the lambda Red recombinase system to rapidly generate mutants in *Pseudomonas aeruginosa,' BMC molecular biology*, 9(1), pp. 20.

Lin, C., Chen, Y., Jinn, T., Wu, C., Hong, Y. and Wu, W. (2013). Role of the cAMP-Dependent Carbon Catabolite Repression in Capsular Polysaccharide Biosynthesis in *Klebsiella pneumoniae*. PLoS ONE, 8(2), p.e54430.

Livak, K. and Schmittgen, T. (2001) 'Analysis of relative gene expression data using real-time quantitative PCR and the 2− ΔΔCT method,' *methods*, 25(4), pp. 402-408.

Llobet, E., Martínez-Moliner, V., Moranta, D., Dahlström, K., Regueiro, V., Tomás, A., Cano, V., Pérez-Gutiérrez, C., Frank, C., Fernández-Carrasco, H. and Insua, J., 2015. Deciphering tissue-induced *Klebsiella pneumoniae* lipid A structure. *Proceedings of the National Academy of Sciences*, *112*(46), pp.E6369-E6378.

Loureiro, I., Faria, J., Clayton, C., Ribeiro, S., Roy, N., Santarém, N. & Cordeiro-da-Silva, A. (2013). Knockdown of asparagine synthetase A renders Trypanosoma brucei auxotrophic to asparagine. *PLoS neglected tropical diseases*, *7*(12), p.e2578.

Lynch, N., Roscher, S., Hartung, T., Morath, S., Matsushita, M., Maennel, D. N., Schwaeble, W. J. (2004). L-ficolin specifically binds to lipoteichoic acid, a cell wall constituent of gram-positive bacteria, and activates the lectin pathway of complement. The Journal of Immunology, 172(2), 1198-1202.

Lubkowski, J.; Wlodawer, A.; Ammon, H. ; Copeland, T. ;and Swain, A. (1994). Structural characterization of Pseudomonas 7A glutaminase-asparaginase. J.Biochem. 33: P.10257-10265

Macaluso, A., Best, E. and Bender, R. (1990). Role of the nac gene product in the nitrogen regulation of some NTR-regulated operons of Klebsiella aerogenes. Journal of Bacteriology, 172(12), pp.7249-7255.

Magasanik, B. 1961. Catabolite repression. Cold Spring Harb. Symp. Quant. Biol. 26:249-25.

Maniatis, T., Fritsch, E., and Sambrook, J. (1982) *Molecular cloning: a laboratory manual.* Cold Spring harbor laboratory Cold Spring Harbor, NY.

Martinko, J. and Parker, J. Brock Biology of Microorganisms, 9th ed. Prentice-Hall, Inc. Englewood Cliffs: New Jersey, 2003. p. 69–73.

Matsushita, M. (2010). Ficolins: Complement-activating lectins involved in innate immunity. *Journal of Innate Immunity*, 2(1), 24-32.

Matsushita, M. & Fujita, T. (2002). The role of ficolins in innate immunity. Immunobiology, 205(4-5), 490-497.

Matsushita, M., Kuraya, M., Hamasaki, N., Tsujimura, M., Shiraki, H. & Fujita, T. (2002). Activation of the lectin complement pathway by H-ficolin (hakata antigen). The Journal of Immunology, 168(7), 3502-3506.

Merino, S., Altarriba, M., Izquierdo, L., Nogueras, M., Regué, M. and Tomás, J., 2000. Cloning and Sequencing of the *Klebsiella pneumoniae* O5wb Gene Cluster and Its Role in Pathogenesis. *Infection and immunity*, *68*(5), pp.2435-2440.

Merle, N., Noe, R., Halbwachs-Mecarelli, L., Fremeaux-Bacchi, V., & Roumenina, L. (2015). Complement system part II: Role in immunity. Frontiers in Immunology, 6, 257.

Merrick, M.J. and Edwards, R.A., (1995). Nitrogen control in bacteria. *Microbiological reviews*, *59*(4), pp.604-622.

Miles, A.A., Misra, S.S. and Irwin, J.O., 1938. The estimation of the bactericidal power of the blood. *Epidemiology & Infection*, *38*(6), pp.732-749.

Miller. M.; Rao, J.; Wlodawer, A. and Gribskov, M. (1993). A lefthanded crossover involved in amidohydrolase catalysis. Crystal structure of Erwinia chrysanthemil-asparaginase with bound l-aspartate, J. FEBS Let. 328:P.275–279.

Miethke, M. and Marahiel, M. (2007) 'Siderophore-Based Iron Acquisition and Pathogen Control', *Microbiology and Molecular Biology Reviews*, 71(3), pp. 413–451. doi: 10.1128/MMBR.00012-07.

Mosberg, J., Lajoie, M. and Church, G. (2010) 'Lambda red recombineering in Escherichia coli occurs through a fully single-stranded intermediate', *Genetics,* 186(3), pp. 791-799.

Murphy, K. (1998) 'Use of bacteriophage lambda recombination functions to promote gene replacement in *Escherichia coli,' Journal of Bacteriology,* 180(8), pp. 2063-2071.

Müller, H. and Boos, J. (1998) 'Use of L-asparaginase in childhood ALL.' *Critical reviews in oncology/hematology*, 28(2), pp. 97–113. Available at: http://www.ncbi.nlm.nih.gov/pubmed/9768345 (Accessed: 18 April 2018).

Neves-Petersen, M., Fojan, P. & Petersen, S., 2001. How do lipases and esterases work: the electrostatic contribution. J Biotechnol, 85, 115-47.

Newsholme, P. (2001). Glutamine metabolism: nutritional and clinical significance. J Nutr,131,25152522.

Nishi, T. and Tsuchiya, K. (1980) 'Experimental respiratory tract infection with *Klebsiella pneumoniae* DT-S in mice: chemotherapy with kanamycin.' Antimicrobial Agents and Chemotherapy, 17(3), pp. 494-505.

Ollenschläger, G., Roth, E., Linkesch, W., Jansen, S., Simmel, A. and Mödder, B. (1988). Asparaginase-induced derangements of glutamine metabolism: the pathogenetic basis for some drug-related side-effects. European Journal of Clinical Investigation, 18(5), pp.512-516.

O'donovan, D. J., & Lotspeich, W. D. (1966). Activation of kidney mitochondrial glutaminase by inorganic phosphate and organic acids. *Nature*, *212*(5065), 930.

Ortlund, E., Lacount, M.W., Lewinski, K. and Lebioda, L. (2000). Reactions of Pseudomonas 7A glutaminase-asparaginase with diazo analogues of glutamine and asparagine result in unexpected covalent inhibitions and suggests an unusual catalytic triad Thr-Tyr-Glu, J. Biochem. 39:p.1199–1204.

Özbek, B. and Ülgen, K. (2000) 'The stability of enzymes after sonication,' *Process Biochemistry*, 35(9), pp. 1037-1043.

Paczosa, M. and Mecsas, J., 2016. *Klebsiella pneumoniae*: going on the offense with a strong defense. *Microbiology and Molecular Biology Reviews*, *80*(3), pp.629-661.

Pan, Y., Fang, H., Yang, H., Lin, T., Hsieh, P., Tsai, F., Keynan, Y. and Wang, J., 2008. Capsular polysaccharide synthesis regions in *Klebsiella pneumoniae* serotype K57 and a new capsular serotype. *Journal of clinical microbiology*, *46*(7), pp.2231-2240.

Pan, Y., Lin, T., Chen, Y., Hsu, C., Hsieh, P., Wu, M. and Wang, J., 2013. Capsular types of *Klebsiella pneumoniae* revisited by wzc sequencing. *PloS one*, *8*(12), p.e80670.

Paul, J. and Cooksey, K. (1981). Regulation of Asparaginase, Glutamine Synthetase, and Glutamate Dehydrogenase in Response to Medium Nitrogen Concentrations in a Euryhaline Chlamydomonas Species. PLANT PHYSIOLOGY, 68(6), pp.1364-1368.

Pech, L.L. and Strand, M. (1996) 'Granular cells are required for encapsulation of foreign targets by insect haemocytes,' Journal of cell science, 109(8), pp. 2053-2060.

Perry, R., Balbo, P., Jones, H., Fetherston, J. and DeMoll, E., 1999. Yersiniabactin from Yersinia pestis: biochemical characterization of the siderophore and its role in iron transport and regulation. *Microbiology*, *145*(5), pp.1181-1190.

Petersen, S., Thiel, S., Jensen, L., Vorup-Jensen, T., Koch, C., & Jensenius, J. C. (2000). Control of the classical and the MBL pathway of complement activation. Molecular Immunology, 37(14), 803-811.

Philippe, N., Alcaraz, J., Coursange, E., Geiselmann, J. and Schneider, D. (2004) 'Improvement of pCVD442, a suicide plasmid for gene allele exchange in bacteria', *Plasmid,* 51(3), pp. 246-255.

Podschun, R. and Ullmann, U. (1998) 'Klebsiella spp. as nosocomial pathogens: epidemiology, taxonomy, typing methods, and pathogenicity factors.', Clinical microbiology reviews, 11(4), pp. 589–603. Available at: http://www.ncbi.nlm.nih.gov/pubmed/9767057 (Accessed: 11 April 2018).

Pokrovskii, V., Pokrovskaya, M., Aleksandrova, S., Anrianov, R., Zhdanov, D., Osmel'yanyuk, N., & Sokolov, N. (2013). Physicochemical properties and antiproliferative activity of recombinant *Yersinia pseudotuberculosis* L-asparaginase. *Applied biochemistry and microbiology*, *49*(1), 18-22.

Prusiner, S., Miller, R. and Valentine, R. (1972). Adenosine 3':5'-Cyclic Monophosphate Control of the Enzymes of Glutamine Metabolism in Escherichia coli. Proceedings of the National Academy of Sciences, 69(10), pp.2922-2926.

Quin, L., Carmicle, S., Dave, S., Pangburn, M., Evenhuis, J., & McDaniel, L. (2005). In vivo binding of complement regulator factor H by *streptococcus pneumoniae*. The Journal of Infectious Diseases, 192(11), 1996-2003.

Rammaert, B., Goyet, S., Beauté, J., Hem, S., Te, V., Try, P., Mayaud, C., Borand, L., Buchy, P., Guillard, B. and Vong, S. (2011). *Klebsiella pneumoniae related community-acquired acute lower respiratory infections in CAMBODIA*: *clinical characteristics and treatment*. BMC Proceedings, 5(Suppl 1), p.P72.

Raynal, A., Karray, F., Tuphile, K., Darbon-Rongère, E. and Pernodet, J., 2006. Excisable cassettes: new tools for functional analysis of Streptomyces genomes. *Applied and environmental microbiology*, *72*(7), pp.4839-4844.

Reitzer, L. (2003). Nitrogen assimilation and global regulation in *Escherichia coli*. *Annual Reviews in Microbiology*, *57*(1), 155-176.

Resnick, A. and Magasanik, B. (1976). L-Asparaginase of *Klebsiella aerogenes*. Activation of its synthesis by glutamine synthetase. *J Biol Chem*. 251(9), pp.2722–2728.

Rimbara, E., Mori, S., Kim, H. and Shibayama, K. (2013) 'Role of γ-glutamyltranspeptidase in the pathogenesis of Helicobacter pylori infection,' Microbiology and immunology, 57(10), pp. 665-673.

Ronneau, S., Moussa, S., Barbier, T., Conde-Álvarez, R., Zuniga-Ripa, A., Moriyon, I. & Letesson, J. (2014). *Brucella*, nitrogen and virulence. *Critical reviews in microbiology*, (0), 1-

Runza, V., Schwaeble, W. and Männel, D., 2008. Ficolins: novel pattern recognition molecules of the innate immune response. *Immunobiology*, *213*(3-4), pp.297-306.

Ruzzo, E., Capo-Chichi, J., Ben-Zeev, B., Chitayat, D., Mao, H., Pappas, A. & Goldstein, D. (2013). Deficiency of asparagine synthetase causes congenital microcephaly and a progressive form of encephalopathy. *Neuron*, *80*(2), 429-441.

Saito, H. and Miura, K. (1963) 'Preparation of transforming deoxyribonucleic acid by phenol treatment,' *Biochimica et Biophysica Acta (BBA)-Specialized Section on Nucleic Acids and Related Subjects*, 72, pp. 619-629.

Sanchez, D., Pieckenstain, F., Escaray, F., Erban, A., Kraemer, U., Udvardi, M. and Kopka, J. (2011). 'Comparative ionomics and metabolomics in extremophile and glycophytic Lotus species under salt stress challenge the metabolic preadaptation hypothesis,' Plant, Cell & Environment, 34(4), pp. 605-617.

Sanches, M., Krauchenco, S. and Polikarpov, I. (2007) 'Structure, Substrate Complexation and Reaction Mechanism of Bacterial Asparaginases,' *Current Chemical Biology*, 1(1), pp. 75–86. doi: 10.2174/187231307779814057.

Savitri, N.A. and W. Azmi, 2003. Microbial L-asparaginase: A potent antitumour enzyme. Indian J. Biotechnol., (2), pp. 184-194.

Schalk, A.M., Nguyen, H.A., Rigouin, C. and Lavie, A., 2014. Identification and Structural Analysis of an L-asparaginase Enzyme from Guinea Pig with Putative Tumor Cell-killing Properties. *Journal of Biological Chemistry*, pp.jbc-M114.

Schmit, A. and Ratcliffe, N. (1977) 'The encapsulation of foreign tissue implants in Galleria mellonella larvae,' Journal of insect physiology, 23(2), pp. 175-184.

Schmitz, R., Klopprogge, K. and Grabbe, R. (2002) 'Regulation of nitrogen fixation in *Klebsiella pneumoniae* and Azotobactervinelandii: NifL, transducing two environmental signals to the nif transcriptional activator NifA,' *Journal of molecular microbiology and biotechnology*, 4(3), pp. 235–42.

Schwaeble, W., Lynch, N., Clark, J., Marber, M., Samani, N., Ali, Y., . . . Wallis, R. (2011). Targeting of mannan-binding lectin-associated serine protease-2 confers protection from myocardial and gastrointestinal ischemia/reperfusion injury. Proceedings of the National Academy of Sciences, 108(18), 7523-7528.

Schwaeble, W. & Reid, K. (1999). Does properdin crosslink the cellular and the humoral immune response? Immunology Today, 20(1), 17-21.

Schwaeble, W., Schäfer, M., Petry, F., Fink, T., Knebel, D., Weihe, E. and Loos, M., 1995. Follicular dendritic cells, interdigitating cells, and cells of the monocyte-macrophage lineage are the C1q-producing sources in the spleen. Identification of specific cell types by in situ hybridization and immunohistochemical analysis. *The Journal of Immunology*, *155*(10), pp.4971-4978.

Scoble, M. (1991) 'Classification of the Lepidoptera,' The moths and butterflies of Great Britain and Ireland, 7.

Scorzoni, L., de Lucas, M., Mesa-Arango, A., Fusco-Almeida, A., Lozano, E., Cuenca-Estrella, M., Mendes-Giannini, M., and Zaragoza, O. (2013) 'Antifungal efficacy during Candida krusei infection in non-conventional models correlates with the yeast in vitro susceptibility profile,' PloS one, 8(3), pp. e60047.

Scotti, C., Sommi, P., Pasquetto, M., Cappelletti, D., Stivala, S., Mignosi, P., Savio, M., Chiarelli, L., Valentini, G., Bolanos-Garcia, V., Merrell, D., Franchini, S., Verona, M.,

Bolis, C., Solcia, E., Manca, R., Franciotta, D., Casasco, A., Filipazzi, P., Zardini, E. and Vannini, V. (2010). Cell-Cycle Inhibition by Helicobacter pylori L-Asparaginase. PLoS ONE, 5(11), p.e13892.

Selander, B., Mårtensson, U., Weintraub, A., Holmström, E., Matsushita, M., Thiel, S., Jensenius, J.C., Truedsson, L. and Sjöholm, A., 2006. Mannan-binding lectin activates C3 and the alternative complement pathway without involvement of C2. *The Journal of clinical investigation*, *116*(5), pp.1425-1434.

Sezonov, G., Joseleau-Petit, D., & D'Ari, R. (2007). Escherichia coli physiology in Luria-Bertani broth. *Journal of bacteriology*, *189*(23), 8746-8749.

Shankar-Sinha, S., Valencia, G., Janes, B., Rosenberg, J., Whitfield, C., Bender, R., . . . Younger, J. (2004). The *Klebsiella pneumoniae* O antigen contributes to bacteremia and lethality during murine pneumonia. Infection and Immunity, 72(3), 1423-1430.

Sheng, Y., Mancino, V. and Birren, B. (1995) 'Transformation of Escherichia coli with large DNA molecules by electroporation,' *Nucleic acids research,* 23(11), pp. 1990-1996.

Shibayama, K., Takeuchi, H., Wachino, J., Mori, S. & Arakawa, Y. (2011). Biochemical and pathophysiological characterization of *Helicobacter pylori* asparaginase. *Microbiology and immunology*, 55(6), 408-417.

Shrivastava, A., Khan, A., Khurshid, M., Kalam, M., Jain, K. & Singhal, K. (2015). Recent Developments in L-asparaginase Discovery and Its Potential as Anticancer Agent. *Critical Reviews in Oncology/Hematology*.

Shu, H., Fung, C., Liu, Y., Wu, K., Chen, Y., Li, L., Liu, T., Kirby, R. and Tsai, S., 2009. Genetic diversity of capsular polysaccharide biosynthesis in *Klebsiella pneumoniae* clinical isolates. *Microbiology*, *155*(12), pp.4170-4183.

Singh, J., Srivastava, A., Jha, P., Sinha, K. and Kundu, B. (2015). L-Asparaginase as a new molecular target against leishmaniasis: insights into the mechanism of action and structure-based inhibitor design. Mol. BioSyst., 11(7), pp.1887-1896.

Siu, L., Yeh, K., Lin, J., Fung, C. & Chang, F., 2012. *Klebsiella pneumoniae* liver abscess: a new invasive syndrome. *The Lancet infectious.*

Somerville, G. and Proctor, R. (2009). At the Crossroads of Bacterial Metabolism and Virulence Factor Synthesis in Staphylococci. Microbiology and Molecular Biology Reviews, 73(2), pp.233-248.

Sonawane, A., Klöppner, U., Derst, C. and Röhm, K. (2003) 'Utilization of acidic amino acids and their amides by pseudomonads: role of periplasmic glutaminase-asparaginase,' *Archives of Microbiology,* 179(3), pp. 151-159.

Soupene, E., He, L., Yan, D. and Kustu, S., 1998. Ammonia acquisition in enteric bacteria: physiological role of the ammonium/methylammonium transport B (AmtB) protein. *Proceedings of the National Academy of Sciences*, *95*(12), pp.7030-7034.

Srikhanta, N., Atack, M., Beacham, R. & Jennings, P. (2013). Distinct physiological roles for the two L-asparaginase isozymes of *Escherichia coli*. *Biochemical and biophysical research communications, 436*(3), 362-365.

Standiford, L., Standiford, T., Newstead, M., Zeng, X., Ballinger, M., Kovach, M., Reka, A. and Bhan, U., 2011. TLR4-dependent GM-CSF protects against lung injury in Gram-negative bacterial pneumonia. *American Journal of Physiology-Lung Cellular and Molecular Physiology*, *302*(5), pp.L447-L454.

Stark, M., Suleiman, S., Hassan, J., Greenman, J. & Millar, R., (1997). Amino acid utilisation and deamination of glutamine and asparagine by Helicobacter pylori. Journal of medical microbiology, 46(9), 793-800.

Stover, C., Lynch, N., Dahl, M., Hanson, S., Takahashi, M., Frankenberger, M., . . . Schwaeble, W. (2003). Murine serine proteases MASP-1 and MASP-3, components of the lectin pathway activation complex of complement, are encoded by a single structural gene. Genes and Immunity, 4(5), 374.

Straus, D. C. (1998) *'Klebsiella, Infection and Immunity,' in Encyclopedia of Immunology*. Elsevier, pp. 1522–1523. doi: 10.1006/rwei.1999.0390.

Streicher, S., Shanmugam, K., Ausubel, F., Morandi, C. and Goldberg, R., 1974. Regulation of nitrogen fixation in *Klebsiella pneumoniae*: evidence for a role of glutamine synthetase as a regulator of nitrogenase synthesis. *Journal of bacteriology*, *120*(2), pp.815-821.

Struve, C. and Krogfelt, K. (2003) 'Role of capsule in *Klebsiella pneumoniae* virulence: lack of correlation between in vitro and in vivo studies,' FEMS microbiology letters, 218(1), pp. 149-154.

Stumvoll, M., Perriello, G., Meyer, C. and Gerich, J. (1999). Role of glutamine in human carbohydrate metabolism in kidney and other tissues. Kidney International, 55(3), pp.778-792.

Stülke, J. and Hillen, W. (1999). Carbon catabolite repression in bacteria. Current Opinion in Microbiology, 2(2), pp.195-201.

Tapiero, H., Mathé, G., Couvreur, P. and Tew, K. (2002). II. Glutamine and glutamate. Biomedicine & Pharmacotherapy, 56(9), pp.446-457.

Takahashi, K., & Ezekowitz, R. (2005). The role of the mannose-binding lectin in innate immunity. Clinical Infectious Diseases, 41(Supplement_7), S444.

Takahashi, M., Ishida, Y., Iwaki, D., Kanno, K., Suzuki, T., Endo, Y., Fujita, T. (2010). Essential role of mannose-binding lectin-associated serine protease-1 in activation of the complement factor D. Journal of Experimental Medicine, 207(1), 29-37.

Thiel, S., Vorup-Jensen, T., Stover, C., Schwaeble, W., Laursen, S., Poulsen, K., . . . Holmskov, U. (1997). A second serine protease associated with mannan-binding lectin that activates complement. Nature, 386(6624), 506.

Thomas, X., Cannas, Y., Chelghoum and Gougounon, A. (2010). Therapeutic alternatives to native L-asparaginase in the treatment of adult acute lymphoblastic leukemia. Bull. Cancer, (97), pp. 1105-1117.

Tojo, S., Naganuma, F., Arakawa, K. and Yokoo, S. (2000) 'Involvement of both granular cells and plasmatocytes in phagocytic reactions in the greater wax moth, Galleria mellonella,' *Journal of insect physiology*, 46(7), pp. 1129-1135.

Tomas, J., Camprubi, S. & Williams, P. 1988. Surface exposure of the O-antigen in *Klebsiella pneumoniae* O1: K1 serotype strains. *Microbial pathogenesis*.

Tsai, C., Loh, J. and Proft, T. (2016) 'Galleria mellonella infection models for the study of bacterial diseases and for antimicrobial drug testing,' *Virulence*, 7(3), pp. 214-229.

Turvey, S., & Broide, D. (2010). Innate immunity. Journal of Allergy and Clinical Immunology, 125(2), S32.

van Aartsen, J. and Rajakumar, K. (2011) 'An optimized method for suicide vector-based allelic exchange in *Klebsiella pneumoniae*,' *Journal of microbiological methods*, 86(3), pp. 313-319.

Vidya, J., Vasudevan1, U., Soccol, C., and Pandey, A. (2011). Cloning, functional expression and characterization of L-Asparaginase II from E. coli MTCC 739, Food Technol. Biotechnol., 49 (3):P.286–290.

Villiers, C., Arlaud, G., Colomb, M., & . (1985). Domain structure and associated functions of subcomponents C1r and C1s of the first component of human complement. Proceedings of the National Academy of Sciences, 82(13), 4477-4481.

Vu, B., Chen, M., Crawford, R. and Ivanova, E. (2009) 'Bacterial extracellular polysaccharides involved in biofilm formation,' *Molecules*, 14(7), pp. 2535-2554.

Wallis, R., Dodds, A., Mitchell, D., Sim, R., Reid, K., & Schwaeble, W. (2007). Molecular interactions between MASP-2, C4, and C2 and their activation fragments leading to complement activation via the lectin pathway. Journal of Biological Chemistry, 282(11), 7844-7851.

Wallis, R., Mitchell, D., Schmid, R., Schwaeble, W., & Keeble, A. (2010). Paths reunited: Initiation of the classical and lectin pathways of complement activation. Immunobiology, 215(1), 1-11.

Walsh, M., Bourcier, T., Takahashi, K., Shi, L., Busche, M., Rother, R., . . . Stahl, G. L. (2005). Mannose-binding lectin is a regulator of inflammation that accompanies myocardial ischemia and reperfusion injury. The Journal of Immunology, 175(1), 541-546.

Wand, M., McCowen, J., Nugent, P. and Sutton, J. (2013) 'Complex interactions of *Klebsiella pneumoniae* with the host immune system in a Galleria mellonella infection model,' *Journal of medical microbiology*, 62(12), pp. 1790-1798.

Washington, E., Banfield, M. and Dangl, J. (2013). What a Difference a Dalton Makes: Bacterial Virulence Factors Modulate Eukaryotic Host Cell Signaling Systems via Deamidation. *Microbiology and Molecular Biology Reviews*, 77(3), pp.527-539.

Weis, W., Taylor, M. & Drickamer, K. (1998). The c-type lectin superfamily in the immune system. Immunological Reviews, 163(1), 19-34.

Widdel, F. (2007) 'Theory and measurement of bacterial growth,' *Di dalamGrundpraktikumMikrobiologie*, 4(11).

Wriston, J. and Yellin, T. (1973) 'L-asparaginase: a review,' *Adv EnzymolRelat Areas Mol Biol*, 39, pp. 185-248.

Wu, M. and Li, X. (2015) *'Klebsiella pneumoniae and Pseudomonas aeruginosa,'* in *Molecular Medical Microbiology*. Elsevier, pp. 1547–1564. doi: 10.1016/B978-0-12-397169-2.00087-1.

Xiong, H., Carter, R., Leiner, I., Tang, Y., Chen, L., Kreiswirth, B., & Pamer, E. G. (2015). Distinct contributions of neutrophils and CCR2 monocytes to pulmonary clearance of different *Klebsiella pneumoniae* strains. Infection and Immunity, 83(9), 3418-3427.

Yan, D. (2007) 'Protection of the glutamate pool concentration in enteric bacteria,' *Proceedings of the National Academy of Sciences*, 104(22), pp. 9475-9480.

Yesilkaya, H., Manco, S., Kadioglu, A., Terra, V. and Andrew, P. (2007) 'The ability to utilize mucin affects the regulation of virulence gene expression in *Streptococcus pneumoniae*,' *FEMS microbiology letters*, 278(2), pp. 231-235.

Yongqing, T., Drentin, N., Duncan, R., Wijeyewickrema, L. C. & Pike, R. (2012). Mannose-binding lectin serine proteases and associated proteins of the lectin pathway of complement: Two genes, five proteins and many functions? Biochimica Et Biophysica Acta (BBA)-Proteins and Proteomics, 1824(1), 253-262.

Yoshida, K., Matsumoto, T., Tateda, K., Uchida, K., Tsujimoto, S. and Yamaguchi, K., 2000. Role of bacterial capsule in local and systemic inflammatory responses of mice during pulmonary infection with *Klebsiella pneumoniae*. *Journal of medical microbiology*, *49*(11), pp.1003-1010.

Yuste, J., Ali, S., Sriskandan, S., Hyams, C., Botto, M. & Brown, J. (2006). Roles of the alternative complement pathway and C1q during innate immunity to streptococcus pyogenes. The Journal of Immunology, 176(10), 6112-6120.

Zhang, G., Ducatelle, R., De Bruyne, E., Joosten, M., Bosschem, I., Smet, A., Haesebrouck, F. and Flahou, B. (2015). Role of γ-glutamyltranspeptidase in the pathogenesis of Helicobacter suis and Helicobacter pylori infections. Veterinary Research, 46(1), p.31.